FIFTH EDITION

CARDIAC MAPPING

Edited by
Mohammad Shenasa, Gerhard Hindricks,
David J. Callans, John M. Miller,
and Mark E. Josephson

Foreword by
Douglas P. Zipes and A. John Camm

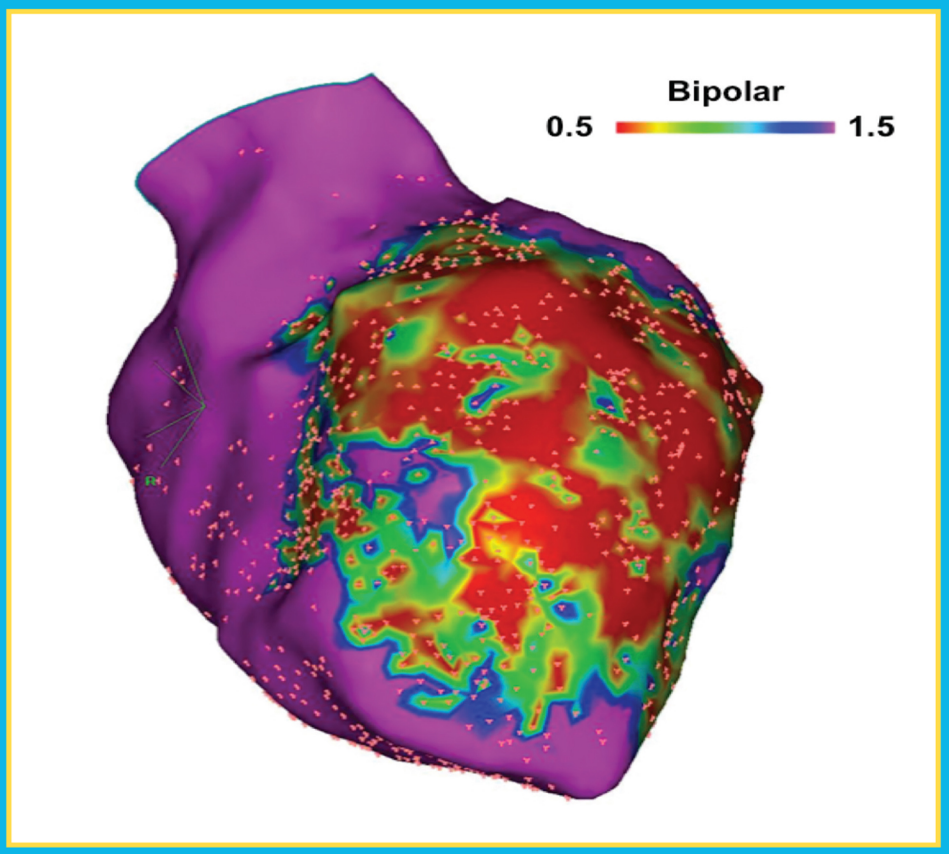

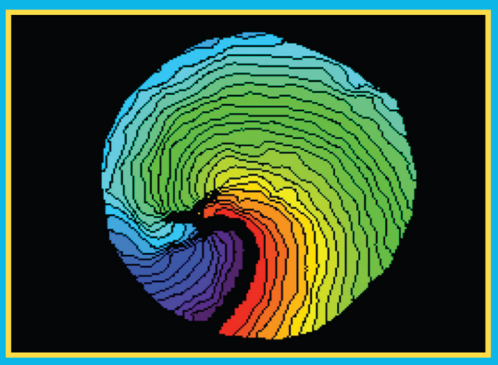

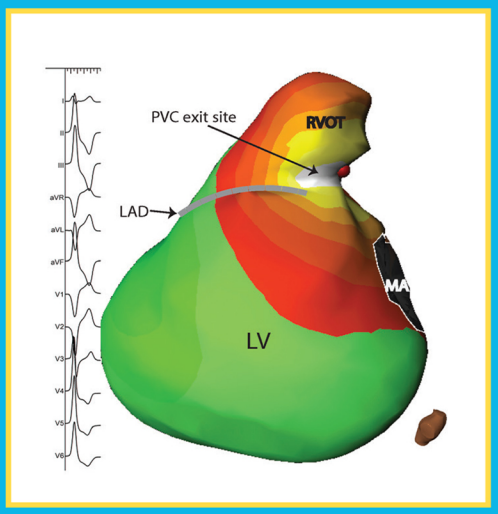

digital companion website

WILEY Blackwell

Cardiac Mapping

We are honored to dedicate this volume to Mark Josephson, MD (January 27, 1943 – January 11, 2017), who mentored and inspired all of us as well as many others in the field of cardiac electrophysiology. Above all, he was a sincere friend and left an indelible mark on our understanding and treatment of cardiac arrhythmias.

Cardiac Mapping

Fifth Edition

Edited by

Mohammad Shenasa, MD, PhD
Heart & Rhythm Medical Group
Department of Cardiovascular Services, O'Connor Hospital
San Jose, CA, USA

Gerhard Hindricks, MD
Professor of Medicine (Cardiology)
University of Leipzig, Heart Center
Director, Department of Electrophysiology
Leipzig, Germany

David J. Callans, MD
Professor of Medicine
Cardiovascular Division
University of Pennsylvania
Philadelphia, PA, USA

John M. Miller, MD
Professor of Medicine
Indiana University School of Medicine
Krannert Institute of Cardiology, Department of Medicine
Indianapolis, IN, USA

Mark E. Josephson, MD[†]
Chief, Cardiovascular Medicine Division
Director, Harvard-Thorndike Electrophysiology Institute and Arrhythmia Service
Beth Israel Deaconess Medical Center
Herman C. Dana Professor of Medicine
Harvard Medical School
Boston, MA, USA

WILEY Blackwell

This edition first published 2019

Edition History
(2e, 1993; 3e, 2009; 4e, 2013) Blackwell Publishing Ltd.

Registered Office(s)
John Wiley & Sons, Inc., 111 River Street, Hoboken, NJ 07030, USA
John Wiley & Sons Ltd, The Atrium, Southern Gate, Chichester, West Sussex, PO19 8SQ, UK

Editorial Office
9600 Garsington Road, Oxford, OX4 2DQ, UK

For details of our global editorial offices, customer services, and more information about Wiley products visit us at www.wiley.com.

Wiley also publishes its books in a variety of electronic formats and by print-on-demand. Some content that appears in standard print versions of this book may not be available in other formats.

Library of Congress Cataloging-in-Publication Data

Names: Shenasa, Mohammad, editor. | Hindricks, Gerhard, editor. | Callans, David J., editor. | Miller, John M. (John Michael), 1954– editor. | Josephson, Mark E., editor.
Title: Cardiac mapping / edited by Mohammad Shenasa, Gerhard Hindricks, David J. Callans, John M. Miller, Mark E. Josephson.
Description: Fifth edition. | Hoboken, NJ, USA : Wiley-Blackwell, 2019. | Includes bibliographical references and index. |
Identifiers: LCCN 2018040052 (print) | LCCN 2018041069 (ebook) | ISBN 9781119152620 (Adobe PDF) | ISBN 9781119152613 (ePub) | ISBN 9781119152590 (hardcover)
Subjects: | MESH: Arrhythmias, Cardiac–physiopathology | Arrhythmias, Cardiac–diagnosis | Electrophysiologic Techniques, Cardiac | Electrocardiography | Cardiac Imaging Techniques
Classification: LCC RC685.A65 (ebook) | LCC RC685.A65 (print) | NLM WG 330 | DDC 616.1/28–dc23
LC record available at https://lccn.loc.gov/2018040052

Cover Design: Wiley
Cover Images: © Lior Gepstein (Top-right), © Elad Anter (Left), Courtesy of Ghassen Chniti (Bottom-right)

Set in 10/12pt Warnock by SPi Global, Pondicherry, India

Hb printing 10 9 8 7 6 5 4 3 2 1

Contents

About the Companion Website and Companion Digital Edition

Companion website

This book is accompanied by a companion website:

http://www.wiley.com/go/cardiacmapping5e

The website includes:

- Video clips showing procedures described in the book

All video clips are referenced in the text where you see this logo 

Companion digital edition

This book is also accompanied by a companion digital edition. Simply find your unique companion digital edition redemption code on the inside front cover of this book by carefully scratching away the top coating on the label. Then visit http://www.vitalsource.com/software/bookshelf/downloads to get started. For more detailed instructions, go to the companion website. Full support is also available at http://support.vitalsource.com

If you purchased this title as an e-book, Wiley Customer Care will provide your access code for the companion digital edition. Visit http://support.wiley.com to request via the "Live Chat" or "Ask a Question" tabs, within 90 days of purchase, and please have your receipt for verification.

Please note that the book cannot be returned once the label is scratched off, and the unique PIN cannot be shared. The site is for individual use by purchasers only and cannot be networked.

List of Videos

Video clip 8.1 Dense mapping in the suspected area of flutter allowed understanding of a small reentrant circuit in the left atrial roof close to the left superior pulmonary vein. Map showing activation in atrial flutter from superior and posterior view.

Video clip 8.2 Right and left atrial map in LAO view showing mitral isthmus flutter in a patient with prior cavotricuspid isthmus ablation. The entire tachcyardia cycle length can be noted also in the right atrium coincidentally.

Video clip 13.1 Optogenetics pacing of the isolate Langendorff-perfused rat heart preparation. As can be seen, the application of flashes of blue light to the site of ChR2 transgene delivery (*apex*) resulted in efficient capture of the ventricle. Note the increase in the contraction rate from ~75 bpm at baseline to 200 bpm during application of flashes of blue light at the same frequency.

Video clip 15.1 Assessment of pulmonary vein anatomy with MDCT prior to RFCA. Analysis of the MDCT axial images is the first step to evaluate pulmonary vein anatomy. Scrolling through them in the caudal to cranial direction as this video shows, we can identify first the left and right inferior pulmonary veins draining into the left atrium, the right superior pulmonary vein, the left atrial appendage, and finally the left superior pulmonary vein.

Video clip 15.2 Evaluation of left ventricular arrhythmogenic substrate with MRI. The left ventricular two-chamber view shows a large, thinned, and akinetic anteroapical wall that corresponds to a prior anterior myocardial infarction. On contrast-enhanced MRI, this area will appear as an extensive bright, hyperenhanced area.

Video clip 25.1 Simultaneous optical mapping of the posterior wall and the appendage of the left atrium (PLA/LAA) with two synchronized CCD cameras. Time series of voltage-sensitive fluorescence were transformed to the phase domain and color-coded according to the stages of the action potential (wavefront is the blue–purple boundary). The phase movies show a rotor with its center of rotation (a phase singularity point representing the surface end point of a filament perpendicular to the field of view) drifting towards the LAA (right). As soon as the rotor enters in the field of view of the LAA, the patterns of activation switch from breakthroughs to reentry and the meandering rotor becomes the main source driving the AF at DF_{Max}. Similarly, once the rotor travels outside of the field of view, the pattern of activation in the LAA switches back to breakthroughs and DF decreases.

Video clip 25.2 Spiral wave reentries (rotors) initiated by S1–S2 cross-field protocol in two-dimensional computer models of paroxysmal (left) and paroxysmal-to-persistent transition (right) AF. Paroxysmal AF rotors exhibited lower frequency than that in transition AF. Rotors in paroxysmal AF meandered considerably and eventually self-terminated on collision with boundary. In transition AF, the rotors were more stable, had higher frequency, and persisted throughout the simulation.

Video clip 31.1 Figure-of-eight reentrant ventricular tachycardia in the anterior septal wall of a swine with chronic anterior wall infarction.

Video clip 33.1 Chaotic Ca^{2+} dynamics at subcellular resolution during VF.

Video clip 40.1 (a) A Carto™ three-dimensional propagation map (derived from electroanatomical mapping) during typical or counterclockwise CTI-dependent AFL. Note the counterclockwise activation sequence around the tricuspid valve annulus. (b) A Carto 3™ three-dimensional propagation map (derived from electroanatomical mapping) during reverse typical or clockwise CTI-dependent AFL. Note the clockwise activation sequence around the tricuspid valve annulus. The red circles indicate the area in the CTI ablated after creating the propagation/activation map.

Video clip 40.2 A Velocity™ three-dimensional propagation map (derived from electroanatomical mapping) during typical AFL. Note the clockwise activation sequence around the tricuspid valve annulus.

Video clip 40.3 A Velocity™ three-dimensional propagation map (derived from electroanatomical mapping) following CTI ablation during pacing from the proximal coronary sinus. Note the conduction block from medial to lateral at the line of ablation in the CTI. Lateral to medial conduction block was also demonstrated (not shown) and AFL was non-inducible. The white circles indicate the area in the CTI ablated prior to creating the propagation/activation map.

Video clip 40.4 (a) A three-dimensional propagation (voltage) map of typical AFL created using the Ensite™ balloon array electrode. Note the counterclockwise activation sequence around the tricuspid valve annulus in this patient. TV, tricuspid valve; CSO, coronary sinus ostium; IVC, inferior vena cava. (b) A three-dimensional propagation (voltage) map following CTI ablation, during pacing from the low lateral right atrium using the Ensite™ balloon array electrode (same patient as in Video clip 40.2). Note the absence of lateral to medial conduction through the CTI with a strictly descending activation at the interatrial septum, confirming lateral to medial conduction block. However, typical AFL was still reinducible after CTI ablation. (c) A three-dimensional propagation (voltage) map following CTI ablation, during pacing from the proximal coronary sinus using the Ensite™ balloon array electrode (same patient as in Video clip 40.2). This patient had typical AFL reinduced after CTI ablation. Note the delayed propagation through the CTI from medial to lateral, with narrowly spaced double potentials (right panel) recorded along the ablation line, indicating incomplete CTI block, resulting in slow conduction and reinducible typical AFL. Repeat ablation eliminated CTI conduction and rendered AFL non-inducible.

Video clip 40.5 A Carto 3™ three-dimensional propagation map (RAO view of right atrium) during atypical scar AFL. Note the double loop reentry pattern using an isthmus between areas of dense scar intermixed with viable atrial myocardium, across which a series of ablation lesions terminated AFL rendering it non-inducible.

Video clip 41.1 Three-dimensional reconstructed CT model (gray shell) of a patient who received mitral valve repair and biatrial cryoablation 2 years before electrophysiological study. At several (43) characteristic sites in the left atrium, post-pacing interval (PPI) measurements were performed and the difference between PPI and the tachycardia cycle length (TCL) is color-coded by using the LAT function of the three-dimensional mapping system. Point by point the reentrant circuit is visualized: in this example the reentrant circuit involved the septal wall, the posterior wall in an oblique direction, and crossed between left atrial appendage (LAA) and left superior pulmonary vein (LSPV). The patient was successfully ablated by creating a linear lesion between the superior mitral annulus and the LSPV anterior to the LAA.

Video clip 41.2 Biatrial activation map using the Rhythmia system. Almost 15 000 electrograms were automatically annotated in a mapping time of less than 20 min using a 64-electrode basket catheter. The active reentry circuit was affecting the right atrium; when reaching the interatrial connection, the passive activation of the entire left atrium can be nicely seen in this high-resolution activation map.

Video clip 41.3 Three-dimensional reconstructed CT with superimposed PPI map of a patient who presented with atypical atrial flutter and 2 : 1 conduction following pulmonary vein isolation 6 months previously. Spots where the post-pacing return cycle equaled tachycardia cycle length are displayed in red. Greater differences are shown in yellow, blue and purple. The reentrant circuit involves the antrum of the left pulmonary veins, probably due to gaps in the circumferential lesions. Ablation of the anterior "ridge" close to the left atrial appendage terminated the tachycardia and made the patient non-inducible after completion of reisolation of the pulmonary veins.

Video clip 80.1 A video of subxiphoid epicardial access in the AP projection. CS, His, RVA catheters were present along with an ICD RV lead. The ablation catheter entered the pericardial space via an inferior approach. Diaphragmatic staining along with free-flowing contrast in the pericardial space was noted.

Video clip 80.2 A video of epicardial mapping in the RAO projection. CS, His, RVA catheters were present along with an ICD RV lead. The ablation catheter and sheath entered the pericardial space via an inferior approach and coursed laterally and superiorly over the left ventricle. The ablation catheter looped over the right ventricular free wall and positioned at the inferior interventricular septum. Coronary angiography showed the course of the right coronary artery (RCA) and the close proximity to the ablation catheter tip.

Video clip 83.1 Animation of MRI-derived left ventricular signal intensity maps projected over color-coded shells from endocardium to epicardium from a patient with healed inferior myocardial infarction. Tridimensional reconstruction of the aortic root is shown in purple. Paths of the border zone channels are highlighted with colored lines. Normal myocardium is represented in purple, core of the infarct in red, and border zone in blue-green-yellow.

Video clip 83.2 Substrate ablation guided by MRI-derived scar. Signal intensity map obtained from MRI projected over subendocardial shell in a patient with a healed inferior myocardial infarction. Areas of dense

scar (signal intensity >60% of the maximal pixel signal intensity) are represented in red. Border zone (signal intensity 40–60%) in green. Normal healthy myocardium is coded in purple. Blue dots represent local abnormal electrograms with delayed components recorded during sinus rhythm. Black dots represent "conducting channel entrances" (local abnormal electrograms with shortest delay between the far-field component and local component). Ablation catheter successively moves to the channel entrances for applying radiofrequency in order to isolate the areas of slow conduction.

Video clip 86.1 Diffusion tensor MRI-derived myocardial fiber disarray in hypertensive left ventricular hypertrophy: visualization, quantification, and effect on mechanical function.

Video clip 96.1 Preprocedure MRI showing distribution of scar tissue in patient with previous myocardial infarction. Myocardial thinning and akinesis of the basal to mid inferior wall with hypokinesis of the inferior apex. Hypokinesis of the basal inferior septum and basal to mid inferolateral wall with mild myocardial thinning inferolaterally. No dyskinetic segments identified. Subendocardial resting first-pass myocardial perfusion defect involving the basal inferior wall with extension into the inferior septum and inferolateral wall.

Video clip 96.2 Myocardial PET metabolic evaluation plus PET perfusion imaging at rest. Moderate perfusion abnormality with focal myocardial FDG uptake. Probable peak active inflammatory cardiac sarcoidosis. Abnormalities involve the apex, lateral, anterior, and septum and do not fit a coronary distribution.

Video clip 96.3 Intracardiac echocardiography. A: Prominent Chiari network/Eustachian ridge. B: Contact during ablation. C: Moderator band mapping. D: Papillary muscle mapping.

Video clip 96.4 Rhythmia maps. RA (**A**) and LA (plus CS) (**B**) maps of an atypical atrial flutter **(C)** post repair of ASD.

List of Contributors

Juan Acosta
Arrhythmia Section, Cardiology Department, Virgen del Rocío University Hospital, Seville, Spain
Chapter 83 Scar-related Ventricular Tachycardia Mapping and Ablation using Contrast-enhanced Magnetic Resonance Imaging

Olujimi A. Ajijola MD, PhD
UCLA Cardiac Arrhythmia Center, UCLA Neurocardiology Research Center, Los Angeles, CA, USA
Chapter 91 Mapping and Ablation in Patients with VT Storm: Role of Neuraxial Therapeutics

Amin Al-Ahmad MD
Texas Cardiac Arrhythmia Institute at St. David's Medical Center, Austin, TX, USA
Chapter 44 Revisiting Non-pulmonary Vein Triggers
Chapter 69 Substrate Ablation for Ventricular Tachycardia in Structural Heart Disease

Vincent Algalorrondo MD
Department of Medicine, Montreal Heart Institute and Université de Montréal, Montreal, QC, Canada
Chapter 37 Clinical Relevance of Functional Models of Atrial Reentry and Fibrillation

Sana M. Al-Khatib MD, MHS
Duke University Hospital and Duke Clinical Research Institute, Durham, NC, USA
Chapter 92 Appropriateness of Mapping and Imaging Modalities in Interventional Electrophysiology

Mohamed Aljaabari MD
Cardiovascular Center, Tufts Medical Center, Tufts University School of Medicine, Boston, MA, USA
Chapter 62 Imaging and Mapping of Arrhythmias in Hypertrophic Cardiomyopathy

Maurits A. Allessie MD, PhD
Department of Cardiology, Erasmus Medical Center, Rotterdam, The Netherlands
Chapter 26 Atrial Fibrillation from a Unipolar, High-resolution Perspective

Jesus Almendral MD
Electrophysiology Laboratory and Arrhythmia Unit, Hospital Monteprincipe, University CEU-San Pablo, Madrid, Spain
Chapter 72 Resetting and Entrainment Phenomena: Application to Mapping of Ventricular Tachycardia

Robert Altman MD
SMG Arrhythmia Center, Summit Medical Group, Short Hills, NJ, USA
Chapter 90 Robotic Navigation for Atrial Fibrillation: Mapping and Ablation

Elad Anter MD
Cardiac Electrophysiology Section, Beth Israel Deaconess Medical Center, Boston, MA, USA
Chapter 31 Experimental VT: A New Porcine Model of Infarct-related Reentrant VT

Charles Antzelevitch PhD, FHRS, FACC, FAHA
Lankenau Institute for Medical Research and Lankenau Heart Institute, Wynnewood, PA; Sidney Kimmel Medical College, Thomas Jefferson University, Philadelphia, PA, USA
Chapter 27 Mechanisms Underlying Arrhythmogenesis in the J-wave Syndromes

Kedar K. Aras PhD
Department of Biomedical Engineering, George Washington University, Washington, DC, USA
Chapter 35 Optical Mapping of Successful and Failed Defibrillation

Mariana Argenziano
Lankenau Institute for Medical Research, Wynnewood, PA, USA
Chapter 27 Mechanisms Underlying Arrhythmogenesis in the J-wave Syndromes

Samuel J. Asirvatham MD
Department of Cardiovascular Diseases, and Department of Pediatrics and Adolescent Medicine, Mayo Clinic, Rochester, MN, USA

Chapter 5 Cardiac Morphology Relevant to Mapping
Chapter 8 Troubleshooting to Avoid Failed Ablation

Fabrizio Assis MD
ARVD/C Program, Division of Cardiology, Johns Hopkins University School of Medicine, Baltimore, MD, USA
Chapter 74 Mapping and Ablation in Arrhythmogenic Right Ventricular Dysplasia Cardiomyopathy: Epicardial and Endocardial Mapping and Long-Term Results

Teresa Barrio-Lopez
Electrophysiology Laboratory and Arrhythmia Unit, Hospital Monteprincipe, University CEU-San Pablo, Madrid, Spain
Chapter 72 Resetting and Entrainment Phenomena: Application to Mapping of Ventricular Tachycardia

Cristina Basso MD, PhD
Department of Cardiac, Thoracic, and Vascular Sciences, University of Padua Medical School, Padova, Italy
Chapter 2 Embryology, Anatomy, and Pathology of Ventricular Outflow Tracts Related to Cardiac Mapping and Arrhythmias

Jeroen J. Bax MD, PhD
Department of Cardiology, Leiden University Medical Center, Leiden, The Netherlands
Chapter 15 Towards Non-invasive Mapping and Imaging of Cardiac Arrhythmias

Tina Baykaner MD, MPH
Stanford University, Palo Alto, CA, USA
Chapter 19 Contact Mapping and Ablation of Complex Cardiac Arrhythmias
Chapter 38 Rotor Mapping in Patients with Atrial Fibrillation

Victor Bazan MD, PhD
Electrophysiology Unit, Cardiology Department, Germans Trias i Pujol, Barcelona, Spain
Chapter 81 Usefulness of the 12-Lead ECG to Identify Epicardial Ventricular Substrate and Epicardial Ventricular Tachycardia Site of Origin

Omer Berenfeld PhD
Cardiac Arrhythmia Service and Center for Arrhythmia Research, University of Michigan, Ann Arbor, MI, USA
Chapter 25 Rotors in Animal Models of Atrial Fibrillation
Chapter 53 Phase Mapping of Human Atrial Fibrillation

Antonio Berruezo MD, PhD
Cardiology Department, Heart Institute, Teknon Medical Center, Barcelona, Spain
Chapter 83 Scar-related Ventricular Tachycardia Mapping and Ablation using Contrast-Enhanced Magnetic Resonance Imaging

Deepak Bhakta MD
Krannert Institute of Cardiology, Department of Medicine, Indiana University School of Medicine, Indiana University Health, Indianapolis, IN, USA
Chapter 71 Endocardial Catheter Pace Mapping of Ventricular Tachycardias

Ad J.J.C. Bogers MD, PhD
Department of Cardiothoracic Surgery, Erasmus Medical Center, Rotterdam, The Netherlands
Chapter 26 Atrial Fibrillation from a Unipolar, High-resolution Perspective

Frank Bogun MD
University of Michigan Hospital, Ann Arbor, MI, USA
Chapter 82 Mapping and Imaging of Fascicular Ventricular Tachycardia

Bastiaan J.D. Boukens PhD
Department of Medical Biology, Academic Medical Center, Amsterdam UMC, Amsterdam, The Netherlands
Chapter 2 Embryology, Anatomy, and Pathology of Ventricular Outflow Tracts Related to Cardiac Mapping and Arrhythmias
Chapter 35 Optical Mapping of Successful and Failed Defibrillation

Mohamed Boutjdir MD
State University of New York, Downstate Medical Center, Brooklyn, NY; New York University School of Medicine, New York, NY; VA New York Harbor Healthcare System, Brooklyn, NY, USA
Chapter 24 Electrophysiological Substrates for Gender Difference in the Incidence of Torsades de Pointes Arrhythmias

Jason Bradfield MD
UCLA Cardiac Arrhythmia Center, UCLA Neurocardiology Research Center, Los Angeles, CA, USA
Chapter 6 Anatomy of the Outflow Tract Region: Relevance to Arrhythmias and Catheter Ablation

Günter Breithardt MD
Department of Cardiovascular Medicine, Division of Electrophysiology, University Hospital Münster, Münster, Germany
Chapter 1 History of Cardiac Mapping

Jaclyn A. Brennan MS
Department of Biomedical Engineering, George Washington University, Washington, DC, USA
Chapter 34 Optical Mapping of Arrhythmogenic Remodeling in the Failing Human Heart

David Briceno MD
Montefiore Medical Center, Albert Einstein College of Medicine, Bronx, NY, USA
Chapter 43 Image-based Risk Stratification for Stroke in Atrial Fibrillation
Chapter 69 Substrate Ablation for Ventricular Tachycardia in Structural Heart Disease

Chad Brodt
Stanford University, Palo Alto, CA, USA
Chapter 38 Rotor Mapping in Patients with Atrial Fibrillation

Josep Brugada MD, PhD
Arrhythmia Section, Cardiology Department, Thorax Institute, Hospital Clínic and IDIBAPS (Institut d'Investigacións Biomèdiques Agustí Pi i Sunyer), Barcelona, Spain
Chapter 83 Scar-related Ventricular Tachycardia Mapping and Ablation using Contrast-enhanced Magnetic Resonance Imaging

J. David Burkhardt MD
Texas Cardiac Arrhythmia Institute at St. David's Medical Center, Austin, TX, USA
Chapter 44 Revisiting Non-pulmonary Vein Triggers
Chapter 69 Substrate Ablation for Ventricular Tachycardia in Structural Heart Disease

Bryan J. Caldwell PhD
Auckland Bioengineering Institute, The University of Auckland, New Zealand;
Institute for Translational Sciences, University of Texas Medical Branch, Galveston, TX, USA
Chapter 32 Experimental Mapping of Ventricular Arrhythmias: Intramural Pathways and Substrate

Hugh Calkins MD
Cardiac Arrhythmia Service, Johns Hopkins Hospital, Baltimore, MD, USA
Chapter 94 Summary and Consensus of Guidelines for Cardiac Mapping and Ablation

David J. Callans MD
Department of Medicine, Perelman School of Medicine, University of Pennsylvania, Philadelphia, PA, USA
Chapter 9 Intracardiac Echocardiography
Chapter 65 Mapping and Ablation of Ventricular Tachycardia in Normal Hearts

Chris D. Cantwell PhD
Department of Aeronautics, Imperial College London; Imperial Centre for Cardiac Engineering, Imperial College London, UK
Chapter 7 Fundamentals of Cardiac Mapping

Riccardo Cappato MD
Humanitas Clinical and Research Center, Rozzano – Milan; Humanitas University, Department of Biomedical Sciences, Pieve Emanuele – Milan, Italy
Chapter 54 Trials on Atrial Fibrillation Mapping and Ablation

René Cardinal PhD
Centre de Recherche, Hôpital du Sacré-Cœur de Montréal; Department of Pharmacology, Faculty of Medicine, Université de Montréal, Montreal, QC, Canada
Chapter 36 Atrial Patterns of Neurally Induced Repolarization Changes: Neuroablative Studies in Canines

Eduardo Castellanos MD
Electrophysiology Laboratory and Arrhythmia Unit, Hospital Monteprincipe, University CEU-San Pablo, Madrid, Spain
Chapter 72 Resetting and Entrainment Phenomena: Application to Mapping of Ventricular Tachycardia

Shih-Ann Chen MD
Faculty of Medicine and Institute of Clinical Medicine, National Yang-Ming University, Taipei, Taiwan; Heart Rhythm Center, Division of Cardiology, Department of Medicine, Taipei Veterans General Hospital, Taiwan
Chapter 39 Rotor Mapping and Ablation in Persistent Atrial Fibrillation

Ghassen Cheniti MD
Bordeaux University Hospital (CHU), Electrophysiology and Cardiac Stimulation Unit;
IHU Liryc, Electrophysiology and Heart Modeling Institute, Fondation Bordeaux Université, Bordeaux, France
Chapter 73 Mapping and Ablation of Idiopathic Ventricular Fibrillation

Anthony J. Choi MD
Massachusetts General Hospital, Cardiac Arrhythmia Service, Boston, MA, USA
Chapter 51 Mapping and Ablation of the Left Atrial Appendage

Jonathan Chrispin MD
Department of Medicine, Division of Cardiology, Johns Hopkins University School of Medicine, Baltimore, MD, USA
Chapter 77 Magnetic Resonance Imaging Mapping of Ventricular Tachycardia in Patients with Different Cardiomyopathies (Arrhythmogenic Right Ventricular Dysplasia, Amyloidosis, etc.)

Fa-Po Chung MD
Faculty of Medicine and Institute of Clinical Medicine, National Yang-Ming University, Taipei, Taiwan; Heart Rhythm Center, Division of Cardiology, Department of Medicine, Taipei Veterans General Hospital, Taiwan
Chapter 39 Rotor Mapping and Ablation in Persistent Atrial Fibrillation

Gopi Dandamudi MD
Krannert Institute of Cardiology, Department of Medicine, Indiana University School of Medicine, Indianapolis, IN, USA
Chapter 55 Entrainment Mapping in Supraventricular Tachycardias
Chapter 56 The Problematic Postpacing Interval
Chapter 71Endocardial Catheter Pace Mapping of Ventricular Tachycardias

Mithilesh K. Das MD
Krannert Institute of Cardiology, Department of Medicine, Indiana University School of Medicine, Indianapolis, IN, USA
Chapter 71 Endocardial Catheter Pace Mapping of Ventricular Tachycardias

James P. Daubert MD
Clinical Cardiac Electrophysiology, Cardiology Division, Department of Medicine and Duke Clinical Research Institute, Duke University Medical Center, Durham, NC, USA
Chapter 12 Multimodel Imaging for Cardiac Mapping
Chapter 16 New High-Density and Automated Mapping Systems
Chapter 57 Mapping and Ablation of Typical and Atypical Accessory Pathways

André D'Avila MD, PhD
Cardiac Arrhythmia Service, Hospital SOS Cardio Florianópolis, Florianópolis, SC, Brazil
Chapter 76 Cardiac Mapping and Imaging in Patients with Ventricular Arrhythmias in Chagas Disease Undergoing Catheter Ablation of Ventricular Tachycardia

Natasja M.S. de Groot MD, PhD
Department of Cardiology, Erasmus Medical Center, Rotterdam, The Netherlands
Chapter 26 Atrial Fibrillation from a Unipolar, High-resolution Perspective

Victoria Delgado MD, PhD
Department of Cardiology, Leiden University Medical Center, Leiden, The Netherlands
Chapter 15 Towards Non-invasive Mapping and Imaging of Cardiac Arrhythmias

Arnaud Denis MD
Bordeaux University Hospital (CHU), Electrophysiology and Cardiac Stimulation Unit;
IHU Liryc, Electrophysiology and Heart Modeling Institute, Fondation Bordeaux Université, Bordeaux, France
Chapter 73 Mapping and Ablation of Idiopathic Ventricular Fibrillation

Makarand Deo PhD
Department of Engineering, Norfolk State University, Norfolk, VA, USA
Chapter 25 Rotors in Animal Models of Atrial Fibrillation

Nicholas Derval MD
Bordeaux University Hospital (CHU), Electrophysiology and Cardiac Stimulation Unit;
IHU Liryc, Electrophysiology and Heart Modeling Institute, Fondation Bordeaux Université, Bordeaux, France
Chapter 17 Non-invasive Body Surface Potential Mapping of Reentrant Drivers in Human Atrial Fibrillation
Chapter 73 Mapping and Ablation of Idiopathic Ventricular Fibrillation

Elizabeth DeWitt MD
Cardiac Electrophysiology Division, Department of Cardiology, Boston Children's Hospital; Harvard Medical School, Boston, MA, USA
Chapter 68 Mapping and Ablation of Ventricular Arrhythmias in Patients with Congenital Heart Disease

Luigi Di Biase MD, PhD
Montefiore Medical Center, Albert Einstein College of Medicine, Bronx, NY; Texas Cardiac Arrhythmia Institute at St. David's Medical Center, Austin, TX, USA;
Department of Biomedical Engineering, University of Texas, Austin, TX, USA;
Department of Cardiology, University of Foggia, Foggia, Italy
Chapter 43 Image-based Risk Stratification for Stroke in Atrial Fibrillation
Chapter 44 Revisiting Non-pulmonary Vein Triggers
Chapter 69 Substrate Ablation for Ventricular Tachycardia in Structural Heart Disease

Timm Dickfeld MD, PhD
Division of Cardiology/Electrophysiology, University of Maryland, Baltimore, MD, USA
Chapter 11 Role of Cardiac Magnetic Resonance Imaging and Late Gadolinium Enhancement in Relation to Arrhythmias in Different Cardiomyopathies

Maxim Didenko MD, PhD
Kuprianov's Cardiovascular Surgery Clinic, Military Medical Academy, Saint Petersburg, Russia;
Department of Cardiology, Cardiovascular Research Institute Maastricht (CARIM), Maastricht University Medical Center, The Netherlands
Chapter 4 The Impact of Embryology and Anatomy on Cardiac Electrophysiology

Remi Dubois PhD
Bordeaux University Hospital (CHU), Electrophysiology and Cardiac Stimulation Unit;
IHU Liryc, Electrophysiology and Heart Modeling Institute, Fondation Bordeaux Université, Bordeaux, France
Chapter 17 Non-invasive Body Surface Potential Mapping of Reentrant Drivers in Human Atrial Fibrillation
Chapter 73 Mapping and Ablation of Idiopathic Ventricular Fibrillation

Josselin Duchateau MD
Bordeaux University Hospital (CHU), Electrophysiology and Cardiac Stimulation Unit;
IHU Liryc, Electrophysiology and Heart Modeling Institute, Fondation Bordeaux Université, Bordeaux, France
Chapter 73 Mapping and Ablation of Idiopathic Ventricular Fibrillation

John Duell MD
Hawthorn Medical Associates, Dartmouth, MA, USA
Chapter 11 Role of Cardiac Magnetic Resonance Imaging and Late Gadolinium Enhancement in Relation to Arrhythmias in Different Cardiomyopathies

Srikant Duggirala MD
Section of Cardiac Electrophysiology, University of California, San Francisco, CA, USA
Chapter 78 Mapping and Ablation of Ventricular Arrhythmias of Unusual Sites

Lars Eckardt MD
Department of Cardiovascular Medicine, Division of Electrophysiology, University Hospital Münster, Germany
Chapter 1 History of Cardiac Mapping
Chapter 45 Mechanisms of Antifibrillatory Agents for Atrial Fibrillation: Evidence Obtained from Experimental Models

Igor R. Efimov PhD
Department of Biomedical Engineering, George Washington University, Washington, DC, USA
Chapter 34 Optical Mapping of Arrhythmogenic Remodeling in the Failing Human Heart
Chapter 35 Optical Mapping of Successful and Failed Defibrillation

Kenneth A. Ellenbogen MD
Division of Cardiology, VCU School of Medicine, and the McGuire VA Medical Center, Richmond, VA, USA
Chapter 42 Mapping and Ablation of Atrial Tachycardia

Nabil El-Sherif MD
State University of New York, Downstate Medical Center, Brooklyn, NY; VA New York Harbor Healthcare System, Brooklyn, NY, USA
Chapter 24 Electrophysiological Substrates for Gender Difference in the Incidence of Torsades de Pointes Arrhythmias

Andres Enriquez MD
Division of Cardiology, Queen's University, Kingston, ON, Canada
Chapter 6 Anatomy of the Outflow Tract Region: Relevance to Arrhythmias and Catheter Ablation

Sabine Ernst MD
Department of Cardiology, Imperial College London, and Royal Brompton and Harefield NHS Foundation Trust, London, UK
Chapter 64 Cardiac Mapping and Imaging: Arrhythmias in Patients with Congenital Heart Disease

N. A. Mark Estes, III MD
Department of Medicine, Division of Cardiology, University of Pittsburgh Medical Center, Pittsburgh, PA, USA
Chapter 62 Imaging and Mapping of Arrhythmias in Hypertrophic Cardiomyopathy

Thomas H. Everett IV, PhD
Krannert Institute of Cardiology, Indiana University School of Medicine, Indianapolis, IN, USA
Chapter 48 Remodeling in Atrial Fibrillation: Novel Mapping Studies

Gregory K. Feld MD
Division of Cardiology, Clinical Cardiac Electrophysiology Program, University of California, San Diego, CA, USA
Chapter 40 Mapping and Ablation of Atrial Flutter and its Variants

Juan Fernández-Armenta
Arrhythmia Section, Cardiology Department, Puerta del Mar University Hospital, Cadiz, Spain

Chapter 83 Scar-related Ventricular Tachycardia Mapping and Ablation using Contrast-enhanced Magnetic Resonance Imaging

David Filgueiras-Rama MD, PhD
Fundación Centro Nacional de Investigaciones Cardiovasculares, Carlos III (CNIC), Madrid, Spain; Hospital Universitario Clínico San Carlos, Madrid, Spain
Chapter 25 Rotors in Animal Models of Atrial Fibrillation

Gerrit Frommeyer MD
Department of Cardiovascular Medicine, Division of Electrophysiology, University of Münster, Germany
Chapter 45 Mechanisms of Antifibrillatory Agents for Atrial Fibrillation: Evidence Obtained from Experimental Models

Antonio Frontera MD
Bordeaux University Hospital (CHU), Electrophysiology and Cardiac Stimulation Unit;
IHU Liryc, Electrophysiology and Heart Modeling Institute, Fondation Bordeaux Université, Bordeaux, France
Chapter 73 Mapping and Ablation of Idiopathic Ventricular Fibrillation

Marco Galeazzi MD
Cardiovascular Department, San Filippo Neri Hospital, Rome, Italy
Chapter 3 Arrythmogenic Venous Extremity of the Cardiac Tube

Paul Garabelli MD
Heart Rhythm Institute and Cardiovascular Section, University of Oklahoma Health Sciences Center, Oklahoma City, OK, USA
Chapter 47 Mapping and Ablation of the Cardiac Autonomic Nervous System to Treat Atrial Fibrillation

Fermin C. Garcia MD
Department of Medicine, Perelman School of Medicine, University of Pennsylvania, Philadelphia, PA, USA
Chapter 6 Anatomy of the Outflow Tract Region: Relevance to Arrhythmias and Catheter Ablation
Chapter 65 Mapping and Ablation of Ventricular Tachycardia in Normal Hearts

Mario Garcia MD
Montefiore Medical Center, Albert Einstein College of Medicine, Bronx, NY, USA
Chapter 43 Image-based Risk Stratification for Stroke in Atrial Fibrillation

Lior Gepstein MD, PhD
Sohnis Laboratory for Cardiac Electrophysiology and Regenerative Medicine, Rambam Medical Center; Cardiology Department, Rappaport Institute and Faculty of Medicine, Technion-Israel Institute of Technology, Haifa, Israel
Chapter 13 Light and the Heart: Cardiac Optogenetics

Edward P. Gerstenfeld MD
Section of Cardiac Electrophysiology, University of California, San Francisco, CA, USA
Chapter 78 Mapping and Ablation of Ventricular Arrhythmias of Unusual Sites

Carola Gianni MD
Texas Cardiac Arrhythmia Institute at St. David's Medical Center, Austin, TX, USA
Chapter 43 Image-based Risk Stratification for Stroke in Atrial Fibrillation
Chapter 44 Revisiting Non-pulmonary Vein Triggers
Chapter 69 Substrate Ablation for Ventricular Tachycardia in Structural Heart Disease

Christopher R. Gloschat PhD
Department of Biomedical Engineering, George Washington University, Washington, DC, USA
Chapter 35 Optical Mapping of Successful and Failed Defibrillation

Amit Gruber
Sohnis Laboratory for Cardiac Electrophysiology and Regenerative Medicine, Rambam Medical Center; Cardiology Department, Rappaport Institute and Faculty of Medicine, Technion-Israel Institute of Technology, Haifa, Israel
Chapter 13 Light and the Heart: Cardiac Optogenetics

Lorne J. Gula MD, MSc
Division of Cardiology, Western University, London, ON, Canada
Chapter 60 Electrical Stimulation Maneuvers to Differentiate Different Forms of Supraventricular Tachycardias

David E. Haines MD
Department of Cardiovascular Medicine, Oakland University William Beaumont School of Medicine, and Beaumont Health, Royal Oak, MI, USA
Chapter 93 How to Avoid Complications of Mapping and Ablation

Michel Haissaguerre MD, PhD
Department of Cardiology, Cardiac Electrophysiology and Pacing, Bordeaux University Hospital-University of Bordeaux, France
Chapter 17 Non-invasive Body Surface Potential Mapping of Reentrant Drivers in Human Atrial Fibrillation
Chapter 73 Mapping and Ablation of Idiopathic Ventricular Fibrillation

Seeongwook Han MD, PhD
Keimyung University School of Medicine, Daegu, South Korea
Chapter 55 Entrainment Mapping in Supraventricular Tachycardias
Chapter 56 The Problematic Postpacing Interval

Donald D. Hegland MD
Clinical Cardiac Electrophysiology, Cardiology Division, Department of Medicine,
Duke University Medical Center, Durham, NC, USA
Chapter 12 Multimodel Imaging for Cardiac Mapping

Sebastian Hilbert MD
Heart Center, Department of Electrophysiology, University of Leipzig, Germany
Chapter 89 Real-Time MRI Mapping and Ablation

Herman D. Himel PhD
VA New York Harbor Healthcare System, Brooklyn, NY, USA
Chapter 24 Electrophysiological Substrates for Gender Difference in the Incidence of Torsades de Pointes Arrhythmias

Gerhard Hindricks MD
Heart Center, Department of Electrophysiology, University of Leipzig, Germany
Chapter 41 Mapping and Ablation of Left Atrial Flutter and Tachycardia: New Observations
Chapter 89 Real-Time MRI Mapping and Ablation

Mélèze Hocini MD
Bordeaux University Hospital (CHU), Electrophysiology and Cardiac Stimulation Unit;
IHU Liryc, Electrophysiology and Heart Modeling Institute, Fondation Bordeaux Université, Bordeaux, France
Chapter 17 Non-invasive Body Surface Potential Mapping of Reentrant Drivers in Human Atrial Fibrillation
Chapter 73 Mapping and Ablation of Idiopathic Ventricular Fibrillation

Boris A. Hoffmann MD
Department of Cardiology II/Electrophysiology, Center of Cardiology, University Medical Center, Johannes Gutenberg-University Mainz, Germany
Chapter 46 Stepwise Approach to AF Mapping and Ablation in Persistent and Long-standing Persistent AF: Short- and Long-term Results

Darren A. Hooks MBChB, PhD, FRACP
Auckland Bioengineering Institute, The University of Auckland;
Cardiology Service, Wellington Hospital, Wellington South, New Zealand
Chapter 32 Experimental Mapping of Ventricular Arrhythmias: Intramural Pathways and Substrate

Rodney P. Horton MD
Texas Cardiac Arrhythmia Institute at St. David's Medical Center, Austin, TX, USA
Chapter 44 Revisiting Non-pulmonary Vein Triggers

Patrick M. Hranitzky MD
Texas Cardiac Arrhythmia Institute at St. David's Medical Center, Austin, TX, USA
Chapter 44 Revisiting Non-pulmonary Vein Triggers

Henry H. Hsia MD, FHRS
San Francisco Veteran Administration Medical Center, University of California, San Francisco, CA, USA
Chapter 80 Epicardial Mapping in Different Ventricular Tachycardia Substrates: Technique and Instrumentation, Short and Long-term Results

Jonathan Hsu MD, MAS
Division of Cardiology, Clinical Cardiac Electrophysiology Program, University of California, San Diego, CA, USA
Chapter 40 Mapping and Ablation of Atrial Flutter and its Variants

Ayman A. Hussein MD
Cleveland Clinic, Heart and Vascular Institute, Section of Cardiac Pacing and Electrophysiology, Cleveland, OH, USA
Chapter 52 Electrogram-based Mapping and Ablation in Atrial Fibrillation

Mathew D. Hutchinson MD
Cardiac Electrophysiology, University of Arizona, Tucson, AZ, USA
Chapter 9 Intracardiac Echocardiography

Kevin P. Jackson MD
Clinical Cardiac Electrophysiology, Cardiology Division, Department of Medicine,
Duke University Medical Center, Durham, NC, USA
Chapter 12 Multimodel Imaging for Cardiac Mapping

Arnold F. Jacobson MD, PhD
Icahn School of Medicine at Mount Sinai, New York, NY, USA
Chapter 22 Advances in Molecular Imaging Relevant to Arrhythmias

Cosima Jahnke MD
Heart Center, Department of Electrophysiology, University of Leipzig, Germany
Chapter 89 Real-Time MRI Mapping and Ablation

Rahul Jain MD, MPH
Krannert Institute of Cardiology, Department of Medicine, Indiana University School of Medicine, Indianapolis, IN, USA
Chapter 55 Entrainment Mapping in Supraventricular Tachycardias
Chapter 56 The Problematic Postpacing Interval

Pierre Jais MD, PhD
Bordeaux University Hospital (CHU), Electrophysiology and Cardiac Stimulation Unit;
IHU Liryc, Electrophysiology and Heart Modeling Institute, Fondation Bordeaux Université, Bordeaux, France
Chapter 17 Non-invasive Body Surface Potential Mapping of Reentrant Drivers in Human Atrial Fibrillation
Chapter 73 Mapping and Ablation of Idiopathic Ventricular Fibrillation

Michiel J. Janse MD
Academic Medical Center, University of Amsterdam, The Netherlands
Chapter 29 Fibrosis and Arrhythmogenesis

Beatriz Jáuregui MD
Cardiology Department, Heart Institute, Teknon Medical Center, Barcelona, Spain
Chapter 83 Scar-related Ventricular Tachycardia Mapping and Ablation using Contrast-Enhanced Magnetic Resonance Imaging

Mohammad-Ali Jazayeri MD
Division of Cardiovascular Diseases, University of Kansas Health System, Kansas City, KS, USA
Chapter 58 Preexcited Atrioventricular Junctional Reentrant Tachycardia: Electrophysiological Characteristics of the Reentrant Circuits

Mohammad-Reza Jazayeri MD
Heart & Vascular Center, Bellin Health, Green Bay, WI, USA
Chapter 58 Preexcited Atrioventricular Junctional Reentrant Tachycardia: Electrophysiological Characteristics of the Reentrant Circuits

Roy M. John MBBS, PhD
Department of Medicine, Vanderbilt University Medical Center, Nashville, TN, USA
Chapter 67 Mapping and Ablation of Ventricular Arrhythmias: Patients with Non-ischemic Cardiomyopathy

Mark E. Josephson MD†
Formerly at Beth Israel Deaconess Medical Center, Harvard Medical School, Boston, MA, USA
Chapter 31 Experimental VT: A New Porcine Model of Infarct-related Reentrant VT
Chapter 59 Mapping and Ablation of Atrioventricular Nodal Reentry Tachycardia and its Variants: Current Understanding and Controversies
Chapter 72 Resetting and Entrainment Phenomena: Application to Mapping of Ventricular Tachycardia

Jonathan M. Kalman MBBS, PhD
Department of Cardiology, Royal Melbourne Hospital; Department of Medicine, University of Melbourne, Australia
Chapter 61 Mechanisms of Persistent Atrial Fibrillation: What Do the Clinical Mapping Studies Teach Us?

Thomas R. Kambur MD
Novant Health, Charlotte, NC, USA
Chapter 55 Entrainment Mapping in Supraventricular Tachycardias
Chapter 56 The Problematic Postpacing Interval
Chapter 71 Endocardial Catheter Pace Mapping of Ventricular Tachycardias

Krishna Kancharla MBBS
Heart and Vascular Institute, University of Pittsburgh Medical Center, Pittsburgh, PA, USA
Chapter 8 Troubleshooting to Avoid Failed Ablation

Suraj Kapa MD
Department of Cardiovascular Diseases, Mayo Clinic, Rochester, MN, USA
Chapter 8 Troubleshooting to Avoid Failed Ablation

Hrayr S. Karagueuzian PhD, MSc, FHRS, FACC
Translational Arrhythmia Research Section, UCLA Cardiovascular Research Laboratory, Department of Medicine (Cardiology), David Geffen School of Medicine at UCLA, Los Angeles, CA, USA
Chapter 30 Triggered Ventricular Tachyarrhythmias Initiated by Enhanced Late Inward Na and Ca Currents: Novel Therapeutic Targets

Demosthenes G. Katritsis MD, PhD
Hygeia Hospital, Athens, Greece
Chapter 59 Mapping and Ablation of Atrioventricular Nodal Reentry Tachycardia and its Variants: Current Understanding and Controversies

Karoly Kaszala MD, PhD
Division of Cardiology, VCU School of Medicine, and the McGuire VA Medical Center, Richmond, VA, USA
Chapter 42 Mapping and Ablation of Atrial Tachycardia

Paul Khairy MD, PhD
Department of Cardiology, Montreal Heart Institute, University of Montréal, Montreal, QC, Canada
Chapter 63 Mapping and Ablation of Supraventricular Arrhythmias in Congenital Heart Disease

Jong J. Kim PhD
RSS Center, Advanced Medical Device Research Division, Korea Electrotechnology Institute, Seoul, Korea;
University of Pittsburgh School of Medicine, Department of Bioengineering, Pittsburgh, PA, USA
Chapter 33 The Molecular Basis of Long QT Type 2 (LQT2)-related Arrhythmias: How Sex Modifies the Risk of Torsades de Pointes

Soo Kim MD
Montefiore Medical Center, Albert Einstein College of Medicine, Bronx, NY, USA
Chapter 69 Substrate Ablation for Ventricular Tachycardia in Structural Heart Disease

Bettina Kirstein MD
Department of Electrophysiology, Cardiac Centre, University Hospital, TU Dresden, Germany
Chapter 14 Cardiac Mapping and Imaging in Patient Selection for Cardiac Resynchronization Therapy: How to Identify Super-responders, Responders, and Non-responders

Takeshi Kitamura MD
Bordeaux University Hospital (CHU), Electrophysiology and Cardiac Stimulation Unit;
IHU Liryc, Electrophysiology and Heart Modeling Institute, Fondation Bordeaux Université, Bordeaux, France
Chapter 73 Mapping and Ablation of Idiopathic Ventricular Fibrillation

André G. Kléber MD
Department of Pathology, Beth Israel and Deaconess Medical Center, Harvard Medical School, Boston, MA, USA
Chapter 29 Fibrosis and Arrhythmogenesis

George J. Klein MD
Division of Cardiology, Western University, London, ON, Canada
Chapter 60 Electrical Stimulation Maneuvers to Differentiate Different Forms of Supraventricular Tachycardias

Jayanthi Koneru MD
Division of Cardiology, VCU School of Medicine, and the McGuire VA Medical Center, Richmond, VA, USA
Chapter 42 Mapping and Ablation of Atrial Tachycardia

Elisa Konofagou PhD
Departments of Biomedical Engineering and Radiology, Columbia University, New York, NY, USA
Chapter 84 Myocardial Elastography
Chapter 85 Electromechanical Wave Imaging

Hans Kottkamp MD
Department of Electrophysiology, Hirslanden Hospital, Zurich, Switzerland
Chapter 50 Fibrotic Atrial Cardiomyopathy: Implications for Ablation of Atrial Fibrillation

Christopher A.B. Kowalewski
Stanford University, Palo Alto, CA, USA
Chapter 38 Rotor Mapping in Patients with Atrial Fibrillation

Fred Kusumoto MD
Heart Rhythm Services, Department of Cardiovascular Disease, Mayo Clinic, Jacksonville, FL, USA
Chapter 4 The Impact of Embryology and Anatomy on Cardiac Electrophysiology

Nirusha Lachman PhD
Department of Anatomy, Mayo Clinic, Rochester, MN, USA
Chapter 5 Cardiac Morphology Relevant to Mapping

Gautam Lalani MD
Division of Cardiology, Clinical Cardiac Electrophysiology Program, University of California, San Diego, CA, USA
Chapter 40 Mapping and Ablation of Atrial Flutter and its Variants

Rakesh Latchamsetty MD
University of Michigan Hospital, Ann Arbor, MI, USA
Chapter 82 Mapping and Imaging of Fascicular Ventricular Tachycardia

Geoffrey Lee MBBS, PhD
Department of Cardiology, Royal Melbourne Hospital; Department of Medicine, University of Melbourne, Australia
Chapter 61 Mechanisms of Persistent Atrial Fibrillation: What Do the Clinical Mapping Studies Teach Us?

Ian J. LeGrice MBChB, PhD
Auckland Bioengineering Institute and Department of Physiology, The University of Auckland, New Zealand
Chapter 32 Experimental Mapping of Ventricular Arrhythmias: Intramural Pathways and Substrate

Peter Leong-Sit MD, MSc
Division of Cardiology, Western University, London, ON, Canada
Chapter 60 Electrical Stimulation Maneuvers to Differentiate Different Forms of Supraventricular Tachycardias

Nigel A. Lever MBChB, FRACP
Green Lane Cardiovascular Service, Auckland City Hospital;
Department of Medicine and Auckland Bioengineering Institute, The University of Auckland, New Zealand
Chapter 32 Experimental Mapping of Ventricular Arrhythmias: Intramural Pathways and Substrate

Yenn-Jiang Lin MD, PhD
Faculty of Medicine and Institute of Clinical Medicine, National Yang-Ming University, Taipei, Taiwan; Heart Rhythm Center, Division of Cardiology, Department of Medicine, Taipei Veterans General Hospital, Taiwan
Chapter 39 Rotor Mapping and Ablation in Persistent Atrial Fibrillation

Mark S. Link MD
Department of Medicine, Division of Cardiology, UT Southwestern Medical Center, Dallas, TX, USA
Chapter 62 Imaging and Mapping of Arrhythmias in Hypertrophic Cardiomyopathy

Li-Wei Lo MD
Faculty of Medicine and Institute of Clinical Medicine, National Yang-Ming University, Taipei, Taiwan; Heart Rhythm Center, Division of Cardiology, Department of Medicine, Taipei Veterans General Hospital, Taiwan
Chapter 39 Rotor Mapping and Ablation in Persistent Atrial Fibrillation

Men-Tzung Lo PhD
Institute of Translational and Interdisciplinary Medicine and Department of Biomedical Sciences and Engineering, National Central University, Chung-Li, Taiwan
Chapter 39 Rotor Mapping and Ablation in Persistent Atrial Fibrillation

Jaimie Manlucu MD
Division of Cardiology, Western University, London, ON, Canada
Chapter 60 Electrical Stimulation Maneuvers to Differentiate Different Forms of Supraventricular Tachycardias

Moussa Mansour MD
Massachusetts General Hospital, Cardiac Arrhythmia Service, Boston, MA, USA
Chapter 51 Mapping and Ablation of the Left Atrial Appendage

Francis E. Marchlinski MD
Electrophysiology Section, Cardiovascular Division, University of Pennsylvania, Philadelphia, PA, USA
Chapter 81 Usefulness of the 12-Lead ECG to Identify Epicardial Ventricular Substrate and Epicardial Ventricular Tachycardia Site of Origin

Joseph E. Marine MD
Section of Electrophysiology, Division of Cardiology, Department of Medicine, Johns Hopkins University School of Medicine, Baltimore, MD, USA
Chapter 79 Mapping and Ablation of Ventricular Tachycardia in Coronary Artery Disease

Nassir F. Marrouche MD, FHRS
Comprehensive Arrhythmia Research and Management Center (CARMA), University of Utah School of Medicine, Salt Lake City, UT, USA
Chapter 49 MRI Mapping of Atrial Fibrosis and Atrial Fibrillation

Ruairidh Martin MD
Bordeaux University Hospital (CHU), Electrophysiology and Cardiac Stimulation Unit;
IHU Liryc, Electrophysiology and Heart Modeling Institute, Fondation Bordeaux Université, Bordeaux, France
Chapter 17 Non-invasive Body Surface Potential Mapping of Reentrant Drivers in Human Atrial Fibrillation
Chapter 73 Mapping and Ablation of Idiopathic Ventricular Fibrillation

Gregoire Massoullie MD
Bordeaux University Hospital (CHU), Electrophysiology and Cardiac Stimulation Unit;
IHU Liryc, Electrophysiology and Heart Modeling Institute, Fondation Bordeaux Université, Bordeaux, France
Chapter 73 Mapping and Ablation of Idiopathic Ventricular Fibrillation

Choukri Mekkaoui PhD
Harvard Medical School, Athinoula A. Martinos Center for Biomedical Imaging, Department of Radiology, Massachusetts General Hospital, Boston, MA, USA
Chapter 87 Diffusion Magnetic Resonance Imaging Tractography of the Heart

Christian Meyer MD
Department of Electrophysiology, University Heart Center Hamburg, University Hospital Hamburg Eppendorf, Hamburg, Germany

Chapter 46 Stepwise Approach to AF Mapping and Ablation in Persistent and Long-standing Persistent AF: Short- and Long-term Results

John M. Miller MD
Krannert Institute of Cardiology, Department of Medicine, Indiana University School of Medicine, Indianapolis, IN, USA
Chapter 55 Entrainment Mapping in Supraventricular Tachycardias
Chapter 56 The Problematic Postpacing Interval
Chapter 71 Endocardial Catheter Pace Mapping of Ventricular Tachycardias

Federico Migliore MD
Department of Cardiac, Thoracic, and Vascular Sciences, University of Padua Medical School, Padova, Italy
Chapter 2 Embryology, Anatomy, and Pathology of Ventricular Outflow Tracts Related to Cardiac Mapping and Arrhythmias

Sanghamitra Mohanty MD
Texas Cardiac Arrhythmia Institute at St. David's Medical Center, Austin, TX, USA
Chapter 43 Image-based Risk Stratification for Stroke in Atrial Fibrillation
Chapter 44 Revisiting Non-pulmonary Vein Triggers
Chapter 69 Substrate Ablation for Ventricular Tachycardia in Structural Heart Disease

Lluís Mont MD, PhD
Arrhythmia Section, Cardiology Department, Thorax Institute, Hospital Clínic and IDIBAPS (Institut d'Investigacións Biomèdiques Agustí Pi i Sunyer), Barcelona, Spain
Chapter 83 Scar-related Ventricular Tachycardia Mapping and Ablation using Contrast-enhanced Magnetic Resonance Imaging

Fabian Moser MD
Department of Electrophysiology, Hirslanden Hospital, Zurich, Switzerland
Chapter 50 Fibrotic Atrial Cardiomyopathy: Implications for Ablation of Atrial Fibrillation

Yuji Nakazato MD, PhD
Department of Cardiology, Juntendo University Urayasu Hospital, Urayasu, Japan
Chapter 66 The Combination of a Basket Catheter and Ensite Mapping System Improves Catheter Ablation of Right Ventricular Outflow Premature Ventricular Contraction

Niyada Naksuk MD
Department of Cardiovascular Diseases, Mayo Clinic, Rochester, MN, USA
Chapter 5 Cardiac Morphology Relevant to Mapping

Kumaraswamy Nanthakumar MD
Institute of Medical Science, University of Toronto; and Heart Rhythm Disorders, Toronto General Hospital, University Health Network, Toronto, ON, Canada
Chapter 97 The Evolution of Cardiac Mapping: Past, Present, Future

Sanjiv M. Narayan MB, MD, FRCP
Stanford University, Palo Alto, CA, USA
Chapter 19 Contact Mapping and Ablation of Complex Cardiac Arrhythmias
Chapter 38 Rotor Mapping in Patients with Atrial Fibrillation

Jagat Narula MD, PhD
Icahn School of Medicine at Mount Sinai, New York, NY, USA
Chapter 22 Advances in Molecular Imaging Relevant to Arrhythmias

Andrea Natale MD
Texas Cardiac Arrhythmia Institute at St. David's Medical Center, Austin, TX, USA;
Department of Biomedical Engineering, University of Texas, Austin, TX, USA
Chapter 43 Image-based Risk Stratification for Stroke in Atrial Fibrillation
Chapter 44 Revisiting Non-pulmonary Vein Triggers
Chapter 69 Substrate Ablation for Ventricular Tachycardia in Structural Heart Disease

Stanley Nattel MD
Department of Medicine, Montreal Heart Institute and Université de Montréal; and Department of Pharmacology and Therapeutics, McGill University, Montreal, Canada; Institute of Pharmacology, West German Heart and Vascular Center, Faculty of Medicine, University Duisburg-Essen, Essen, Germany; L'Institut de Rythmologie et Modelisation Cardiaque (LIRYC), CHU Bordeaux, Bordeaux, France
Chapter 37 Clinical Relevance of Functional Models of Atrial Reentry and Fibrillation

Leenhapong Navaravong MD, FACC, FHRS
UnityPoint Clinic, Iowa Methodist Medical Center, Des Moines, IA, USA
Chapter 49 MRI Mapping of Atrial Fibrosis and Atrial Fibrillation

Saman Nazarian MD, PhD
Department of Medicine, Hospital of the University of Pennsylvania, Philadelphia, PA, USA
Chapter 77 Magnetic Resonance Imaging Mapping of Ventricular Tachycardia in Patients with Different Cardiomyopathies (Arrhythmogenic Right Ventricular Dysplasia, Amyloidosis, etc.)

Jan Němec MD
University of Pittsburgh School of Medicine, Heart and Vascular Institute, Pittsburgh, PA, USA
Chapter 33 The Molecular Basis of Long QT Type 2 (LQT2)-related Arrhythmias: How Sex Modifies the Risk of Torsades de Pointes

Fu Siong Ng MRCP, PhD
National Heart and Lung Institute, Imperial College London, UK
Imperial Centre for Cardiac Engineering, Imperial College London, UK
Chapter 7 Fundamentals of Cardiac Mapping
Chapter 34 Optical Mapping of Arrhythmogenic Remodeling in the Failing Human Heart

Kevin Ng MD
Division of Cardiology, Western University, London, ON, Canada
Chapter 60 Electrical Stimulation Maneuvers to Differentiate Different Forms of Supraventricular Tachycardias

Zhenning Nie MD
Cardiology Department, Zhongshan Hospital, Fudan University, Shanghai, China
Chapter 80 Epicardial Mapping in Different Ventricular Tachycardia Substrates: Technique and Instrumentation, Short and Long-term Results

Sercan Okutucu MD
Department of Cardiology, Memorial Ankara Hospital, Ankara, Turkey
Chapter 70 Coronary Mapping and Ablation of Arrhythmias

Jeffrey E. Olgin MD
Division of Cardiology, University of California, San Francisco, CA, USA
Chapter 48 Remodeling in Atrial Fibrillation: Novel Mapping Studies

Hakan Oral MD
Cardiac Arrhythmia Service and Center for Arrhythmia Research, University of Michigan, Ann Arbor, MI, USA
Chapter 53 Phase Mapping of Human Atrial Fibrillation

Mercedes Ortiz PhD
Electrophysiology Laboratory and Arrhythmia Unit, Hospital Monteprincipe, University CEU-San Pablo, Madrid, Spain
Chapter 72 Resetting and Entrainment Phenomena: Application to Mapping of Ventricular Tachycardia

Ali Oto MD
Head of Cardiology Department, Memorial Ankara Hospital, Ankara, Turkey
Chapter 70 Coronary Mapping and Ablation of Arrhythmias

Douglas L. Packer MD
Department of Cardiovascular Medicine, Mayo Clinic, Rochester, MN, USA
Chapter 96 Future of Cardiac Mapping

Deepak Padmanabhan MD
Department of Cardiovascular Medicine, Mayo Clinic, Rochester, MN, USA
Chapter 96 Future of Cardiac Mapping

Ingo Paetsch MD
Heart Center, Department of Electrophysiology, University of Leipzig, Germany
Chapter 89 Real-Time MRI Mapping and Ablation

Pierre Pagé MD
Centre de Recherche, Hôpital du Sacré-Cœur de Montréal; Department of Surgery, Faculty of Medicine, Université de Montréal, Montreal, QC, Canada
Chapter 36 Atrial Patterns of Neurally Induced Repolarization Changes: Neuroablative Studies in Canines

Diego Penela MD, PhD
Arrhythmia Section, Ospedale Guiglielmo da Saliceto, Piacenza, Italy
Chapter 83 Scar-related Ventricular Tachycardia Mapping and Ablation using Contrast-enhanced Magnetic Resonance Imaging

Nicholas S. Peters FRCP, MD
National Heart and Lung Institute, Imperial College London, UK
Imperial Centre for Cardiac Engineering, Imperial College London, UK
Chapter 7 Fundamentals of Cardiac Mapping

Christopher Phelan MD
Cardiovascular Center, Tufts Medical Center, Tufts University School of Medicine, Boston, MA, USA
Chapter 62 Imaging and Mapping of Arrhythmias in Hypertrophic Cardiomyopathy

Jonathan P. Piccini MD, MHS
Clinical Cardiac Electrophysiology, Cardiology Division, Department of Medicine, and Duke Clinical Research Institute, Duke University Medical Center, Durham, NC, USA
Chapter 16 New High-Density and Automated Mapping Systems

Christopher Piorkowski MD, PhD
Department of Electrophysiology, Cardiac Centre, University Hospital, TU Dresden, Germany
Chapter 14 Cardiac Mapping and Imaging in Patient Selection for Cardiac Resynchronization Therapy: How to Identify Super-responders, Responders, and Non-responders

Cristiano Faria Pisani
Instituto do Coração, São Paulo, SP, Brazil
Chapter 76 Cardiac Mapping and Imaging in Patients with Ventricular Arrhythmias in Chagas Disease Undergoing Catheter Ablation of Ventricular Tachycardia

Sunny S. Po MD, PhD
Heart Rhythm Institute and Cardiovascular Section, University of Oklahoma Health Sciences Center, Oklahoma City, OK, USA
Chapter 47 Mapping and Ablation of the Cardiac Autonomic Nervous System to Treat Atrial Fibrillation

Christian Poenisch MD
Department of Electrophysiology, Hirslanden Hospital, Zurich, Switzerland
Chapter 50 Fibrotic Atrial Cardiomyopathy: Implications for Ablation of Atrial Fibrillation

Edgard A. Prihadi MD
Department of Cardiology, Leiden University Medical Center, Leiden, The Netherlands
Chapter 15 Towards Non-invasive Mapping and Imaging of Cardiac Arrhythmias

Zhilin Qu PhD
UCLA Cardiovascular Research Laboratory, Departments of Medicine (Cardiology) and Physiology, David Geffen School of Medicine at UCLA, Los Angeles, CA, USA
Chapter 28 Relationship Between Cardiac Alternans, Calcium Cycling, and Ventricular Arrhythmias

Javad Rahimian PhD
Southern California Permanente Medical Group, Department of Radiation Oncology, Los Angeles, CA, USA
Chapter 86 Principles of Diffusion Tensor Imaging of the Myocardium: Clinical Applications
Chapter 95 A Roadmap to a Non-invasive Radiosurgical Approach to Ablate the Pulmonary Vein Antra for an Effective Treatment of Atrial Fibrillation: Basic and Technical Principles

Wouter-Jan Rappel PhD
Department of Physics, University of California, San Diego, CA, USA
Chapter 19 Contact Mapping and Ablation of Complex Cardiac Arrhythmias
Chapter 38 Rotor Mapping in Patients with Atrial Fibrillation

Mark Restivo PhD
VA New York Harbor Healthcare System, Brooklyn, NY, USA
Chapter 24 Electrophysiological Substrates for Gender Difference in the Incidence of Torsades de Pointes Arrhythmias

Andreas Rieger MD
Department of Electrophysiology, Hirslanden Hospital, Zurich, Switzerland
Chapter 50 Fibrotic Atrial Cardiomyopathy: Implications for Ablation of Atrial Fibrillation

Crystal M. Ripplinger PhD
Department of Pharmacology, School of Medicine, University of California, Davis, CA, USA
Chapter 23 Optical Mapping of Sarcoplasmic Reticulum Ca^{2+} and Transmembrane Potential in the Intact Heart: Insights into Ca^{2+}-mediated Arrhythmias
Chapter 35 Optical Mapping of Successful and Failed Defibrillation

Stefania Rizzo MD, PhD
Department of Cardiac, Thoracic, and Vascular Sciences, University of Padua Medical School, Padova, Italy
Chapter 2 Embryology, Anatomy, and Pathology of Ventricular Outflow Tracts Related to Cardiac Mapping and Arrhythmias

Jorge Romero MD
Montefiore Medical Center, Albert Einstein College of Medicine, Bronx, NY, USA
Chapter 43 Image-based Risk Stratification for Stroke in Atrial Fibrillation
Chapter 69 Substrate Ablation for Ventricular Tachycardia in Structural Heart Disease

Caroline Roney PhD
National Heart and Lung Institute, Imperial College London; King's College, London, UK
Imperial Centre for Cardiac Engineering, Imperial College London, UK
Chapter 7 Fundamentals of Cardiac Mapping

Thomas Rostock MD
Department of Cardiology II/Electrophysiology, Center of Cardiology, University Medical Center, Johannes Gutenberg-University Mainz, Germany
Chapter 46 Stepwise Approach to AF Mapping and Ablation in Persistent and Long-standing Persistent AF: Short- and Long-term Results

Yoram Rudy PhD
Washington University in St. Louis, MO, USA
Chapter 18 Electrophysiology of Heart Failure: Non-invasive Mapping of Substrate and Guidance of Cardiac Resynchronization Therapy with Electrocardiographic Imaging

Frederic Sacher MD
Bordeaux University Hospital (CHU), Electrophysiology and Cardiac Stimulation Unit;
IHU Liryc, Electrophysiology and Heart Modeling Institute, Fondation Bordeaux Université, Bordeaux, France
Chapter 73 Mapping and Ablation of Idiopathic Ventricular Fibrillation

Mohammed Saeed MD, PhD
Cardiac Arrhythmia Service and Center for Arrhythmia Research, University of Michigan, Ann Arbor, MI, USA
Chapter 53 Phase Mapping of Human Atrial Fibrillation

Guy Salama PhD
University of Pittsburgh School of Medicine, Heart and Vascular Institute and Department of Bioengineering; McGowan Institute of Regenerative Medicine, Pittsburgh, PA, USA
Chapter 33 The Molecular Basis of Long QT Type 2 (LQT2)-related Arrhythmias: How Sex Modifies the Risk of Torsades de Pointes

Walid Saliba MD
Cleveland Clinic, Heart and Vascular Institute, Section of Cardiac Pacing and Electrophysiology, Cleveland, OH, USA
Chapter 52 Electrogram-based Mapping and Ablation in Atrial Fibrillation

Javier E. Sanchez MD
Texas Cardiac Arrhythmia Institute at St. David's Medical Center, Austin, TX, USA
Chapter 44 Revisiting Non-pulmonary Vein Triggers

Pasquale Santangeli MD, PhD
Department of Medicine, Perelman School of Medicine, University of Pennsylvania, Philadelphia, PA, USA
Chapter 9 Intracardiac Echocardiography
Chapter 65 Mapping and Ablation of Ventricular Tachycardia in Normal Hearts

Farhood Saremi MD
Department of Radiology, University of Southern California, Los Angeles, CA, USA
Chapter 10 Role of Cardiac Computed Tomography Imaging to Guide Catheter Ablation of Arrhythmias in Complex Cardiac Morphologies

William H. Sauer MD
Division of Cardiology, Section of Cardiac Electrophysiology, University of Colorado, Denver, CO, USA
Chapter 75 Mapping and Ablation of Ventricular Arrhythmias in Patients with Cardiac Sarcoidosis

Eleonora Savio-Galimberti MD, PhD
Lankenau Institute for Medical Research, Wynnewood, PA, USA
Chapter 27 Mechanisms Underlying Arrhythmogenesis in the J-wave Syndromes

Mauricio Scanavacca MD, PhD
Universidade de São Paulo (USP), São Paulo, SP, Brasil
Chapter 76 Cardiac Mapping and Imaging in Patients with Ventricular Arrhythmias in Chagas Disease Undergoing Catheter Ablation of Ventricular Tachycardia

Benjamin Schaeffer MD
Department of Electrophysiology, University Heart Center Hamburg, University Hospital Hamburg Eppendorf, Hamburg, Germany
Chapter 46 Stepwise Approach to AF Mapping and Ablation in Persistent and Long-standing Persistent AF: Short- and Long-term Results

Benjamin J. Scherlag PhD
Heart Rhythm Institute and Cardiovascular Section, University of Oklahoma Health Sciences Center, Oklahoma City, OK, USA
Chapter 47 Mapping and Ablation of the Cardiac Autonomic Nervous System to Treat Atrial Fibrillation

Richard Schilling MB, BS, MRCP(UK), MD (London), CCS
Barts Heart Centre, St Bartholomew's Hospital, London, UK
Chapter 21 Integration of Contact Force into Mapping and Ablation Systems: Does It Improve the Results?

Doreen Schreiber MD
Department of Electrophysiology, Hirslanden Hospital, Zurich, Switzerland
Chapter 46 Stepwise Approach to AF Mapping and Ablation in Persistent and Long-standing Persistent AF: Short- and Long-term Results

Amir Schricker MD
Division of Cardiology, Clinical Cardiac Electrophysiology Program, University of California, San Diego, CA, USA
Chapter 40 Mapping and Ablation of Atrial Flutter and its Variants

Naim Shaheen
Sohnis Laboratory for Cardiac Electrophysiology and Regenerative Medicine, Rambam Medical Center; Cardiology Department, Rappaport Institute and Faculty of Medicine, Technion-Israel Institute of Technology, Haifa, Israel
Chapter 13 Light and the Heart: Cardiac Optogenetics

Fatemah Shenasa BS
Stanford University, Palo Alto, CA, USA
Chapter 19 Contact Mapping and Ablation of Complex Cardiac Arrhythmias

Hossein Shenasa MD, MSc
Heart and Rhythm Medical Group; Department of Cardiovascular Services, O'Connor Hospital, San Jose, CA, USA
Chapter 86 Principles of Diffusion Tensor Imaging of the Myocardium: Clinical Applications

Mohammad Shenasa MD, PhD
Heart & Rhythm Medical Group; Department of Cardiovascular Services, O'Connor Hospital, San Jose, CA, USA
Chapter 20 Advances in Atrial Fibrillation Ablation
Chapter 86 Principles of Diffusion Tensor Imaging of the Myocardium: Clinical Applications
Chapter 95 A Roadmap to a Non-invasive Radiosurgical Approach to Ablate the Pulmonary Vein Antra for an Effective Treatment of Atrial Fibrillation: Basic and Technical Principles
Chapter 97 The Evolution of Cardiac Mapping: Past, Present, Future

Kalyanam Shivkumar MD
UCLA Cardiac Arrhythmia Center, UCLA Neurocardiology Research Center, Los Angeles, CA, USA
Chapter 6 Anatomy of the Outflow Tract Region: Relevance to Arrhythmias and Catheter Ablation
Chapter 91 Mapping and Ablation in Patients with VT Storm: Role of Neuraxial Therapeutics

Allan C. Skanes MD
Division of Cardiology, Western University, London, ON, Canada
Chapter 60 Electrical Stimulation Maneuvers to Differentiate Different Forms of Supraventricular Tachycardias

Bruce H. Smaill PhD
Auckland Bioengineering Institute and Department of Physiology, The University of Auckland, New Zealand
Chapter 32 Experimental Mapping of Ventricular Arrhythmias: Intramural Pathways and Substrate

Philipp Sommer MD
Heart and Diabetes Center NRW, Clinic for Electrophysiology, University of Bochum, Bad Oeynhausen, Germany
Chapter 41 Mapping and Ablation of Left Atrial Flutter and Tachycardia: New Observations
Chapter 89 Real-Time MRI Mapping and Ablation

Antonio Sorgente MD, PhD
Heart and Vascular Institute, Cleveland Clinic Abu Dhabi, United Arab Emirates
Chapter 54 Trials on Atrial Fibrillation Mapping and Ablation

David E. Sosnovik MD, FACC
Harvard Medical School, Athinoula A. Martinos Center for Biomedical Imaging, Department of Radiology, Massachusetts General Hospital, Boston, MA, USA
Chapter 87 Diffusion Magnetic Resonance Imaging Tractography of the Heart
Chapter 88 Molecular Magnetic Resonance Imaging in Cardiac Electrophysiology

David Spragg MD
Cardiac Arrhythmia Service, Johns Hopkins Hospital, Baltimore, MD, USA
Chapter 94 Summary and Consensus of Guidelines for Cardiac Mapping and Ablation

Stavros Stavrakis MD, PhD
Heart Rhythm Institute and Cardiovascular Section, University of Oklahoma Health Sciences Center, Oklahoma City, OK, USA
Chapter 47 Mapping and Ablation of the Cardiac Autonomic Nervous System to Treat Atrial Fibrillation

Jonathan S. Steinberg MD
University of Rochester School of Medicine and Dentistry, Rochester, NY; SMG Arrhythmia Center, Summit Medical Group, Short Hills, NJ, USA
Chapter 90 Robotic Navigation for Atrial Fibrillation: Mapping and Ablation

Daniel Steven MD
Department of Electrophysiology, University Hospital Cologne, Germany
Chapter 46 Stepwise Approach to AF Mapping and Ablation in Persistent and Long-standing Persistent AF: Short- and Long-term Results

William G. Stevenson MD
Department of Medicine, Vanderbilt University Medical Center, Nashville, TN, USA
Chapter 67 Mapping and Ablation of Ventricular Arrhythmias: Patients with Non-ischemic Cardiomyopathy

Arian Sultan MD
Department of Electrophysiology, University Hospital Cologne, Germany
Chapter 46 Stepwise Approach to AF Mapping and Ablation in Persistent and Long-standing Persistent AF: Short- and Long-term Results

Albert Y. Sun MD
Clinical Cardiac Electrophysiology, Cardiology Division, Department of Medicine, and Duke Clinical Research Institute, Duke University Medical Center, Durham, NC, USA
Chapter 16 New High-Density and Automated Mapping Systems

Edward Sze MD
Clinical Cardiac Electrophysiology, Cardiology Division, Department of Medicine, and Duke Clinical Research Institute, Duke University Medical Center, Durham, NC, USA
Chapter 57 Mapping and Ablation of Typical and Atypical Accessory Pathways

Masateru Takigawa MD
Bordeaux University Hospital (CHU), Electrophysiology and Cardiac Stimulation Unit;
IHU Liryc, Electrophysiology and Heart Modeling Institute, Fondation Bordeaux Université, Bordeaux, France
Chapter 73 Mapping and Ablation of Idiopathic Ventricular Fibrillation

Tanyanan Tanawuttiwat PhD
Section of Electrophysiology, Division of Cardiology, Department of Medicine, Johns Hopkins University School of Medicine, Baltimore, MD, USA; Section of Electrophysiology, Division of Cardiology, Department of Medicine, University of Mississippi Medical Center, Jackson, MS, USA
Chapter 79 Mapping and Ablation of Ventricular Tachycardia in Coronary Artery Disease

Harikrishna Tandri MD
ARVD/C Program, Division of Cardiology, Johns Hopkins University School of Medicine, Baltimore, MD, USA
Chapter 74 Mapping and Ablation in Arrhythmogenic Right Ventricular Dysplasia/Cardiomyopathy: Epicardial and Endocardial Mapping and Long-term Results

Gaetano Thiene MD
Department of Cardiac, Thoracic, and Vascular Sciences and Public Health, University of Padua Medical School, Padova, Italy
Chapter 2 Embryology, Anatomy, and Pathology of Ventricular Outflow Tracts Related to Cardiac Mapping and Arrhythmias

Nathaniel Thompson MD
Bordeaux University Hospital (CHU), Electrophysiology and Cardiac Stimulation Unit;
IHU Liryc, Electrophysiology and Heart Modeling Institute, Fondation Bordeaux Université, Bordeaux, France
Chapter 73 Mapping and Ablation of Idiopathic Ventricular Fibrillation

Takashi Tokano MD, PhD
Department of Cardiology, Juntendo University Urayasu Hospital, Urayasu, Japan
Chapter 66 The Combination of a Basket Catheter and Ensite Mapping System Improves Catheter Ablation of Right Ventricular Outflow Premature Ventricular Contraction

Artour Torossian MD
Antelope Valley Cancer Center, Palmdale, CA, USA
Chapter 95 A Roadmap to a Non-invasive Radiosurgical Approach to Ablate the Pulmonary Vein Antra for an Effective Treatment of Atrial Fibrillation: Basic and Technical Principles

Mark L. Trew PhD
Auckland Bioengineering Institute, The University of Auckland, New Zealand
Chapter 32 Experimental Mapping of Ventricular Arrhythmias: Intramural Pathways and Substrate

Chintan Trivedi MD, MPH
Texas Cardiac Arrhythmia Institute at St. David's Medical Center, Austin, TX, USA
Chapter 44 Revisiting Non-pulmonary Vein Triggers

Wendy S. Tzou MD
Division of Cardiology, Section of Cardiac Electrophysiology, University of Colorado, Denver, CO, USA
Chapter 75 Mapping and Ablation of Ventricular Arrhythmias in Patients with Cardiac Sarcoidosis

Waqas Ullah MD
University Hospital Southampton, Southampton, UK
Chapter 21 Integration of Contact Force into Mapping and Ablation Systems: Does It Improve the Results?

Vaibhav R. Vaidya MBBS
Department of Cardiovascular Diseases, Mayo Clinic, Rochester, MN, USA
Chapter 5 Cardiac Morphology Relevant to Mapping

Lisette J.M.E. van der Does MD
Department of Cardiology, Erasmus Medical Center, Rotterdam, The Netherlands
Chapter 26 Atrial Fibrillation from a Unipolar, High-resolution Perspective

Marmar Vaseghi MD, PhD
UCLA Cardiac Arrhythmia Center, UCLA Neurocardiology Research Center, Los Angeles, CA, USA
Chapter 91 Mapping and Ablation in Patients with VT Storm: Role of Neuraxial Therapeutics

Atul Verma MD
Heart Rhythm Program, Southlake Regional Health Centre, Newmarket, ON; Faculty of Medicine, University of Toronto; McGill University, Montreal, QC, Canada
Chapter 20 Advances in Atrial Fibrillation Ablation
Chapter 97 The Evolution of Cardiac Mapping: Past, Present, Future

David Vidmar MS
Department of Physics, University of California, San Diego, CA, USA
Chapter 38 Rotor Mapping in Patients with Atrial Fibrillation

Konstantinos Vlachos MD
Bordeaux University Hospital (CHU), Electrophysiology and Cardiac Stimulation Unit;
IHU Liryc, Electrophysiology and Heart Modeling Institute, Fondation Bordeaux Université, Bordeaux, France
Chapter 73 Mapping and Ablation of Idiopathic Ventricular Fibrillation

Julia Vogler MD
Department of Electrophysiology, University Heart Center Hamburg, University Hospital Hamburg Eppendorf, Hamburg, Germany
Chapter 46 Stepwise Approach to AF Mapping and Ablation in Persistent and Long-standing Persistent AF: Short- and Long-term Results

Edward P. Walsh MD
Cardiac Electrophysiology Division, Department of Cardiology, Boston Children's Hospital, and Harvard Medical School, Boston, MA, USA
Chapter 68 Mapping and Ablation of Ventricular Arrhythmias in Patients with Congenital Heart Disease

Tomos E. Walters MBBS, PhD
Department of Cardiology, University of California, San Francisco, CA, USA
Chapter 61 Mechanisms of Persistent Atrial Fibrillation: What Do the Clinical Mapping Studies Teach Us?

Lianguo Wang MD
Department of Pharmacology, School of Medicine, University of California, Davis, CA, USA
Chapter 23 Optical Mapping of Sarcoplasmic Reticulum Ca^{2+} and Transmembrane Potential in the Intact Heart: Insights into Ca^{2+}-mediated Arrhythmias

James N. Weiss MD
UCLA Cardiovascular Research Laboratory, Departments of Medicine (Cardiology) and Physiology, David Geffen School of Medicine at UCLA, Los Angeles, CA, USA
Chapter 28 Relationship Between Cardiac Alternans, Calcium Cycling, and Ventricular Arrhythmias

Stephan Willems MD
Department of Electrophysiology, University Heart Center Hamburg, University Hospital Hamburg Eppendorf, Hamburg, Germany
Chapter 46 Stepwise Approach to AF Mapping and Ablation in Persistent and Long-standing Persistent AF: Short- and Long-term Results

Andrew L. Wit PhD
Department of Pharmacology, Columbia University Medical Center, New York, NY, USA
Chapter 31 Experimental VT: A New Porcine Model of Infarct-related Reentrant VT

Michael Wolf MD
Bordeaux University Hospital (CHU), Electrophysiology and Cardiac Stimulation Unit;
IHU Liryc, Electrophysiology and Heart Modeling Institute, Fondation Bordeaux Université, Bordeaux, France
Chapter 73 Mapping and Ablation of Idiopathic Ventricular Fibrillation

Raymond Yee MD
Division of Cardiology, Western University, London, ON, Canada
Chapter 60 Electrical Stimulation Maneuvers to Differentiate Different Forms of Supraventricular Tachycardias

Yuan Yue PhD
VA New York Harbor Healthcare System, Brooklyn, NY, USA
Chapter 24 Electrophysiological Substrates for Gender Difference in the Incidence of Torsades de Pointes Arrhythmias

Junaid A. B. Zaman MA, BMBCh, MRCP
Stanford University, Palo Alto, CA, USA; Imperial College, London, UK

Chapter 19 Contact Mapping and Ablation of Complex Cardiac Arrhythmias
Chapter 38 Rotor Mapping in Patients with Atrial Fibrillation

Emily P. Zeitler MD, MHS
Dartmouth-Hitchcock Medical Center and Geisel School of Medicine at Dartmouth, Lebanon, NH, USA
Chapter 92 Appropriateness of Mapping and Imaging Modalities in Interventional Electrophysiology

Stephan Zellerhoff MD
Department of Internal Medicine and Cardiology, Heart Center Osnabrück – Bad Rothenfelde, Niels-Stensen-Kliniken, Marienhospital Osnabrück, Osnabrück, Germany
Chapter 1 History of Cardiac Mapping

Matthew M. Zipse MD
Division of Cardiology, Section of Cardiac Electrophysiology, University of Colorado, Denver, CO, USA
Chapter 75 Mapping and Ablation of Ventricular Arrhythmias in Patients with Cardiac Sarcoidosis

Editors of Previous Editions

First Edition Editors:
Mohammad Shenasa, Martin Borggrefe, Gunter Breithardt
Assistant Editors: Willhelm Haverkamp, Gerhard Hindricks

Second Edition Editors:
Mohammad Shenasa, Martin Borggrefe, Gunter Breithardt

Third Edition Editors:
Mohammad Shenasa, Gerhard Hindricks, Martin Borggrefe, Gunter Breithardt

Fourth Edition Editors:
Mohammad Shenasa, Gerhard Hindricks, Martin Borggrefe, Gunter Breithardt, Mark E. Josephson
Foreword by: Douglas P. Zipes, A. John Camm

Fifth Edition Editors:
Mohammad Shenasa, Gerhard Hindricks, David Callans, John M. Miller, Mark E. Josephson†
Foreword by: Douglas P. Zipes, A. John Camm

Preface to the Fifth Edition

It is our pleasure to provide our readers with the 5th edition of this textbook on cardiac mapping. Since the publication of the 4th edition in 2013, the field of cardiac mapping has progressed at an unprecedented speed. Many new concepts in mapping and ablation of cardiac arrhythmias, from mechanisms to management, have been introduced and continue to move forward. Similarly, several new technological advances have been made and are already in clinical practice.

Cardiac mapping has always been an integral part of basic and clinical electrophysiology and, indeed, was developed before clinical cardiac electrophysiology from the time of Walter Gaskell and Sir Thomas Lewis.

This volume is not an updated version of previous editions but rather is completely revised, with 17 new chapters added to cover all aspects of fundamentals and technologies on the subject. This provides the reader with all they need to know in one volume. This edition is accompanied by an online version as well as videos on certain topics to help "hands-on" in real time.

As in the previous edition, the chapters are arranged in eight parts: Part I includes eight chapters on the fundamentals of cardiac mapping, Part II contains six chapters describing imaging technologies in cardiac mapping and ablation, while Part III has eight chapters discussing advances in technology. Part IV contains 14 chapters examining mapping in experimental models of cardiac arrhythmias. Part V consists of 18 chapters covering all aspects of mapping and imaging in atrial fibrillation, flutter, and atrial tachycardias. Part VI has 10 chapters discussing mapping of supraventricular arrhythmia, and Part VII has 19 chapters describing the mapping and imaging of ventricular arrhythmias. Finally, Part VIII encompasses 14 chapters exploring the future directions and technologies in cardiac mapping and imaging of cardiac arrhythmias.

We sincerely appreciate all of the contributors who have unanimously accepted our invitations and also presented their state-of-the-art manuscripts in a timely fashion. A project such as this, with 97 chapters, was not an easy task and could not have been done without the support of all the leaders on this fascinating subject. As Douglas Zipes mentioned in his previous Foreword, this textbook on cardiac mapping is "the GPS for electrophysiologists" that guides you to unknown places of cardiac anatomy.

We are deeply saddened by the untimely loss, in January of 2017, of our mentor and friend, the late Mark E. Josephson, who supported us and contributed to both this and previous editions of the book up to the last few days of his life, which was well lived. He will be greatly missed in the cardiology and electrophysiology community.

New to this edition are editors David Callans and John Miller, both former colleagues and friends of Mark E. Josephson. They are both well known to the community of cardiac mapping and electrophysiology. We also wish to thank our previous editors, Gunter Breithardt and Martin Borggrefe, who were instrumental to the success of previous editions.

We sincerely acknowledge our wives and families for their unlimited support, passion, love, and encouragement to finish this project.

Finally, we would like to acknowledge the Wiley team, including Claire Bonnett, Jennifer Seward, Tom Bates, and Gillian Whitley for their outstanding professional work to put this text together. Likewise, we wish to thank Ms Mariah Smith, who was always available, for her superb assistance from the beginning to the end of this project.

We are confident that the electrophysiology community, fellows, attendings, and those who participate in taking care of patients with cardiac arrhythmias will find this text useful. Professor Hein Wellens complimented the previous edition by saying that "it should be in the hands of every person handling an arrhythmia in the catheter room!"

The Editors
Mohammad Shenasa
Gerhard Hindricks
David J. Callans
John M. Miller

Preface to the First Edition

Cardiac mapping has always been an integral part of both experimental and clinical electrophysiology. Indeed, Sir Thomas Lewis systematically investigated the activation sequence of the dog ventricle as early as 1915. The detailed activation map from that experiment is shown in Figure 1. Since then, cardiac mapping has evolved from single sequential probe mapping to very sophisticated computerized three-dimensional mapping. By the time cardiac mapping began being used in the surgical management of ventricular as well as supraventricular tachycardias, a large body of literature had already been collected.

Despite this significant progress, a collective textbook that attempted to discuss all aspects of cardiac mapping did not exist. When we first considered working on such a project, we were not sure if our friends and colleagues who had paved the road to this point would think it necessary to join us in this effort, especially in this era of implantable devices. We were surprised and encouraged by their unanimous positive support to go ahead with this text. (Many of the contributors have already asked about the second revised edition!) The contributors unanimously agreed to prepare manuscripts that discussed their latest work that would subsequently be published in this, the only comprehensive book to present state-of-the-art on all aspects of cardiac mapping from computer simulation to online clinical application. Thus, we would like to thank all the contributors for presenting their best work here. Without them this book would not have been possible.

A unique feature of this book is that chapters are followed by critical editorial comments by the pioneer of that specific area, so that the state-of-the-art is discussed. We hope this book will serve as impetus to stimulate new ideas for cardiac mapping in the future.

The Editors

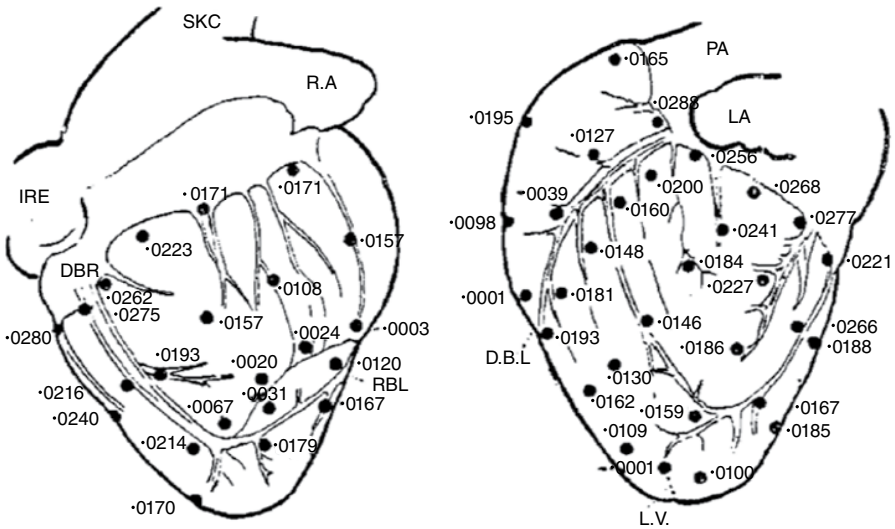

Foreword

We are pleased to write a foreword to the 5th edition of *Cardiac Mapping*, edited by Mohammad Shenasa, Gerhard Hindricks, David Callans, John Miller, and (the late) Mark Josephson. Fittingly, the book is dedicated to Mark Josephson who died in January 2017 before publication. Mark left an indelible imprint on all of us in electrophysiology with his personality, teaching, and contributions to research and patient care. We are certain he would have been proud of this edition.

As with the previous editions, *Cardiac Mapping* continues to be a stellar contribution by world experts in cardiac electrophysiology. The book assumes even more importance in today's world as our navigation in and around the heart becomes more complex and requires more precision. We commented for the last edition that "It is impossible to travel unknown places without a map, or today, more likely, with a GPS in your cell phone, car, computer or iPad. *Cardiac Mapping* is the cardiac electrophysiologist's GPS. It will guide you to new places in the heart and help you find the old places more easily."

We also said, "Cardiac mapping techniques provide extraordinary tools to advance this science (of electrophysiology). But there is still far to go, for unlike the assertion of Sir Thomas Lewis on giving up his research on atrial fibrillation that the "cream was off the milk," we can anticipate accelerated and exciting progress in this arena – "the cat has still to get to the cream."

This text provides many places to look for the cream that will improve our understanding of mechanisms, diagnoses, and treatment. In addition to revising old chapters, new ones have been added to keep pace with our accelerated accumulation of knowledge. Major sections include imaging for ablation, technological advances, mapping in experimental models of cardiac arrhythmias, mapping in challenging arrhythmia substrates of supra- and ventricular tachyarrhythmias, and the new frontiers. The future is dripping with new cream as we explore noninvasive mapping and ablation. In the not-too-distant future, a patient will have a map, an ablation cure, and never have a skin incision. Wouldn't that astound Sir Thomas!

Fortunately for the reader, this text has it all.

Douglas P. Zipes
A. John Camm

Part I

Fundamentals of Cardiac Mapping

1

History of Cardiac Mapping

Stephan Zellerhoff[1], *Lars Eckardt*[2], *and Günter Breithardt*[2]

[1] *Department of Internal Medicine and Cardiology, Heart Center Osnabrück – Bad Rothenfelde, Niels-Stensen-Kliniken, Marienhospital Osnabrück, Osnabrück, Germany*
[2] *Department of Cardiovascular Medicine, Division of Electrophysiology, University Hospital Münster, Germany*

Summary

Cardiac mapping involves recording of electrical activity invasively by electrodes in contact with the heart or non-invasively from the body surface to provide information on myocardial depolarization and/or repolarization over time. The present chapter gives a brief overview on major historical steps in cardiac mapping. Early investigations allowed the registration of only one signal at a time, necessitating sequential point-by-point mapping by repositioning of the mapping catheter. With the advent of more powerful computing capabilities, not only three-dimensional (3D) reconstructions of such sequential mappings, but also the simultaneous mapping of unstable rhythm disorders by invasive and non-invasive multielectrode recording systems have become possible.

Introduction

Knowledge of the time course of electrical activation of the heart is fundamental to the understanding of cardiac arrhythmias – from a scientific as well as from a clinical standpoint. Cardiac mapping involves the recording of electrical activity invasively by electrodes in contact with the heart or non-invasively from the body surface to provide information on changes in depolarization and/or repolarization over time. Early investigations allowed the registration of only one signal at a time, necessitating a sequential point-by-point mapping by repositioning of the mapping catheter. With the advent of more powerful computing capabilities, not only three-dimensional (3D) reconstructions of such sequential mappings, but also the simultaneous mapping of unstable rhythm disorders by invasive and non-invasive multielectrode recording systems became possible.

In this chapter, a short description of the history of cardiac mapping is given which partly refers to chapters in previous editions of this book [1–4]. From the many contributions, both experimentally as well as clinically, only a few can be mentioned here.

Early days of electrocardiography: indirect recordings of the electrical activity of the heart

The late nineteenth and early twentieth century experienced remarkable advances in the indirect recording of the electrical activity of the heart [1]. In 1878, Theodor Wilhelm Engelmann recorded a primitive electrocardiogram (ECG) in isolated frog hearts using a Bernstein rheotome [5]. Shortly thereafter, the first ECG registration from the body surface in man was performed by Augustus Desiré Waller in 1887 (Figure 1.1a) [6]. Potential differences were traced by a Lippmann's capillary electrometer consisting of a mercury column connected to the patient's chest and a sulfuric acid column connected to the back. Willem Einthoven replaced this instrument by a string galvanometer developed by Clément Ader in 1897 [7]. This galvanometer provided, amongst other things, a better response compared to the capillary electrometer owing to the inertness of the mercury column (Figure 1.1b) [8].

Mechanisms of reentrant arrhythmias

Basic features and diagnostic criteria of reentrant arrhythmias, which are still applied nowadays, were initially discovered in the early twentieth century [1]. Mayer, who made ring-like preparations of the muscular tissue of the subumbrella of the scyphomedusa *Cassiopeia*, described rapid, rhythmical pulsation upon stimulation of the disk [9]. Janse portrayed the outstanding but often overlooked role of George Ralph Mines in detail in the second edition of this volume [2]. In brief, in 1913 and 1914 (posthumously), Mines published landmark papers on ring-like preparations of a tortoise heart demonstrating three key criteria of reentrant arrhythmias.

Cardiac Mapping, Fifth Edition. Edited by Mohammad Shenasa, Gerhard Hindricks, David J. Callans, John M. Miller, and Mark E. Josephson.

Companion website: www.wiley.com/go/cardiacmapping5e

(a)

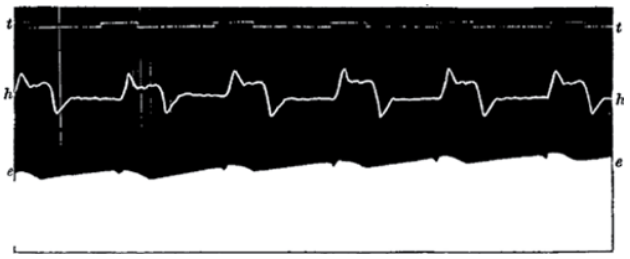

(b)

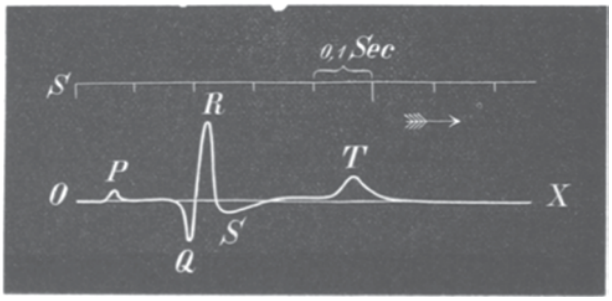

Figure 1.1 (a) A cardiograph recorded by AD Waller in 1887 (front to Hg; back to H_2SO_4). *Source:* Adapted from Waller [6]. Reproduced with permission of John Wiley & Sons. (b) An electrocardiogram recorded by Einthoven. *Source:* Adapted from Einthoven W. Ueber die Form des menschlichen Electrocardiogramms. *Archiv für die gesamte Physiologie des Menschen und der Tiere* 1895;**60**(3):101–23. Reproduced with permission of Springer Nature.

- For the initiation of reentry, an area of unidirectional block must be present.
- The movement of the excitatory pathway should be observed to progress through the pathway, to return to its point of origin, and then again to follow the same pathway.
- "The best test for circulating excitation is to cut through the ring at one point. If the impulse continues to arise in the cut ring, circus movement as a cause can be ruled out" [10,11].

Furthermore, he made predictions on the clinical relevance of these observations in men [11].

> "I venture to suggest that a circulating excitation of this type may be responsible for some cases of paroxysmal tachycardia as observed clinically."

The "multiple wavelet theory" was also envisioned by him.

> "Ordinarily, in the naturally beating heart, the wave of excitation is so long and so rapid that it spreads all over the ventricle long before it has ceased in any one part. Under the altered conditions of increased frequency it is possible that this should no longer be the case, and thus that, the wave being slow and short, more than one could exist at one time in a single chamber …"

Garrey added to these observations.

- The fibrillatory process is not due to a single, rapidly firing focus.
- The demonstration that a minimal tissue mass is required for fibrillation.
- The concept of reentry around a functional obstacle: "The impulse is diverted into different paths weaving and intercoursing through the tissue mass, crossing and recrossing old paths again to course over them or to stop short as it impinges in some barriers of refractory tissue" [12].

Although not studying all criteria proposed by Mines, the experiments of Sir Thomas Lewis in a canine model were the first attempts to document reentry in an intact heart and were of great influence on later studies [13].

Advances in technology: from single-electrode mapping to panoramic four-dimensional mapping

Prior to the aforementioned study, Lewis and Rothschild performed the first *in vivo* mapping of cardiac activation in 1915, trying to elucidate the excitatory process in the canine heart [14]. Point-by-point mapping with a single hand-held probe and the dependency on a string galvanometer made mapping of unstable arrhythmias impossible. Later in the twentieth century, cathode ray oscilloscopes facilitated photographic registration and visual observation of cardiac electrograms during mapping studies.

Beginning in the 1950s, Durrer and colleagues in Amsterdam studied not only the epicardial but also the intramural excitation of the mammalian heart after developing special needle electrodes, which allowed exact registration of the transmural activation, as Hein Wellens reported insightfully in detail in the third edition of this volume as a contemporary witness [3]. After initial observations in canine hearts, Langendorff-perfused human hearts were studied and both 2D and 3D isochronal representations of the ventricular activation of the isolated human heart were reported in a landmark publication in *Circulation* [15].

Meanwhile, Puech et al. in Mexico City studied the process of atrial excitation in the dog's heart by a combination of uni- and bipolar epicardial electrogram recordings while the interatrial septum was explored by introducing special electrodes through different points of the atrial surface, thereby providing detailed data on the spread of activation and conduction velocities in different regions of the right and left atrium [16].

Alanis et al., also based in Mexico City, performed early experiments in Langendorff-perfused canine hearts, specifically recording electrograms from the bundle of His [17]. They were able to show where the decrement in atrioventricular (AV) conduction is located and that His bundle electrogram is part of neither the atrial nor the ventricular electrogram by pacing and by destroying the sinus node and AV node, respectively. After initial case reports in patients with congenital heart disease [18,19], Scherlag et al. introduced the percutaneous His bundle registration clinically [20]. In the following years, this method gained widespread acceptance as a diagnostic tool in various conduction disturbances and arrhythmias [21,22].

Information on activation of cardiac chambers not directly accessible to the diagnostic catheters is sometimes crucial to the understanding of the arrhythmia. The basic feasibility of registering electrical cardiac activity from anatomical structures in the vicinity of the heart was shown by Cremer as early as 1906 [23]. Other proof of principle studies were later undertaken in New York by Kossmann et al. [24], while Breithardt and colleagues in Düsseldorf and Lacombe and co-workers in Montreal were able to perform more sophisticated mapping studies of activation in the left-sided cardiac structures without accessing them [25,26].

In clinical electrophysiology, interpretations of noninvasive as well as invasive recordings were reliant on spontaneously occurring changes in cardiac rhythm, as these zones of transition might give additional clues on the arrhythmias' mechanisms. Two groups independently introduced programmed electrical stimulation as a key technique for the analysis of atrial as well as ventricular arrhythmias into clinical electrophysiology, thereby enabling the operator to provoke similar events and paving the way for subsequent mapping studies: Philippe Coumel and co-workers from Paris and Dirk Durrer's group from Amsterdam [27–29].

A fruitful milieu with seminal contributions to ventricular tachycardia mechanisms and management arose in Philadelphia with Neill Moore and Joe Spear and their team in the experimental laboratory and Mark Josephson and his many colleagues in the clinic, in collaboration with the cardiac surgeon Alden Harken and his team. Their early studies focused on the mechanisms of ventricular tachycardia and endocardial activation during ventricular tachycardia, facilitating surgical treatment [30,31]. Reentry was assumed to be the predominant mechanism of recurrent ventricular tachycardia in 21 patients studied, supporting earlier findings by Wellens et al. [28,30,32]. Interestingly, Josephson described three cases of recurrent ventricular tachycardia in which induction of ventricular tachycardia was dependent on a critical degree of fractionation and delay in local left ventricular electrograms [33]. Continuous electrical activity spanning diastole was necessary for sustenance of the tachycardia whereas after termination, these areas exhibited local prolonged electrical activity exceeding 100 ms even beyond the QRS complex, a phenomenon which was called postexcitation syndrome by Fontaine et al. [34]. Nowadays, these so-called "late potentials" represent one target of substrate-based ablation approaches in ventricular tachycardia in the presence of structural heart disease [35,36].

During the late 1970s and 1980s, the treatment of recurrent supraventricular tachycardia caused by accessory pathways and of recurrent ventricular tachycardia in structural heart disease consisted of surgical transection of the structures related to reentry [37–39]. Treatment success was highly dependent on accurate mapping results. Results of epicardial mapping were usually manually plotted on a visual grid scheme. The inherent problems of interpolation of data between points of measurement are similar to geographic mapping [40]. In addition, recording techniques and interpretation of local electrograms are very variable [41].

Abendroth et al. studied the reproducibility of activation time during intraoperative epicardial ventricular mapping using a coordinate system for registration of spatiotemporal activation [42]. Wit et al. performed multielectrode epicardial mapping in a canine model of myocardial infarction, circumventing the limitations of a single roving electrode used in clinical mapping [43]. Thereby, they found evidence for reentry during episodes of non-sustained ventricular tachycardia, but not during sustained tachycardia. The latter findings may be explained by the results published by de Bakker et al. in 1988 [44]. Using a balloon-shaped multielectrode catheter, intraoperative mapping revealed an apparent focal origin of majority of the ventricular tachycardia. Histological examination of the resected myocardium revealed subendocardially as well as intramurally located zones of viable tissue, favoring a circuitous pathway that consisted of two separated zones of surviving myocardium leading to a "zigzag" activation [45]. These findings support the earlier results of El-Sherif et al., who provided the first *in vivo* evidence of ventricular reentry in a canine model late after myocardial infarction [46].

The concept of entrainment as a key investigational measure for reentrant arrhythmias was clinically validated by Waldo and colleagues in atrial flutter [47]. Epicardially placed, percutaneous pacing wires were used in 30 patients, who developed atrial flutter following open heart surgery, to study the response to pacing at different rates and for different durations. Fundamental observations of fusion during pacing at a rate faster than the atrial as well as of mechanisms of termination were made.

Further functional characterization of zones of slow conduction and the response to entrainment mapping at different sites within the reentry circuit were studied by

Stevenson et al. in a computer model and clinically in 15 patients with drug-refractory ventricular tachycardia late after myocardial infarction [48]. Combinations of entrainment with concealed fusion, postpacing intervals, stimulus to QRS intervals, and isolated diastolic potentials or continuous electrical activity predicted a more than 35% incidence of ventricular tachycardia termination during radiofrequency current application versus a 4% incidence when none suggested that the site was in the reentry circuit.

While most of the reports so far focused on myocardial excitation, Korsgren et al. established invasive measurements of cardiac repolarization *in vivo* by recording monophasic action potentials using a suction electrode catheter, thereby providing new information on repolarization in the normal and diseased state [49]. Franz and colleagues made its routine examination possible in the early 1980s after major changes in catheter design obviating the need for a suction electrode [50].

With the advent of radiofrequency current ablation in the late 1980s, the treatment of cardiac arrhythmias shifted from a surgical to a percutaneous, catheter-based procedure [51,52]. Detailed mapping was further facilitated by the development of sophisticated three-dimensionalmappingsystems,whichprovide(a)non-fluoroscopic catheter localization in three dimensions, (b) accurate reconstruction of the cardiac chamber of interest, and (c) display of electrogram-derived information regarding activation and voltage on the three-dimensional shel [53,54]l. These systems underwent several modifications and enhancements, including the possibility to integrate image information from various imaging modalities (computed tomography, magnetic resonance imaging, intracardiac echocardiography). Furthermore, the limitations of point-by-point mapping using a single electrode were partly overcome by the simultaneous localization of multiple recording electrodes in three-dimensional space and online electrogram recording and automatic annotation.

Following the seminal study by Haïssaguerre et al., various studies on catheter ablation of atrial fibrillation were conducted [55]. Still, mechanisms of initiation and perpetuation of atrial fibrillation are incompletely understood [56,57]. Recently, further advances in mapping of atrial fibrillation have been accomplished by the development of novel invasive and non-invasive mapping systems [4,58,59]. Both systems make use of newly developed algorithms, which include phase mapping for the detection of phase singularities as a marker of functional reentry causing the maintenance of the fibrillatory process. Especially with regard to the spatiotemporal stability of the events mapped, the results of the novel mapping systems differ considerably and an explanation for this is still lacking. Nevertheless, especially non-invasive mapping might provide further *in vivo* insight into the complex pathophysiological mechanisms in inherited arrhythmogenic syndromes, which are not easily amenable to conventional mapping [60].

References

1 Janse MJ. Some historical notes on the mapping of arrhythmias. In: Shenasa M, Borggrefe M, Breithardt G (eds), *Cardiac Mapping*. London: Futura Publishing, 1993: pp. 3–10.

2 Janse MJ. Historical notes: George Ralph Mines. In: Shenasa M, Borggrefe M, Breithardt G (eds), *Cardiac Mapping*, 2nd edn. London: Futura Publishing, 2003: pp. 3–11.

3 Wellens HJ. Cardiac activation mapping: the Amsterdam years. In: Shenasa M, Hindricks G, Borggrefe M, Breithardt G, Josephson ME (eds), *Cardiac Mapping*, 3rd edn. Philadelphia: John Wiley & Sons, 2009: pp. 3–9.

4 de Bakker JM, Vos MA. Evolution of cardiac mapping: From direct analog to digital multi-dimensional recording. In: Shenasa M, Hindricks G, Borggrefe M, Breithardt G, Josephson ME, editors. *Cardiac Mapping*, 4th edn. Oxford: Wiley-Blackwell, 2013: pp. 3–11.

5 Engelmann TW. Ueber das electrische Verhalten des thätigen Herzens. *Pflüger Arch* 1878;**17**:68–99.

6 Waller AD. A demonstration on man of electromotive changes accompanying the heart's beat. *J Physiol* 1887;**8**:229–34.

7 Ader C. Sur un nouvel appareil enregistreur pour cables sous-marins. *Compt Rend Acad Sci* 1897;**124**:1440–2.

8 Einthoven W. Die galvanometrische Registrirung des menschlichen Elektrokardiogramms, zugleich eine Beurtheilung der Anwendung des Capillar-Elektrometers in der Physiologie. *Pflüger Arch* 1903;**99**:472–80.

9 Mayer AG. *Rhythmical Pulsation in Scyphomedusae*. Washington, DC: Carnegie Institute of Washington, 1906: p. 47.

10 Mines GR. On dynamic equilibrium in the heart. *J Physiol* 1913;**46**:349–83.

11 Mines GR. Further experiments on the action of the vagus on the electrogram of the frog's heart. *J Physiol* 1914;**47**:419–30.

12 Garrey WE. The nature of fibrillary contraction of the heart. Its relation to tissue mass and form. *Am J Physiol* 1914;**33**:397.

13 Lewis T, Feil HS, Stroud WD. Observations upon flutter and fibrillation. II. The nature of auricular flutter. *Heart* 1920;**7**:191–233.

14 Lewis T, Rothschild MA. The excitatory process in the dog's heart. Part II. The ventricles. *Phil Trans Roy Soc London B* 1915;**206**:181–226.

15 Durrer D, van Dam RT, Freud GE, Janse MJ, Meijler FL, Arzbaecher RC. Total excitation of the isolated human heart. *Circulation* 1970;**41**:899–912.

16 Puech P, Esclavissat M, Sodi-Pallares D, Cisneros F. Normal auricular activation in the dog's heart. *Am Heart J* 1954;**47**:174–91.

17 Alanís J, González H, López E. The electrical activity of the bundle of His. *J Physiol* 1958;**142**:127–40.

18 Giraud G, Puech P, Latour H. L'activite electrique physiologique du noeud de Tawara et du faisceau de His chez l'homme. *Acad Nat Med* 1960;**363**.

19 Watson H, Emslie-Smith D, Lowe KG. The intracardiac electrocardiogram of human atrioventricular conducting tissue. *Am Heart J* 1967;**74**:66–70.

20 Scherlag BJ, Lau SH, Helfant RH, Berkowitz WD, Stein E, Damato AN. Catheter technique for recording His bundle activity in man. *Circulation* 1969;**39**:13–18.

21 Akhtar M, Gilbert C, Wolf FG, Schmidt DH. Reentry within the His–Purkinje system. Elucidation of reentrant circuit using right bundle branch and His bundle recordings. *Circulation* 1978;**58**:295–304.

22 Castillo CA, Castellanos A. His bundle recordings in patients with reciprocating tachycardias and Wolff-Parkinson-White syndrome. *Circulation* 1970;**42**:271–85.

23 Cremer M. Über die direkte Ableitung der Aktionsströme des menschlichen Herzens vom Oesophagus und über das Elektrokardiogramm des Fötus. *Münch Med Wochenschr* 1906;**53**:811–13.

24 Kossmann CE, Berger AR, Rader B, Brumlik J, Briller SA, Donnelly JH. Intracardiac and intravascular potentials resulting from electrical activity of the normal human heart. *Circulation* 1950;**2**:10–30.

25 Lacombe P, Sadr-Ameli MA, Pagé P, Cardinal R, Nadeau RA, Shenasa M. Catheter recording of left atrial activation from left pulmonary artery in the Wolff-Parkinson-White syndrome: validation of the technique with intraoperative mapping results. *Pacing Clin Electrophysiol* 1988;**11**:2168–79.

26 Breithardt G, Seipel L. Recording of left atrial potentials from pulmonary artery in man. *Br Heart J* 1980;**43**:689–94.

27 Durrer D, Schoo L, Schuilenburg RM, Wellens HJJ. The role of premature beats in the initiation and the termination of supraventricular tachycardia in the Wolff-Parkinson-White syndrome. *Circulation* 1967;**36**:644–62.

28 Wellens HJJ, Schuilenburg RM, Durrer D. Electrical stimulation of the heart in patients with ventricular tachycardia. *Circulation* 1972;**46**:216–26.

29 Coumel PH, Cabrol C, Fabiato A, Gourgon R, Slama R. Tachycardie permanente par rythme reciproque. *Arch Mal Coeur* 1967;**60**:1830–64.

30 Josephson ME, Horowitz LN, Farshidi A, Kastor JA. Recurrent sustained ventricular tachycardia. 1. Mechanisms. *Circulation* 1978;**57**:431–40.

31 Josephson ME, Horowitz LN, Farshidi A, Spear JF, Kastor JA, Moore EN. Recurrent sustained ventricular tachycardia. 2. Endocardial mapping. *Circulation* 1978;**57**:440–7.

32 Wellens HJJ, Lie KI, Durrer D. Further observations on ventricular tachycardia as studied by electrical stimulation of the heart: chronic recurrent ventricular tachycardia and ventricular tachycardia during acute myocardial infarction. *Circulation* 1974;**49**:647–53.

33 Josephson ME, Horowitz LN, Farshidi A. Continuous local electrical activity. A mechanism of recurrent ventricular tachycardia. *Circulation* 1978;**57**:659–65.

34 Fontaine G, Guiraudon GM, Frank R. Intramyocardial conduction defects in patients prone to chronic ventricular tachycardia. I. The post-excitation syndrome in sinus rhythm. In: Sandoe E, Julian DG, Bell JW (eds), *Management of Ventricular Tachycardia – Role of Mexiletine*. Amsterdam: Excerpta Medica, 1978: p. 39.

35 Arenal A, Glez-Torrecilla E, Ortiz M, *et al*. Ablation of electrograms with an isolated, delayed component as treatment of unmappable monomorphic ventricular tachycardias in patients with structural heart disease. *J Am Coll Cardiol* 2003;**41**:81–92.

36 Breithardt G, Cain ME, El-Sherif N, *et al*. Standards for analysis of ventricular late potentials using high resolution or signal-averaged electrocardiography. A statement by a Task Force Committee between the European Society of Cardiology, the American Heart Association and the American College of Cardiology. *Eur Heart J* 1991;**12**:473–80.

37 Gallagher JJ, Gilbert M, Svenson RH, Sealy WC, Kasell J, Wallace AG. Wolff-Parkinson-White syndrome. The problem, evaluation, and surgical correction. *Circulation* 1975;**51**:767–85.

38 Gallagher JJ, Oldham HN, Wallace AG, Peter RH, Kasell J. Ventricular aneurysm with ventricular tachycardia. Report of a case with epicardial mapping and successful resection. *Am J Cardiol* 1975;**35**:696–700.

39 Iwa T, Kazui T, Sugii S, Wada J. [Surgical treatment of Wolff-Parkinson-White syndrome]. *Japan J Thorac Surg* 1970;**23**:513–18.

40 Breithardt G, Shenasa M, Biermann M, *et al*. Precision and reproducibility of isochronal electrical cardiac mapping. In: Shenasa M, Borggrefe M, Breithardt G (eds), *Cardiac Mapping*. London: Futura Publishing, 1993: pp. 35–62.

41 Biermann M, Shenasa M, Borggrefe M, Hindricks G, Haverkamp W, Breithardt G. The interpretation of cardiac electrograms. In: Shenasa M, Borggrefe M, Breithardt G (eds), *Cardiac Mapping*. London: Futura Publishing, 1993: pp. 11–34.

42 Abendroth RR, Ostermeyer J, Breithardt G, Seipel L, Bircks W. Reproducibility of local activation times during intraoperative epicardial mapping. *Circulation* 1980;**62**:75–9.

43 Wit AL, Allessie MA, Bonke FI, Lammers W, Smeets J, Fenoglio JJ. Electrophysiologic mapping to determine the mechanism of experimental ventricular tachycardia initiated by premature impulses. Experimental approach and initial results demonstrating reentrant excitation. *Am J Cardiol* 1982;**49**:166–85.

44 de Bakker JM, van Capelle FJ, Janse MJ, *et al*. Reentry as a cause of ventricular tachycardia in patients with chronic ischemic heart disease: electrophysiologic and anatomic correlation. *Circulation* 1988;**77**:589–606.

45 de Bakker JM, van Capelle FJ, Janse MJ, *et al*. Slow conduction in the infarcted human heart. "Zigzag" course of activation. *Circulation* 1993;**88**:915–26.

46 El-Sherif N, Scherlag BJ, Lazzara R, Hope RR. Re-entrant ventricular arrhythmias in the late myocardial infarction period. 1. Conduction characteristics in the infarction zone. *Circulation* 1977;**55**:686–702.

47 Waldo AL, MacLean WA, Karp RB, Kouchoukos NT, James TN. Entrainment and interruption of atrial flutter with atrial pacing: studies in man following open heart surgery. *Circulation* 1977;**56**:737–45.

48 Stevenson WG, Khan H, Sager P, et al. Identification of reentry circuit sites during catheter mapping and radiofrequency ablation of ventricular tachycardia late after myocardial infarction. *Circulation* 1993;**88**:1647–70.

49 Korsgren M, Leskinen E, Sjöstrand U. Intracardiac recording of monophasic action potentials in the human heart. *Scand J Clin Lab Invest* 1966;**18**:561–4.

50 Franz M, Schöttler M, Schaefer J, Seed WA. Simultaneous recording of monophasic action potentials and contractile force from the human heart. *Klin Wochenschr* 1980;**58**:1357–9.

51 Borggrefe M, Budde T, Podczeck A, Breithardt G. High frequency alternating current ablation of an accessory pathway in humans. *J Am Coll Cardiol* 1987;**10**:576–82.

52 Budde TH, Breithardt G, Borggrefe M, Podczeck A, Langwasser J. Erste Erfahrungen mit der Hochfrequenzstromablation des AV-leitungssystems beim Menschen. *Z Kardiol* 1987;**76**:204–10.

53 Gepstein L, Hayam G, Ben-Haim SA. A novel method for nonfluoroscopic catheter-based electroanatomical mapping of the heart. *Circulation* 1997;**95**:1611–22.

54 Wittkampf FH, Wever EF, Derksen R, *et al*. LocaLisa: new technique for real-time 3-dimensional localization of regular intracardiac electrodes. *Circulation* 1999;**99**:1312–17.

55 Haïssaguerre M, Jaïs P, Shah DC, Takahashi A, Hocini M, Quiniou G, et al. Spontaneous initiation of atrial fibrillation by ectopic beats originating in the pulmonary veins. *N Engl J Med* 1998;**339**:659–66.

56 Moe GK, Rheinboldt WC, Abildskov JA. A computer model of atrial fibrillation. *Am Heart J* 1964;**67**:200–20.

57 Jalife J, Berenfeld O, Mansour M. Mother rotors and fibrillatory conduction: a mechanism of atrial fibrillation. *Cardiovasc Res* 2002;**54**:204–16.

58 Narayan SM, Krummen DE, Shivkumar K, Clopton P, Rappel W-J, Miller JM. Treatment of atrial fibrillation by the ablation of localized sources: CONFIRM (Conventional Ablation for Atrial Fibrillation With or Without Focal Impulse and Rotor Modulation) trial. *J Am Coll Cardiol* 2012;**60**:628–36.

59 Haïssaguerre M, Hocini M, Denis A, *et al*. Driver domains in persistent atrial fibrillation. *Circulation* 2014;**130**:530–8.

60 Zhang J, Sacher F, Hoffmayer K, et al. Cardiac electrophysiologic substrate underlying the ECG phenotype and electrogram abnormalities in Brugada syndrome patients. *Circulation* 2015;**131**:1950–9.

2

Embryology, Anatomy, and Pathology of Ventricular Outflow Tracts Related to Cardiac Mapping and Arrhythmias

Bastiaan J.D. Boukens[1], Cristina Basso[2], Federico Migliore[2], Stefania Rizzo[2], and Gaetano Thiene[2]

[1] *Department of Medical Biology, Academic Medical Center, Amsterdam UMC, Amsterdam, The Netherlands*
[2] *Department of Cardiac, Thoracic, and Vascular Sciences, University of Padua Medical School, Padova, Italy*

Summary

Ventricular arrhythmias, especially those of non-ischemic heart diseases, arise mostly from the outflows. Differences in embryonic origin and phenotype may account for arrhythmogenic propensity of right ventricular outflow tract (RVOT). The anatomy of the ventricles may be divided into inflow, apex, and outflow. As far as RVOT (pulmonary infundibulum) is concerned, it goes from the moderation band to the semilunar pulmonary valves. Since some myocardium extends distally from the "nadir" of the valve ring, arrhythmias may originate from the "pulmonary artery." This is true also on the aortic side, where the myocardium located within the coronary Valsalva sinuses may be the source of "aortic" arrhythmias. Arrhythmias with substrate from the RVOT may be genetically determined (arrhythmogenic cardiomyopathy), immune mediated (sarcoidosis) or infective (viral myocarditis), or form without substrate (idiopathic RVOT tachycardia). It is still controversial whether Brugada syndrome occurs in normal hearts or presents a substrate at the infundibular level.

Electroanatomical mapping plays a crucial role in establishing the existence of lacking electrical activity ("electric scars"), but it is unable to establish the precise nature of the underlying disease. Endomyocardial biopsy in this setting is the gold standard for diagnosis.

Introduction

Sudden cardiac death accounts for 300 000 deaths per year in the USA [1] and up to 5% are due to arrhythmias related to genetic abnormalities [2]. Many of these arrhythmias originate in the right ventricle (RV) and, in particular, the right ventricular outflow tract (RVOT) [3,4]. Although the mechanisms underlying these arrhythmias have been thoroughly investigated over the last 15 years, several aspects remain insufficiently understood. In particular, it is still unclear why the RVOT is the preferential site of origin of these arrhythmias. Animal studies show that during embryonic heart development, the RVOT forms from the embryonic outflow tract (OFT) [5] which, in contrast to the developing ventricles, has slow-conducting properties [6]. The OFT is in turn derived from a pool of cardiac precursor cells that differs from those of the left ventricle (LV) [7]. The differences in embryonic origin and phenotype between the LV and RV may provide insight into the arrhythmogenic nature of the RVOT [8].

Development of the outflow tract

Early development of the embryonic outflow tract

Studies in mice and chickens have shown that the heart forms from a pool of cardiac precursor cells located in a crescent-shaped field. The heart field can be divided into progenitor cells, that are located laterally in the embryo and differentiate early into myocardium (referred to as the first heart field) [7], and cells that are located medially and caudally and differentiate later during cardiac development (referred to as the second heart field).

The cells from the first heart field fuse at the midline and form a tube. This early heart tube is composed of primary (embryonic) myocardium and has an inflow tract and an OFT interconnected at the dorsal side by the fusing mesocardium. The early heart tube grows by recruitment of progenitor cells of the second heart field, which are added at the inflow tract, OFT, and dorsal mesocardium. During this elongation phase, the heart tube loops and ventricular working myocardium differentiates at the ventral side and atrial working myocardium at the dorsal side of the tube [9]. The chambers expand by rapid proliferation of the differentiating myocytes, whereas the parts flanking the chambers, the atrioventricular (AV) canal, the OFT, and the inner curvature, neither proliferate nor expand, and do not differentiate into working myocardium [9].

The LV starts to differentiate first, followed by the RV, which differentiates and expands cranially of the LV.

Cardiac Mapping, Fifth Edition. Edited by Mohammad Shenasa, Gerhard Hindricks, David J. Callans, John M. Miller, and Mark E. Josephson.

Companion website: www.wiley.com/go/cardiacmapping5e

Because these structures are formed subsequently, the progenitor cells of these three compartments have a different developmental history and have been exposed to different signals and gene programs prior to their differentiation [10]. In the embryonic heart, the OFT extends at the outer curvature from the RV to the pericardial cavity and at the inner curvature from the LV (here connected to the AV canal) to the pericardial cavity. At this stage, the OFT myocardium still retains its primary myocardial phenotype – slow conduction and low contractility – while the LV and RV acquire the working myocardial phenotype – fast conduction and high contractility (Figure 2.1).

Transition from embryonic outflow tract to left and right ventricular outflow tracts

Since the embryonic OFT is commonly defined as the tubular structure connecting the embryonic RV with the pericardial deflection, its cell composition changes immensely over time. This is because during development, cells from the pharyngeal mesoderm pass through the embryonic OFT towards the RV, enabling ventricular growth [11]. At 28–32 days of human development (embryonic), the OFT fully consists of myocardial cells. Further in development, the distal part will become composed of non-myocardial

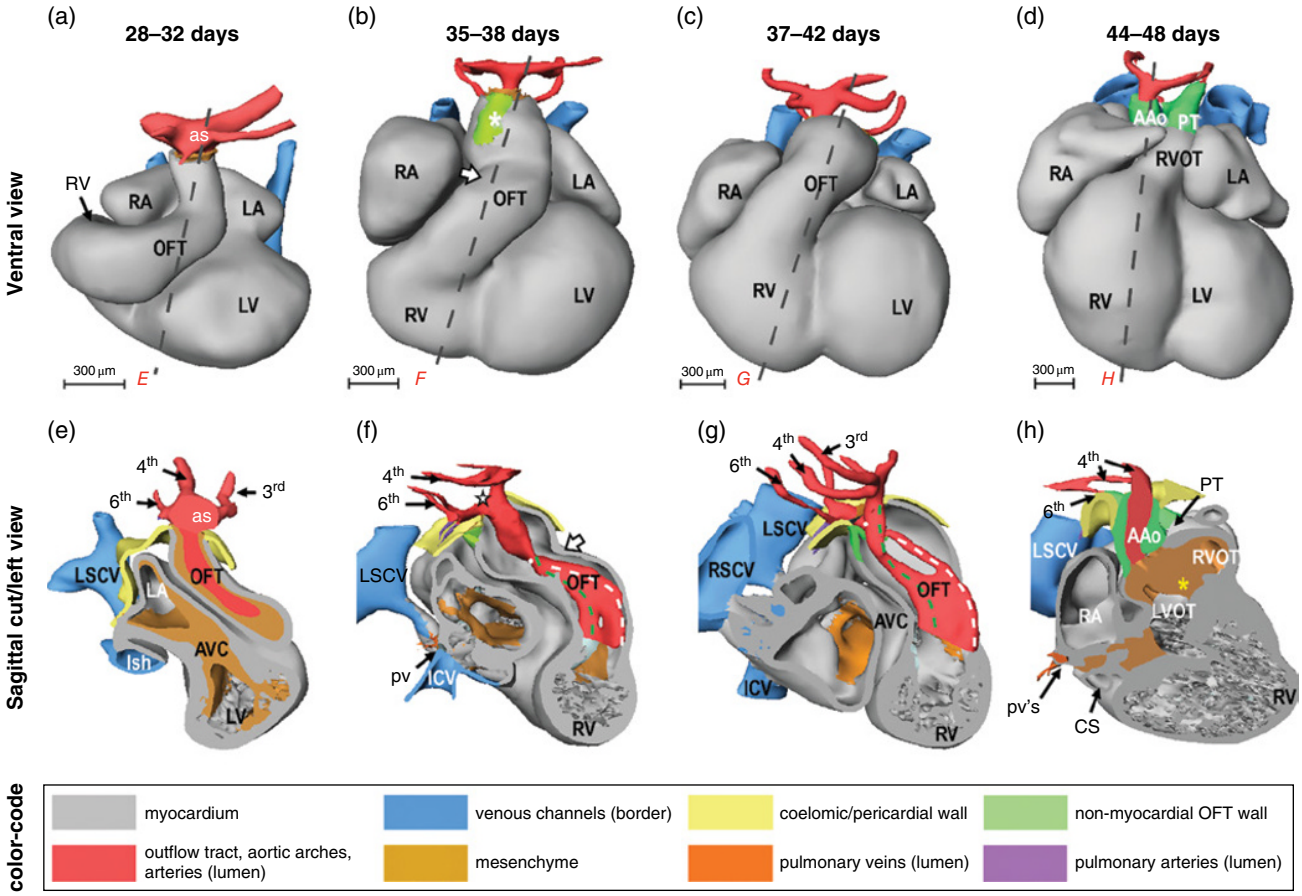

Figure 2.1 The developing outflow tract of the human heart. (a) At this stage the myocardial outflow tract (OFT), connecting the right ventricle with the aortic sac (as), is tubular. The 3rd, 4th, and 6th aortic arches originate directly from the aortic sac. (b) The intrapericardial mesenchymal tissue forming the column-like structures at the ventral and dorsal aspects of the distal outflow tract (asterisks in (a)). (c) The muscular outflow tract has further shortened, and the mass of the right ventricle is ventrally recognizable. The extrapericardial portions of the perpendicularly oriented ascending aorta and pulmonary trunk are separated from each other by mesenchymal tissue. (d) The myocardial outflow tract has further shortened, along with formation of the right ventricular infundibulum (RVOT). The intrapericardial ascending aorta and pulmonary trunk now possess their own discrete non-myocardial walls. The arrows in (b) and (f) point to the characteristic bend of the myocardial outflow tract, dividing it into proximal and distal parts. Dotted lines in (f) refer to the spirally oriented channels in the proximal outflow tract connecting the unseptated distal outflow tract with the right ventricle (*white line*) and the primary interventricular foramen (*green line*). (g) The relations between the developing ascending aorta and pulmonary trunk (*white and green dotted lines, respectively*) now resemble the situation seen in the formed heart. The asterisk in (h) refers to the myocardializing mesenchyme between the ventricular outflow tracts. *Source:* Modified from Sizarov et al. [12] with permission of John Wiley & Sons. AVC, atrioventricular canal; e/tr, (undivided) developing esophagus and trachea; LA/RA, left/right atrium; LSCV, left superior cardinal vein; lsh, left sinus horn; LV/RV, left/right ventricle; SV, sinus venosus; pv, pulmonary vein; tr, trachea; cs, coronary sinus.

cells, which will later, after septation, give rise to the intrapericardial aortic and pulmonary components [12,13]. The proximal part of the embryonic OFT will ventricularize and be incorporated into the ventricular free wall and form the left ventricular outflow tract (LVOT) and RVOT, respectively.

Thus, the RVOT and LVOT have a common origin, which may point to a common mechanism underlying outflow tract arrhythmias. Interestingly, however, the inferior part of the embryonic OFT gives rise to the subpulmonary myocardium (corresponding to the RVOT), and the superior part to the subaortic myocardium (corresponding to the LVOT). These two parts show differential gene expression (e.g. inferior part expresses *Sema3C*) and the subpulmonary myocardium is specifically affected and possibly largely absent in Tbx1 mutant mice [14]. Therefore, the RVOT and LVOT are not molecularly identical, but both are different from the LV and RV. The RVOT and LVOT acquire the working myocardial phenotype just before birth [15].

Developmental basis for RVOT arrhythmias

Electrophysiological characteristics of the RVOT

Conduction in the myocardium depends on the availability of sodium (Na^+) channels (encoded by *SCN5A*) and intercellular electrical coupling by gap junctions, which are formed by connexin (Cx) subunits. In the developing human working myocardium, the expression of *SCN5A*, *CX40*, and *CX43* is high [16], which results in relatively fast conduction (±20 cm/s) [6]. In the embryonic OFT, however, the expression of *SCN5A* is low and the expression of *Cx40* and *Cx43* is absent, resulting in slow conduction (±1–5 cm/s) [6]. Accordingly, myocytes isolated from the embryonic OFT have a slower upstroke velocity and a less depolarized resting membrane potential than myocytes from the RV or LV [17,18].

During the fetal stage of development, the embryonic OFT is fully incorporated into the RV myocardium and forms the RVOT and LVOT. In the fetal RVOT, conduction is faster (±5–10 cm/s) than in the embryonic OFT (±1–5 cm/s). However, it still remains slower than in the working myocardium (±40 cm/s) [15]. The expression of *Cx43* is maintained in the ventricles, but remains absent from the RVOT. In the adult heart, the *Cx43*-negative myocardium only remains present just below the pulmonary valves, thereby resembling the ring of primary myocardium that is present at the entrance of the RV and LV [19,20]. Primary myocardium is spontaneously active and is often, although incorrectly, referred to as nodal myocardium. These primary myocardial cells could give rise to spontaneous activity.

In the adult heart, the expression of Cx43 is lower in the RVOT than in the remainder of the heart. Despite this, the conduction velocity in the adult RVOT is not slower than in the remaining RV (±40 cm/s in both). The low expression of *Cx43* and *SCN5A* in the RVOT, however, indicates a lower safety factor [21] for conduction than in the RV. Indeed, when the safety factor of cardiac conduction is decreased pharmacologically (sodium channel blockade) or genetically (heterozygous mutation in *SCN5A*), conduction becomes slower in the RVOT than in the RV or LV [15]. This suggests that, at least in mice, this aspect of the slowly conducting embryonic OFT is retained in the free wall of the adult RVOT (Figure 2.2).

Predisposition of the RVOT to arrhythmias

Arrhythmias originating predominantly in the RVOT include idiopathic outflow tract tachycardia, Brugada syndrome, and, to a lesser extent, arrhythmogenic cardiomyopathy. Arrhythmias in these cardiac pathologies usually do not occur at a pediatric age but rather in young adulthood, indicating that postnatal development and maturation play an important role in disease development. The electrophysiological characteristics of the RVOT, however, develop prenatally and are different from those of the LV and RV [15]. The developmental history and phenotype of the RVOT are not intrinsically arrhythmogenic, but may predispose to arrhythmias in the setting of an active pathological mechanism that progresses during life.

Brugada syndrome

The Brugada syndrome is characterized by ST segment elevation in the right precordial leads and highly fractionated local electrograms in the RVOT and ventricular arrhythmias [22–26]. The mechanism underlying these characteristics is debated, but evidence supporting conduction delay or block as a potential mechanism is accumulating. In 20–30% of Brugada syndrome patients, a loss of function mutation in *SCN5A* has been found [24]. A reduction in the Na + current itself, however, does not lead to Brugada characteristics [26a]. In contrast, reducing the Na + current is used to discriminate between patients who have Brugada syndrome and those who do not [24]. In patients with Brugada syndrome, subtle, small structural discontinuities have been demonstrated in the RV free wall and RVOT [23,27,28]. Experimental and clinical studies have shown that conduction can be delayed in the myocardium with small structural discontinuities or even be blocked by a mechanism called current-to-load mismatch [29,30]. Conduction block is a prerequisite for reentry and may generate a substrate for reentrant-based arrhythmias as seen in Brugada syndrome patients [27].

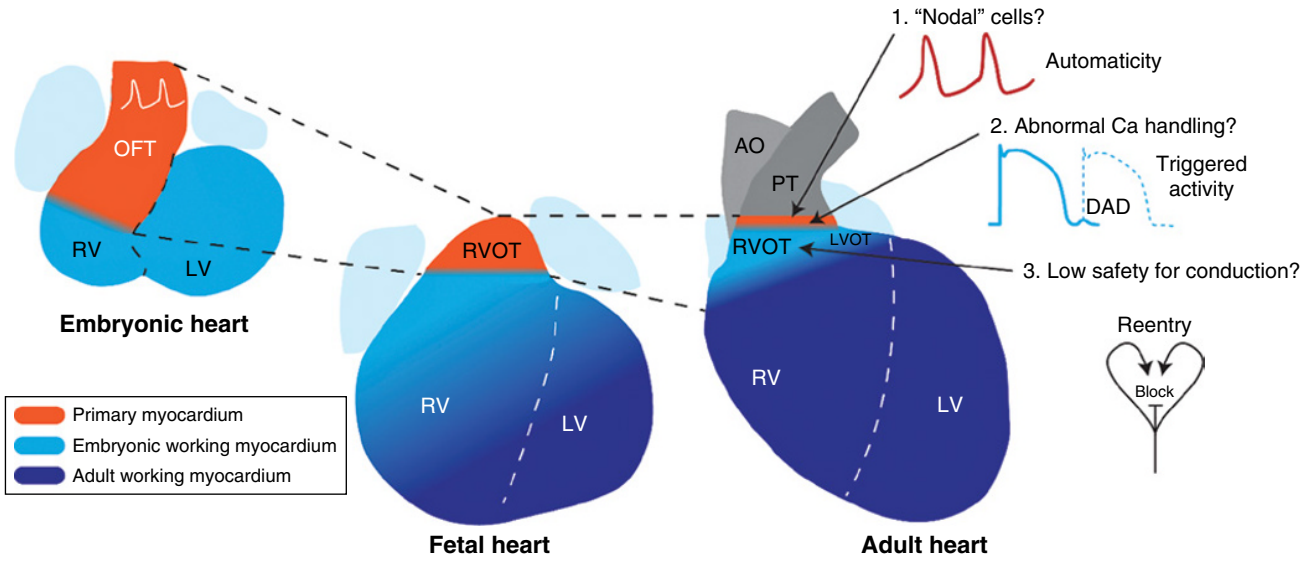

Figure 2.2 Developmental basis for RVOT arrhythmias. The adult RVOT has formed from the embryonic outflow tract (*left*), which is composed primarily of the myocardium exhibiting slow conduction and spontaneous activity. During development, the embryonic outflow tract acquires a working myocardial phenotype, e.g. fast conduction, and transforms into the RVOT. A small ring of primary myocardium, however, still remains just below the pulmonary valve which may give rise to automaticity as seen in patients with idiopathic RVOT tachycardia. The myocardium of the free wall and septum of the adult RVOT has a working myocardial phenotype, although expression of *Cx43* and *SCN5A* is lower than in the right ventricle. This may set the stage for reentrant-based arrhythmias as seen in patients with the Brugada syndrome. LV, left ventricle; OFT, outflow tract; RV, right ventricle; RVOT, right ventricular outflow tract.

In addition, conduction delay or block can cause ST segment elevation on the body surface electrocardiogram (ECG), which is a hallmark of Brugada syndrome [31,32].

Although a unifying mechanism explaining arrhythmias in Brugada syndrome patients has been proposed [32], it does not offer an explanation for the preferential location of these arrhythmias in the RVOT. We thus surmise that genes of the ventricular working myocardial genetic program are less active in the RVOT, resulting in a reduced safety of conduction, thereby facilitating current-to-load mismatch and subsequently arrhythmias. Indeed, lower expression of Cx43 protein has been found in the epicardial region of the RVOT when compared to the RV in patients with Brugada syndrome [33].

Idiopathic outflow tract tachycardias

The mechanism underlying idiopathic RVOT tachycardias is, by definition, unknown. However, these arrhythmias are catecholamine sensitive, suggesting automaticity or triggered activity as an underlying mechanism. Indeed, idiopathic arrhythmias can be treated with adenosine or beta-blockers [4]. A subset of myocytes in the RVOT have long action potentials, do not depolarize fully to the resting membrane potential, and easily develop early afterdepolarizations [34]. This electrophysiological phenotype is expected from the primary ring myocardium that is present just below, and above, the valves of the pulmonary artery. These primary myocytes may, in the presence of structural changes or uncoupling, give rise to spontaneous activity [19,35]. Consistently, ectopic beats in the RVOT are reported to originate from the myocardium just below the pulmonary valve and even from myocardial sleeves in the pulmonary artery [36,37]. For the moment, however, the direct relation between these primary cells and idiopathic RVOT tachycardia remains elusive and further research is required to determine a causal relation.

Anatomy of the right ventricle

The RV is the chamber between the tricuspid AV valve and pulmonary semilunar cusps, located anteriorly and right sided, just underneath the sternum. When seen from outside, it is easily identifiable, being located on the right between the anterior and posterior interventricular grooves, where the anterior and posterior descending coronary arteries and great cardiac vein and middle cardiac vein run, respectively. The shape is triangular, with the base corresponding to the AV sulcus and the pulmonary valve orifice, and the apex distally.

The RV is a coarse trabeculated chamber, which may be divided in three parts: inflow, apex, and outlet (Figure 2.3). The inflow corresponds to the part which hosts the tricuspid valve apparatus, from the AV ring to the base of papillary muscles. The outlet, known also as the pulmonary infundibulum, is the part of the RV which goes from the moderator band and the sigmoid pulmonary valves. The apical segment is what remains distally up to the apex.

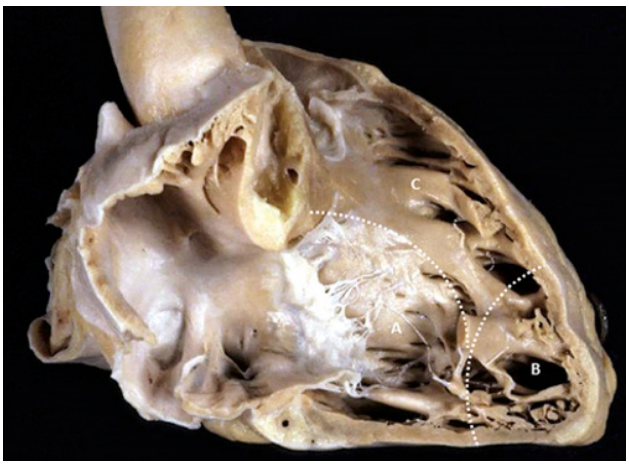

Figure 2.3 The tripartite, coarsely trabeculated right ventricle. A, Inflow, hosting the tricuspid valve. B, Apex. C, Outflow from the moderator band to the pulmonary valve.

Tricuspid valve

The tricuspid valve is a complex valvular structure which, despite being called AV because it is interposed between the atrium and ventricle, is a ventricular structure like the mitral valve, both anatomically and embryologically. It consists of three leaflets (tri-cuspid). The base of the septal leaflet is attached to the septal AV junction and goes from the anteroseptal to the posteroseptal commissures. The anteroseptal commissure corresponds to the area of the membranous septum and is indicated by fan-like chordae tendinae originating from the so-called Lancisi (conal) papillary muscle attached to the ventricular septum. The posteroseptal commissure is indicated by fan-like chordae arising from the group of posterior papillary muscles. A peculiar feature of the tricuspid valve consists in the attachment of the septal leaflet to the ventricular septum by chordae tendinae, directly or mediated by tiny papillary muscles.

The anterior leaflet is a large curtain in between the anteroseptal and anteroposterior commissures. The latter is indicated by the anterior papillary muscle, a long pillar from the tip of which chordae tendinae arise to join both the anterior and posterior leaflets, including the fan-like chordae for the anteroposterior commissure. The base of the anterior leaflet is attached to the AV ring of the anterior free wall. The difference between the anterior mitral valve leaflet and the anterior leaflet of the tricuspid valve is that the latter is not in fibrous continuity with the pulmonary semilunar cusps, because of the crista supraventricularis, a muscular structure wedged in between and consisting of septal and parietal components. This big structure, hanging over the RV, accounts for the anterior position of the RVOT when compared to the LVOT. The posterior leaflet of the tricuspid valve is attached to the ring of the posterior AV sulcus, from the acute margin to the crux cordis, and delimited by the anterolateral and posteroseptal commissures. Seen from outside, the acute margin of the heart roughly indicates the border between the anterior and posterior RV free walls and anterior and posterior leaflets. It corresponds to the anteroposterior commissure of the tricuspid valve.

The tricuspid valve commissures, defined as the boundary between two leaflets where the distance from the free margin to the AV ring is shorter, show leaflet continuity. However, anteroseptal commissure discontinuity is seen in 20–30% of cases so that the underlying membranous septum appears bare. This facilitates intracavitary recording of His bundle electrical activity as well as ablation to achieve iatrogenic AV block when necessary [38].

Tricuspid valve leaflets exhibit first-order chordae, attached to the free margin, and second-order chordae attached to the ventricular surface (rough zone of the leaflets), anchoring the subvalvular apparatus (so-called strut chordae). Third-order short chordae arise close to the basal attachment of the mural leaflets (anterior and posterior), as seen in the mitral valve.

Right ventricular outflow tract

The outlet part of the RV corresponds to the embryonic "conus" or bulbus cordis, so-called because of its conical shape (Figure 2.4). It starts proximally from the moderator band, a peculiar muscular bundle originally described by Leonardo da Vinci in his outstanding anatomical pictures (Figure 2.5). Leonardo employed the adjective "moderator" due to the alleged function to restrain the action of the anterior papillary muscle of the tricuspid valve, anchoring its base to the ventricular septum. It connects the anterior papillary muscle of the tricuspid valve to the septal band. Together, they are known as the trabecula septomarginalis or septomarginal band. The septal band, namely the septal part of the trabecular septomarginalis, is a prominent, distinct structure of the right-sided surface of the ventricular septum and represents a landmark of the RV (see Figure 2.4). The right bundle branch runs under the subendocardium and, when reaching the moderator band, divides with a distinctive branch coursing along the anterior papillary muscle of the tricuspid valve. The proximal part of the septal band, at the level of the Lancisi (conal) muscle, divides into two limbs, one anterior and one posterior, with a sling configuration, hosting the septal branch of the crista supraventricularis. The anterior wall of the pulmonary infundibulum may show thick trabeculae originating from the ventricular septum (septoparietal bands), different from the parietal band of the crista (see Figure 2.4).

There are three semilunar cusps (anterior, postero-right, and postero-left) within the sinuses of Valsalva and separated by commissures. The cusps are attached to the

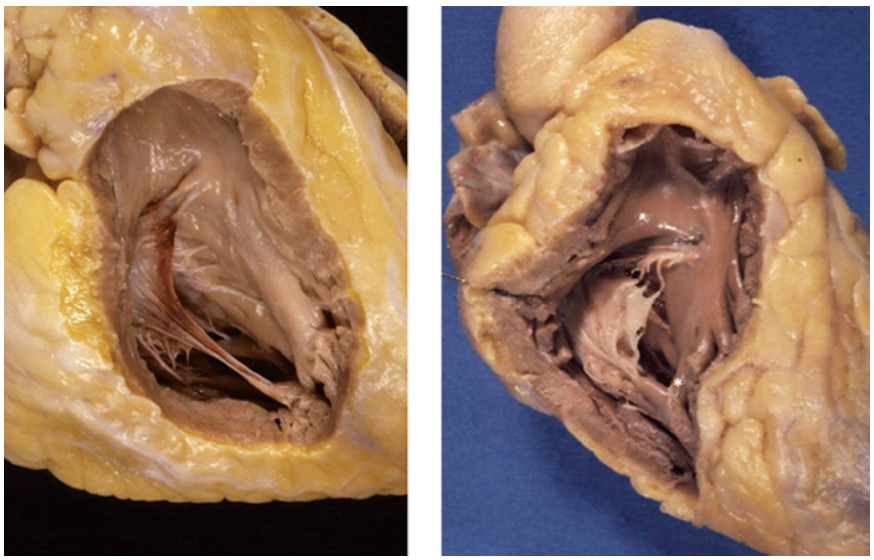

Figure 2.4 The outflow tract of the right ventricle from the moderator band to the pulmonary valve.

(a) (b)

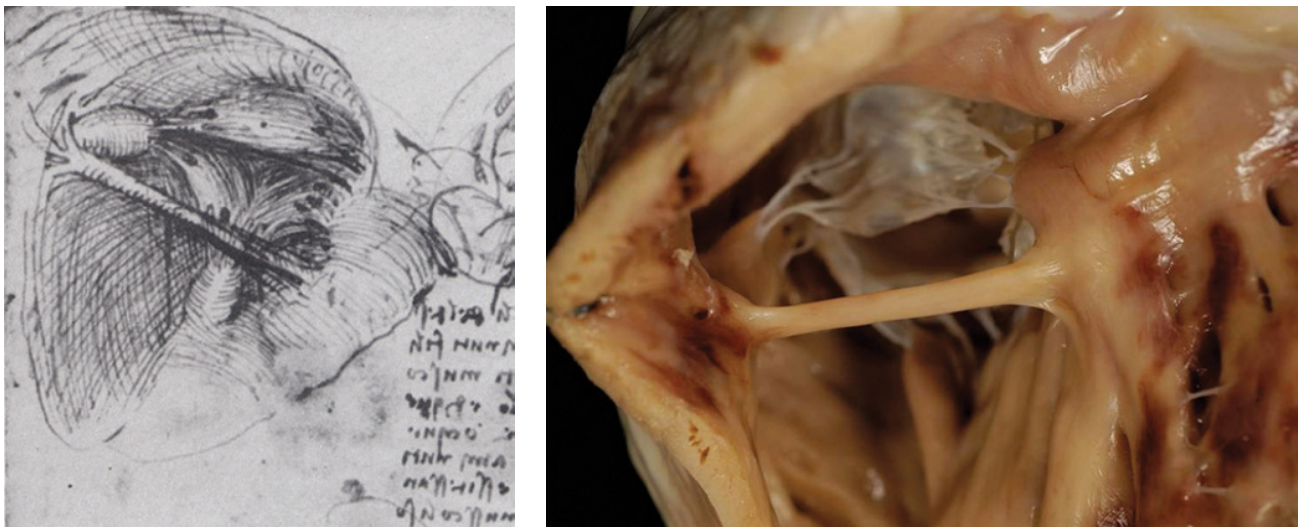

Figure 2.5 (a) Original drawing of the moderator band by Leonardo da Vinci. (b) The same in an ovine heart.

pulmonary wall, which is an essential part of the valve apparatus. Overall, they show a crown-shaped ring and lie over the infundibular myocardium (Figures 2.6, 2.7). The latter regularly extends over the ring, so the myocardium of the RV is located beyond the hemodynamic ventriculoarterial boundary (see Figure 2.7). This explains the apparent paradox of arrhythmias originating from the pulmonary artery. Indeed, the pulmonary root is higher than the aortic root. Thus, the infundibular septum (namely, the septal band of the crista supraventricularis) separates the pulmonary infundibulum from the sinus portion of the aorta, like a ventriculoarterial septum (Figures 2.8, 2.9). Thus, the infundibular septum is within the sinus portion of the aorta, seen from the left side. This may explain "aortic" arrhythmias, originating from the aortic side of the infundibular septum.

The myocardium of the RV free wall is 3–4 mm thick in the normal adult, with a variable amount of fatty tissue infiltrating the subepicardial layer. In obese people, an extensive lipomatous infiltration may be observed ("adipositas cordis"), equivalent to the subcutaneous adipose tissue. This should not be confused with the fibrofatty replacement of arrhythmogenic cardiomyopathy [39].

Anatomy of the left ventricle

The LV is a posterior chamber between the mitral and aortic valves. Seen from the outside with an epicardial view, it may be easily identified on the left side of the heart, between the anterior and posterior descending coronary arteries, which run in the anterior and posterior

interventricular grooves, respectively. The shape of the cavity is oval with inflow and outflow tracts separated by the anterior (aortic) mitral leaflet (Figure 2.10). The LV may be divided into three parts: inlet, apex, and outlet.

The inflow contains the left AV apparatus, which consists of two leaflets, chordae tendinae, and two groups of papillary muscles. The shape of the mitral valve apparatus mimics a bishop's miter, thus explaining why Andreas Vesalius coined the term "mitral." The anterior leaflet is a large curtain receiving chordae from both anterolateral and posteromedial papillary muscles. It is deeper and narrower than the posterior one. It is in fibrous continuity with the aortic valve (all posterior and part of the left coronary cusps), and is not inserted into the AV ring (Figure 2.11). The posterior ("mural") mitral leaflet is larger and less deep than the anterior but the areas of both are almost equal. It is attached to the AV ring, which provides discontinuity between the atrial and ventricular myocardium. The posterior leaflet usually consists of three scallops, separated by commissural-like indentations, known as "cleft commissures," marked by fan cleft-like

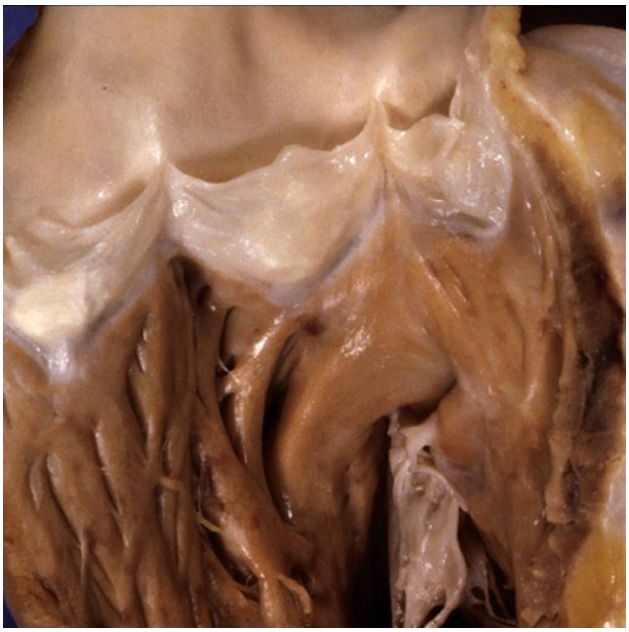

Figure 2.6 Close-up of the pulmonary infundibulum (right ventricular outflow tract). Note the Lancisi muscle: the crista supraventricularis with parietal and septal bands. All of the pulmonary semilunar cusps lie over musculature.

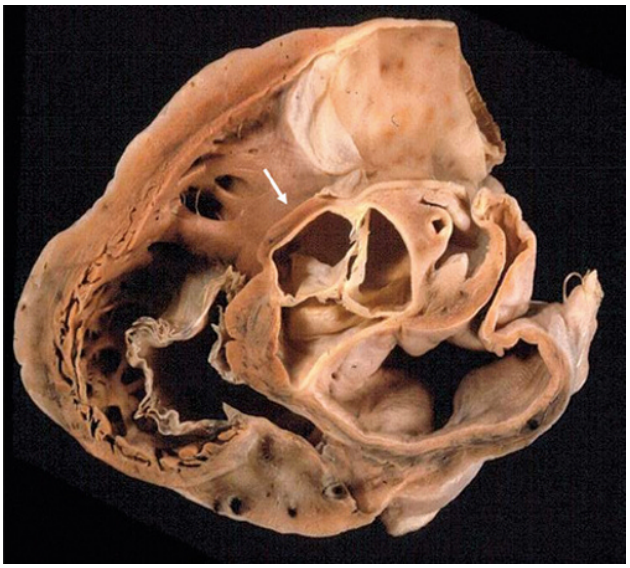

Figure 2.8 Basal short axis section of a cardiac specimen. The right and left outflow tracts are crossing over. Arrow indicates the so-called infundibular septum (septal band of crista supraventricularis) separating the subvalvular pulmonary outflow from the supravalvular right aortic sinus.

Figure 2.7 (a) Pulmonary arterial root: all the cusps are attached to muscle. (b) Histology of the postero-left pulmonary semilunar cusp: the myocardium is well over the basal ring (hemodynamic border between the ventricular and pulmonary artery), and may be the source of "pulmonary" arrhythmias.

(a)

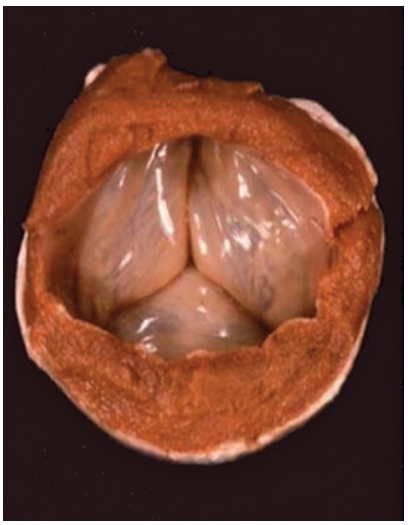

(b)

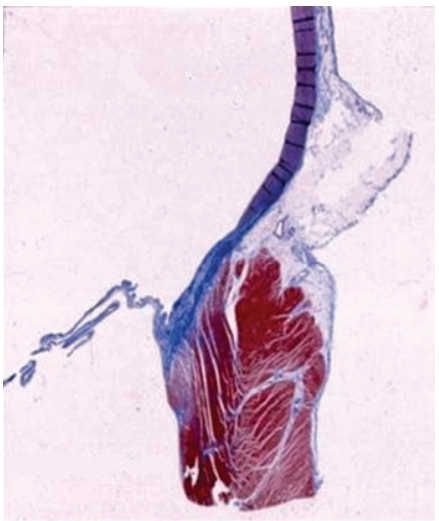

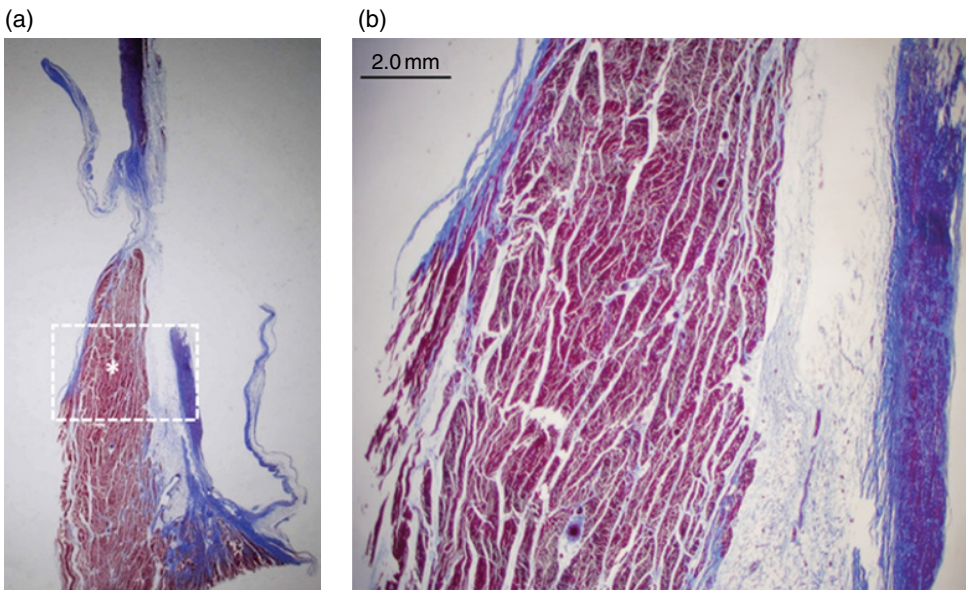

Figure 2.9 (a) Long axis view of the ventricular outflow tract. Asterisk indicates the "infundibular septum" separating the subpulmonary infundibulum from the right aortic sinus. (b) Histology of the "infundibular septum," located just in front of the right aortic sinus. Access for ablating outflow tracts arrhythmias may be through the aorta.

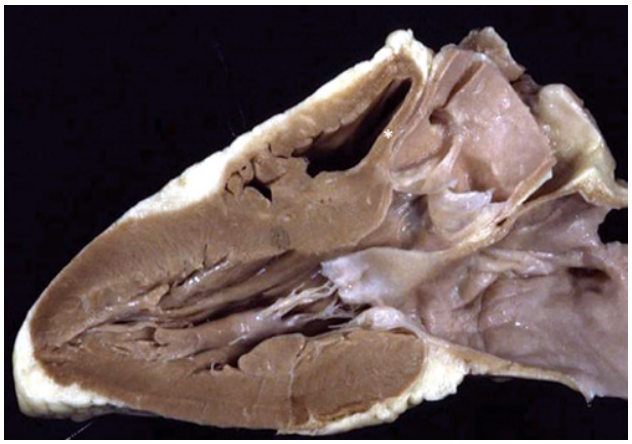

Figure 2.10 Left ventricle in a long axis view. Note the inflow hosting the mitral valve, the apex with thin trabeculations, and the outflow tract corresponding to the smooth basal ventricular septum. Note the anterior (aortic) leaflet of the mitral valve separating the inflow from the outflow tract. The asterisk indicates the "infundibular" septum separating the pulmonary outflow tract from the sinus portion of the aorta.

chordae taking origin from the tips of the posteromedial papillary muscle. The anterolateral papillary muscle, which consists of a single pillar, is different from the posteromedial, which consists of two or more pillars with several tips to support the wider leaflet. The anterolateral and posteromedial commissures represent the boundary between the leaflets, where they approximate each other but still keep in continuity. The commissures are well indicated by fan-like chordae arising from the apex of the

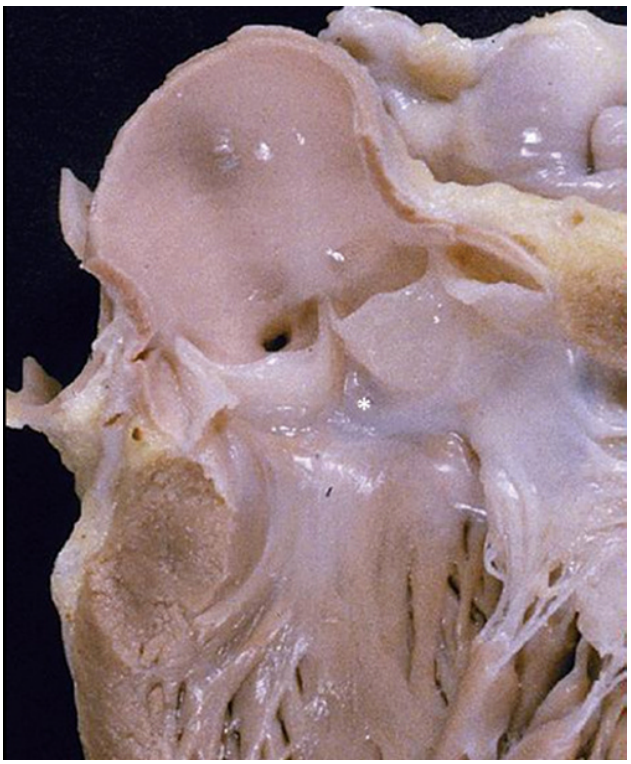

Figure 2.11 The left ventricular outflow tract. Note the mitral valve free from attachment to the ventricular septum, the membranous septum (*) in between the right and non-coronary cusps. The latter and partially the left are in fibrous continuity with the anterior ("aortic") leaflet of the mitral valve. Note the smooth basal part of the ventricular septum.

papillary muscle pillars or tips. The chordae tendinae consist of three orders: the first order is attached to the free margin of the leaflet, the second order is attached to the ventricular surface (rough zone), and the third order arises from the posterolateral free wall (mediated or not by tiny papillary muscles), anchoring the posterior leaflet close to the AV ring. Some of the second-order chordae to the anterior (aortic) leaflet are particularly long and thick and act as strut chordae to sustain the systolic closure of the mitral valve at high pressure.

The apical portion of the LV consists of tiny trabeculae and a thinner wall (see Figure 2.10). It usually forms the apex of the heart, although a bifid apex from both the RV and LV is not a rare occurrence.

The LVOT is posterior and inferior to the RVOT. They cross each other, with the anterosuperior right one running from right to left and the posteroinferior left one running from left to right.

Because of the discontinuity between the tricuspid and pulmonary valves by the crista supraventricularis, the pulmonary root is superior and to the left and the aortic root inferior and to the right.

The LVOT is wedged between the ventricular septum (anterosuperiorly) and the aortic mitral leaflet (posteroinferiorly). Here, the septum is smooth without a septal band. At difference from the RVOT, which starts from the moderator band, it is hard to establish a landmark origin of the LVOT. We might mark it in the border between the smooth and the trabecular parts of the left side of the ventricular septum, which corresponds to the free margin of the anterior (aortic) mitral leaflet in diastole. The length of the LVOT varies according to the cardiac phases. It is long and tubular during diastole at the opening of the anterior (aortic) mitral leaflet and much shorter during systole, when the anterior leaflet moves posteroinferiorly to close the mitral orifice and stick with the posterior leaflet. No muscular structure, such as the crista supraventricularis of the RV, is interposed in between the aorta and the mitral valve (see Figure 2.11). An anterolateral muscle band, variable in thickness, is located between the ventricular septum and the anterior leaflet of the mitral valve, just underneath the left coronary cusp.

The aortic valve apparatus is housed within the sinus portion of the ascending aorta (sinuses of Valsalva). The aortic valve is tricuspid (see Figure 2.11) and consists of:

- a posterior, non-coronary sigmoid cusp, which is in fibrous continuity with the anterior (aortic) leaflet of the mitral valve
- a left coronary cusp, in continuity with both the anterior mitral leaflet and the anterolateral muscle band
- an anterior right coronary cusp, lying over the myocardium of the ventricular septum.

Compared to the pulmonary valve, which is entirely over the myocardium of the pulmonary infundibulum, the aortic valve attaches either to the septal and anterolateral myocardium or to fibrous tissue of the aortic-mitral continuity (Figure 2.12). The aortic ring is crown-shaped with intercuspal triangles, their apex representing the commissures, namely the highest attachment of the cusps to the aortic wall (see Figure 2.11).

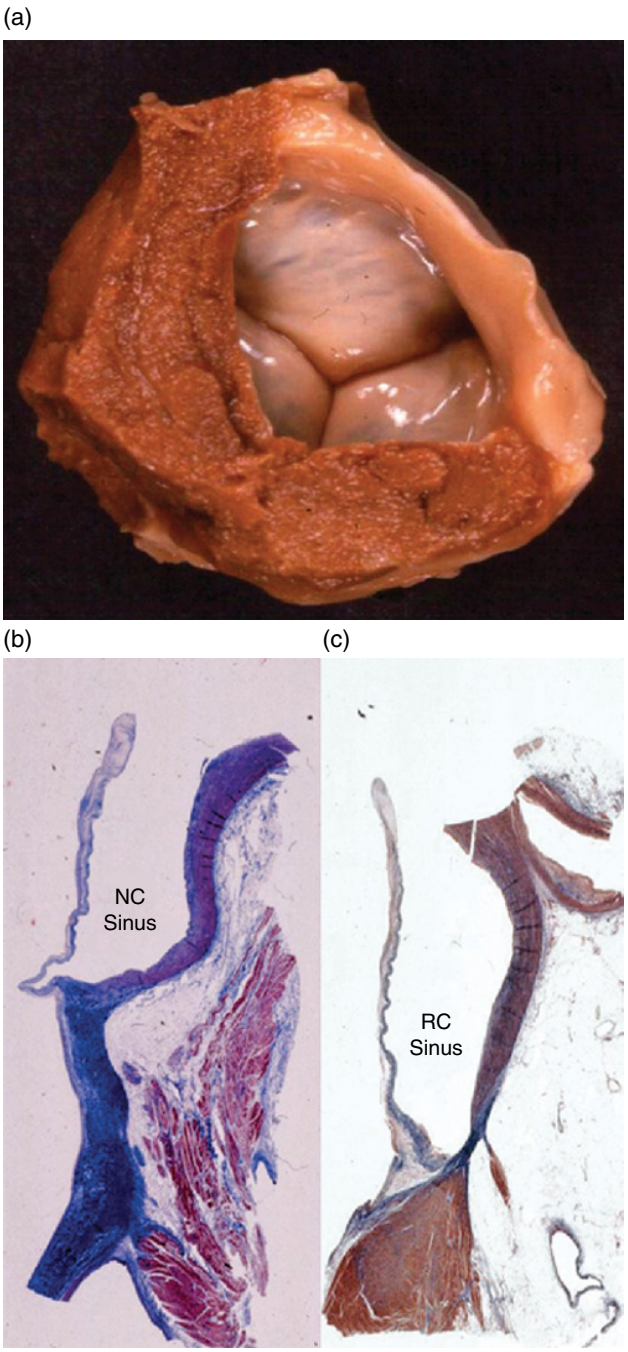

Figure 2.12 (a) Aortic root: the whole non-coronary cusp and part of the left coronary cusp are in fibrous continuity with the mitral valve, whereas the entire right coronary and part of the left coronary cusp are attached to muscle. (b) Histology of the mitro-aortic fibrous continuity. (c) Histology of the right coronary sinus with ventricular septal myocardium over the valve ring. NC, non-coronary; RC, right coronary.

Compared to the mitral valve leaflets, which are still in continuity at the commissures, both the pulmonary and aortic semilunar cusps are in discontinuity at the commissural level.

Atrioventricular conduction system and ventricular outflow tracts

The axis of the AV conduction, the specialized structure joining the atria to the ventricles, is topographically related on the right side to the inflow and on the left side to the outflow [38]. The AV node is located on the right side of the atrial septum within the so-called triangle of Koch, in front of the opening of the coronary sinus. The His bundle penetrates the central fibrous ring at the apex of the Koch triangle and runs underneath the membranous septum over the crest (or on the left) of the ventricular septum, and then divides into right and left bundle branches. The right bundle branch at the level of the Lancisi (conal) septum turns down with either a subendocardial or, more frequently, an intramyocardial course. The left bundle branch spreads out like a sheet in the subendocardium of the left side of the ventricular septum, subdividing into anterior and posterior fascicles. Because of the crista supraventricularis, the His bundle is not exposed to the RVOT whereas it is an intrinsic part of the LVOT. When seen from above (aorta), the commissure in between the non-coronary and right aortic cusps is a landmark, being located just above the His bundle. The distance between the aortic surgical ring (the so-called cusp "nadir") and the His bundle in the adult is about 3–5 mm (Figure 2.13).

Pathology of non-ischemic arrhythmias from the ventricular outflow tract

Most of the tachyarrhythmias arising from the ventricular outflow have a substrate, accounting for triggered activity or reentry circuits, and are mostly non-ischemic. More rarely, the culprits are merely functional disorders, including ion channel diseases. Differential diagnosis between the two entities (organic versus functional) may be pursued *in vivo* with the help of tissue characterization imaging tools and endomyocardial biopsy, which still remains the gold standard in some patients. The latter tool is in fact able to detect histological or ultrastructural abnormalities like inflammation, fibrosis, necrosis or adipose tissue, storage disease or infiltrative interstitial deposits.

(a)

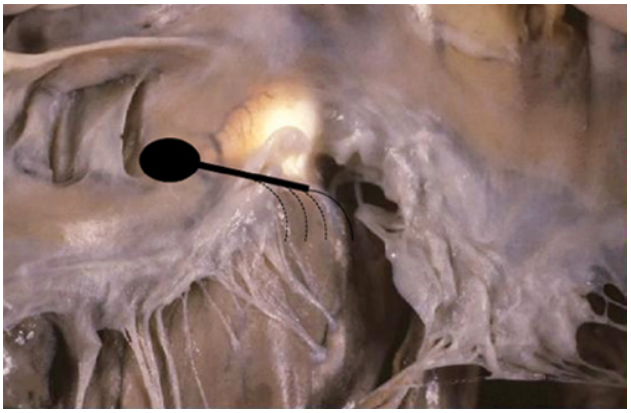

(b)

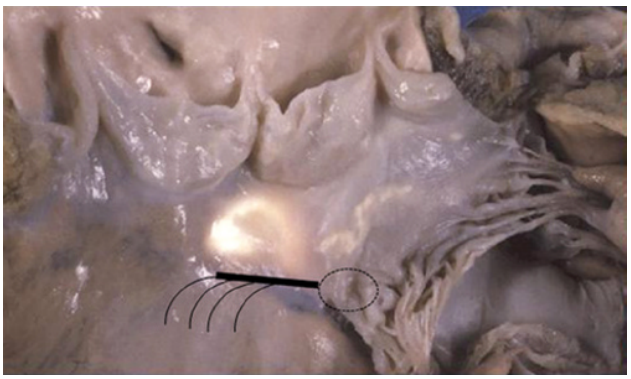

Figure 2.13 The AV conduction system, which is mostly exposed to the left ventricular outflow tract, in a tight relationship with the membranous septum. (a) View from the right side. (b) View from the left side.

Non-ischemic arrhythmic substrates of the RVOT

Arrhythmogenic cardiomyopathy

Arrhythmogenic cardiomyopathy is heredo-familial disorder due to mutations of genes encoding cell junction proteins (desmosome), characterized by a pathognomonic substrate, namely fibro-fatty replacement of the ventricular myocardium (Figures 2.14, 2.15) [40–43].

Originally believed to be confined to the RV and featured by ventricular arrhythmias with left bundle branch morphology, it has been recently recognized as biventricular cardiomyopathy or even involving only the LV with isolated non-ischemic scars and polymorphic ventricular arrhythmias. Nowadays, the original term arrhythmogenic RV cardiomyopathy has been replaced with arrhythmogenic cardiomyopathy.

Ventricular electrical instability is high, which explains the propensity to sustained ventricular tachycardia/fibrillation with cardiac arrest, mostly occurring during effort. It has been well demonstrated, in both human and animal models, that it is a genetically determined

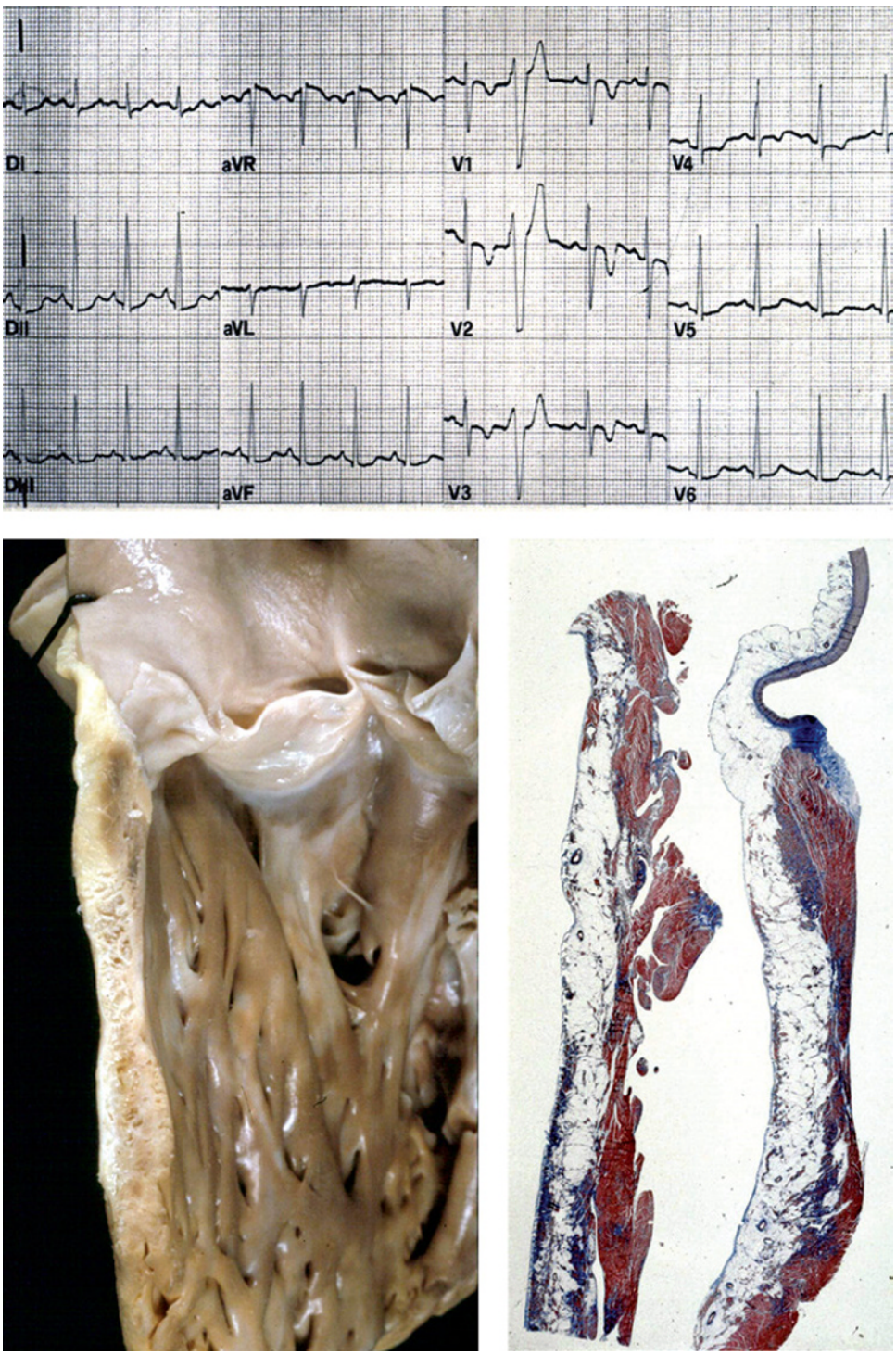

Figure 2.14 Arrhythmogenic cardiomyopathy with fibro-fatty replacement of the right ventricular outflow tract. The ECG shows inverted T waves in the precordial leads and an apparently innocent premature ventricular beat.

cardiomyopathy, with onset and progression of myocyte death and fibro-fatty replacement occurring during childhood, adolescence, and adulthood. Since loss of the myocardium begins after birth, arrhythmogenic cardiomyopathy cannot be considered a congenital heart disease (defect present at birth). The phenomenon of cell death, with fibro-fatty replacement as a consequence of repair, starts from the epicardium. In the RV it extends progressively deeper into the endocardium like a wave front phenomenon, so it is reachable by the bioptome at

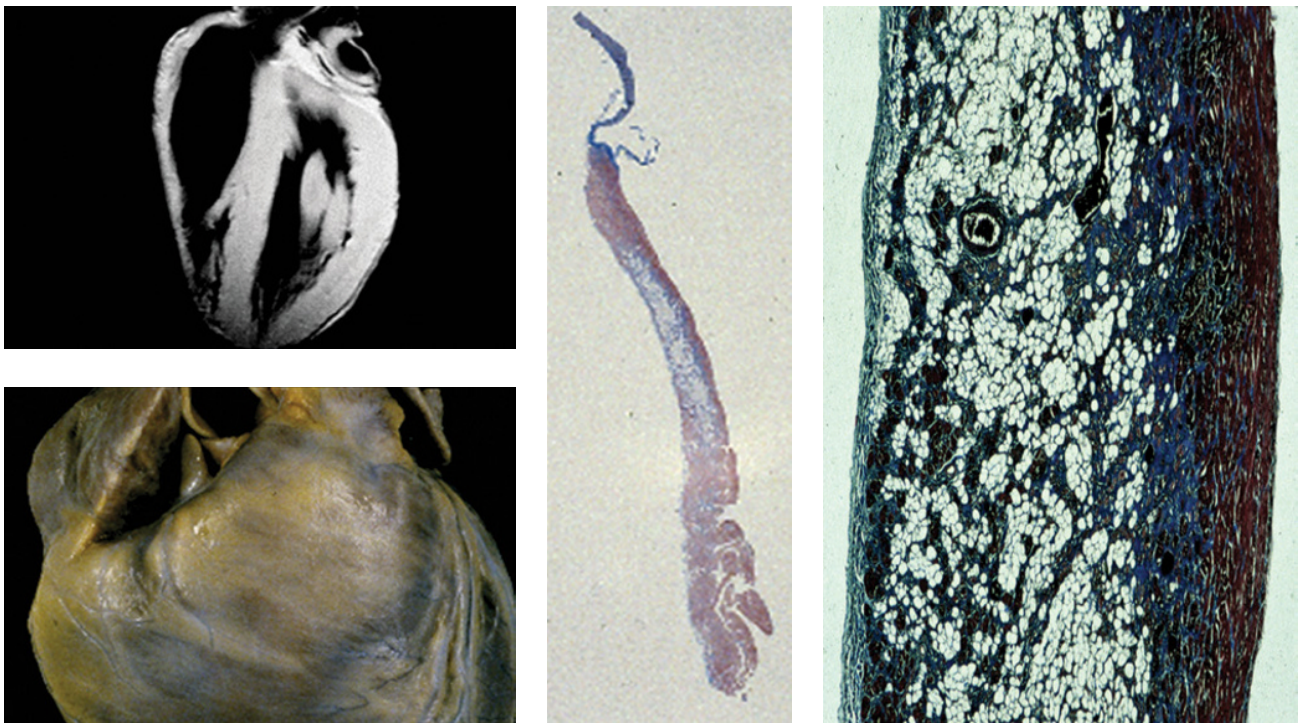

Figure 2.15 Segmental arrhythmogenic cardiomyopathy with fibro-fatty replacement limited to the pulmonary infundibulum (postmortem CMR, gross view, panoramic and close-up histology of the RVOT).

endomyocardial biopsy. When transmurally replaced by fibro-fatty tissue, the RV wall becomes thin and weak, leading to remodeling with the development of ventricular aneurysms in the so-called triangle of dysplasia (inflow, apex, outflow). The RV cavity becomes enlarged with depressed contractility and decreased ejection fraction. RVOT dilation is a common occurrence, easily seen by echocardiography. The aneurysm located at the inflow in the subtricuspid diaphragmatic wall should be considered a pathognomonic marker of arrhythmogenic cardiomyopathy.

The RV remodeling explains the typical phenotype of this cardiomyopathy.

- Electrical disorders consisting of delayed ventricular depolarization (large QRS, epsilon wave, late potentials), repolarization abnormalities (inverted T waves in right precordial leads exploring the outlet and anterior wall of the RV), ventricular tachyarrhythmias with left bundle branch block morphology, positive electrophysiological test at ventricular stimulation. The aneurysms favor reentry circuits of the electrical stimulus with onset of ventricular arrhythmias.
- Depressed ventricular contractility, which may lead to congestive heart failure. In advanced stages, it may be so severe that it may require cardiac transplantation. Arrhythmogenic cardiomyopathy, mimicking dilated cardiomyopathy, accounts for 4% of indications of cardiac transplantation [44]. RV enlargement, aneurysms and depressed contractility are well visible by two-dimensional echocardiography, which represents a low-cost, rapid tool for assessment of ventricular remodeling and dysfunction. Contrast cardiac magnetic resonance imaging, with late enhancement by gadolinium, adds information on tissue composition by visualizing fibro-fatty replacement [45].
- In 80% of cases of fibro-fatty infiltration, the phenomenon is topographically diffused with the occurrence of aneurysms [41]. Oddly enough, the ventricular septum is almost always spared and cannot be considered the target for endomyocardial biopsy as a source of fibro-fatty tissue. The RV disease may be segmental, with sole involvement of the RVOT, as a source of infundibular tachyarrhythmias and may require differential diagnosis with idiopathic RVOT tachycardia (Figures 2.17, 2.18). The pathology of the LV in arrhythmogenic cardiomyopathy includes "non-ischemic scars," typically located in the subepicardium – midwall. Since the disease is biventricular in 70% of cases, and the LV "scars" are easily detectable by cardiac magnetic resonance, the LV may be considered the diagnostic "mirror" of the RV in arrhythmogenic cardiomyopathy [45].
- "Electrical" scars, namely myocardial areas that are electrically silent at electroanatomical mapping. No electrical activity may originate from areas with

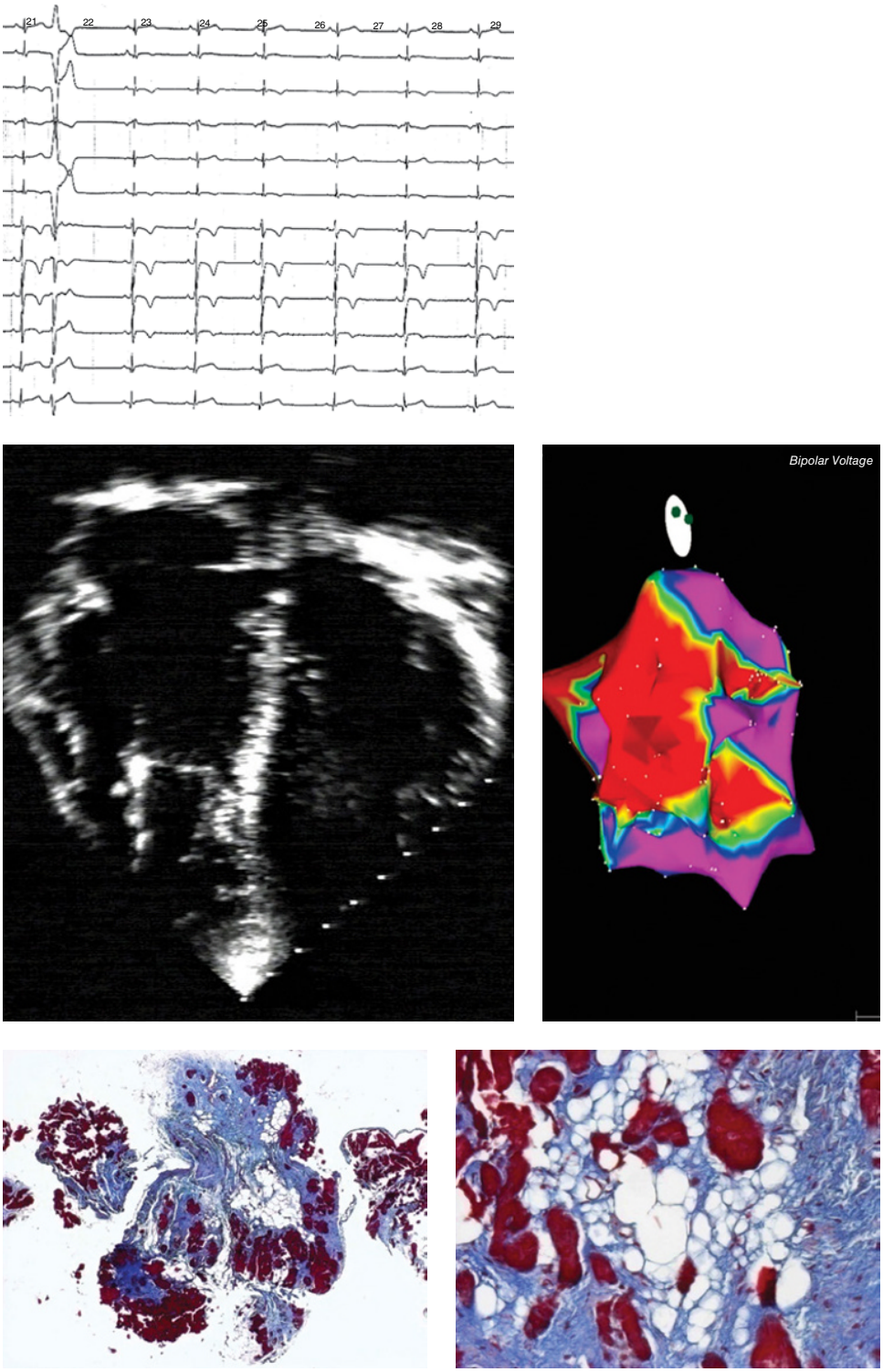

Figure 2.16 Electrophysiological mapping of extensive electrical scars and an endomyocardial biopsy showing severe fibro-fatty replacement in a patient with ECG and echocardiographic features of arrhythmogenic cardiomyopathy.

fibro-fatty replacement (see Figures 2.16, 2.17, 2.18) [45,46]. It is interesting to note that, as far as the RV free wall, because of the pathological thinning, electro-anatomical mapping is superior to contrast cardiac magnetic resonance to visualize areas of "non-ischemic" fibro-fatty scars.

- Right ventricular endomyocardial biopsy plays a pivotal role in the *in vivo* diagnosis by detecting the substrate

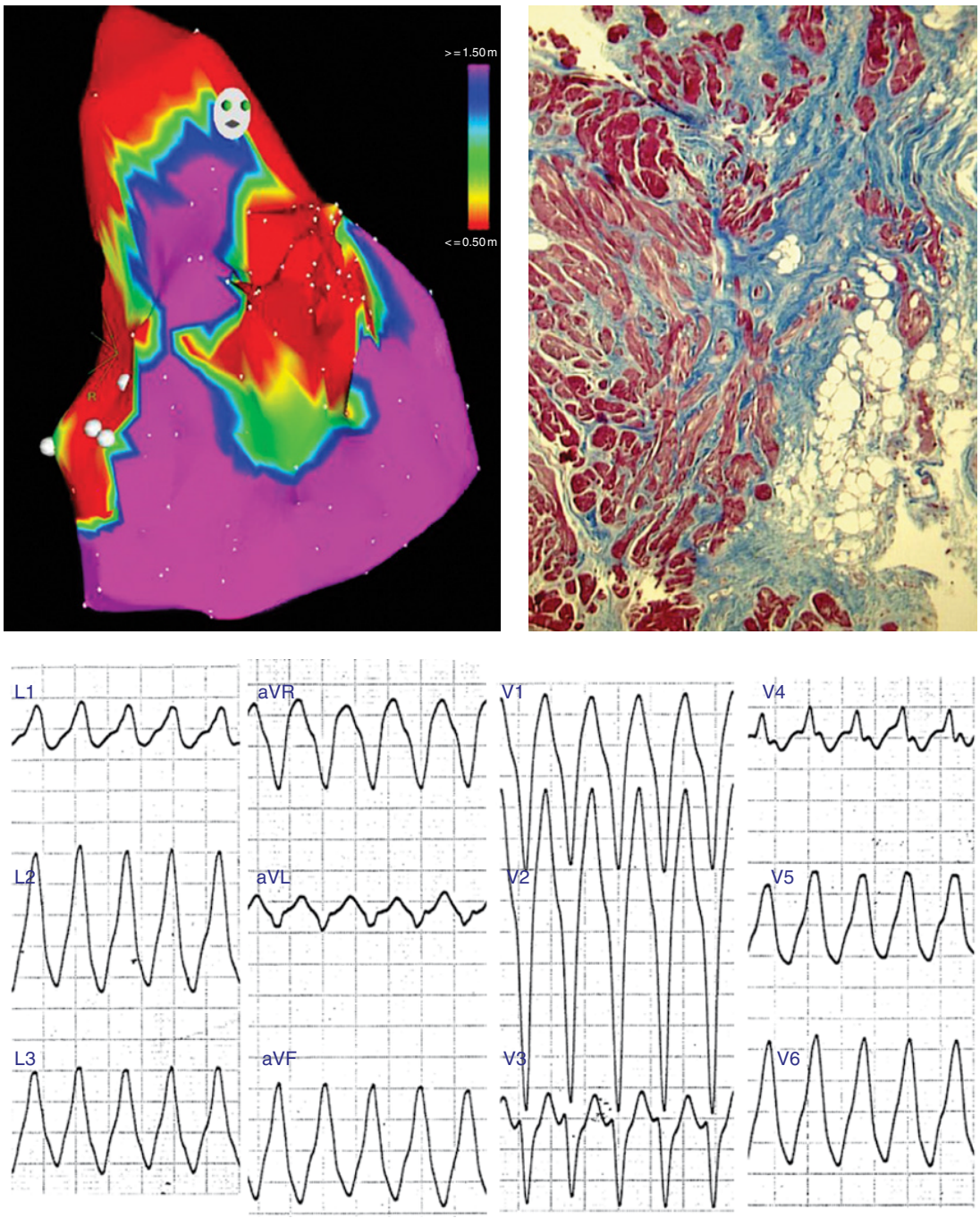

Figure 2.17 Electrophysiological mapping showing infundibular electrical scars and an endomyocardial biopsy with fibro-fatty replacement. The ECG shows left bundle branch block ventricular tachycardia with inferior axis.

of fibro-fatty replacement. Histomorphometric quantitative parameters have been calculated, thus providing major and minor criteria for the tissue characterization category [47,48]. When the residual myocardium (which accounts for 85% of the area in the normal heart) is less than 60% in a bioptic sample due to fibro-fatty replacement, the histological examination is pathognomonic for arrhythmogenic cardiomyopathy and is nowadays considered one of the major criteria for achieving the final diagnosis (see Figures 2.16, 2.17). To increase the sensitivity, the bioptome should point to the free wall where the fibro-fatty replacement

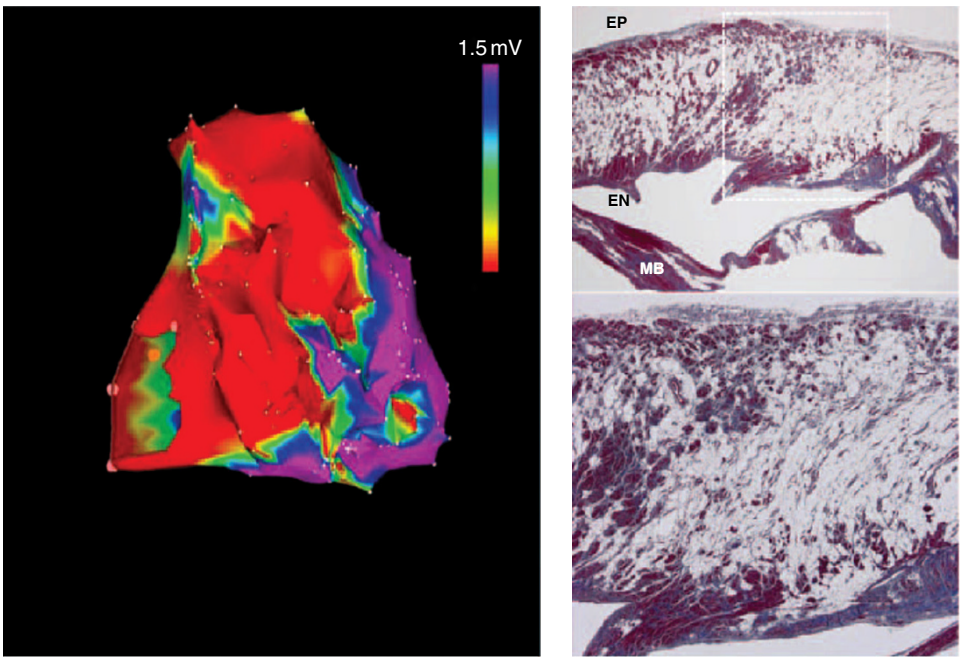

Figure 2.18 Extensive electrical scar by electroanatomical mapping and transmural fibro-fatty replacement of the pulmonary infundibulum at postmortem histology. EP, epicardium; EN, endocardium; MB, moderator band.

may be transmural, reaching the endocardium, and not the ventricular septum which is exceptionally involved. Perforation is rare and the risk is acceptable since it is not life-threatening and cardiac tamponade remains exceptional. However, bleeding may occur although rarely. Immunostaining for plakoglobin has been proposed as an additional diagnostic marker of arrhythmogenic cardiomyopathy [49], but additional validation is required.

Myocarditis

Ventricular arrhythmias are one of the clinical presentations of myocarditis, especially when focal without impairment of contractility and congestive heart failure [50]. Acute myocarditis may be localized in the RVOT and be the origin of ventricular arrhythmias with left bundle branch block morphology [51]. Lymphocyte infiltrates associated with myocyte death and inflammatory edema may interfere with Na + or K+ inflow-outflow and myocyte depolarization-repolarization, thus accounting for electrical instability.

Endomyocardial biopsy is still the gold standard for diagnosis, even though in cases of focal myocarditis the sampling error may be high. Several pieces of endomyocardium are mandatory to avoid sampling errors and increased sensitivity. Molecular investigation with polymerase chain reaction in acute early phase may help to establish the precise etiological diagnosis, whether RNA (especially enterovirus) or DNA (especially adenovirus) viruses. It is interesting to note that myocarditis in the acute phase may not be associated with extensive loss of myocardium so that electroanatomical mapping may produce negative results. In this setting, the coupling of electroanatomical mapping and endomyocardial biopsy plays a key role in differential diagnosis between arrhythmogenic cardiomyopathy (electroanatomical mapping and biopsy both positive because of fibro-fatty replacement) and myocarditis (electroanatomical mapping negative and endomyocardial biopsy positive) (Figure 2.19), as well as idiopathic tachycardia of the RVOT (electroanatomical mapping and endomyocardial biopsy both negative) [51,52] (Figure 2.20).

Sarcoidosis

Clinically evident cardiac involvement may occur in 5% of patients with sarcoidosis, even as a primary manifestation [53]. Another 20–25% of pulmonary/systemic sarcoidosis patients have asymptomatic cardiac involvement (clinically silent disease). Although conduction disturbances and heart failure are the main clinical signs, ventricular arrhythmias are also a common presentation.

The disease is mostly a multisystem, non-infective, granulomatous morbid entity, with non-caseating granulomas as a pathological hallmark. No specific pattern of

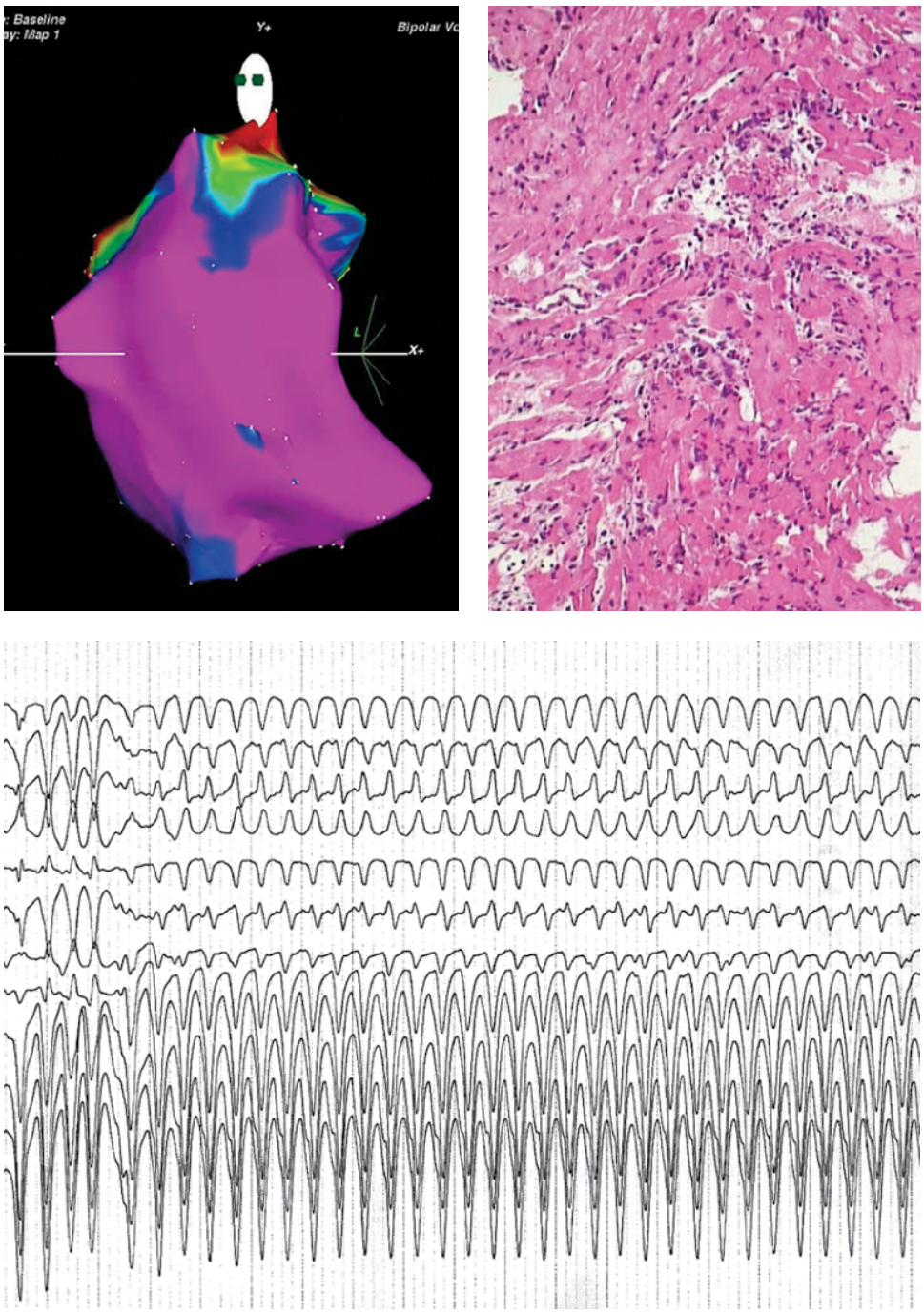

Figure 2.19 Negative electroanatomical mapping and acute myocarditis from an endomyocardial biopsy in a patient with ventricular tachycardia of left bundle branch morphology.

late enhancement is diagnostic for cardiac involvement, although it is most often seen in basal segments (particularly of the septum and lateral wall). By fluorodeoxyglucose positron emission tomography (PET), focal or diffuse fluorodeoxyglucose uptake patterns suggest active cardiac sarcoidosis. Differential diagnosis with other diseases (myocarditis, arrhythmogenic cardiomyopathy) is achieved by endomyocardial biopsy (Figure 2.21) [54,55]. Unfortunately, the sensitivity of biopsy is low (nearly 25%), due to sampling error because the focal nature of the disease. To increase the sensitivity, imaging-guided (PET-cardiac magnetic

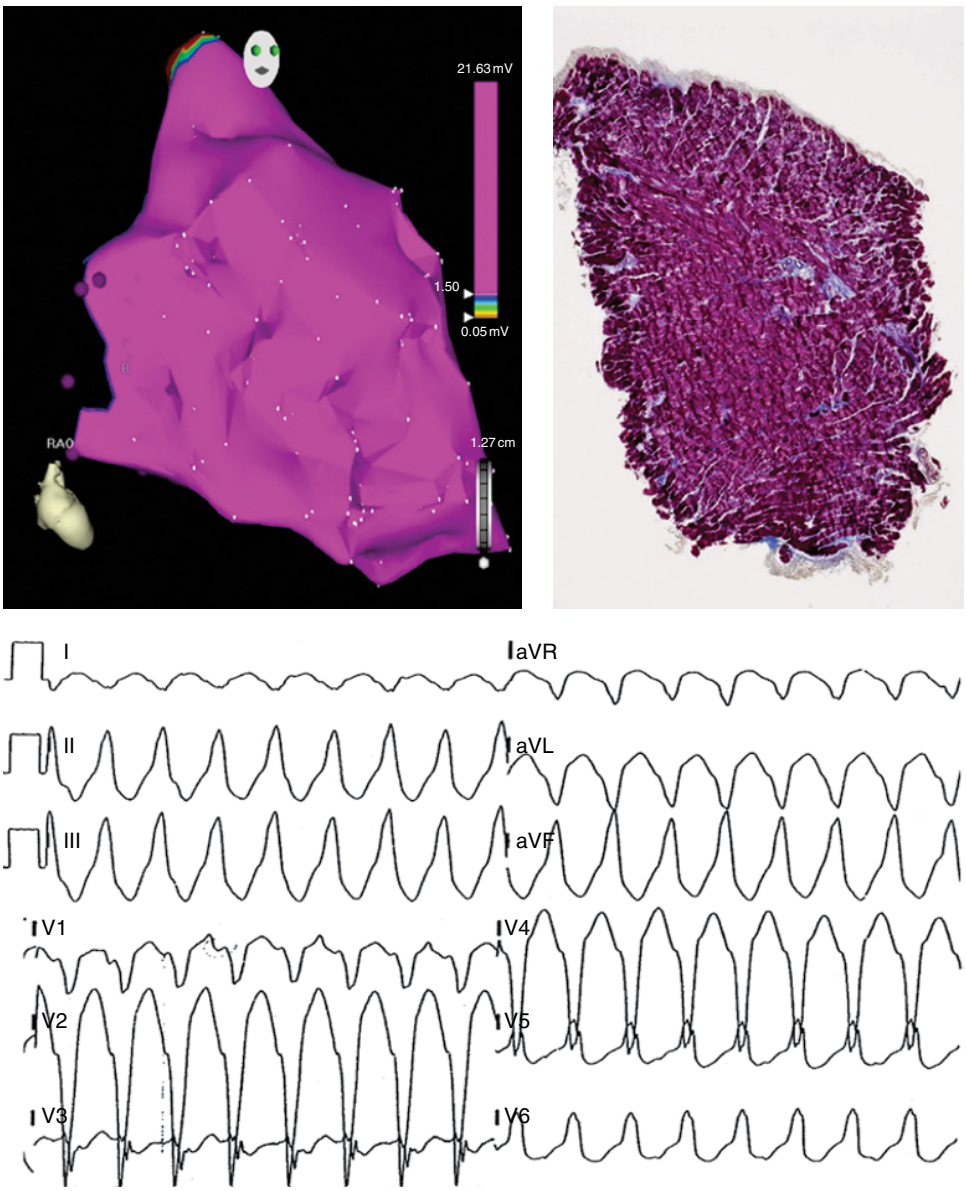

Figure 2.20 Normal electrical activity (negative electrophysiological mapping) and endomyocardial biopsy (preserved myocardium) in a patient with left bundle branch block ventricular tachycardia (idiopathic RVOT tachycardia).

resonance (CMR)) biopsy procedures, especially of the lymph nodes, are recommended and may increase sensitivity up to 50%. In cardiac sarcoidosis, electro-anatomical mapping is positive but non-specific. Thus, endomyocardial biopsy is pathognomonic and still the gold standard for a certain diagnosis of cardiac sarcoidosis.

RVOT ventricular arrhythmias without substrate

RVOT or LVOT tachyarrhythmias (premature ventricular beats, non-sustained and sustained monomorphic ventricular tachycardia, ventricular fibrillation) may occur in the absence of structural myocardial disease. They may originate from either the subvalvular or supravalvular regions in the ventricular outflows. They include myocardium located within the sinus of Valsalva beyond the hemodynamical border of the crown-shaped valve ring of both the pulmonary and aortic semilunar valves [56]. Outflow tract arrhythmias are identified by an electrocardiographic pattern consistent with a left bundle branch block morphology with inferior axis. They are caused by cAMP-mediated triggered activity and terminated by administration of adenosine. They are benign and not genetically determined. Of course, being ventricular arrhythmias without

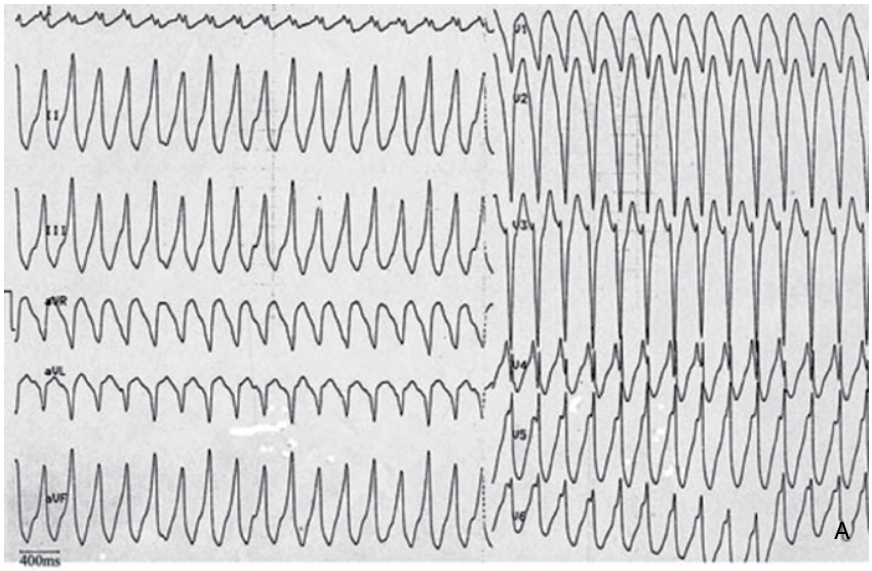

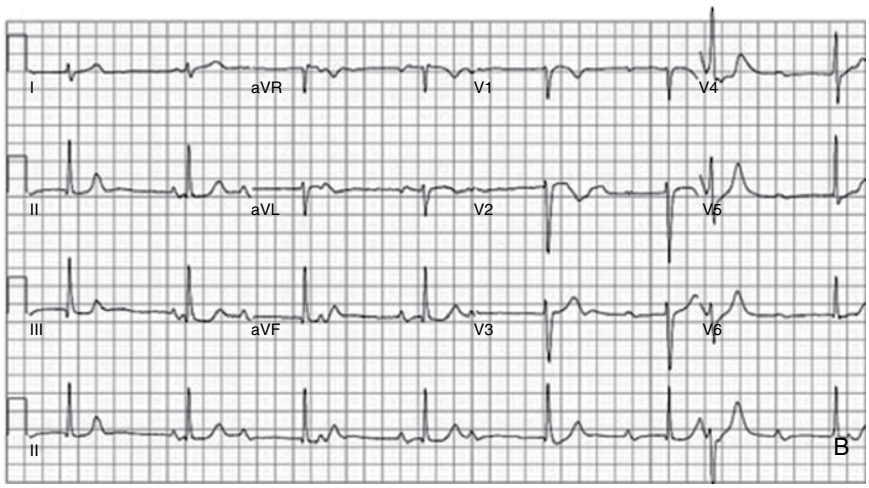

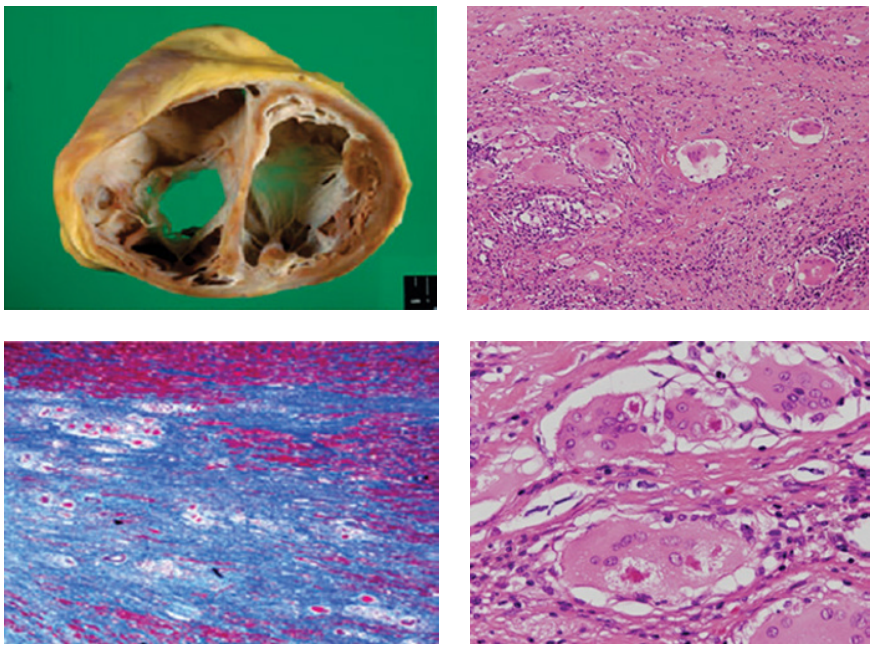

Figure 2.21 Ventricular tachycardia with left bundle branch morphology in a patient with an ECG-clinical diagnosis of arrhythmogenic cardiomyopathy and sarcoidosis identified in the explanted heart at transplantation. Note the non-caseous granuloma.

substrate, unipolar or bipolar electroanatomical mapping results are negative (Figure 2.20). Nonetheless, catheter-based radiofrequency ablation may represent definitive treatment [57].

Brugada syndrome

This is an inherited arrhythmic disorder featuring a non-ischemic ST segment elevation in right precordial leads in a 12-lead ECG [22–25] (Figure 2.22). Mutations of the *SCN5A* gene have been found in about 20% of cases. While the report by the Brugada brothers described a syndrome in survivors of cardiac arrest without structural disease [22], the original description in the literature was of "ventricular fibrillation without apparent heart disease." In fact, structural abnormalities of the RV determined by either autopsy or endomyocardial biopsy were found in five out of six patients [23]. Since then, the presence of a substrate has remained a matter of debate in the literature.

There are two main theories to explain the pathogenesis of Brugada syndrome: repolarization and depolarization. Yan and Antzelevitch first advanced the theory of an abnormal transmural repolarization in the RVOT due to heterogeneous loss of the cardiomyocyte action potential dome in the epicardium [58]. The most compelling evidence in support of the depolarization hypothesis comes from the studies by Nademanee [25,33]. In particular, myocardial fibrosis has been suggested by abnormal, low-voltage,

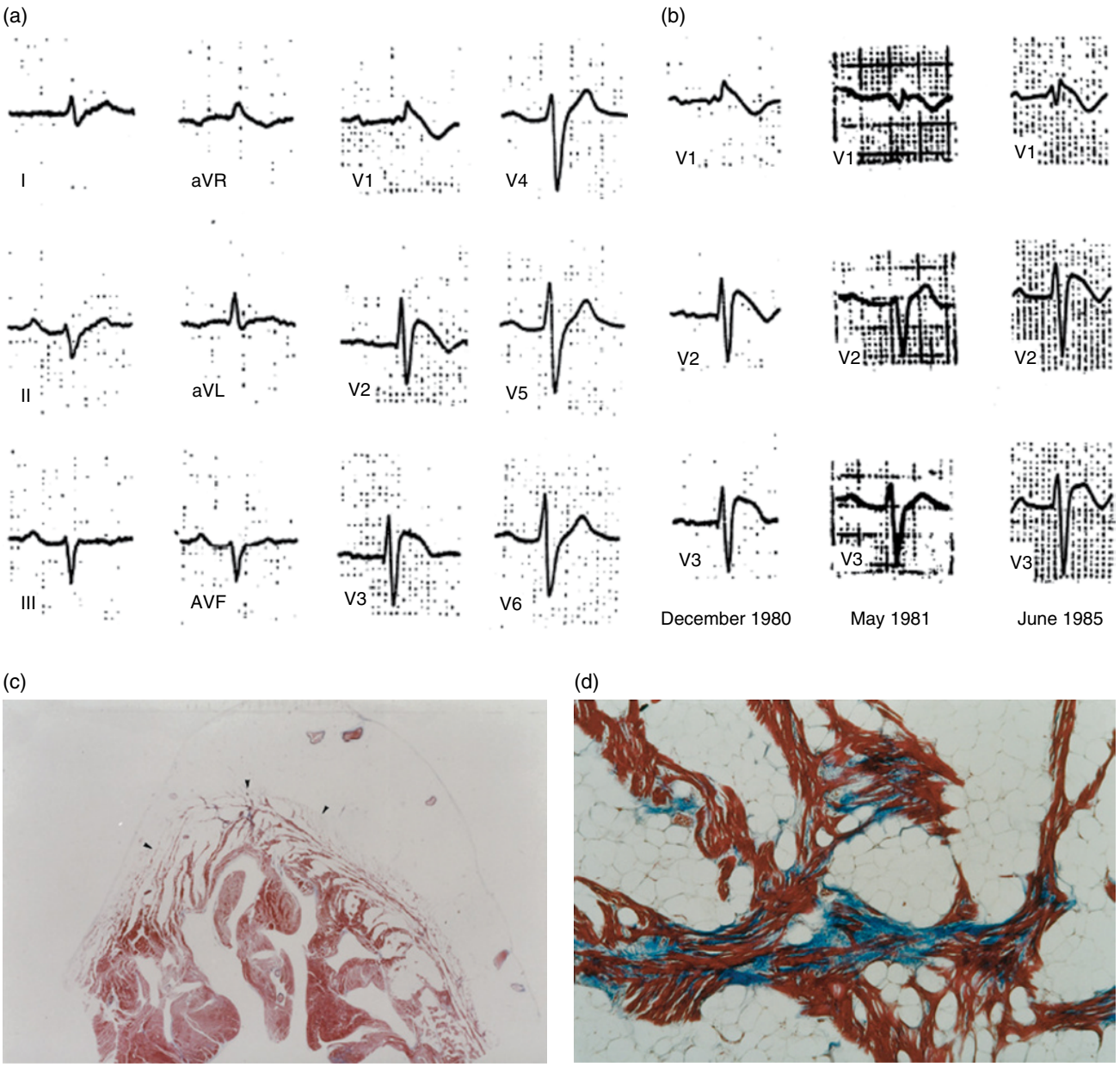

Figure 2.22 Fatty infiltration with mild fibrosis of the right ventricle in a patient with an *in vivo* diagnosis of ST segment elevation, right bundle branch, prolonged PQ interval, and aborted sudden death.

fractionated electrograms localized to the RVOT at the epicardium. The recent description of increased fibrosis, as well as reduced gap junction signaling protein Cx43 in the RVOT in a series of sudden death cases with family history of Brugada syndrome and without evident structural disease, is in favor of the depolarization hypothesis. Furthermore, electrophysiological and imaging studies have identified subtle structural abnormalities in the RVOT of affected patients [29,59,60]. Elimination of the sites of slow conduction gives the rationale for the efficacy of ablation therapy [61,62]. However, Szel et al. provided an alternative cellular electrophysiological mechanism as the basis for late potentials and fractionated electrogram activity in Brugada syndrome, demonstrating that the ECG abnormalities are due to repolarization and not to depolarization defects [63]. Future studies in genotyped cases should address the roles of fibrosis and gap junction proteins in Brugada syndrome.

Although repolarization and depolarization theories may indeed be synergistic and not mutually exclusive, correct assessment of the cellular pathophysiology remains a main target for appropriate therapy. It is important to note that AV conduction disturbances are a common finding in Brugada syndrome (PR prolongation, right bundle branch block). This is not surprising, considering that familial AV block has been explained by mutation of *SCN5A* [64]. Again, whether conduction disturbances are the result of merely functional changes or structural abnormalities of the specialized myocardium (Figure 2.22) remains to be addressed [65,66].

References

1 Chugh SS, Reinier K, Teodorescu C, *et al.* Epidemiology of sudden cardiac death: clinical and research implications. *Prog Cardiovasc Dis.* 2008;**51**:213–28.

2 Huikuri HV, Castellanos A, Myerburg RJ. Sudden death due to cardiac arrhythmias. *N Engl J Med* 2001;**345**:1473–82.

3 Morita H, Fukushima-Kusano K, Nagase S, *et al.* Site-specific arrhythmogenesis in patients with Brugada syndrome. *J Cardiovasc Electrophysiol* 2003;**14**:373–9.

4 Shimizu W. Arrhythmias originating from the right ventricular outflow tract: how to distinguish "malignant" from "benign"? *Heart Rhythm* 2009;**6**:1507–11.

5 de la Cruz MV, Sanchez GC, Arteaga MM, Arguello C. Experimental study of the development of the truncus and the conus in the chick embryo. *J Anat* 1977;**123**:661–86.

6 de Jong F, Opthof T, Wilde AA, *et al.* Persisting zones of slow impulse conduction in developing chicken hearts. *Circ Res* 1992;**71**:240–50.

7 Buckingham M, Meilhac S, Zaffran S. Building the mammalian heart from two sources of myocardial cells. *Nat Rev Genet* 2005;**6**:826–35.

8 Boukens BJ, Christoffels VM, Coronel R, Moorman AF. Developmental basis for electrophysiological heterogeneity in the ventricular and outflow tract myocardium as a substrate for life-threatening ventricular arrhythmias. *Circ Res* 2009;**104**:19–31.

9 Moorman AF, Christoffels VM. Cardiac chamber formation: development, genes, and evolution. *Physiol Rev* 2003;**83**:1223–67.

10 Kelly RG, Brown NA, Buckingham ME. The arterial pole of the mouse heart forms from Fgf10-expressing cells in pharyngeal mesoderm. *Dev Cell* 2001;**1**:435–40.

11 Rana MS, Horsten NC, Tesink-Taekema S, Lamers WH, Moorman AF, van den Hoff MJ. Trabeculated right ventricular free wall in the chicken heart forms by ventricularization of the myocardium initially forming the outflow tract. *Circ Res* 2007;**100**:1000–7.

12 Sizarov A, Lamers WH, Mohun TJ, Brown NA, Anderson RH, Moorman AF. Three-dimensional and molecular analysis of the arterial pole of the developing human heart. *J Anat* 2012;**220**:336–49.

13 Lamers WH, Moorman AF. Cardiac septation: a late contribution of the embryonic primary myocardium to heart morphogenesis. *Circ Res* 2002;**91**:93–103.

14 Theveniau-Ruissy M, Dandonneau M, Mesbah K, *et al.* The del22q11.2 candidate gene Tbx1 controls regional outflow tract identity and coronary artery patterning. *Circ Res* 2008;**103**:142–8.

15 Boukens BJ, Sylva M, de Gier–de Vries C, *et al.* Reduced sodium channel function unmasks residual embryonic slow conduction in the adult right ventricular outflow tract. *Circ Res* 2013;**113**:137–41.

16 Sizarov A, Devalla HD, Anderson RH, Passier R, Christoffels VM, Moorman AF. Molecular analysis of patterning of conduction tissues in the developing human heart. *Circ Arrhythm Electrophysiol* 2011;**4**:532–42.

17 Fijnvandraat AC, van Ginneken AC, de Boer PA, *et al.* Cardiomyocytes derived from embryonic stem cells resemble cardiomyocytes of the embryonic heart tube. *Cardiovasc Res* 2003;**58**:399–409.

18 Sadauskas VM, Mutskus KS, Puodzhius SS, Bukauskas FF. Electrical activity of human embryo heart cells under hypoxic conditions. *Akush Ginekol (Mosk)* 1976:19–22.

19 Dobrzynski H, Anderson RH, Atkinson A, *et al.* Structure, function and clinical relevance of the cardiac conduction system, including the atrioventricular ring

and outflow tract tissues. *Pharmacol Ther* 2013;**139**:260–88.
20 Christoffels VM, Moorman AF. Development of the cardiac conduction system: why are some regions of the heart more arrhythmogenic than others? *Circ Arrhythm Electrophysiol* 2009;**2**:195–207.
21 Kleber AG, Rudy Y. Basic mechanisms of cardiac impulse propagation and associated arrhythmias. *Physiol Rev* 2004;**84**:431–88.
22 Brugada P, Brugada J. Right bundle branch block, persistent ST segment elevation and sudden cardiac death: a distinct clinical and electrocardiographic syndrome. A multicenter report. *J Am Coll Cardiol* 1992;**20**:1391–6.
23 Martini B, Nava A, Thiene G, *et al.* Ventricular fibrillation without apparent heart disease: description of six cases. *Am Heart J* 1989;**118**:1203–9.
24 Antzelevitch C, Brugada P, Borggrefe M, *et al.* Brugada syndrome: report of the second consensus conference. *Heart Rhythm* 2005;**2**:429–40.
25 Nademanee K, Veerakul G, Chandanamattha P, *et al.* Prevention of ventricular fibrillation episodes in Brugada syndrome by catheter ablation over the anterior right ventricular outflow tract epicardium. *Circulation* 2011;**123**:1270–9.
26 Chen Q, Kirsch GE, Zhang D, *et al.* Genetic basis and molecular mechanism for idiopathic ventricular fibrillation. *Nature* 1998;**392**:293–6.
26a Kyndt F, Probst V, Potet F, *et al.* Novel SCN5A mutation leading either to isolated cardiac conduction defect or Brugada syndrome in a large French family. *Circulation* 2001;**104**:3081–6.
27 Coronel R, Casini S, Koopmann TT, *et al.* Right ventricular fibrosis and conduction delay in a patient with clinical signs of Brugada syndrome: a combined electrophysiological, genetic, histopathologic, and computational study. *Circulation* 2005;**112**:2769–77.
28 Frustaci A, Priori S, Pieroni M, *et al.* Cardiac histological substrate in patients with clinical phenotype of Brugada syndrome. *Circulation* 2005;**112**:3680–7.
29 Postema PG, van Dessel PF, de Bakker JM, *et al.* Slow and discontinuous conduction conspire in Brugada syndrome: a right ventricular mapping and stimulation study. *Circ Arrhythm Electrophysiol* 2008;**1**:379–86.
30 Hoogendijk MG, Potse M, Vinet A, de Bakker JM, Coronel R. ST segment elevation by current-to-load mismatch: an experimental and computational study. *Heart Rhythm* 2011;**8**:111–18.
31 Hoogendijk MG, Potse M, Linnenbank AC, *et al.* Mechanism of right precordial ST-segment elevation in structural heart disease: excitation failure by current-to-load mismatch. *Heart Rhythm* 2010;**7**:238–48.
32 Hoogendijk MG, Opthof T, Postema PG, Wilde AA, de Bakker JM, Coronel R. The Brugada ECG pattern: a marker of channelopathy, structural heart disease, or neither? Toward a unifying mechanism of the Brugada syndrome. *Circ Arrhythm Electrophysiol* 2010;**3**:283–90.
33 Nademanee K, Raju H, de Noronha SV, *et al.* Fibrosis, Connexin-43, and conduction abnormalities in the Brugada syndrome. *J Am Coll Cardiol* 2015;**66**:1976–86.
34 Liang S, Lin C, Li Y, Liu T, Wang Y. L-type calcium current in right ventricular outflow tract myocytes of rabbit heart. *Sci China Life Sci* 2012;**55**:41–6.
35 Xie Y, Sato D, Garfinkel A, Qu Z, Weiss JN. So little source, so much sink: requirements for afterdepolarizations to propagate in tissue. *Biophys J* 2010;**99**:1408–15.
36 Liu CF, Cheung JW, Thomas G, Ip JE, Markowitz SM, Lerman BB. Ubiquitous myocardial extensions into the pulmonary artery demonstrated by integrated intracardiac echocardiography and electroanatomic mapping: changing the paradigm of idiopathic right ventricular outflow tract arrhythmias. *Circ Arrhythm Electrophysiol* 2014;**7**:691–700.
37 Timmermans C, Rodriguez LM, Crijns HJ, Moorman AF, Wellens HJ. Idiopathic left bundle-branch block-shaped ventricular tachycardia may originate above the pulmonary valve. *Circulation* 2003;**108**:1960–7.
38 Basso C, Ho SY, Rizzo S, Thiene G. Anatomic and histopathologic characteristics of the conductive tissues of the heart. In: Gussak I, Antzelevitch C (eds), *Electrical Diseases of the Heart.* London: Springer Verlag, 2013: pp. 47–71.
39 Basso C, Thiene G. Adipositas cordis, fatty infiltration of the right ventricle, and arrhythmogenic right ventricular cardiomyopathy. Just a matter of fat? *Cardiovasc Pathol* 2005;**14**:37–41.
40 Thiene G, Nava A, Corrado D, Rossi L, Pennelli N. Right ventricular cardiomyopathy and sudden death in young people. *N Engl J Med* 1988;**318**:129–33.
41 Basso C, Thiene G, Corrado D, Angelini A, Nava A, Valente M. Arrhythmogenic right ventricular cardiomyopathy. Dysplasia, dystrophy, or myocarditis? *Circulation* 1996;**94**:983–91.
42 Basso C, Bauce B, Corrado D, Thiene G. Pathophysiology of arrhythmogenic cardiomyopathy. *Nat Rev Cardiol* 2011;**9**:223–33.
43 Pilichou K, Thiene G, Bauce B, *et al.* Arrhythmogenic cardiomyopathy. *Orphanet J Rare Dis* 2016;**11**:33.
44 McKenna WJ, Maron B, Thiene G. Classification, epidemiology, and global burden of cardiomyopathies. *Circ Res* 2017;**121**:722–30.
45 Marra MP, Leoni L, Bauce B, *et al.* Imaging study of ventricular scar in arrhythmogenic right ventricular cardiomyopathy: comparison of 3D standard

electroanatomical voltage mapping and contrast-enhanced cardiac magnetic resonance. *Circ Arrhythm Electrophysiol* 2012;**5**:91–100.

46 Migliore F, Zorzi A, Silvano M, *et al.* Prognostic value of endocardial voltage mapping in patients with arrhythmogenic right ventricular cardiomyopathy/dysplasia. *Circ Arrhythm Electrophysiol* 2013;**6**:167–76.

47 Basso C, Ronco F, Marcus F, *et al.* Quantitative assessment of endomyocardial biopsy in arrhythmogenic right ventricular cardiomyopathy/dysplasia: an in vitro validation of diagnostic criteria. *Eur Heart J* 2008;**29**:2760–71.

48 Marcus FI, McKenna WJ, Sherrill D, *et al.* Diagnosis of arrhythmogenic right ventricular cardiomyopathy/dysplasia: proposed modification of the Task Force Criteria. *Eur Heart J* 2010;**31**:806–14.

49 Asimaki A, Tandri H, Huang H, *et al.* A new diagnostic test for arrhythmogenic right ventricular cardiomyopathy. *N Engl J Med* 2009;**360**:1075–84.

50 Basso C, Calabrese F, Angelini A, Carturan E, Thiene G. Classification and histological, immunohistochemical, and molecular diagnosis of inflammatory myocardial disease. *Heart Fail Rev* 2013;**18**:673–81.

51 Corrado D, Basso C, Leoni L, *et al.* Three-dimensional electroanatomic voltage mapping increases accuracy of diagnosing arrhythmogenic right ventricular cardiomyopathy/dysplasia. *Circulation* 2005;**111**:3042–50.

52 Corrado D, Basso C, Leoni L, *et al.* Three-dimensional electroanatomical voltage mapping and histologic evaluation of myocardial substrate in right ventricular outflow tract tachycardia. *J Am Coll Cardiol* 2008;**51**:731–9.

53 Birnie DH, Kandolin R, Nery PB, Kupari M. Cardiac manifestations of sarcoidosis diagnosis and management. *Eur Heart J* 2017;**38**:2663–70.

54 Vasaiwala SC, Finn C, Delpriore J, *et al.* Prospective study of cardiac sarcoid mimicking arrhythmogenic right ventricular dysplasia. *J Cardiovasc Electrophysiol* 2009;**20**:473–6.

55 Ladyjanskaia GA, Basso C, Hobbelink MG, *et al.* Sarcoid myocarditis with ventricular tachycardia mimicking ARVD/C. *J Cardiovasc Electrophysiol* 2010;**21**:94–8.

56 Vaseghi M, Lai C, Huang A, Fishbein MC, Shivkumar K. The relationship of the ventricular septum and right ventricular outflow tract to the right and non-coronary sinuses: implications for ablation of ventricular tachycardias. *Circulation* 2007;**116**:II–366.

57 Lerman BB. Mechanism, diagnosis, and treatment of outflow tract tachycardia. *Nat Rev Cardiol* 2015;**12**:597–608.

58 Yan GX, Antzelevitch C. Cellular basis for the Brugada syndrome and other mechanisms of arrhythmogenesis associated with ST-segment elevation. *Circulation* 1999;**100**:1660–6.

59 Catalano O, Antonaci S, Moro G, *et al.* Magnetic resonance investigations in Brugada syndrome reveal unexpectedly high rate of structural abnormalities. *Eur Heart J* 2009;**30**:2241–8.

60 Letsas KP, Efremidis M, Vlachos K, *et al.* Right ventricular outflow tract high-density endocardial unipolar voltage mapping in patients with Brugada syndrome: evidence for electroanatomical abnormalities. *Europace* 2018;**20**(FI1):f57–f63.

61 Morita H, Zipes DP, Morita ST, *et al.* Epicardial ablation eliminates ventricular arrhythmias in an experimental model of Brugada syndrome. *Heart Rhythm* 2009;**6**:665–71.

62 Brugada J, Pappone C, Berruezo A, *et al.* Brugada syndrome phenotype elimination by epicardial substrate ablation. *Circ Arrhythm Electrophysiol* 2015;**8**:1373–81.

63 Szél T, Antzelevitch C. Abnormal repolarization as the basis for late potentials and fractionated electrograms recorded from epicardium in experimental models of Brugada syndrome. *J Am Coll Cardiol* 2014;**63**:2037–45.

64 Schott JJ, Alshinawi C, Kyndt F, *et al.* Cardiac conduction defects associate with mutations in SCN5A. *Nat Genet* 1999;**23**:20–1.

65 Corrado D, Nava A, Buja G, *et al.* Familial cardiomyopathy underlies syndrome of right bundle branch block, ST segment elevation and sudden death. *J Am Coll Cardiol* 1996;**27**:443–8.

66 Migliore F, Testolina M, Zorzi A, et al. First-degree atrioventricular block on basal electrocardiogram predicts future arrhythmic events in patients with Brugada syndrome: a long-term follow-up study from the Veneto region of Northeastern Italy. *Europace* 2018 Jul **6** [Epub ahead of print]

3

Arrhythmogenic Venous Extremity of the Cardiac Tube

Marco Galeazzi

Cardiovascular Department, San Filippo Neri Hospital, Rome, Italy

Summary

Although much progress has been made since imaging techniques started to be used in the setting of cardiac arrhythmia ablation, it is interesting to observe that very few electrophysiologists have sufficient awareness about the embryological basis of their "battlefield." Therefore, a quick glance at the embryogenetic processes leading to the development of certain anatomical structures may be helpful in understanding the related arrhythmogenic substrate, thus giving the specialist some basic tools to evaluate the appropriateness and effects of their therapeutic choices.

Introduction

The primitive heart starts developing (and contracting) in the third week of pregnancy. Several components arising from different substrates participate in the genesis of the cardiac conduction system. Neural crest-derived cells turn out to be crucial, especially as far as particular cardiac districts are concerned. Common arrhythmias originating from the extremities of the cardiac tube (i.e. venous–atrial and ventricular–arterial junctions) reflect the complexity of the local embryogenesis. The highly specialized cells spreading to these districts, in addition to the complexity of the developement of the local anatomical structures, may explain local arrhythmogenic behaviors.

The cardiac tube

The tubular primordial heart has a mesodermal origin, very early during cardiogenesis, through the fusion of two endothelial strands. The cranial extremity of the tube represents the future cardiac outflow tract and is continuous with the aortic arches. On the other hand, the caudal extremity represents the inflow tract and is continuous with the vitteloumbilical veins. After the looping and segmental dilation of several segments of the cardiac tube have occurred, it is possible to recognize different primitive structures: (1) the sinus venosus (which forms the venous inflow chamber), (2) the primitive atrium, (3) the primitive ventricle, and (4) the conus arteriosus. A complex activation of several regulatory genes and transcription factors is responsible for the correct sequential steps of this embryogenetic phase. At the same time, it is possible to recognize a primitive sequential contraction of these structures, thus reflecting the presence of a primitive specialized cardiac conduction system.

As far as the development of this conduction system is concerned, great importance has been given to the migration and influence of the neural crest-derived cells. These cells are able to differentiate into several types and can contribute to the development of the craniofacial cartilage of the bones and connective tissue. Moreover, they differentiate into nerves and accessory cells (involved in the layered myelin insulation of the nerves) and can contribute to smooth muscle progenitors in the great vessels of the heart.

The population of crest cells coming from the posterior rhombencephalic segments of the neural tube contribute to multiple aspects of cardiac development and function. They have an active influence on several steps in the embryogenesis of the outflow pole of the heart. Indeed, the ablation of the premigratory cardiac neural crest results in a defective development of the cardiac outflow tract.

Moreover, some evidence has been provided for an association between ablation of the neural crest cells and a significant reduction in myocardial calcium transients, which are a measure of excitation-contraction coupling in both the inflow and outflow portions of the looped heart tube. Furthermore, a complete recovery of the myocardial transients can be obtained by replacing the cardiac neural crest.

Cardiac Mapping, Fifth Edition. Edited by Mohammad Shenasa, Gerhard Hindricks, David J. Callans, John M. Miller, and Mark E. Josephson.

Companion website: www.wiley.com/go/cardiacmapping5e

It is also known that ablation of neural crest cells inhibits compaction and electrical function of the conduction system bundles.

Finally, the neural crest plays an important role in the development of the parasympathetic postganglionic innervation of the heart.

For these reasons, it was formerly believed that development of the myocardial specialized conduction tissue was entirely dependent on the correct migration of these cells, thus ascribing an extracardiac origin. Indeed, it is possible to document this migration, especially around the great arteries and the atrioventricular septum.

The most recent investigations ascribe this phenomenon to the differentiation of some multipotent cardiomyogenic cells that can be addressed to form the contractile or conduction tissue. In the case of conduction tissue, these cells could be inhibited from a full maturation to contractile elements by the influence of the epicardium-derived cells or by the neural crest cells themselves which contribute to insulate the future conduction tissue from the rest of the heart.

The cardiac neural crest may also play a role in the late phase of cardiac conduction system cell maturation. Many developmental components are necessary for the specification and function of cardiac conduction; for example, it has been demonstrated that an altered expression of the *HF-1B* gene in the ventricular myocardium and in the neural crest cells can lead to many arrhythmic problems.

It is still unclear why some primitive myocytes develop into conduction cells rather than into contractile elements. These cells typically show a slower proliferation that leads to the formation of some constriction areas (the "multiple ring theory") so the cardiac tube modifies its morphology simply by folding around them. Another theory postulates that a model of the conduction system is already present in the primitive heart and evolves into its final structure by a progressive recruitment of the adjacent myocytes. On the other hand, according to the "early specification model," the development of the conduction system could be due to the expression of some "conduction genes" causing a slow proliferation and progressive differentatiation into mature conduction elements (Figure 3.1). The observation of different kinds of arrhythmias developing at different ages could be explained if we postulate that this expression will show up during any period of human life.

Regardless of the embryogenetic mechanism that takes place, it is well known that the conduction of the action potentials generated in these cells is able to spread to the adjacent ones by the presence of gap junctions and the action of different types of connexins that allow the passage of ions from one cell to another.

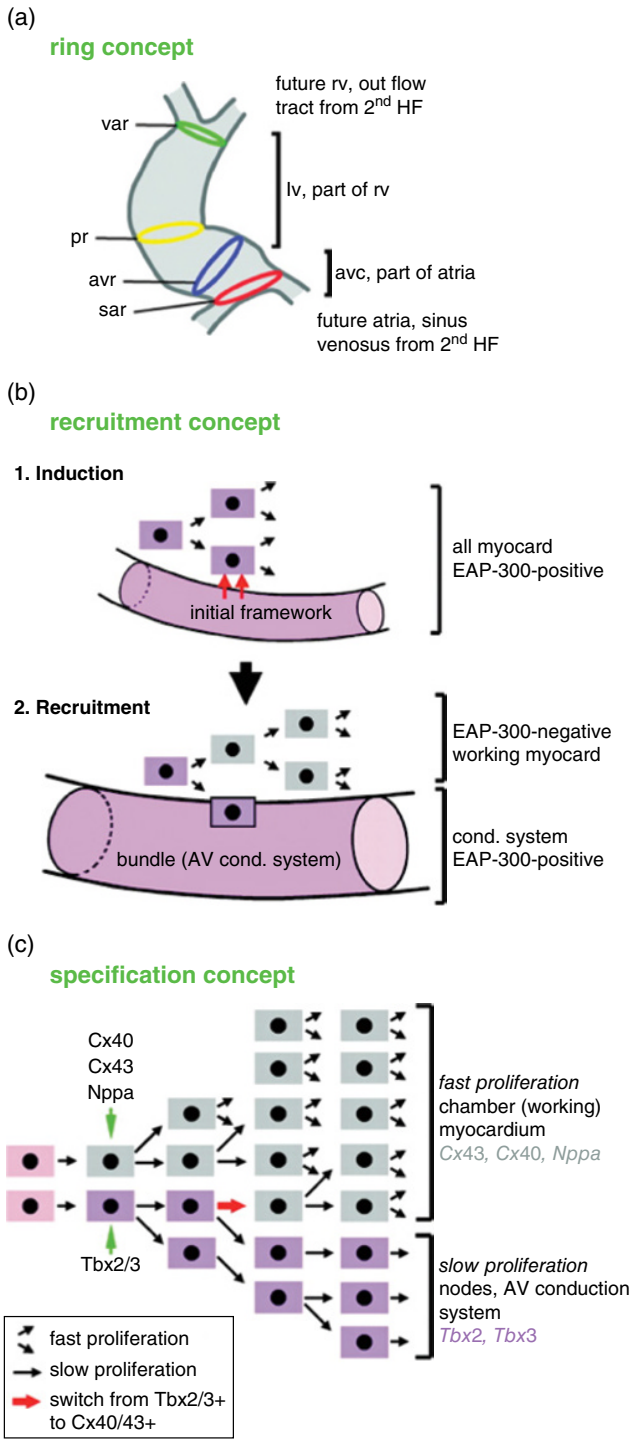

Figure 3.1 The three hypotheses of conduction system development. (a) The four-ring theory, with four conduction system rings represented in the tubular heart. avr, atrioventricular ring; pr, primary ring; sar, sinuatrial ring; var, ventriculoarterial ring. (b) Two-step model of recruitment of myocardial cells to the conduction system (recruitment model). (c) Early specification model: the primary myocardium of the heart tube (*pink*) can give rise either to conduction elements (*purple*) that maintain an undifferentiated phenotype and a low proliferation profile or to chamber (working) ones (*gray*, more differentiated). *Source:* Christoffels et al. [1]. Reproduced with permission of Wolters Kluwer.

Different types of connexins allow different ion passage velocities between the cells. Four types of connexins have so far been identified, and they are diffused in different amounts according to the features of the specialized cells. For example, Cx43 is more concentrated in fast-conducting tissues, whereas Cx45 is more likely to be identified in slow-conducting ones (like sinoatrial and atrioventricular nodes).

Soon after cardiac looping has occurred, the primordial atrium starts behaving as a primitive pacemaker, thus allowing a sequential cardiac tube contraction. This regulatory function rapidly migrates to the sinus venosus and then to the sinoatrial node; at the end of the fifth week after conception, the final pacemaker of the heart is already developed.

It is well known by electrophysiologists that, although every region of the mature heart is able to host arrhythmogenic areas, some of them display this feature much more frequently. While the primitive heart tube does not have a definite conduction system during its progressive lengthening, it is possible to identify either fast-conducting muscle cells (the contractile elements) or slow-conducting cells that amount to a primitive conduction network. It has been shown that altered expression of factors like Tbx3 in the embryonic heart influences the development of some cardiac regions that can therefore express a higher arrhythmogenic pattern. This could be the case, for instance, for the orifice of the coronary sinus, the terminal crest, and the atrial tissue surrounding the tricuspid and mitral valves.

The venous extremity of the cardiac tube

The development of the sinus venosus at the transition with the vitelline veins is characterized by the formation of thin myocardial sleeves inside the future pulmonary veins. These sleeves are well known as a potential source of arrhythmias. In fact, as was observed many years ago, the pulmonary veins show an independent pulsation, thus suggesting that they host an electrical automaticity.

The orientation of the fibers at the ostium of the pulmonary veins is also very important. It is easier to observe action potentials at the ostium of the left upper vein, since circumferential fibers (which are able to create more propagation delay) are present. Longitudinal fibers are more frequently located in the left lower vein, where the observation of action potentials is less likely.

Although an apparent continuity is observable between the myocardium of the pulmonary venous sleeves and that coming from the sinus venosus, these two elements show different embryogenetic pathways. Indeed, the pulmonary veins are of mesenchimal origin inside the mediastinum, where a plexus of veins starts growing around the primitive bronchial buds. These veins organize into four distinct blood vessels meeting and fusing with a single common vein breaking out from the posterior left atrial region as a "pulmonary pit" (Figure 3.2a). This common vein gets progressively incorporated inside the posterior atrial wall, where the four pulmonary veins finally originate separately (Figure 3.2b).

The development of the myocardial sleeves inside the veins differs as far as the single veins are concerned; longer sleeves can be detected in the left superior vein, whereas shorter sleeves are observed in the right inferior vein (Figures 3.3, 3.4). This is an important concept since the clinical arrhythmogenicity of the veins depends on the length of the circumpherential sleeves. Several electrophysiological properties (which are distinct from those arising from the atrial miocardium) have been identified, including the resting membrane potentials, phase 0 upstroke velocities, and action potential duration. It has not yet been confirmed how these properties contribute to the arrhythmogenic process.

A relevant amount of pacemaker P cells and Purkinje cells have been observed in the veins of atrial fibrillation patients; however, strong evidence does exist against the presence of "nodal" cells, since the pacemaker channel gene *HCN4* (a fundamental feature of these cells) is not expressed.

Although the pulmonary myocardial sleeves express a certain amount of markers associated with the conduction tissue (like CCSlacZ), these markers are also expressed by the cells of active working myocardium. For this reason, no evidence is available to consider the myocardial sleeves as a component of the developing conduction system.

The right atrial posterior region arises from venous structures, mainly from the sinus venosus. On the other hand, the left and right atrial appendages come from the atrial region of the cardiac tube.

While the inferior vena cava is of little importance to the genesis of arrhythmias, the superior vena cava and particularly the coronary sinus are well-known arrhythgmogenic elements. Indeed, they are not part of the cardiac conduction system, but participate in the genesis and maintenance of atrial ectopies.

The superior vena cava comes from the right horn of the sinus venosus, and a certain amount of myocardial sleeves can be detected inside its ostium. The coronary sinus comes from the left horn. Initially, it gives rise to the left superior vena cava, which progressively degenerates and broadens (Figure 3.5). In a small percentage of normal adults (about 0.5%), when the left common cardinal vein has failed to occlude, it is possible to observe a persistency of the left superior vena cava which drains into the coronary sinus. When the left superior vena cava is occluded, it gives rise to the ligament of Marshall

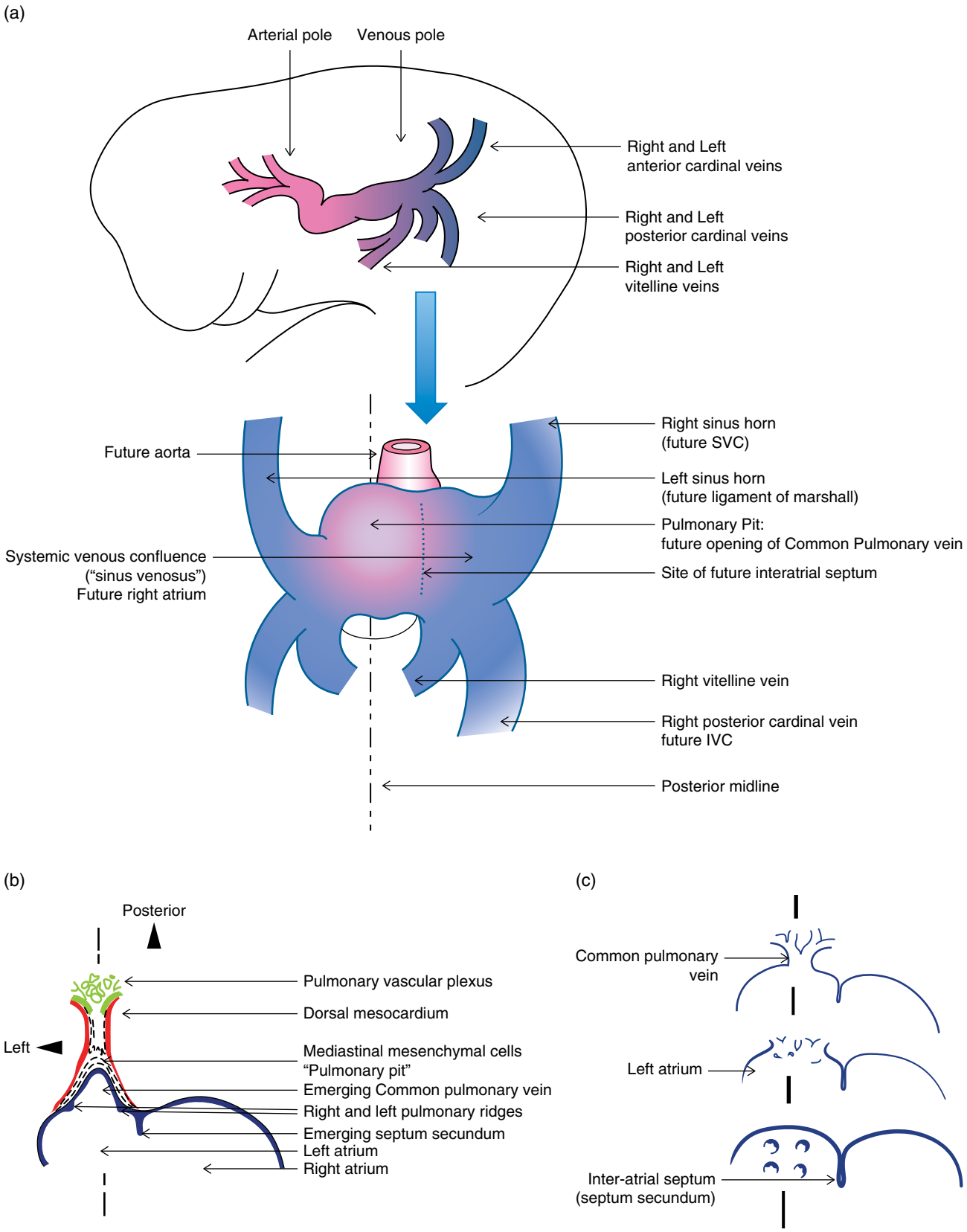

Figure 3.2 (a) Schematic depiction of the cardiac tube in a developing embryo at 22–24 days. Early stages of looping of the tube. The arterial pole is located in the cranial region of the tube, whereas the venous pole is on the opposite site. At the level of the posterior wall of the future left atrium, a pulmonary pit (*red*) starts growing. It will progressively give rise to the common pulmonary vein. *Source:* Modified from Sherif. *Eur J Cardiothorac Surg* 2013;**44**:792–9. Reproduced with permission of Oxford University Press. (b) Cross-section at the level of the developing atria in a six-week-old human embryo. The pulmonary pit of the left atrial wall (*blue*) is growing and tends to fuse with some elements of the pulmonary vascular plexus (*green*) at the level of the future mediastinal myocardium originating from the mesenchymal cells of the posterior mesocardium (*black*). After two more weeks, the left atrial wall will incorporate the common pulmonary vein and its first bifurcation, thus leading to four separate openings of the pulmonary veins (c). *Source:* Sherif. *Eur J Cardiothorac Surg* 2013;**44**:792–9. Reproduced with permission of Oxford University Press.

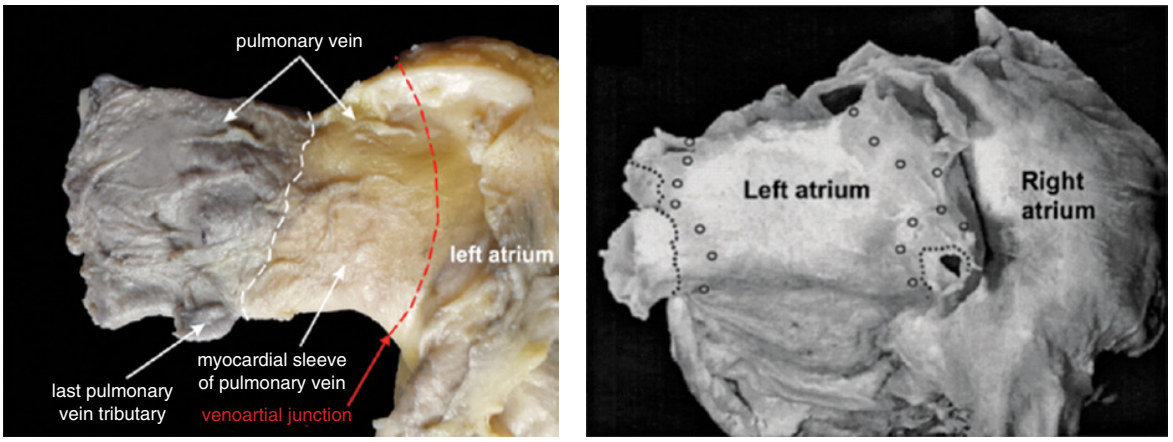

Figure 3.3 Details regarding the presence of the myocardial sleeves in the pulmonary veins. (*Left*) Photograph of the left superior pulmonary vein in a cadaveric heart specimen; evidence of the myocardial sleeves. *Source:* Klimek-Piotrowska et al. *PeerJ* 2016;**4**:e1579. https://peerj.com/about/contact/. Licensed under CC BY 4.0. (*Right*) Posterior aspect of a cadaveric heart specimen. The epicardium has been removed and the different extension of the atrial musculature over the four pulmonary veins to form the myocardial sleeves is shown. The broken lines mark the extent of the sleeves over the veins. The circles mark the veno–atrial junction. *Source:* de Bakkera et al. *Cardiovasc Res* 2002;**54**:287–94. Reproduced with permission of Oxford University Press.

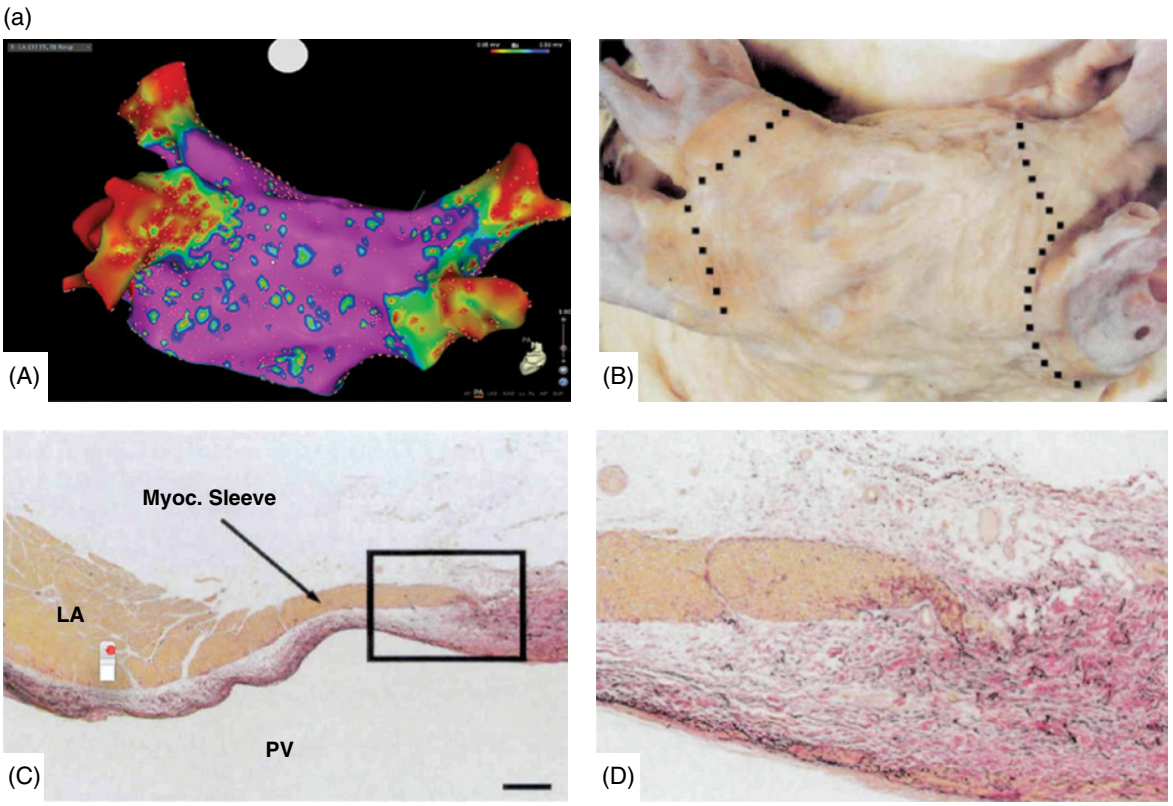

Figure 3.4 (a) Details regarding the presence of myocardial sleeves in the pulmonary arteries. (*Panel A*) Multipolar high-density CARTO mapping (obtained using Confidense software and a multipolar Pentaray catheter) of the left atrium belonging to an atrial fibrillation patient; posterior view. In the four pulmonary veins, a significant difference in the distribution of the areas of valid atrial potentials corresponding to the myocardial sleeves (*purple*) is visible. (*Panel B*) Gross dissection of the left atrial muscular fiber arrangement (the dotted lines mark the atrial–venous junctions). In both panels A and B, a higher density of sleeves is visible inside the right and left upper vein and left lower vein, whereas the right lower vein appears nearly devoid of them. (*Panels C and D*) Microscopic appearance (elastic van Gieson stain; two different magnifications) of the myocardial sleeves in a left atrial human specimen, extending along a pulmonary vein on the adventitial side. LA, left atrial myocardium; Myoc. Sleeve, myocardial sleeve; PV, pulmonary vein. *Source:* Panels B, C, and D modified from Saito et al. J *Cardiovasc Electrophysiol* 2000;**8**:888–94. Reproduced with permission of John Wiley & Sons. (b) Details of the anatomical and electrophysiological mapping features of the myocardial sleeves in different pulmonary veins. (*Panel A*) Anatomical heart specimen showing a relevant amount of sleeves getting into the left upper pulmonary vein (*black stars*); the venous–atrial junction is shown by a dotted line. (*Panel B*) Multipolar high-density CARTO mapping (obtained using Confidense software and a multipolar Pentaray catheter) of the left upper pulmonary vein in an atrial fibrillation patient. Wide areas of valid atrial potentials corresponding to the myocardial sleeves are visible (*white stars in purple areas*). (*Panel C*) Anatomical heart specimen showing a small amount of sleeves going into the right lower pulmonary vein (*black stars*); the venous–atrial junction is shown by a dotted line. (*Panel D*) Multipolar high-density CARTO mapping (obtained using Confidense software and multipolar Pentaray catheter) of the right lower pulmonary vein in an atrial fibrillation patient. A lower amount of valid atrial potentials corresponding to the myocardial sleeves is present (*white star in purple area*). *Source:* Panels A and C modified from Saito et al. J *Cardiovasc Electrophysiol* 2000;**8**:888–94. Reproduced with permission of John Wiley & Sons.

(b)

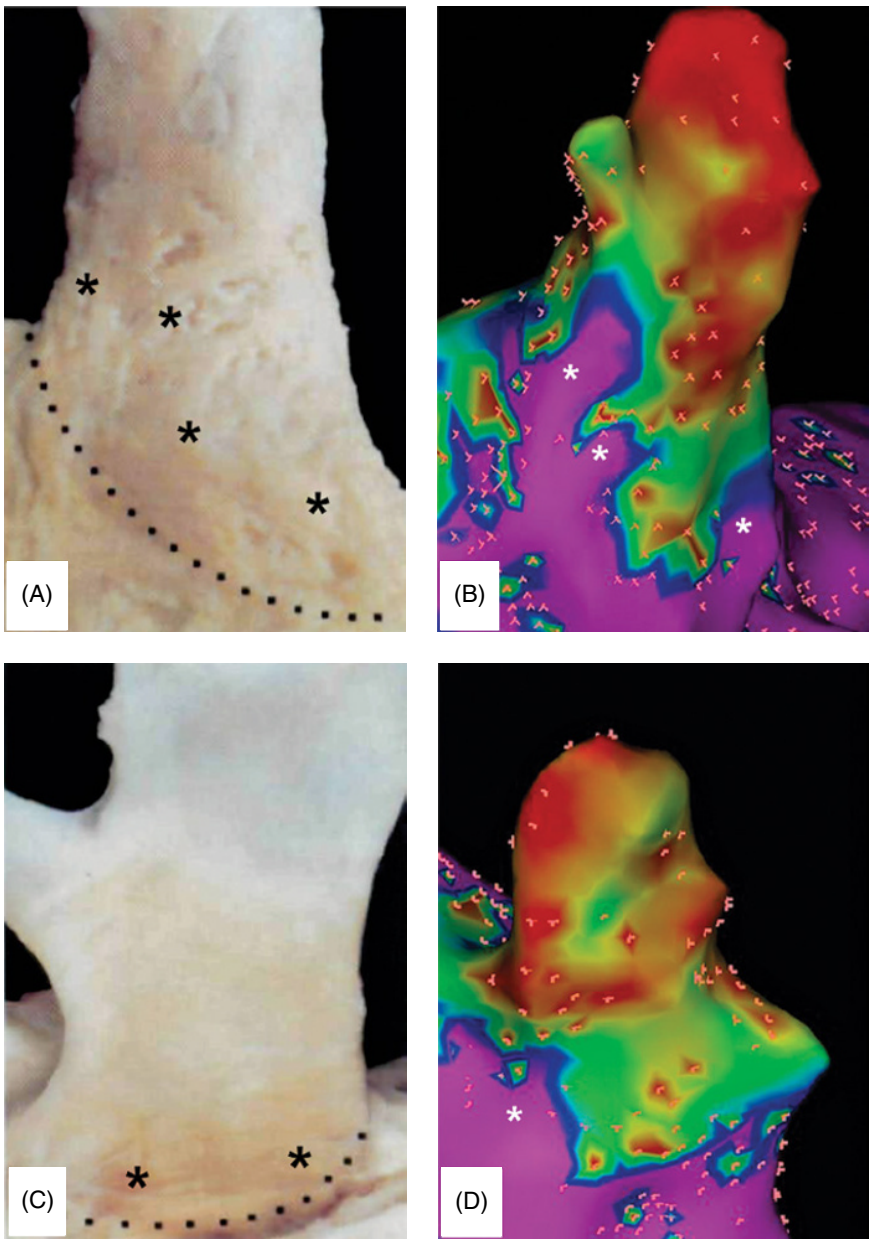

Figure 3.4 *(Cont'd)*

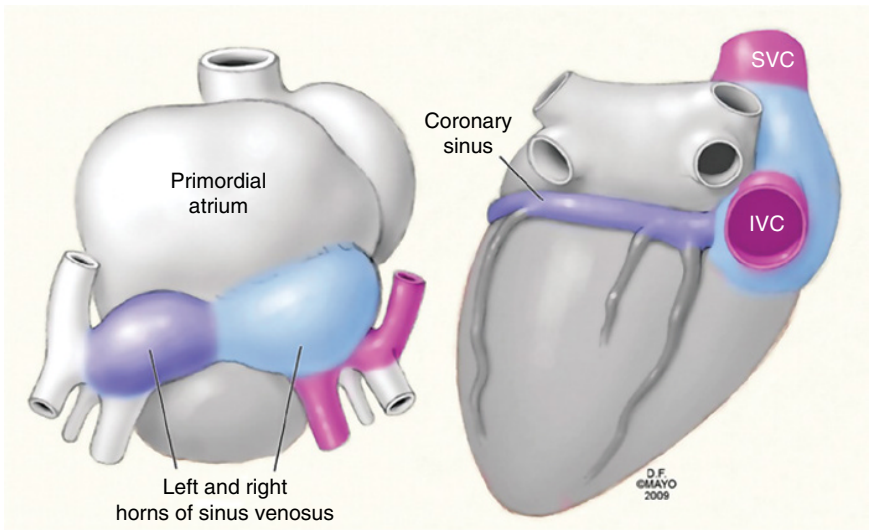

Figure 3.5 Schematic depiction of the coronary sinus development in the human embryo (26 weeks) and its final anatomy in the adult. The right horn of the sinus venosus gives rise to the venous portion of the right atrium (*light blue*) between the superior and inferior vena cava (*purple*). The left horn of the sinus venosus gives rise to the coronary sinus and to part of the great cardiac vein (*dark blue*). *Source:* Habib et al. [2]. Reproduced with permission of Oxford University Press.

that is associated with several arrhythmogenic settings since it carries multiple electrical connections to the left atrium.

Once the migration of the primitive pacemaker cells to the sinus venosus is completed, these cells can be observed in two different areas. The right-sided one evolves to the definitive sinoatrial node, while the left-sided one progressively shifts down towards a lower left atrial territory near the coronary sinus. Therefore, the ability of this tissue to replace, in some situations, the leading electrical activity of the sinoatrial node could justify a certain number of arrhythmias.

Conclusion

The electrical excitability of the cardiac cells is potentially widespread in almost every district of the fully developed heart. Nevertheless, the proximal extremity of the cardiac muscle (at the boundary with the main venous) shows an amplification of this feature, thus leading to abnormally high excitation and/or conduction patterns. Such pathological traits account for the frequent observation of arrhythmogenic phenomena in that setting. Therefore, knowledge of the embryogenetic pathways concerning this critical area is very important for interventional electrophysiologists, not only to understand the underlying mechanisms of the arrhythmogenic substrate, but also to better determine a therapeutic strategy.

References

1 Christoffels VM, Moorman AF. Development of the cardiac conduction system: why are some regions of the heart more arrhythmogenic than others? *Circ Arrhythm Electrophysiol* 2009;**2**:195–207.

2 Habib A, Lachman N, Christensen KN, Asirvatham SJ. The anatomy of the coronary sinus venous system for the cardiac electrophysiologist. *Europace* 2009;**11** Suppl 5:15–21.

Further Reading

Bockman DE, Redmond ME, Kirby ML. Alteration of early vascular development after ablation of cranial neural crest. *Anat Rec* 1989;**225**:209–17.

Campbell M, Deuchar DC. The left-sided superior vena cava. *Br Heart J* 1954;**16**:423.

Chen PS, Wu TJ, Hwang C, *et al*. Thoracic veins and the mechanisms of non-paroxysmal atrial fibrillation. *Cardiovasc Res* 2002;**54**:295–301.

Cheng G, Litchenberg WH, Cole GJ, Mikawa T, Thompson RP, Gourdie RG. Development of the cardiac conduction system involves recruitment within a multipotent cardiomyogenic lineage. *Development* 1999;**126**:5041–9.

Christoffels VM, Burch JBE, Moorman AF. Architectural plan for the heart: early patterning and delineation of the chambers and the nodes. *Trends Cardiovasc Med* 2004;**14**:301–7.

De Jong F, Opthof T, Wilde AAM, Janse MJ, Charles R. Persisting zones of slow impulse conduction in developing chicken hearts. *Circ Res* 1992;**71**:240–50.

Farrell M, Waldo K, Li YX, Kirby ML. A novel role for cardiac neural crest in heart development. *Trends Cardiovasc Med* 1999;**9**:214–20.

Gittenberger-de Groot AC, Bartelings MM, Deruiter MC, Poelmann RE. Basics of cardiac development for the understanding of congenital heart malformations. *Pediatr Res* 2005;**57**:169–76.

Gourdie RG, Harris BS, Bond J, *et al*. Development of the cardiac pacemaking and conduction system. *Birth Defects Res C Embryo Today* 2003;**69**:46–57.

Hatcher CJ, Basson CT. Specification of the cardiac conduction system by transcription factors. *Circ Res* 2009;**105**:620–30.

Ho SY, Sanchez-Quintana D, Cabrera JA, Anderson RH. Anatomy of the left atrium: implications for radiofrequency ablation of atrial fibrillation. *J Cardiovasc Electrophysiol* 1999;**10**:1525–33.

Jongbloed MR, Mahtab EA, Blom NA, Schalij MJ, Gittenberger-de Groot AC. Development of the cardiac conduction system and the possible relation to predilection sites of arrhythmogenesis. *Sci World J* 2008;**8**:239–69.

Jongbloed MR, Schalij MJ, Poelmann RE, *et al*. Embryonic conduction tissue: a spatial correlation with adult arrhythmogenic areas. *J Cardiovasc Electrophysiol* 2004;**15**:349 –55.

Mirzoyev S, McLeod CJ, Asirvatham SJ. Embryology of the conduction system for the electrophysiologist. *Indian Pacing Electrophysiol J* 2010;**10** (8):329–38.

Momma K, Linde LM. Abnormal rhythms associated with persistent left superior vena cava. *Pediatr Res* 1969;**3**:210–16.

Moorman AF, Christoffels VM. Cardiac chamber formation: development, genes, and evolution. *Physiol Rev* 2003;**83**:1223–67.

Moorman AF, Lamers WH. Molecular anatomy of the developing heart. *Trends Cardiovasc Med* 1994;**4**:257–64.

Moorman AF, de Jong F, Denyn MFJ, Lamers WH. Development of the cardiac conduction system. *Circ Res* 1998;**82**:629–44.

Moorman AF, Christoffels VM, Anderson RH. Anatomic substrates for cardiac conduction. *Heart Rhythm*, 2005;**2**:875–86.

Nakamura T, Colbert MC, Robbins J. Neural crest cells retain multipotential characteristics in the developing valves and label the cardiac conduction system. *Circ Res* 2006;**98**:1547–54.

Nattel S. Basic electrophysiology of the pulmonary veins and their role in atrial fibrillation: precipitators, perpetuators, and perplexers. *J Cardiovasc Electrophysiol* 2003;**14**:1372–5.

Perez-Lugones A, McMahon JT, Ratliff NB, *et al*. Evidence of specialized conduction cells in human pulmonary veins of patients with atrial fibrillation. *J Cardiovasc Electrophysiol* 2003;**14**:803–9.

Van Mierop LHS. Localization of pacemaker in chick embryo heart at the time of initiation of heartbeat. *Am J Physiol* 1967;**212**:407– 15.

Waldo K, Zdanowicz M, Burch DH, Kumiski HA, Stadt RE. A novel role for cardiac neural crest in heart development. *J Clin Invest* 1999;**103**:1499–507.

Webb S, Kanani M, Anderson RH, Richardson MK, Brown NA. Development of the human pulmonary vein and its incorporation in the morphologically left atrium. *Cardiol Young* 2001;**11**:632–42.

Zipes DP, Knope RF. Electrical properties of the thoracic veins. *Am J Cardiol* 1972;**29**:372–6.

4

The Impact of Embryology and Anatomy on Cardiac Electrophysiology

Maxim Didenko[1] and Fred Kusumoto[2]

[1] *Kuprianov's Cardiovascular Surgery Clinic, Military Medical Academy, Saint Petersburg, Russia; Department of Cardiology, Cardiovascular Research Institute Maastricht (CARIM), Maastricht University Medical Center, The Netherlands*
[2] *Heart Rhythm Services, Department of Cardiovascular Disease, Mayo Clinic, Jacksonville, FL, USA*

Summary

Our understanding of the embryology of the heart and the importance of complex signaling processes required for cardiac development has improved dramatically over the last decade. Accurate knowledge of the heart embryology and anatomy, supplemented with modern imaging techniques, helps delineate individual anatomy and will likely improve outcomes and reduce complications. The specialized conduction tissues have specific morphological features such as fewer sarcomeres and latent automaticity. However, all cardiac tissues (conduction tissues, atrial and ventricular myocardium) appear to develop from one elementary source of cardiac cells. Genetic abnormalities can lead to specific disorders such as channelopathies and also to anatomical abnormalities. Several genes have been associated with incomplete formation of the fibrous annulus and persistent atrioventricular connections anatomically located away from the penetrating bundle and the Wolff–Parkinson–White syndrome phenotype. Clinical electrophysiologists have identified certain regions of the heart that have specific embryological features and appear to be associated with arrhythmias: the pulmonary veins, crista terminalis, right and left ventricle outflow tracts, and papillary muscles. This chapter summarizes some important aspects of embryology and anatomy of the heart in the context of heart rhythm disorders and their management in clinical electrophysiological practice, with special attention to the anatomy of the pulmonary veins. In addition, historical differences in anatomical nomenclature that can lead to misunderstanding in communication between different specialists will also be addressed.

Introduction

Cardiac embryology and anatomy play a fundamental role in our understanding of clinical electrophysiology and cardiac mapping. Over the last decade, there has been a paradigm shift in embryological research from morphological and histological descriptions of developmental changes to a deeper understanding of the mechanistic processes that mediate these changes. A more complete understanding of the embryological process has provided insight into anatomy which has already translated into changes at the bedside and, in the future, will likely provide clues for novel strategies in arrhythmia management.

Embryology

Development of the cardiac conduction system

The cardiac conduction system is associated with congenital abnormalities linked to arrhythmias such as atrioventricular (AV) septal defects, Ebstein's anomaly, and the Wolff–Parkinson–White syndrome. All components of the system appear to develop from the same source as the atrial and ventricular myocardium so that all cardiac cells have one origin from elementary cardiac cells [1–3]. The suggestion that the cells of the heart conduction system have a neural crest origin has not been supported by evidence although nerve ganglia subtending the conduction system and myocardium are derived from the neural crest [4].

During development, the cardiac conduction system transforms from a simple tube characterized by peristaltic contraction and sinusoidal depolarization to a complex four-chambered structure with sequential contraction due to multiple specialized cells with characteristic depolarization patterns. Although there are differences in the cardiac conduction system among different mammals, the earliest part of development is generally conserved in vertebrates and mediated by the complex interplay of a number of different molecules.

Although macroscopically still a "tube," the atria and ventricles develop from specific areas of growth and these areas develop sodium channels (Scn5a) and are connected by high conductance gap junctions (aggregation

Cardiac Mapping, Fifth Edition. Edited by Mohammad Shenasa, Gerhard Hindricks, David J. Callans, John M. Miller, and Mark E. Josephson.

Companion website: www.wiley.com/go/cardiacmapping5e

of Cx 40 and Cx 43 connexins) that allow rapid depolarization and contraction of these tissues. This process is not observed in the inflow region or the "waist-like" endocardial cushion that will eventually develop into the specialized AV components of the cardiac conduction system.

The sinus node develops within the sinus venosus due to a number of transcription factors including the T-box family (Tbx5 and Tbx3) [1,5,6].The T-box proteins are characterized by a highly conserved 180 amino acid sequence that binds DNA and are critical for embryological development. Additional transcription factors also important in this complex process include short stature homeox transcription factor 2 (Shox2), and bone morphogenetic protein 2 (Bmp2), among others [5]. Expression of these factors appears to initiate a set of gene programs that actively suppress Cx40, Cx43, and Scn5a production and instead encourage calcium channel (Cacna1g) and potassium channel (Hcn4) and production of Cx30.2 (a connexin associated with slower intercellular conduction). In addition, it appears that the pituitary homeobox-2 (Pitx2) gene that regulates left–right organ asymmetry is one of the main factors responsible for development of the sinus node in the right atrium [5,6].

A similar process of suppression of atrial and ventricular phenotypes also occurs at the myocytes at the "waist" of the tube that will eventually be the precursor of the AV canal area. Myocytes in these regions appear to be protected from the processes that lead to more advanced development due to the physical barrier formed from cardiac jelly. As a consequence, these myocytes do not develop abundant Na^+ ion channels and Cx40 and Cx43 expression and instead undergo a similar gene program as described for the sinus node region.

The specialized conduction tissues in the ventricle develop in a thin layer just below the endocardium and appear to be derived from portions of AV canal tissue that extend into the primitive ventricle. The specialized conduction tissue has some specific morphological features similar to sinus node and AV node tissues, such as fewer sarcomeres and latent automaticity. However, the cells differ from these tissues and have high expression of Scn5a and Cxn40 that along with other cellular architecture properties mediate the fast conduction properties characteristic of these cells. There is significant heterogeneity among vertebrates for specialized conduction tissue in the ventricle. For example, the Purkinje network is only observed in birds and mammals [5].

Congenital abnormalities of AV conduction and accessory pathways

Although the heart initially can be described as a tube with an outer layer of myocytes and an inner layer of endocardium separated by cardiac jelly, regional tissue proliferation and development of the cardiac cushion lead to a "dumbbell" shape that ultimately folds on itself to produce the characteristic four-chamber anatomy in the developed heart. The atria and ventricles are separated electrically by the formation of the fibroadipose tissues. In humans, some collagenous cords can be found inferolaterally to support the posterior leaflet of the mitral valve but no "fibrous skeleton" is present, although actual bony elements can be found in some large bovines [7]. The penetrating bundle is normally the only tissue that allows electrical conduction from the atria to the ventricles. The AV node forms the atrial portion of this region and develops from the embryological processes described above for the AV canal region. Morphologically, these cells have sparse mitochondria, a poorly developed sarcoplasmic reticulum and poorly organized actin and myosin filaments.

Several inherited diseases of the conduction system are associated with AV block, including mutations of genes that express Na^+ channels (Scn5a) and K^+ channels (Kcnj2) [8]. Abnormalities of Tbx5 cause Holt Oram syndrome: secundum atrial septal defect, progressive AV block, and upper limb abnormalities often involving the radius and thumb [5].

Several genes have been associated with incomplete formation of the fibrous annulus and persistent AV connections anatomically located away from the penetrating bundle and the Wolff–Parkinson–White syndrome phenotype. Over a decade ago, the association between mutations of the PRKAG2 gene and the Wolff–Parkinson–White syndrome was reported [9,10]. The PRKAG2 encodes for an adenosine monophosphate-activated protein kinase (AMPK). It has been postulated that ventricular preexcitation occurs because of incomplete annular formation due to glycogen deposition. It appears that timing of overexpression of mutant PRKAG2 is critical, since animal models in which the mutant PRKAG2 was overexpressed in adulthood resulted in progressive AV conduction disease but no development of AV accessory pathways [11]. More recently, it has been shown that inactivation of the Tbx2 transcription factor is associated with incomplete formation of the fibrous annulus and ventricular preexcitation via AV accessory pathways [12]. Similarly, interruption of the ubiquitous Wnt signaling system (approximately 20 different proteins involved in regulating beta-catenin; the name is derived from two drosophila phenotypes: *wingless* and *int*) also is associated with abnormal AV annulus formation and the Wolff–Parkinson–White phenotype [13].

Embryological origins of arrhythmogenic regions

Clinical electrophysiologists have identified certain regions of the heart that appear to be associated with

arrhythmias. It is interesting to examine the embryological development of these regions for possible clues and explanations of the underlying pathophysiology (Figure 4.1).

- The *pulmonary veins* (PVs) and the *posterior left atrium* (LA) have been identified in clinical studies as a common source for atrial fibrillation and atrial tachycardias. Pulmonary vein development occurs at approximately the third week and is coincident with development of the lung vasculature [1,5,9]. The posterior smooth portion of the left atrium and PVs (as well as lungs) form from the splanchnic plexus and then connect with the primitive LA (which becomes the left atrial appendage). Initially, the pulmonary veins develop as a single orifice adjacent to the left AV junction. Unlike mice, in humans as the right and left lungs develop, four separate orifices located more dorsally and to the roof of the left atrium develop and replace the common pulmonary vein. The pulmonary veins have distinct electrophysiological characteristics when compared to left atrial tissue or the sinus venosus and include differences in automaticity, smaller phase 0 upstrokes, and shorter action potential durations (Figure **4.2**). These differences appear to be mediated in part by a different initial genetic program [1,9]. Early expression of Nkx2-5 and Cx40 appears to be critical for the development of pulmonary vein tissue and these factors are not present in the sinus venosus. The pituitary homeobox (Pitx) family has also been implicated as an important embryological factor associated with arrhythmogenesis. One Pitx isoform (Pitx2c) is expressed in the embryonic pulmonary veins and posterior left atrium. Absent or decreased Pitx2c during development is associated with development of atrial

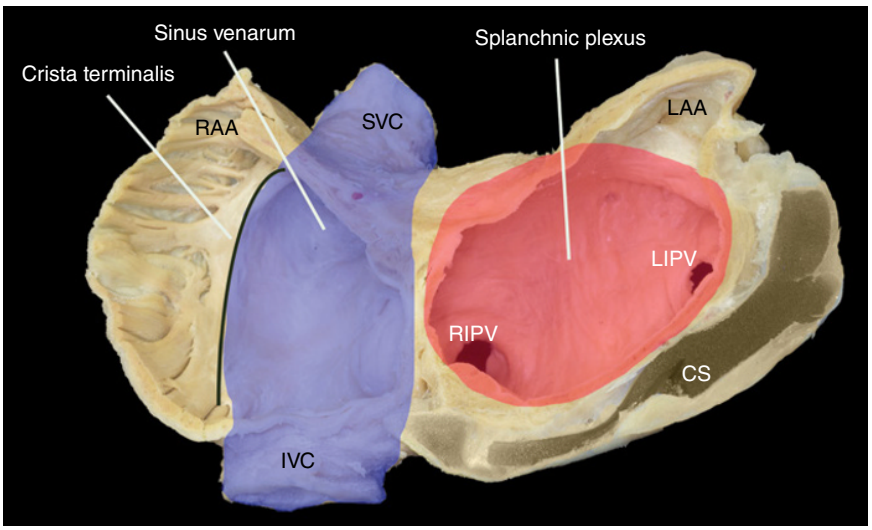

Figure 4.1 Diagramatic representation of the different types of myocardium in the atrial walls on the plastinated specimen of atriums. CS, coronary sinus; IVC, inferior vena cava; LAA, left atrial appendage; LIPV, left inferior pulmonary vein; RAA, right atrial appendage; SVC, superior vena cava; RIPV, right inferior pulmonary vein; SVC, superior vena cava. Black line represents the crista terminalis; blue: atrium myocardium developed from sinus venarum; red: myocardium from splanchnic plexus.

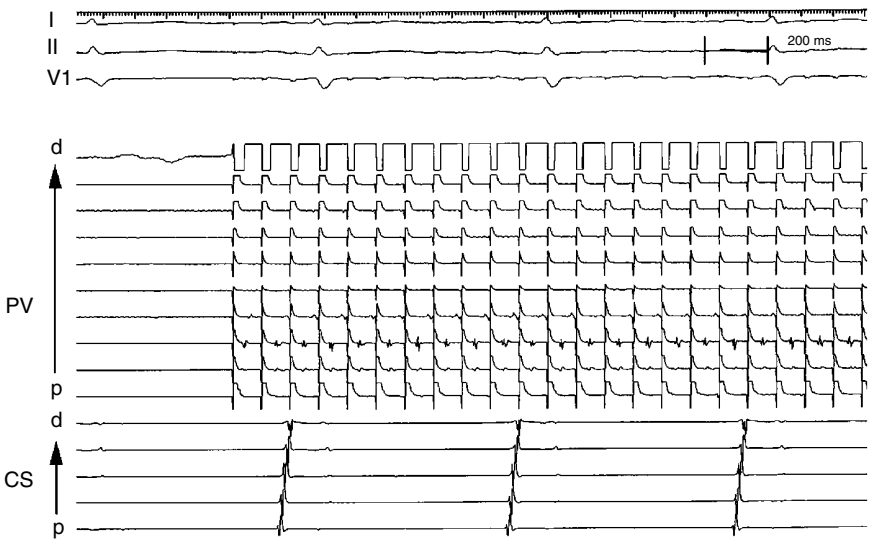

Figure 4.2 Rapid pacing from electrode pair 1,2 of a circular mapping catheter at a cycle length of 90 ms is associated with 1:1 capture, best seen in electrode pairs 15,16 and 17,18. Notice that the pulmonary vein remains isolated with no change in the sinus rate. *Source:* Reproduced with permission from Kusumoto FM. *Understanding Intracardiac EGMs: A Patient Centered Guide*. New York: Wiley, 2015.

fibrillation in adult mice [14]. It is interesting that Pitx2c controls expression of the K^+ channel gene Kcnq1 and that gain-of-function mutation of Kcnq1 has been reported in patients with familial atrial fibrillation [15].

- The venous part of the *right atrium* (RA) as well as the coronary sinus and caval veins originate from a sinus venarum and then connect to the primitive RA, which will be the RA appendage, along the *crista terminalis*. The most abundant connexin in atrial tissue is Cx40. Ectopic impulse formation has been described in knockout (Cx40-/-) mice, suggesting a possible mechanism for atrial tachycardias that can be observed in this region.
- The *right and left outflow tracts* in ventricles form from the connection of the truncus arteriosus to the muscular portions of the ventricles and septation. There are differences in the genetic programs between the left and right outflow tracts, with Tbx5 expressed in the left ventricular outflow tract but not the right. In addition, it has been recognized for many years that the myocytes in the outflow tract regions develop fast conduction properties relatively late in development and the initial cardiac myocytes recruited for outflow tract elongation are morphologically primitive with poorly developed sarcomeres. Some have speculated that a higher likelihood of retaining an embryological phenotype may contribute to the automaticity frequently noted in the outflow tracts [1,9].
- *Papillary muscles* originate from endocardial cushions and then connect with the trabecular part of ventricles at their bases. By five weeks gestation, the primitive left ventricle has significant trabeculae and by seven weeks a prominent horseshoe-shaped ridge can be observed with either end of the horseshoe contiguous with the AV cushions [16]. At approximately eight weeks gestation, the ridge begins to separate from the rest of the ventricular myocardium to form the beginnings of a recognizable papillary muscle. The molecular mechanisms underlying this process are poorly understood.

Anatomical and embryological correlates: practical applications in clinical electrophysiology

There are some common anatomical structures that can lead to misinterpretation when using intracardiac echocardiography or other imaging technologies during electrophysiology studies and also impede catheter manipulation. There are several normal anatomical structures and some minor abnormalities (without significant circulation disorders) in the heart that are embryonic remnants.

During early development the right valve of the sinus venosus forms the border between the right horn of the sinus venosus and the primitive right atrium. The valve is gradually absorbed but the original location of the valve can be identified in the fully developed heart superiorly and anteriorly by the crista terminalis, inferiorly by the Eustachian valve, and continuing more septally by the Thebesian valve. The crista terminalis begins at the anterior ostium of the superior vena cava and courses along the lateral wall toward the anterior ostium of the inferior vena cava (IVC), where it connects contiguously to the Eustachian valve. The crista terminalis defines the border between the venous portion of the RA and the trabecular part of the RA (the right atrial appendage) and can be mistaken for a tumor or thrombus. During embryological development the crista terminalis connects the sinus venosus and primitive RA. It is also important to keep in mind that the thickness of the right atrial appendage (RAA) varies dramatically from several millimeters at the pectinate muscles to "paper thin" in the crevices that separate the pectinate muscles, with obvious implications for catheter manipulation.

The Eustachian valve directs oxygen-rich blood from the placenta to the foramen ovale from the IVC in the embryo and thus shunts blood away from the right ventricle. The Eustachian valve was first described by the Italian anatomist Bartolomeo Eustachi in the early 1500s as a crescent-like structure on the anterior portion of the IVC, attaching on the atrial septum near the coronary sinus. The Eustachian valve can vary dramatically in thickness, width, and height, and is extremely important during cavotricuspid isthmus ablation for typical atrial flutter since it often "protects" the most proximal portion of this region (Figure 4.3). In addition, a prominent Eustachian valve can extend well into the apparent right

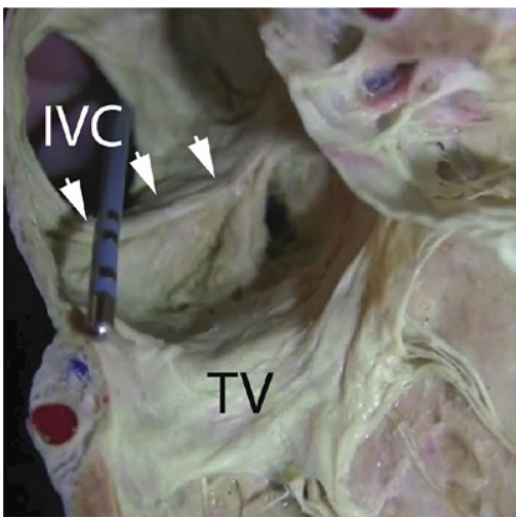

Figure 4.3 Cavotricuspid isthmus. Arrows show the Eustachian valve. IVC, inferior vena cava; TV, tricuspid valve.

atrium and can impede free catheter manipulation in this chamber.

Continuing septally, the final remnant of the right valve of the sinus venosus is the Thebesian valve at the inferior and posterior portion of the coronary sinus os. This valve can be quite variable, from almost absent to almost fully covering the coronary sinus orifice; in a recent anatomical study using magnetic resonance imaging, investigators were able to identify a Thebesian valve in 46% of patients and in 17% of patients the valve was net-like or completely covered the coronary sinus, which would have important implications for coronary sinus cannulation during electrophysiology studies or left ventricular lead placement [17].

An important embryonic remnant of the right valve of the sinus venosus that can also cause confusion in the electrophysiology laboratory is the Chiari network. In approximately 2–4% of patients, incomplete resorption of the right valve is associated with a net-like lattice of tissue that can be observed as an extension of the Eustachian valve and often extends to the coronary sinus [18]. Hans Chiari initially described this anatomical variant in 1897. This structure can also impede catheter manipulation in the right atrium.

Atrial septation is a complex process and a detailed discussion is beyond the scope of this review [19]. However, *in utero* the fossa ovalis allows oxygenated blood to flow from the right atrium to the left atrium and away from the right ventricle. The thin septum secundum is the usual point of entry for electrophysiologists and other interventional cardiologists to access the left atrium. Another septal structure is Bachmann's bundle located on the superior and anterior position of the left atrium. The fibers within Bachmann's bundle travel from the right atrial appendage, from the region of the sinus node as well as from septum surface of the RA, between the aorta and superior vena cava to end at the left atrial appendage (LAA) (Figure 4.4). Conduction velocity along Bachmann's bundle is approximately 20% faster than in other parts of the atrium myocardium and provides rapid depolarization of the left atrium. The rapid conduction appears to be due to parallel orientation of the myocytes and other architectural features and not because of differences in ion channel populations. The embryological mechanism for Bachmann's bundle development has not been well studied but a preliminary study using immunological markers found that it has similarities to conduction tissue in the AV node [20]. It has been suggested that Bachmann's bundle is an important component of unstable reentrant circuits in persistent atrial fibrillation (AF) [21].

Normally, the left sinus horn and the cardinal vein become smaller during development to form the coronary sinus (CS). In 0.3–0.5% of the population, this process will not complete and result in a persistent left-sided

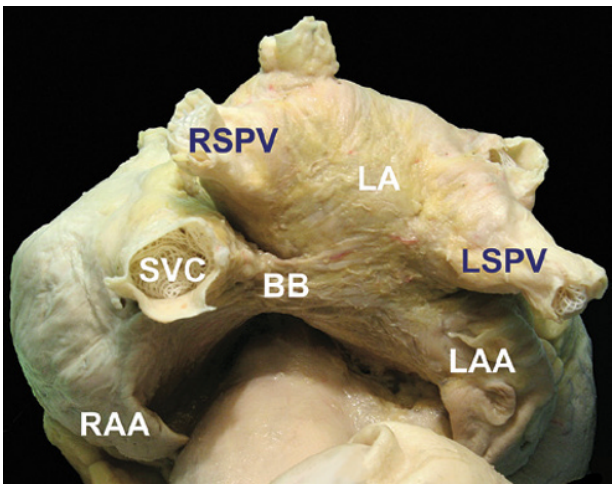

Figure 4.4 Anatomical specimen of human right and left atriums (superior view). Bachmann's bundle (BB) is a group of muscular fibers at the anterosuperior margin of the intraatrial septum. Notice the close relationship of left superior pulmonary vein (LSPV) and left atrial appendage (LAA). LA, left atrium; RAA, right atrial appendage; SVC, superior vena cava.

superior vena cava [22]. Several case reports have reported abnormal automaticity and associated atrial arrhythmias from sites within the persistent left superior vena cava [23].

The smooth part of the left atrium originates from the splanchnic plexus and connects to the LAA, which is formed from primitive left atrium. The LAA is anterior and caudal to the left superior pulmonary vein (LSPV) and in between is the left atrial ridge. Due to its close relationship and superimposition in the left anterior oblique fluoroscopic projection, the LSPV can be confused with the LAA. Generally, the LSPV is characterized by the ability to place a guidewire or catheter outside the cardiac silhouette but it is important to remember that exceptions exist and a portion of the LAA can appear to be outside the cardiac silhouette. The parallel orientation of the anterior LSPV with the posterior wall of the LAA can lead to the appearance of an apparent distinct linear band identified on echocardiography (often called a Coumadin ridge or Q-tip sign) that can sometimes be mistaken for an intracardiac mass.

As previously discussed, the PVs and posterior wall of the LA form from the splanchnic plexus, which is also the origin for the lungs. This fact explains the similar orientation of the PVs from their corresponding lung lobes. Three right lung lobes are the likely reason that a third PV, a right middle PV, is frequently observed (about 15–30%) in the right-sided pulmonary venous system. Moreover, for both the right and left lungs, the superior lobes are located more anterior than the lower lobes. This relationship between the upper and lower lobes is the main reason for the relative anterior angulation of superior PVs when compared to the more posterior

angulation of inferior PVs. In some patients, the LSPV and left infeior pulmonary vein (LIPV) can only be identified in the right anterior oblique (RAO) projection by identifying the LSPV by its anterior direction and the LIPV by its more posterior direction.

Anatomical considerations

Nomenclature

Historically, anatomical nomenclature has been developed by anatomists and surgeons, who viewed the heart outside the body with the apex of ventricles oriented inferiorly, the atria superiorly, with the "right chambers to the right, left chambers to the left," often referred to as the Valentine orientation [19]. Although originally useful, with the advent of advanced imaging modalities such as computed tomography and magnetic resonance imaging and the ability to visualize the heart from myriad different angles, describing the heart in this manner often complicates discussion. For this reason, there has been a general trend and recommendation by all medical professional societies to use descriptors with the heart positioned in the body. This leads to some confusion since structures described as posterior in the Valentine orientation are actually inferior. For example, the posterior leaflet of the mitral valve is actually located inferiorly using modern nomenclature. As a general rule, it is more useful for clinical electrophysiologists to understand and use descriptors with the heart positioned in the body since fluoroscopy is most commonly used for catheter manipulation.

The left anterior oblique (LAO) projection is most useful for differentiating the left atrium and left ventricle (which are more posterior in the body cavity) from the right atrium and right ventricle (which are more anterior in the body cavity). Similarly, within the left atrium itself, the LAO projection is also helpful for distinguishing between the right-sided and left-sided pulmonary veins. An angle of 50° is a general approximation of a perpendicular view to the long axis of the heart for most people but significant variability exists. Catheters located in the coronary sinus and straddling the tricuspid valve are useful for confirming that the chosen LAO angle is perpendicular to the long axis of the heart.

Differentiation of the atria from ventricles usually requires the RAO projection and the coronary sinus catheter is helpful for confirming that the angle chosen is truly parallel to the long axis of the heart.

Finally, it is very important to correctly describe the movement of catheters during the procedure. For example, in the LAO projection when the catheter is moving to the right on the fluoroscopy screen, although this has traditionally been described as leftward movement, it would actually be better described as posterior and leftward. Conversely, leftward motion in this projection would actually represent anterior and rightward movement (Figure 4.5).

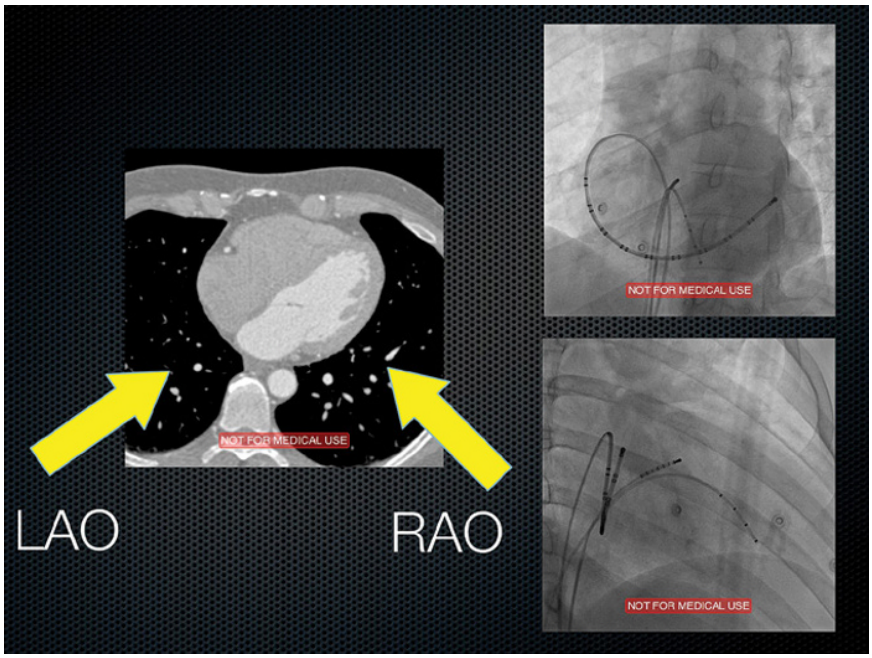

Figure 4.5 Orientation of the heart in the thorax and x-ray projections (*left panel*). Arrows represent direction of projections. (*Right upper panel*) Fluoroscopic view during EP procedure in left anterior oblique (LAO) projection. (*Right inferior panel*) Fluoroscopic view in right anterior oblique (RAO) projection.

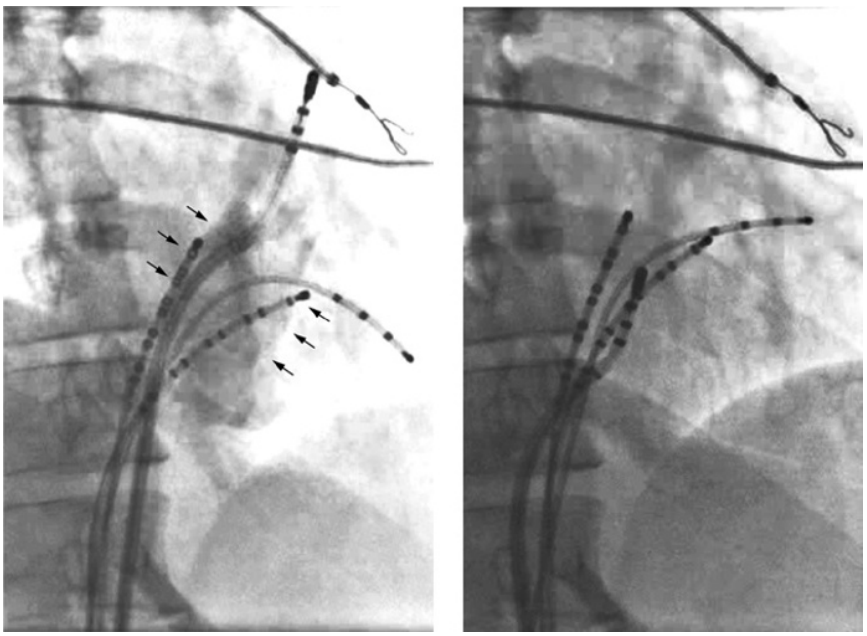

Figure 4.6 (*Left panel*) Angiogram of a patient with persistent left superior vena cava (arrows). (*Right panel*) Successful ablation site identified by slow pathway potentials and typical junctional echoes with a more superior fluoroscopic position than would be expected.

Triangle of koch

For many patients, management of AV node reentrant tachycardia (AVNRT) involves slow pathway modification of the AV node. In most cases, ablation is performed in the atrium between the CS and the tricuspid valve (TV) along the anterior wall of Koch's triangle. Since the TV is more apically displaced when compared to the mitral valve, this region is characterized by larger ventricular electrograms and smaller atrial electrograms. It is important to note that embryological variants can sometimes change the normal location of the slowly conducting pathway. In Figure 4.6, a patient with a persistent left superior vena cava and supraventricular tachycardia is shown. In this case, the slow pathway was likely located more superiorly as this site was associated with a slow pathway potential, typical echoes with retrograde fast pathway conduction were observed during ablation, and no evidence of slow pathway conduction was identified after the ablation.

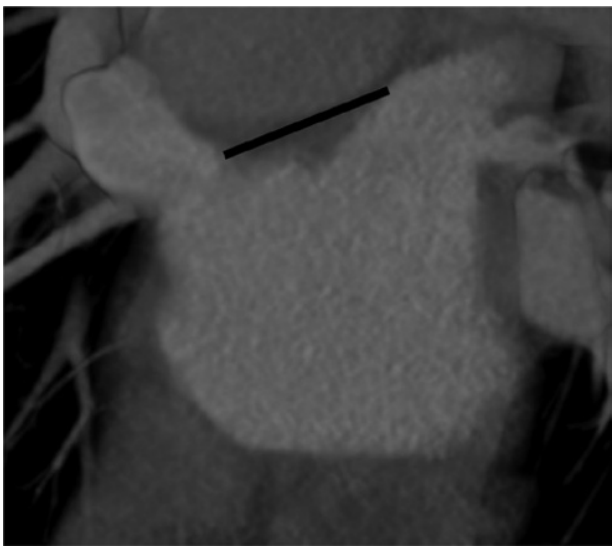

Figure 4.7 Computed tomography of the LA and ostia of superior left and right pulmonary veins. The roof of the LA (*black line*) has an oblique course since the right superior PV ostium is lower than the left superior PV ostium.

Pulmonary vein anatomy

Ablation of AF requires a complete understanding of the LA–PV junction. It is well described that ablation inside the vein itself can produce PV stenosis. The proliferative response to injury may be partially due to the different embryological source of this tissue. Unfortunately, the exact location of the pulmonary vein ostium can be difficult to define, as there is often a gradual change in the pulmonary vein diameter as it enters the left atrium. The roof of the left atrium has an oblique course and the left superior pulmonary vein has a higher take-off than the right superior pulmonary vein (Figure 4.7).

Since the posterior wall of the left atrium has similar embryological origins to the pulmonary veins, it is not surprising that atrial tachycardias can arise from this site. For this reason, some electrophysiologists

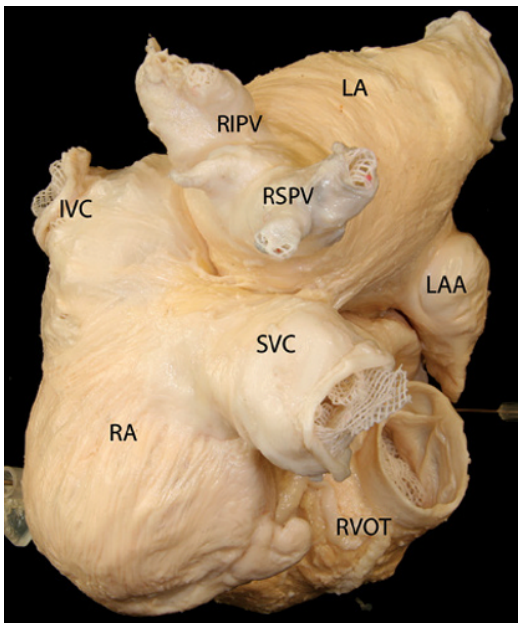

Figure 4.8 Right posterior view of the heart demonstrates the close relationship between the right superior pulmonary vein (RSPV) and the posterior right atrium (RA). IVC, inferior vena cava; LA, left atrium; LAA, left atrial appendage; RIPV, right inferior pulmonary vein; RVOT, right ventricular outflow tract; SVC, superior vena cava.

have advocated isolating all four pulmonary veins and the posterior left atrium as a single unit using a "box" lesion set. However, recent clinical studies have consistently shown that isolation of the pulmonary veins leads to similar outcomes as more aggressive lesion sets.

The LAA develops in the third week of gestation and is formed from the primitive left atrium. The primitive atrium can be identified morphologically by the presence of trabeculae that can be seen at the third week of gestation. The LAA is usually located anterior to the left superior pulmonary vein (see Figure 4.4) and has a much narrower base compared to the RAA. For the purposes of our discussion, the close relationship between the LSPV and LAA can make electrogram interpretation of pulmonary vein signals more difficult. In some cases electrograms recorded within the LSPV can be due to far-field LAA depolarization and may require pacing maneuvers to identify the specific source of an electrogram. Similarly, due to the close relationship between the right-sided pulmonary veins and the posterior right atrium, far-field signals can also be commonly observed in the RSPV (Figure 4.8).

Conclusion

Our understanding of the embryology of the heart and the important and complex signaling processes required for development have dramatically improved over the last decade. Already, the findings are providing clues for the pathophysiological basis of many arrhythmias. When coupled with a complete and clear understanding of anatomy, embryological principles are an important tool for the clinical electrophsyiologist for improving outcomes and avoiding complications. As our knowledge of embryology continues to expand, it is likely that we will be able to treat arrhythmias more mechanistically, perhaps by targeting molecules involved directly during development.

References

1 Christoffels VM, Moorman AF. Development of the cardiac conduction system: why are some regions of the heart more arrhythmogenic than others? *Circ Arrhythm Electrophysiol* 2009;**2**(2):195–207.
2 De Haan RL. Differentiation of the atrioventricular conducting system of the heart. *Circulation* 1961;**24**:458–40.
3 Viragh Sz, Challice CE. The development of the conduction system in the mouse embryo heart. I. The first embryonic A-V conduction pathway. *Dev Biol* 1977;**56**:382–96.
4 Viragh Sz, Challice CE. The development of the conduction system in the mouse embryo heart. II. Histogenesis of the atrioventricular node and bundle. *Dev Biol* 1977;**56**:397– 411.
5 Van Weerd JH, Christoffels VM. The formation and function of the cardiac conduction system. *Development* 2016;**143**(2):197–210.
6 Van Weerd JH, Badi I, van den Boogaard M, *et al*. A large permissive regulatory domain exclusively controls Tbx3 expression in the cardiac conduction system. *Circ Res* 2014;**115**(4):432–41.
7 Spicer DE, Bridgeman JM,Brown NA, Mohun TJ, Anderson RH. The anatomy and development of the cardiac valves. *Cardiol Young* 2014;**24**:1008–22.
8 Priori SG, Wilde AA, Horie M, *et al*. HRS/EHRA/APHRS expert consensus statement on the diagnosis and management of patients with inherited primary arrhythmia syndromes: document endorsed by HRS, EHRA, and APHRS in May 2013 and by ACCF, AHA, PACES, and AEPC in June 2013. *Heart Rhythm* 2013;**10**(12):1932–63.
9 Postma AV, Christoffels VM, Bezzina CR. Developmental aspects of cardiac arrhythmogenesis. *Cardiovasc Res* 2011;**91**(2):243–51.
10 Gollob MH, Green MS, Tang AS, *et al*. Identification of a gene responsible for familial Wolff-Parkinson-White syndrome. *N Engl J Med* 2001;**344**(24):1823–31.
11 Arad M, Moskowitz IP, Patel VV, *et al*. Transgenic mice overexpressing mutant PRKAG2 define the cause of

Wolff-Parkinson-White syndrome in glycogen storage cardiomyopathy. *Circulation* 2003;**107**(22):2850–6.

12 Aanhaanen WT, Boukens BJ, Sizarov A, *et al*. Defective Tbx2-dependent patterning of the atrioventricular canal myocardium causes accessory pathway formation in mice. *Clin Invest* 2011;**121**(2):534–44.

13 Gillers BS, Chiplunkar A, Aly H, *et al*. Canonical wnt signaling regulates atrioventricular junction programming and electrophysiological properties. *Circ Res* 2015;**116**(3):398–406.

14 Wang J, Klysik E, Sood S, Johnson RL, Wehrens XH, Martin JF. Pitx2 prevents susceptibility to atrial arrhythmias by inhibiting left-sided pacemaker specification. *Proc Natl Acad Sci USA* 2010;**107**(21):9753–8.

15 Chen YH, Xu SJ, Bendahhou S, *et al*. KCNQ1 gain-of-function mutation in familial atrial fibrillation. *Science* 2003;**299**(5604):251–4.

16 Oosthoek PW, Wenink ACG, Wisse LJ, Gittenberger-de Groot A. Development of the papillary muscles of the mitral valve: morphogenetic background of parachute-like assymetric mitral valves and other mitral valve anomalies. *J Thorac Cardiovasc Surg* 1998;**116**:36–46.

17 Mlynarski R, Mlynarska A, Haberka M, Golba KS, Sosnowski M. The Thebesian valve and coronary sinus in cardiac magnetic resonance. *J Interv Card Electrophysiol* 2015;**43**(2):197–203

18 Devi Jansirani D, Shiva Deep S, Anandaraja S. Anatomical study of Chiari network and the remnant of left venous valve in the interior of right atrium. *Anat Res Int* 2015;**2015**:247680.

19 Anderson RH, Brown NA, Mohun TJ. Insights regarding the normal and abnormal formation of the atrial and ventricular septal structures. *Clin Anat* 2016;**29**:290–304.

20 Blom NA, Gittenberger-de Groot AC, DeRuiter MC, Poelmann RE, Mentink MM, Ottenkamp J. Development of the cardiac conduction tissue in human embryos using HNK-1 antigen expression: possible relevance for understanding of abnormal atrial automaticity. *Circulation* 1999;**99**:800–6.

21 Ogawa S, Dreifus LS, Osmick MJ. Longitudinal dissociation of Bachmann's bundle as a mechanism of paroxysmal supraventricular tachycardia. *Am J Cardiol* 1977;**40**:915–22.

22 Sheikh AS, Mazhar S. Persistent left superior vena cava with absent right superior vena cava: review of the literature and clinical implications. *Echocardiography* 2014;**31**(5):674–9.

23 Salerno-Uriarte JA, de Ponti R, Storti C, *et al*. The role of catheter ablation in atrial tachycardia, flutter, and fibrillation. *J Interv Cardiol* 1995;**8**(6 Suppl):793–805.

5

Cardiac Morphology Relevant to Mapping

Niyada Naksuk[1], Vaibhav R. Vaidya[1], Nirusha Lachman[2], and Samuel J. Asirvatham[1,3]

[1] *Department of Cardiovascular Diseases, Mayo Clinic, Rochester, MN, USA*
[2] *Department of Anatomy, Mayo Clinic, Rochester, MN, USA*
[3] *Department of Pediatrics and Adolescent Medicine, Mayo Clinic, Rochester, MN, USA*

Summary

In this chapter, we exemplify the method of correlating cardiac anatomy with the challenges of detailed mapping and requirement for safe energy delivery. We use selected examples of common cardiac arrhythmias that are targeted at the most complex anatomical sites in the human heart.

Introduction

An essential component for safe mapping and ablation is a deep understanding of the relevant cardiac morphology and topographical anatomy. In this chapter, we have selected a few key locations that serve as outstanding examples of this underlying concept and our commonly targeted sites during contemporary ablation procedures. All locations are important in terms of appreciating the regional anatomy to be successful and avoid complications, but we believe that these examples and description will allow the reader to develop a similar approach to any site being mapped in a given patient.

Paramount for the invasive electrophysiologist is to know where exactly the mapping or energy delivering catheter is located, correlation of this site fluoroscopically and with intracardiac echo, understanding which variants in regional anatomy may cause difficulty with ablation, and appreciating neighboring structures that may be collaterally injured, giving rise to complications.

Cavotricuspid isthmus

Typical atrial flutter is a common arrhythmia and frequently targeted for permanent ablative cure. It serves historically as the best example of direct correlation between a specific cardiac anatomical location and arrhythmogenic substrate. Although the complete circuit for typical flutter is less exactly understood and likely varies from patient to patient, this circuit invariably involves the myocardial isthmus of tissue between the electrically inert tricuspid valve and inferior vena cava (IVC).

Topographical anatomy

The cavotricuspid isthmus (CVTI) is a complex, three-dimensional structure. The Eustachian ridge routinely divides the CVTI into an anterior smooth muscular and vestibular portion and a posterior downslope made primarily of fibro-fatty tissue [1]. Medially, the CVTI merges with the annular tissue constituting a part of the interatrial septum and laterally with the pectinate muscles emanating from the crista terminalis and lateral vestibular portion of the peritricuspid atrial myocardium. The base and height of the CVTI are variable, typically being relatively narrow in its midportion and with less prominent myocardial bundles more medially. Specific features of both the regional and topographical anatomy have been well studied and described as causes for potential difficulty with ablative elimination of conduction through the CVTI and are summarized as follows (Figure 5.1).

Sub-Eustachian pouch

A sub-Eustachian pouch may be present between the tricuspid valve and the Eustachian ridge and vary from a slight depression of the CVTI floor [2] or a deep recess up to 10 mm at its maximum depth.

When prominent, a sub-Eustachian pouch can cause difficulty with completing the CVTI line for several reasons. If unanticipated by the operator, the depths of this pouch are not ablated with the catheter moving from the anterior to the posterior rim directly, and myocardium is invariably present traversing the pouch and will continue to conduct and allow the maintenance of typical flutter. Even when pouch presence is identified, adequate power delivery

Cardiac Mapping, Fifth Edition. Edited by Mohammad Shenasa, Gerhard Hindricks, David J. Callans, John M. Miller, and Mark E. Josephson.

Companion website: www.wiley.com/go/cardiacmapping5e

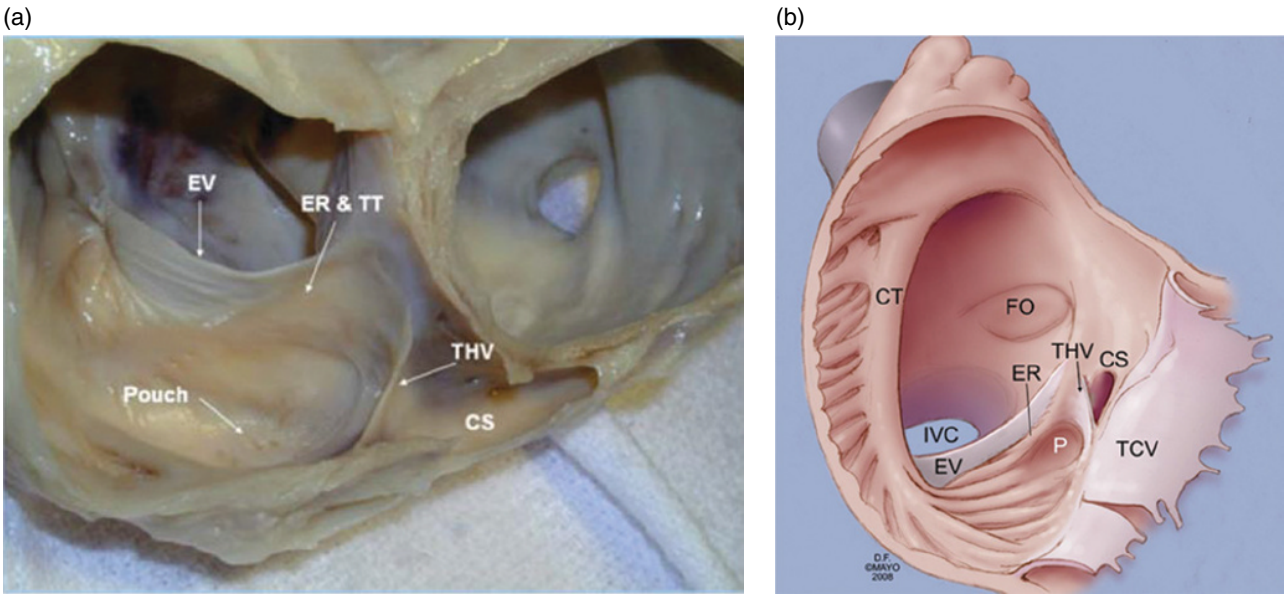

Figure 5.1 (a) Heart cut along the plane of tricuspid annulus (TA); a part of cavotricuspid isthmus (CVTI) is shown. (b) Illustration shows the complete boundary of the CVTI including the tricuspid annulus (TA), inferior vena cava (IVC), crista terminalis (CT)/pectinate muscles, and coronary sinus (CS) from the anterior, posterior, medial, and lateral aspects, respectively. The Eustachian ridge (ER) divides the CVTI into two portions. The anterior portion may have a prominent sub-Eustachian pouch (P) and a Thebesian valve (THV), a ridge separating the pouch from the CS. In the posterior portion, there may be a prominent Eustachian valve guarding the IVC. *Source:* (a) Asirvatham [2]. Reproduced with permission of John Wiley & Sons.

through and including the depth of the pouch can be challenging because of relative stasis of blood and lack of cooling. Thus, the temperature cutoff limit may be reached with very low power, failing to transmurally ablate the myocardium, and in addition, coagulum or thrombus may form. This problem of overheating of the electrode as a result of lack of convective cooling can be remedied by using an open irrigation catheter or a large surface area catheter. However, avoiding an impedance pop and perforation through this relatively thin tissue leading to potential damage, particularly in smaller atria of the adjacent distal right coronary artery, may complicate such an approach.

An anatomical solution is often available to circumvent this variant anatomy contribution to difficulty. Sub-Eustachian pouches are often associated with and adjacent to a prominent Thebesian valve [1,2]. As a result, when a prominent sub-Eustachian pouch is present on the isthmus, ablating further away from the septum on the posterolateral portion of the CVTI will avoid the pouch, albeit with a slightly longer line needing to be created between the tricuspid valve and IVC.

Difficulty with prominent pectinate muscles

The crista terminalis is described as the endpoint or termination site for the pectinate muscles of the right atrium. However, a common variant involves encroachment of the pectinates onto the CVTI, sometimes extending into the proximal coronary sinus. Prominent pectinates may make CVTI ablation challenging since transmural ablation through this thick myocardium may require high energy and prolonged ablation. More importantly, however, a slight movement of the catheter may wedge the tip between two pectinate muscles, thus limiting energy delivery and overheating the surface of the myocardium but without transmural ablation. Once again, open irrigation may help create an adequate line in this location, but since the pectinates originate from the posterolaterally located crista terminalis, they become progressively smaller in size towards the septum. When prominent pectinates are suspected because of large electrogram amplitude or visualized with intracardiac ultrasound, a relatively more septal ablation line will avoid these structures and make ablation more straightforward in this situation.

Eustachian ridge

While it may be anticipated that ablating transmurally across and including the Eustachian ridge would be challenging, in reality this is rarely the case. The reason for this is that the ridge is primarily made up of fibrous tissue and is non-conductive. The myocardial surface is relatively thin, and ablation is straightforward, as long as contact is maintained.

A more nuanced cause of difficulty as a result of this structure when prominent involves catheter manipulation. The crest of the Eustachian ridge serves as a fulcrum for catheters placed via the femoral vein and reaching towards the tricuspid valve. Thus, clockwise rotation of

the catheter that would be anticipated to turn the catheter tip towards the septum will deflect in an opposite direction from balancing on a prominent Eustachian ridge. Such non-intuitive catheter manipulation can be disorienting for the operator and cause difficulty with maintaining appropriate contact through the CVTI line. The problem may be solved by placing the catheter through a sheath with the tip of the sheath balancing on or ventricular to the Eustachian ridge. Once this is accomplished, both sheath and catheter will respond to clockwise or counterclockwise rotation in the usual manner.

Posterior circumferential myocardium around the IVC ostium

The anterior IVC ostium is part of the myocardium that forms the CVTI. In human hearts, myocardium has not been known to extend into the IVC, and ablation when anchored to the IVC is sufficient to prevent conduction across the CVTI. The posterior portion of the circumferential IVC ostial myocardium is not part of the CVTI circuit but may cause confusion when mapping flutter or assessing for CVTI block. When pacing medial to a successfully placed complete CVTI line, conduction utilizing this posterior IVC ostial myocardium will result in low to high activation of the lateral peritricuspid myocardium, giving the impression of continued conduction (pseudo-conduction) [2]. On the other hand, when a gap truly exists in a CVTI line placed in the midportion of the isthmus, conduction utilizing the posterior IVC ostial myocardium may be more rapid than the slow conduction through the partially ablated CVTI and result in the appearance of lateral to medial conduction with medial pacing on the lateral CVTI, giving the appearance of block even though slow conduction is present (pseudo-block). Either situation can be readily clarified by placing closely spaced multielectrode catheters spanning the CVTI or with high density point-to-point mapping [3].

The posterior IVC ostial myocardium does not participate in CVTI-dependent flutter but may be part of another arrhythmia circuit called lower-loop reentry [4]. However, CVTI ablation eliminates lower-loop reentry, and no further ablation of the posterior wall will be required (Figure 5.2).

Relevance to mapping

Double potentials are the hallmark for pathology resulting from scars or previous surgical incisions. However, the normal anatomy of the right atrium relevant for CVTI ablation may have non-pathological double potentials. Posterolaterally, because of the fiber orientation in the crista terminalis, double potentials in sinus rhythm as well as atrial pacing are routinely seen. Similarly, when myocardium is present on both sides of the Eustachian ridge, the ridge frequently shows double potentials that are again physiological. Finally, for unclear reasons, the posterior wall of the right atrium medial to the crista terminalis may also show double potentials and serve as the posterior boundary for atrial flutter in some patients. Pectinate muscles abruptly terminating in a ridge more posteriorly are seen in some hearts and may be the basis for these double potentials [2,5].

Mitral isthmus

The strip of atrial myocardium lying between the orifice of the left inferior pulmonary vein (LIPV) and the mitral valve annulus is the mitral isthmus, which is a frequently targeted site for linear ablation required for the management of one type of atypical left atrial flutter (Figures 5.3, 5.4).

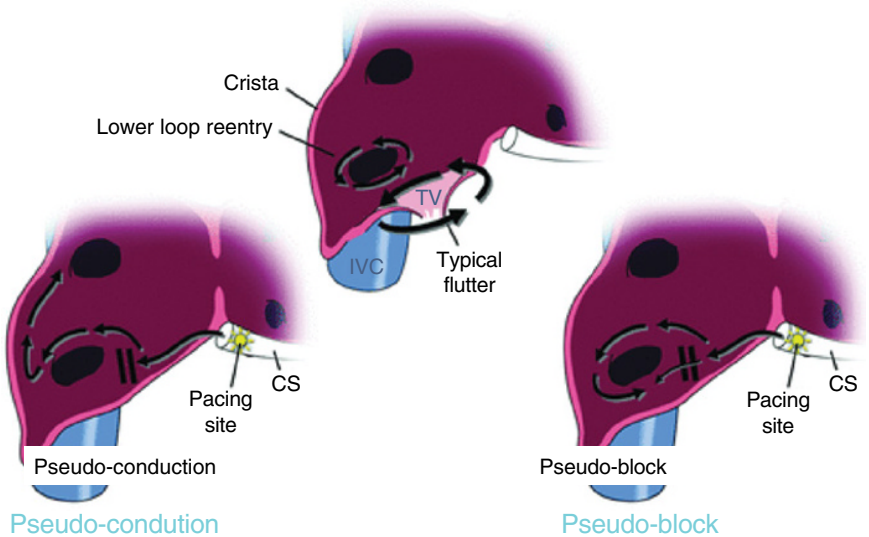

Figure 5.2 Lower loop conduction. The top center panel demonstrates typical atrial flutter circuit that involves the atrial myocardium and the lower loop reentry which is around the inferior vena cava. This arrhythmia is ablated by the cavotricuspid isthmus line anchored to the tricuspid valve and inferior vena cava, similar to that of CVTI-dependent atrial flutter. The bottom left panel shows "pseudo-conduction," with conduction traveling posteriorly through the inferior vena cava giving activation from caudal to cranial on the lateral wall. The bottom right panel shows "pseudo-block," when the conduction preferentially travels through the faster posterior inferior vena cava ostia. See text for details. *Source:* Asirvatham [2]. Reproduced with permission of John Wiley & Sons.

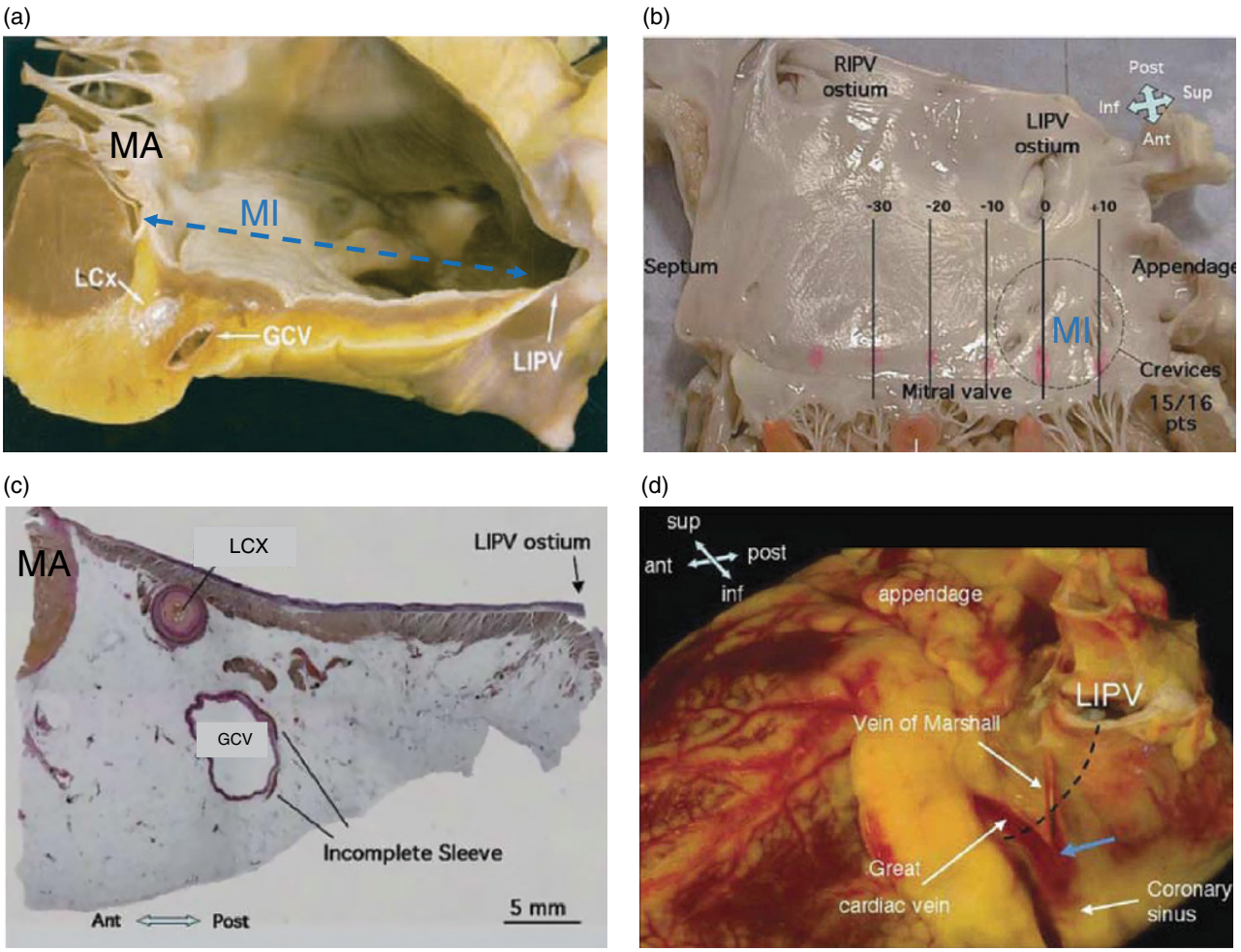

Figure 5.3 (a) Mitral isthmus (MI), a part of the posterior wall of the left atrium, is located between the ostium of the left inferior pulmonary vein (LIPV) and the mitral valve. Note its close relationship to the left atrial appendage (LAA), great cardiac vein (GCV), and left circumflex artery (LCX) (b,c). From the endocardial perspective, the LCX is closer to the MI than the GCV. Myocardial thickness along the floor of the MI is inhomogeneous and extends to form an incomplete muscle sleeve around the GCV. (d) On the epicardium, MI (dotted line) is related to the ligament of Marshall and the GCV posteriorly and the LAA anteriorly. *Source:* (a) Becker [6]. (b–d) Wittkampf FH, van Oosterhout M, Loh P, *et al*. Where to draw the mitral isthmus line in catheter ablation of atrial fibrillation: histological analysis. *Eur Heart J* 2005;**26**(7):689–95. Reproduced with permission of John Wiley & Sons.

Figure 5.4 (a)A deep pouch (d on image) at the mitral isthmus (MI). (b) Branches of the interposed left circumflex artery (Cx) are closer to the MI floor than that of coronary sinus (CS). LA, left atrium, LIPV, left inferior pulmonary vein; MV, mitral valve. *Source:* Yokokawa [8]. Reproduced with permission of Elsevier.

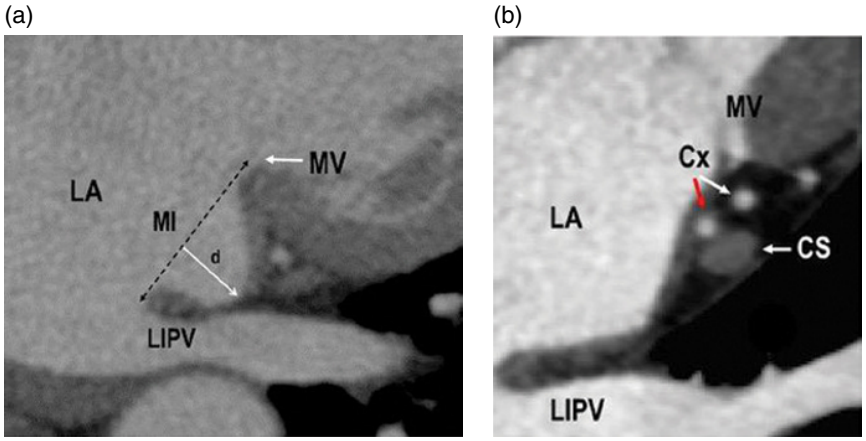

While the mitral isthmus has been described as the left side equivalent of the CVTI, and indeed certain similarities are present, there are major differences between these two isthmuses anatomically that the electrophysiologist needs to keep in mind and which are pointed out below.

The length of the isthmus is variable and usually relatively short, ranging from 17.0 to 51.0 mm [6]. The width of the isthmus is also variable, measuring between 31.4 and 5.3 mm medially and 21.0 and 55.3 mm laterally [7]. When the left atrium dilates, the mitral isthmus is often more prominent with varying thickness of the myocardium at this site [7]. Epicardial to the mitral isthmus lays the great cardiac vein (GCV) more posteriorly and in relation to atrial myocardium and the left circumflex artery as well as its branches closer to the mitral annulus [6]. Each of these relations as well as the variation in the topographical anatomy of the mitral isthmus may give rise to problems with mapping and ablation of this structure [8].

Anchor sites for linear ablation of the mitral isthmus

The boundaries of the CVTI are anatomical and consistent with linear ablation extending from the electrically inert tricuspid valve to the IVC, which has no myocardial extensions. Importantly, the mitral isthmus varies significantly from the CVTI with regard to its posterior boundary. Since in human hearts there are myocardial extensions extending for variable lengths into the LIPV, ablation up to the LIPV ostium results in an incomplete line with continued substrate for mitral isthmus-dependent atrial flutter. Thus, with the mitral isthmus, the anterior boundary of the mitral valve is anatomical but the posterior boundary is not. In order to secure the integrity of the line posteriorly, either ablation needs to be carried into the LIPV up to the limit of where the myocardial extensions are or circumferential isolation of the LIPV is first required with this circle of complete ablation lesions serving as the posterior boundary. Because of the prohibitive risk of pulmonary vein stenosis, when ablation is carried into a pulmonary vein, the latter approach is the only viable one and is routinely used in contemporary ablation practice.

Gaps in the ablation line may also occur anteriorly related to the mitral annulus. A coronary sinus catheter advanced into the GCV is also used by electrophysiologists as a marker for the mitral annulus. However, the GCV's distance from the true mitral annulus varies greatly, ranging from 3 to 15 mm [9]. Thus, extending the ablation line up to where atrial electrograms are no longer seen is critical in avoiding an anterior gap.

In some patients, mitral valve dysjunction is present. In this condition, the mitral valve leaflets insert onto the atrial myocardium [10] (Figure 5.5). When this occurs, ablating the strip of atrial myocardium located ventricular to the point of attachment of the mitral valve leaflet can be challenging since with each cardiac cycle during systole, the mitral valve closes and catheter contact at this site may not be possible. Advancing the catheter into the ventricle and retroflexing the electrode to be positioned between the mitral valve leaflet and the myocardium may be required.

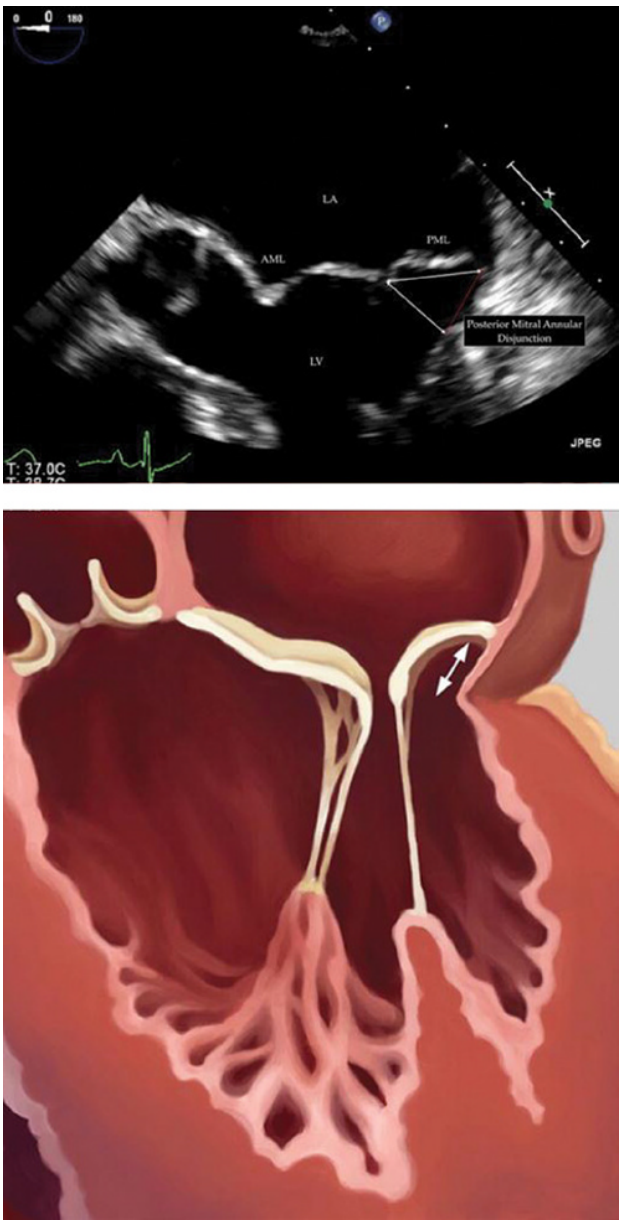

Figure 5.5 Mitral annuli dysjunction is a condition with a separation between the atrial wall–mitral valve junction and the left ventricular attachment, commonly seen in mitral valve prolapse. See text for details. *Source:* Mahmood F, Matyal R. Quantitative approach to the intraoperative echocardiographic assessment of the mitral valve for repair. *Anesth Analg* 2015;**121**(1):34–58. Reproduced with permission of Wolters Kluwer.

Thus, the boundaries for linear ablation in the case of the mitral isthmus are not as straightforward as with the CVTI. When conduction block across this line or continued atypical flutter is present, anatomical reasons for this failure need to be considered and include complete isolation of the left lower pulmonary vein, and approximation of the circular ablation with the mitral isthmus line and ablation up to the true mitral annulus should be considered.

Topographic anatomy of the mitral isthmus

Akin to the CVTI, the mitral isthmus is three-dimensionally complex, having prominences as well as depressions along its course. The lateral left atrial ridge is present and with variable prominence between the left-sided pulmonary veins and the left atrial appendage more superiorly and the mitral annulus inferiorly. Thus, this ridge needs to be negotiated with linear ablation on a mitral isthmus. Unlike the Eustachian ridge, the left lateral ridge is primarily myocardial without significant fibro-fatty components. It is formed by the indentation created between the appendage and the left-sided pulmonary veins in fetal life by the left superior vena cava [11].

A distinct single pouch containing myocardial tissue on its floor similar to a sub-Eustachian pouch may be found in up to 20% of patients. More commonly, however, the pouch is not single but rather pseudo-diverticula-like structures with pectinates and intervening thinner myocardium similar to that found within the left atrial appendage may encroach onto the mitral isthmus. If the operator is unaware of such variation in thickness, these structures may be the site of inadvertent perforation, coagulum formation, or incomplete energy delivery from the absence of local blood flow and cooling of the electrode tissue interface. Thus, cognizance of regional anatomical variation and preprocedural or intraprocedural imaging as with intracardiac echocardiography may be important to strategize where the line should be drawn and assess the potential causes of difficulty along the span of the mitral isthmus. Careful attention to impedance at start of the ablation and using the local electrogram to guide the extent of ablation are necessary given the complexity of this site.

Impact of the cardiac vasculature

Epicardial to the mitral isthmus runs the GCV, the distal left circumflex artery and its branches, and in some cases, a persistent left superior vena cava or its remnant, the vein of Marshall. The GCV may serve as a heat sink when ablating endocardially, giving rise to epicardial gaps close to the GCV. To solve this, ablation can be done within the GCV itself. However, care to avoid injury to the nearby left circumflex artery is required. The anatomical relationship between the circumflex artery and the GCV is variable, but the artery is usually located closer to the left ventricle. The right anterior oblique view may be critical, along with making sure that an atrial electrogram is present at the site of energy delivery at the GCV. In addition, venous ablation should be reserved for remaining gaps after a complete endocardial attempt has been made, ensuring that both the anterior anatomical boundary and the posterior boundary, being the circumferential ablation around the pulmonary vein, have been adequately executed.

An alternate approach involves balloon occlusion of the coronary sinus to remove the heat sink effect and successfully complete mitral isthmus ablation without resorting to venous ablation [12,13]. Less commonly, a persistent left superior vena cava may exaggerate the heat sink effect of the coronary vasculature, creating difficulty with mitral isthmus ablation [14].

In summary, the mitral isthmus, like the CVTI, is an anatomically complex structure that requires detailed study in order to correlate with difficulty in mapping and ablation. The posterior boundary is not anatomical with the mitral isthmus and relies on the adequacy and juxtaposition of the ablation line with complete circumferential isolation of the left lower pulmonary vein.

Ventricular outflow tracts

The ventricular outflow tracts are a common location to target a variety of ventricular arrhythmias including symptomatic premature ventricular contractions (PVCs), ventricular tachycardia, and triggered ventricular fibrillation. Further, the semilunar valve sinuses themselves require ablation for both ventricular and, in the case of the non-coronary sinus of Valsalva (NCSOV) with a close relation to aortomitral continuity, supraventricular arrhythmia [15,16] (Figure 5.6). Perhaps no other location in the heart requires more careful anatomical study to correlate with point-to-point mapping of arrhythmias and safe ablation energy delivery. The outflow tracts are intertwined with each other and also have complex relationships with the conduction system, epicardial space, and coronary vasculature. These difficulties have been made more challenging with inexact terminology (septum of the outflow tract, "cusp" of the aortic sinuses of Valsalva, etc.). In this section, we aim to systematically clarify the detailed regional anatomy of the outflow tracts to allow better correlation with retrieved sensed electrograms and for the invasive electrophysiologist to appreciate the difference between arrhythmia origin and the use of a vantage point to successfully eliminate tachycardia.

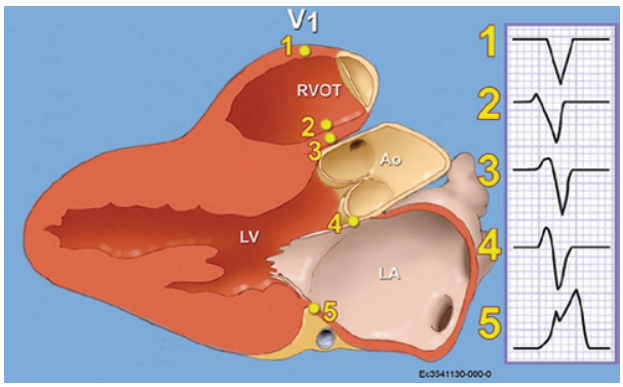

Figure 5.6 The complex outflow tract anatomy and their corresponding characteristic electrocardiogram morphology in lead V1. Note that the right ventricular outflow tract (RVOT), the left ventricular outflow tract (LVOT), and the mitral valve (MV) lie in an anteroposterior position. Because lead V1 is an anterior lead, arrhythmia originating from the anterior RVOT (1) results in a typical left bundle branch block morphology. The posterior RVOT (2) and the right coronary cusp (RCC) (3) are very close to each other, producing a small but variable R wave as consistently seen in lead V1. The more posterior region of the non-coronary cusp (NCC) (4) is characterized on the ECG with a distinct R wave in lead V1. Finally, arrhythmias arising from even more posterior and leftward areas (for example, in the posterior mitral annulus) will have a clear right bundle branch block morphology. *Source:* Asirvatham [18]. Reproduced with permission of John Wiley & Sons.

Sidedness

The inflow portions of the ventricles are appropriately named with regard to their location in the body. Thus, the inflow right ventricle lies to the right of the inflow left ventricle and vice versa. However, the outflow tracts of the two ventricles have a complex relationship with each other such that the distal *right* ventricular outflow tract (RVOT) lies on the *left side* of the body, while the distal *left* ventricular outflow tract (LVOT) lies posterior and to the *left side* of the distal RVOT. This results from the spiral septum forming in fetal life to divide the truncus arteriosus into the two outflow tracts and great arteries and this structure's eventual conjunction and alignment with the inflow intraventricular septum. The RVOT starts on the right side of the body where the inflow right ventricular is located and then wraps around the LVOT such that the distal RVOT and pulmonic valve are to the left, cephalad, and anterior to the aortic valve. The most caudal and rightward portion of the RVOT is in continuity with the tricuspid annulus, and this region includes the normal location of the penetrating bundle of His and membranous septum.

As a result of this unique wrapping around of the RVOT, several important consequences relative to mapping result.

- The LVOT has no epicardial surface and in essence, the posterior wall of the RVOT constitutes the inter outflow tract septum and is the epicardial equivalent for the anterior LVOT.
- Ventricular tachycardia arising in the vicinity of the His bundle, because of its rightward and inferior location, is the only site in the outflow tracts where aVL is not negative during ventricular tachycardia.
- The RVOT shares a portion of its septum with the left ventricular inflow and running in this anterior intraventricular groove epicardially are the left anterior descending and anterior intraventricular veins. As a result, the anterior intraventricular vein may be used as a vantage point to eliminate arrhythmia located in this leftward portion of the RVOT [17].
- The left anterior descending artery may be injured when ablating in the leftward free wall portions of the RVOT. More distally in the RVOT in this orientation, the left anterior descending lies between the distal left atrial appendage and the leftward free wall portion of the RVOT. Thus, when the electrophysiologist notes a significant atrial electrogram in the distal left RVOT, the consistent anatomical of the left anterior descending in this location must be considered.

Interventricular outflow tract septum

Ablationists are used to thinking of the interventricular septum as being leftward of the right ventricle and rightward of the left ventricle because of our long-standing primary manipulations and mapping in the *inflow* portions of the ventricular cavities. However, orienting oneself in a similar manner to recognize where the outflow tract septum is located is an error. Since the RVOT lies superficial and anterior (closer to the sternum) to the LVOT, the septum of the outflow tract is primarily posterior rather than leftward of the RVOT and anterior rather than rightward relative to the LVOT. Even this more appropriate nomenclature and picturing of the septum of the outflow tracts are inexact because of the complex spiral-like nature taken from being a coronal structure between the right and left sides of the body in the inflow portion to being a sagittal structure relative to the outflow tracts.

The relevance of this important but nuanced appreciation of the outflow tract septum for mapping and ablation is significant. When mapping earlier signals as one advance in the RVOT towards the left of the body, we reach the left free wall portion of the RVOT adjacent to the anterior intraventricular vein or directly into the pericardial space. Similarly, in order to ablate an exactly mapped outflow tract septal arrhythmogenic substrate, the operator needs to visualize the catheter in the right

anterior oblique position directed posteriorly in the RVOT or anteriorly from the LVOT.

Because the pulmonary valve is typically located cephalad to the aortic valve, the distal portion of the inter outflow tract septum transitions from being between the two outflow tracts to being between the distal RVOT and the anterior portion of the left sinus of Valsalva (LSOV) (Figure 5.7). This region at the level of the pulmonic valve is juxtaposed with the left main coronary artery as it courses also cephalad to the depths of the LSOV to branch and emerge as the left anterior descending artery in the anterior interventricular groove, in turn the left boundary of the RVOT. Direct visualization of the left main coronary artery with angiography or with careful intracardiac echo is of paramount importance to avoid potentially fatal left main occlusion during ablation in this region of the *right* ventricular outflow tract.

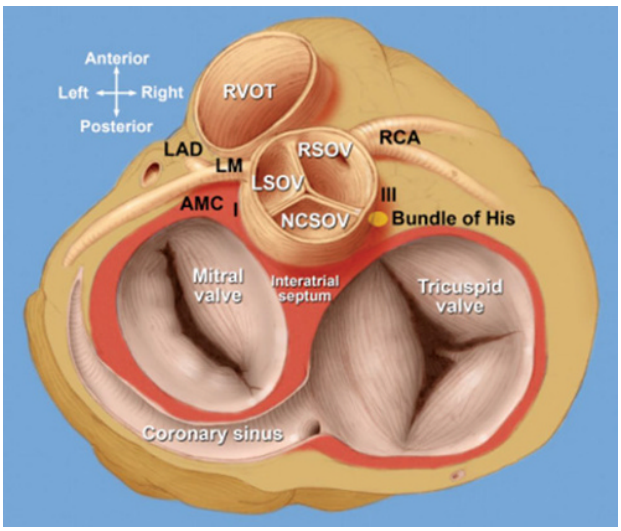

Figure 5.7 View from above demonstrates cross-section of the aortic valve central between the other valves. The pulmonary valve is not seen because of its cephalic position to the aortic valve. Note that the right ventricular outflow tract (RVOT) is on the left and anterior to the left ventricular outflow tract (LVOT). The posterior wall of the RVOT is near the left sinus of Valsalva (LSOV) where the left main (LM) and proximal left anterior descending artery (LAD) lie. Note the area between the junction of the LSOV/non-coronary sinus of Valsalva (NCSOV) and left connected to the aortomitral continuity (AMC, I), which is the fibrous extension from the anterior leaflet of the mitral valve. The NCSOV is the most posterior cusp of the aortic sinuses. The interatrial septum lies underneath the LSOV (II). A commissure between the septal and anterior leaflets, inferior and slightly to the right, close to junction of the NCSOV/right coronary sinus of Valsalva (RSOV), provides a landmark for penetration from the bundle of His (III). Ablationists targeting NCSOV for ablation therefore prefer to manipulate the catheter toward the left to avoid an atrioventricular block. *Source:* Suleiman [21]. Reproduced with permission of Elsevier.

Supravalvar extension of myocardium above the semilunar valves

Circumferential myocardial sleeves extend above the pulmonic valve in most hearts [18,19]. These myocardial sleeves are an important cause of difficulty with mapping and ablation of distal RVOT ventricular arrhythmia. Since retrograde access to the sinuses of the pulmonic valve is not possible, with antegrade mapping and with each diastolic period, the catheter will be pushed out by the filled and closed pulmonic valve leaflets from contact with these myocardial sleeves. Thus, failure to map and, even when adequately mapped and suspected, failure to maintain catheter contact have to be avoided with distal RVOT arrhythmia. Based on understanding this anatomy, the operator may advance the mapping and ablation catheter into the pulmonary artery, place a curve on the catheter, and gently move it back towards the ventricles to maintain contact for mapping and ablation within the sinuses of the pulmonic valve.

Myocardial extensions above the plane of the aortic valve leaflets are more complex and asymmetrical. The primary extension of these sleeves is related to the right sinus of Valsalva (RSOV) and the commissure between this sinus and its neighboring left coronary sinus. The junction of the right and non-coronary sinuses is devoid of myocardium and immediately adjacent to the junction of the anterior and septal leaflet of the tricuspid valve forming the membranous portion of the interventricular septum – the site of location for the penetrating bundle of His. Similarly, the LSOV and commissure with the NCSOV lies adjacent and continuous with the anterior leaflet of the mitral valve, the so-called aortomitral continuity (AMC).

Relevance to mapping and ablation

When ablating in the depths of the RSOV, the actual arrhythmogenic substrate targeted may be the supravalvar extensions in this region or the immediately superficial posterior infundibular portion of the RVOT. Similarly, mapping and ablating in the region of the AMC is unlikely to target any significant neighboring myocardium, being a membranous structure. However, some data suggest that remnant fascicles of Purkinje tissue related to the conduction system may be the source of mapped abnormal signals that have been successfully targeted for ablation [20].

Relevance of anatomy for mapping and ablation in the aortic sinuses of Valsalva

The sinuses of Valsalva represent common sites for mapping and energy delivery. They have unfortunately been referred to as the coronary cusps in both the literature

and common electrophysiology parlance. The cusps themselves are non-arrhythmogenic but rather arrhythmias are routinely targeted in the depths of the sinuses of Valsalva. A detailed understanding of the anatomy of these sinuses, the anticipated electrograms when mapping, and the unique vantage point offered by these structures for ablating a variety of arrhythmogenic substrates is of value [21,22].

A detailed appreciation of the anatomical relations and structure of the aortic valve is key for mapping and safe energy delivery for outflow tract arrhythmia. The aortic valve has proximate relationships with all other cardiac valves, all cardiac chambers, and the cardiac septum. In addition, as explained above, the primary conduction system of the heart and major coronary vessels are related to this valve as well.

The rightward and anterior coronary sinus is the RSOV which is immediately deep and posterior to the relatively thick posterior subvalvar infundibulum of the RVOT. Mapping in this sinus yields a large ventricular electrogram mostly reflective of the overlying posterior RVOT. The signal, however, may be multicomponent with small-amplitude, high-frequency signals likely reflective of the supravalvar sleeves of left ventricular myocardium seen within this sinus. A small far-field atrial electrogram originating in the right atrial appendage may occasionally be seen when mapping in the RSOV as well. Arrhythmias successfully ablated in the RSOV are primarily ventricular arrhythmias originating in either the supravalvar myocardium or the posterior RVOT. Rarely, atrial tachycardia or an accessory pathway may be ablated from this structure as well [23]. A near-field His bundle electrogram is not recordable from the RSOV since this structure lies in the commissure below the junction of the RSOV and NCSOV. However, a far-field His bundle electrogram can occasionally be recorded on the posterior RSOV.

The posterior aortic sinus is the NCSOV. This aortic sinus is essentially an atrial structure directly related to the interatrial septum and cavities of the right and left atria. Mapping in the NCSOV yields a near-field atrial electrogram reflective of activation of the right atrial, left atrial, or septal atrial myocardium. The only ventricular electrograms recorded tend to be of small amplitude and far field. As a result, the NCSOV is a vantage point for ablating primarily atrial tachycardias and occasionally the atrial insertion site for accessory pathways. Care must be taken to visualize the electrode location and the depths of the NCSOV preferably with intracardiac echo since inadvertent slippage of the catheter between the NCSOV and RSOV can result in damage to the His bundle or, if caudal to the non-coronary cusp itself, the fast pathway input to the atrioventricular node.

The cranial anterior and leftward aortic sinus is the LSOV. The regional anatomical relationships of the LSOV are complex and vary greatly based on the exact location. The anterior rightward portion of the LSOV underlies the distal posterior RVOT often at the level of the pulmonic valve. The posterior LSOV and its commissure with the NCSOV are adjacent to the left atrium. The mid and posterior parts of the LSOV are contiguous with the anterior leaflet of the mitral valve and constitute the AMC. Thus, recorded electrograms in the LSOV may be ventricular and/or atrial with the ventricular EGM source in turn being either posterior RVOT origin or subvalvar LVOT. Fragmented low-amplitude, high-frequency signals may be observed in this location as well, possibly from supravalvar extensions or conduction tissue remnants related to the AMC.

The region just beneath the LSOV represents unique heterogenous tissue resulting from the crossing of multiple disparate electrically active sources. Here, depending on the exact location, epicardial perivalvar posterior RVOT myocardium, epicardial left ventricular perimitral myocardium, supravalvar extensions into the sinuses, endocardial left ventricular myocardium, and tissues in the aortic mitral continuity are present. This area is a frequent successful site of ablation for ventricular arrhythmia, sometimes with highly variable QRS morphology. Whether the reason for this apparent preponderance of successful ablation is because of its unique position, enabling energy delivery to multiple locations, or enhanced arrhythmogenesis from this heterogeneity is unclear.

Endocavitary structures and the distal conduction system

Electrophysiologists have long understood the importance of appreciating the three-dimensional anatomy of the ventricular walls, specifically midmyocardial and epicardial substrates and deep septal pathology giving rise to arrhythmia that requires deeper lesions or epicardial access for cure. Of relatively recent importance for anatomical EP correlation are the endocavitary structures of the left and right ventricles [24].

The normal left ventricle includes two papillary structures known commonly as the anterolateral (AL) and posteromedial (PM) papillary muscles. In conjunction with the mitral annulus, mitral valve leaflets and chordae tendineae, the papillary muscles form the mitral valve apparatus. The PM papillary muscle arises from the junction of the left ventricular septum and the posterior wall, and the AL papillary muscle from the anterolateral free wall of the left ventricle (Figure 5.8). There are several finger-like projections from the main body of the papillary muscles, which give rise to the thin non-muscular chordae tendineae attached to the mitral valve leaflets. Chordae tendineae from each papillary muscle insert on

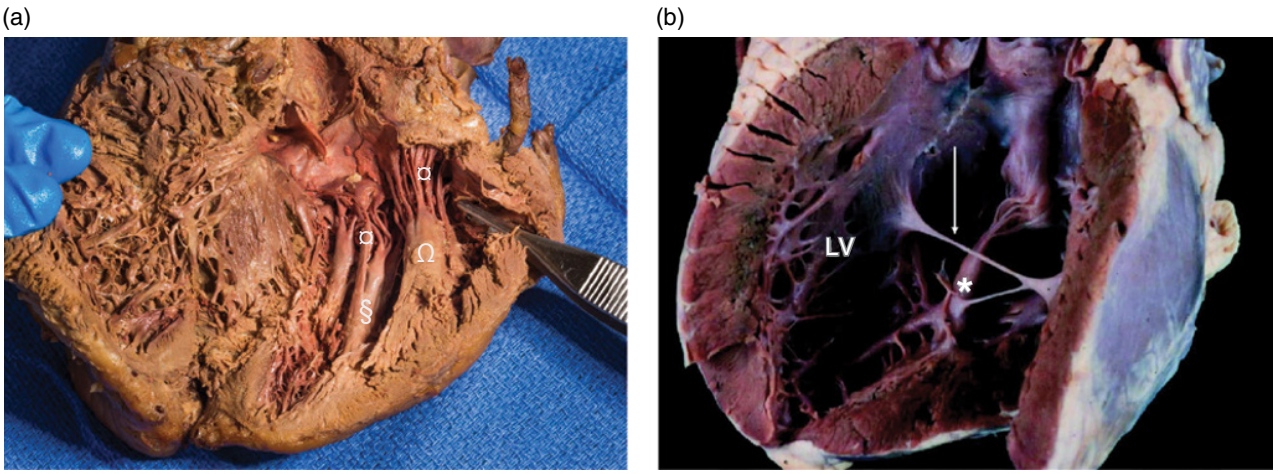

Figure 5.8 (a) The left ventricle (LV) is incised to demonstrate the location of the anterolateral (Ω) and posteromedial (§) papillary muscles. Chordae tendineae (¤) arise from the tips of the papillary muscles and attach on both leaflets of the mitral valve. (b) The anterolateral papillary muscle (*asterisk*) and bifurcated false tendon (*arrow*). *Source:* (b) Madhavan M, Asirvatham SJ. The fourth dimension endocavitary ventricular tachycardia. *Circulation Arrhythmia Electrophysiol* 2010;**3**:302–4. Reproduced with permission of Wolters Kluwer.

both mitral valve leaflets. The base and main bodies of the papillary muscles are as thick as the left ventricular wall. The AL papillary muscle has dual blood supply from the left anterior descending artery and circumflex vessel. However, the PM papillary muscle is supplied usually by the right coronary artery alone in right dominant circulation, and can commonly be affected by inferior wall myocardial infarction.

The right ventricle contains anterior, posterior, and septal (also known as conus) papillary muscles (Figure 5.9). Frequent PVCs can arise from these papillary muscles and can be ablated successfully [25]. While the anterior and posterior right ventricular papillary muscles are apically located, the septal papillary muscle is located in the RVOT. It is notable that PVCs originating from the septal papillary muscle can mimic RVOT PVCs for this reason [7].

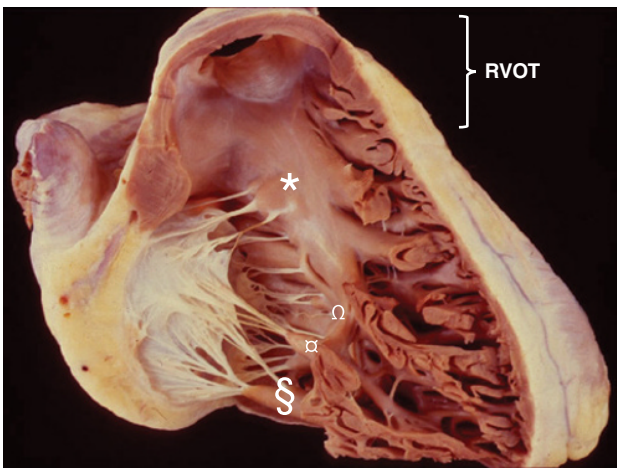

Figure 5.9 The section illustrates papillary muscles of the right ventricle including septal (*), anterolateral (¤), and posteromedial (§) papillary muscles, as well as the moderator band (Ω). See text for details. *Source:* Naksuk N, Kappa S, Asirvatham SJ. Spectrum of ventricular arrhythmias arising from papillary muscle in the structurally normal heart. *Cardiac Electrophysiol Clin* 2016;**8**:555–65. Reproduced with permission of Elsevier.

While the above description is necessarily simplistic, we need to be aware that there is tremendous variation in the number, structure, and interrelationships between the endocavitary structures. Prominent trabeculations may contain conduction tissue and have cord-like attachments to the primary papillary muscles and, in addition, discrete false tendons may bridge the papillary muscles to each other and in turn to the ventricular free wall. The distinction between anatomical conduction tissue-related arrhythmogenesis and those arrhythmias arising from the papillary muscles is to a large extension artificial since the Purkinje network covers the endocardial surface of the papillary muscles, and distinct tendons or prominent trabeculation overlie the primary exit sites of the right and left fascicular networks.

Variation in papillary muscle anatomy can be congenital or acquired. Single papillary muscle resulting in parachute mitral valve, accessory papillary muscles, direct insertion of papillary muscle into the mitral valve leaflets have all been described as congenital anomalies [26–28]. Papillary muscle injury from either ischemia or mitral valve prolapse can result in mitral leaflet tethering or rupture of the papillary muscles, resulting in flail mitral leaflet.

Conduction of electrical impulses from the bundle of His to the ventricular myocardium occurs through a specialized insulated infrahisian conduction system, composed of a network of Purkinje fibers that have a close anatomical relation to the papillary muscle s[29]. The Purkinje fibers are organized into two bundles

proximally – the right and left bundles. The right bundle has a relatively fixed anatomical course, becoming a subendocardial structure at the base of the septal papillary muscle and passing through the moderator band to the right ventricular free wall.

There is considerable variation in the anatomy and connections of the left bundle. The left bundle is a fan-like structure, which divides into the left anterior and left posterior fascicle, and often a left median fascicle. The thin left anterior fascicle courses across the LVOT to the region of the AL papillary muscle, while the broader left posterior fascicle extends posteriorly towards the PM papillary muscle. False tendons are often present within the left ventricular cavity and can house Purkinje fibers (see Figure 5.8) [30,31]. The bundle branches arborize extensively and enter the ventricular myocardium to varying depths. While a transition zone at the Purkinje–cardiomyocyte junction has been described in animals, the existence of this in humans is unclear [32].

Ventricular arrhythmias can arise from endocavitary structures such as papillary muscles, the moderator band, false tendons as well as nearby conduction system [33–36]. Origin from an endocavitary structure must be suspected when there is no specific early site for arrhythmias [37]. These are usually benign, but cardiomyopathy from frequent PVCs and ventricular fibrillation triggered by papillary muscle PVCs have been described [38,39].

Recently, a subset of patients with mitral valve prolapse and malignant arrhythmias originating from the papillary muscles has been described [40]. Catheter ablation of foci originating at the papillary muscles is effective in reducing appropriate implantable cardioverter defibrillator shocks and symptoms of arrhythmia in such patients [7]. Ablation of these arrhythmias can be challenging, particularly due to loss of contact with the muscles in systole [36]. Both transseptal and retrograde approaches have been used to access and ablate in the region of the papillary muscles [33,39]. Intracardiac echocardiography can be a useful adjunct in ablation, and allows for direct visualization of contact between the catheter and the papillary muscles (Figure 5.10) [35]. Arrhythmic foci can exist deep within the papillary muscles, and multiple ablation lesions may be required to eliminate these. Papillary muscle injury is rare, but care must be taken to avoid inadvertent mitral valve pathology from papillary muscle ablation.

The Purkinje fibers are implicated in ventricular arrhythmias [41]. Ablation directed towards early sites can be unsuccessful because of multiple exits from the Purkinje system [42]. Discrete low-amplitude diastolic

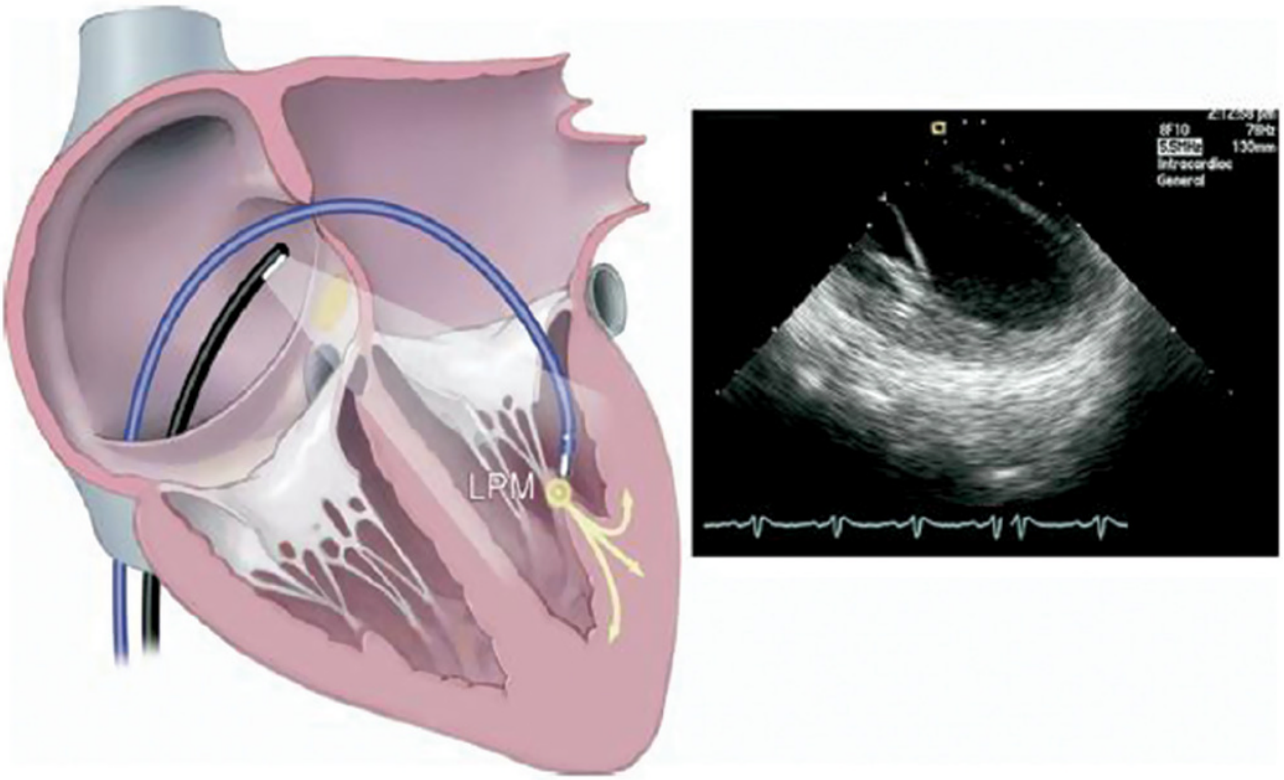

Figure 5.10 Utility of intracardiac echocardiography in visualizing catheter-papillary muscle contact. *Source:* Liu [24]. Reproduced with permission of Elsevier.

Purkinje potentials may be present on mapping and can be targeted for ablation [41]. With regard to bundle branch reentry, the right bundle is easier to ablate since it is a discrete structure compared to the diffuse nature of the left bundle.

The pericardial space

Epicardial ablation for ventricular arrhythmias, atrial fibrillation, and accessory pathway is increasingly being performed. An epicardial approach allows direct access to the pericardial sinuses or recesses important for autonomic modification and introducing devices to protect the esophagus and phrenic nerves. The pericardial cavity is a potential space between the visceral and parietal serous pericardium as it continues along with the fibrous pericardium. The fibrous pericardium then continues as an extension onto the adventitia of the great vessels, reflecting into recesses or sinuses [43].

In order to avoid injury to closely located structures and myocardial puncture, accessing the pericardial space requires appreciation of its 3D anatomy and related cardiac chambers. In a relatively normal-sized heart without enlargement (as seen in the setting of pericardial effusion), directing the needle to halfway between the midline and left shoulder will prevent pulmonary injury in most cases. However, in patients with severe emphysema, where lung parenchyma may extend beyond 50% of the medial mediastinum during full inspiration, other techniques such as a preprocedural CT scan during full inspiration and decreased tidal volume or one-lung ventilation may be required.

Entering from the subxiphoid access can avoid puncture of the diaphragm, liver and related arteries by using the left hand to push away the left lobe of the liver and keeping the needle superficially in contact with the xiphoid process. Once the needle enters the chest cavity, directing the needle deeper and parallel towards the cardiac silhouette will avoid hitting the left internal *mammary* artery which descends approximately 1–2 cm along the sternum. Since we access the pericardial space from the subxiphoid location, the needle is advanced toward the free wall of the right ventricular inflow portion. When access is required for the left ventricular free wall or the left atrial appendage, an exact understanding of the *three-dimensional* nature of the anterior surface of the heart is essential in avoiding trauma. The pulsating RVOT represents a "hill" that requires crossing when a wire, dilator, sheath, or catheter is advanced from the entrance to the pericardial space to the left ventricular free wall. Failure to understand this can severely traumatize the free wall of the RVOT and in some instances has led to fatal outcomes. Placing the sheath parallel to the RVOT is also not recommended since sheath-to-sheath will lie on the anterior intraventricular grove, potentially compressing the left anterior descending artery (LAD). Manipulating the wires and sheath more inferiorly around the apex will avoid trauma to the anterior RVOT or proximal LAD. Generally, injury to coronary vessels can be avoided by directing the needle away from pericardial fat shadow and the ventricular septum where there is an atrioventricular groove housing the distal LAD [44]. Similarly, when ablation along the tricuspid and mitral annuli is required (such as for the epicardial portion of the accessory pathway), careful observation of the fluoroscopic exam is required, as the annuli are intimately related to the left circumflex artery and the coronary sinus. Once the catheter crosses the RVOT cranially and laterally, the left atrial appendage is the first atrial structure to be encountered. Because the RVOT lies over the LVOT, the LVOT is not accessible via the epicardial approach.

The oblique sinus is the pericardial reflection around the pulmonary veins and the inferior vena cava (Figure 5.11). It is a blind-ended sac superiorly and bounded by the left atrium anteriorly. Passing the catheter posterior to the left atrium between the inferior pulmonary veins (the landmark for the opening) will allow ablationists to reach this space located slightly to the left [44]. Caution is needed as the esophagus lies immediately posterior to this oblique sinus. In the situation of an esophageal–atrial fistula, air from the esophagus can reach the oblique sinus, evident as pneumopericardium on a chest X-ray.

Superior to the oblique sinus, but without direct connection, is the transverse sinus that envelops the great arteries. The transverse sinus is bordered by the ascending aorta and the pulmonary trunk anteriorly, and the left atrium and superior pulmonary veins posteriorly and inferiorly (see Figure 5.11). This sinus can be reached by directing the catheter lateral to the left atrial appendage/left ventricular free wall under the pulmonary artery. There, the catheter will be in contact with the roof of the left atrial appendage, which forms part of the transverse sinus floor and allows ablationists to reach the Bachmann's bundle [45]. Anterior to the sinus is the noncoronary and the right coronary sinus of Valsalva via the inferior aortic access [44]. Advancing the catheter across the border of the aortic root will bring it in contact with the aortocaval sinus and superior vena cava [21]. These regions have three parasympathetic ganglia at the junction of the right atrium and the right superior pulmonary vein, the junction of the inferior vena cava-left atrium, and the aortocaval recess [46].

The course of phrenic nerves (PN) passing downward between the pleura and fibrous pericardium varies greatly and is subject to complications (Figure 5.12) [47]. The right PN descends along the right anterolateral border of the SVC and comes in very close proximity to the

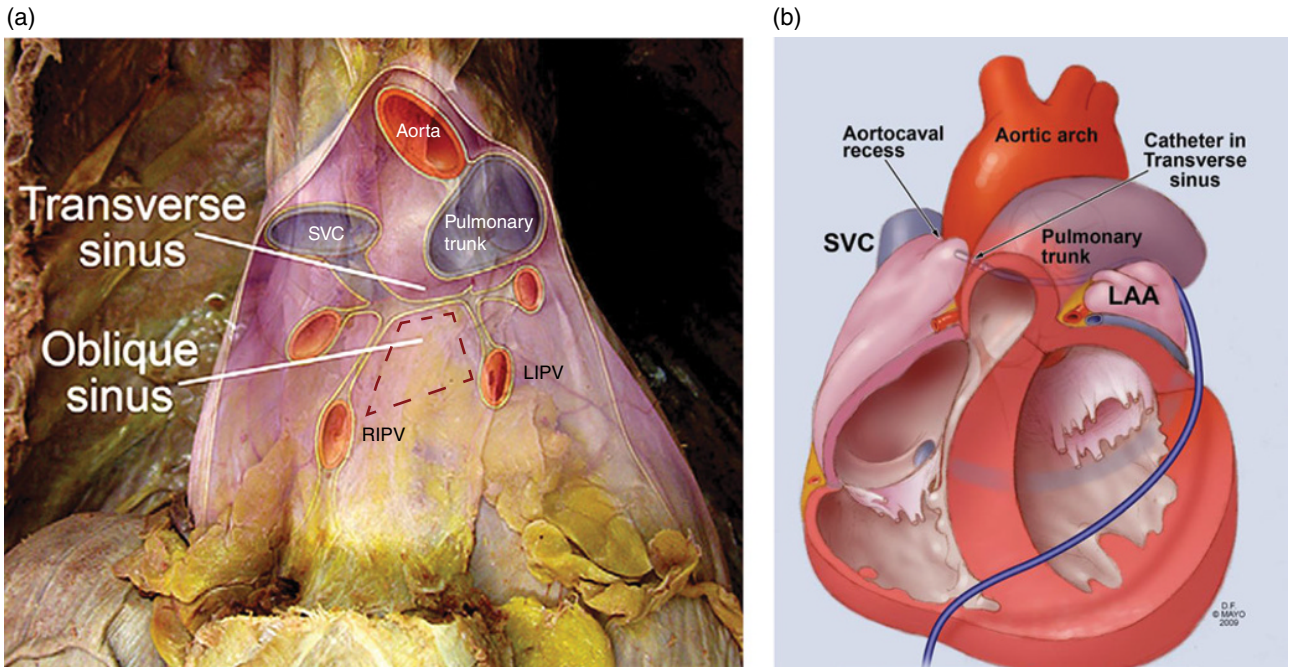

Figure 5.11 (a) The transposed diagram of the pericardium outlines the posteriorly located oblique and transverse sinuses. The heart was removed to demonstrate the oblique sinus behind the left atrium and bordered inferiorly by the right and left inferior pulmonary veins (RIPV and LIPV). (b) Catheter accesses the transverse sinus by passing behind the left atrial appendage (LAA) and the arterial trunks. Note that the catheter sits on the roof of the left atrium and in close proximity to the superior vena cava (SVC). *Source:* Syed [44]. Reproduced with permission of Elsevier.

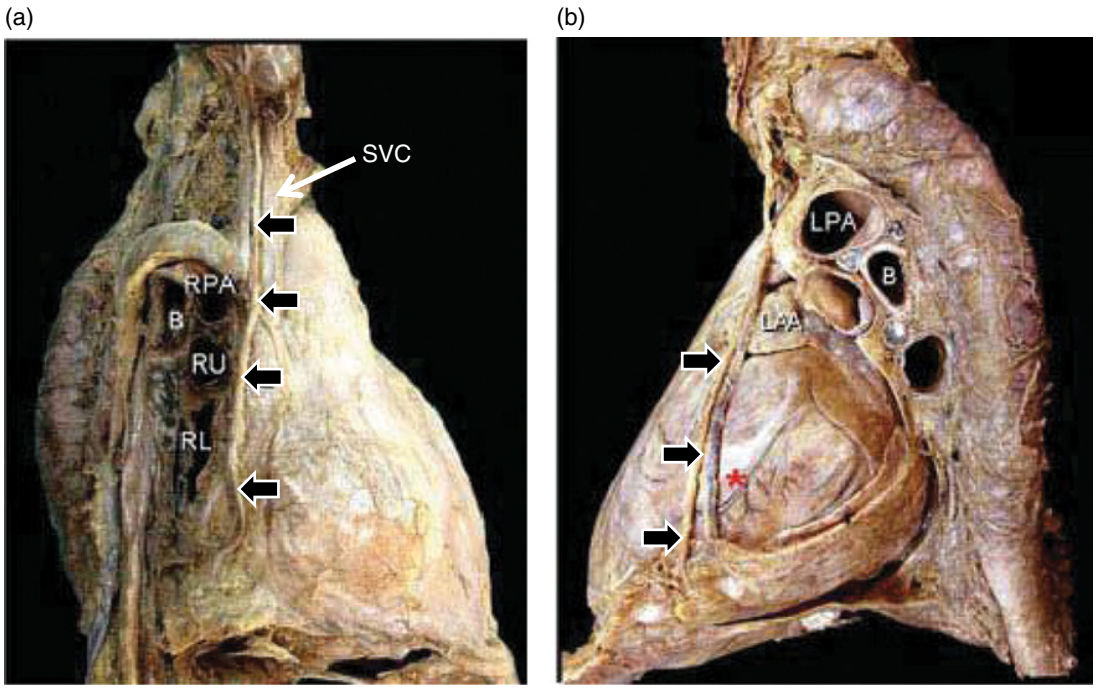

Figure 5.12 View of the specimen without fibrous pericardium to illustrate the course of phrenic nerves (PN). (a) The proximal portion of the right PN locates on the lateral aspect of the SVC and descends near the right upper pulmonary vein (RU). (b) The left PN descends across the left atrial appendage (LAA) and the lateral free wall of the left ventricle where it comes to the area of the obtuse marginal artery and vein (*asterisk*). B, bronchus, LPA, left pulmonary artery, RL, right inferior pulmonary vein. *Source:* Ho et al. *Cardiac Mapping*, 4th edition. Reproduced with permission of John Wiley & Sons.

mid and distal portion of the right superior pulmonary vein prior to descending down along the lateral wall of the right atrium. The inferior course of the right PN is also adjacent to the lateral border of the entrance of the inferior vena cava. On the left, the PN descends over the aortic arch, pulmonary trunk, lateral wall of the left atrial appendage, and high anterolateral left ventricular free wall. It usually reaches the diaphragm behind the tip of the left ventricle [47]. Methods to prevent damage to the PN during the procedure include observation of diaphragmatic stimulation by fluoroscopy while pacing the area of interest. If required, infusion of air and saline (or insertion of balloons) may protect the PN by pushing them away from the pericardium [48].

References

1 Cabrera JA, Sanchez-Quintana D, Farre J, *et al*. The inferior right atrial isthmus: further architectural insights for current and coming ablation technologies. *J Cardiovasc Electrophysiol* 2005;**16**(4):402–8.

2 Asirvatham SJ. Correlative anatomy and electrophysiology for the interventional electrophysiologist. *J Cardiovasc Electrophysiol* 2009;**20**(1):113–22.

3 Friedman PA, Luria D, Munger T, *et al*. Progressive isthmus delay during atrial flutter ablation: the critical importance of isthmus spanning electrodes for distinguishing pseudoblock from block. *Pacing Clin Electrophysiol* 2002;**25**(3):308–15.

4 Cheng J, Cabeen WR, Scheinman MM. Right atrial flutter due to lower loop reentry mechanism and anatomic substrates. *Circulation* 1999;**99**(13):1700–5.

5 Friedman PA, Luria D, Fenton AM, *et al*. Global right atrial mapping of human atrial flutter: the presence of posteromedial (sinus venosa region) functional block and double potentials: a study in biplane fluoroscopy and intracardiac echocardiography. *Circulation* 2000;**101**(13):1568–77.

6 Becker AE. Left atrial isthmus. *J Cardiovasc Electrophysiol* 2004;**15**(7):809–12.

7 Syed FF, Ackerman MJ, McLeod CJ, et al. Sites of successful ventricular fibrillation ablation in bileaflet mitral valve prolapse syndrome. *Circ Arrhythm Electrophysiol* 2016;**9**(5):e004005.

8 Yokokawa M, Sundaram B, Garg A, *et al*. Impact of mitral isthmus anatomy on the likelihood of achieving linear block in patients undergoing catheter ablation of persistent atrial fibrillation. *Heart Rhythm* 2011;**8**(9):1404–10.

9 Takahashi Y, Jais P, Hocini M, *et al*. Acute occlusion of the left circumflex coronary artery during mitral isthmus linear ablation. *J Cardiovasc Electrophysiol* 2005;**16**(10):1104–7.

10 Angelini A, Ho, SY, Anderson, RH, *et al*. A histological study of the atrioventricular junction in hearts with normal and prolapsed leaflets of the mitral valve. *Br Heart J* 1988;**59**(6):712–16.

11 Macedo PG, Kapa S, Mears JA, *et al*. Correlative anatomy for the electrophysiologist:ablation for atrial fibrillation. Part II: regional anatomy of the atria and relevance to damage of adjacent structures during AF ablation. *J Cardiovasc Electrophysiol* 2010;**21**(7):829–36.

12 D'Avila A, Thiagalingam A, Foley L, *et al*. Temporary occlusion of the great cardiac vein and coronary sinus to facilitate radiofrequency catheter ablation of the mitral isthmus. *J Cardiovasc Electrophysiol* 2008;**19**(6):645–50.

13 Wong KC, Jones M, Qureshi N, *et al*. Balloon occlusion of the distal coronary sinus facilitates mitral isthmus ablation. *Heart Rhythm* 2011;**8**(6):833–9.

14 Miyazaki S, Derval N, Shah A, *et al*. Mitral isthmus block in a case of persistent left superior vena cava. *J Cardiovasc Electrophysiol* 2011;**22**(3):343–5.

15 Huang H, Wang X, Ouyang F, *et al*. Catheter ablation of anteroseptal accessory pathway in the non-coronary aortic sinus. *Europace* 2006;**8**(12):1041–4.

16 Suleiman M, Powell BD, Munger TM, *et al*. Successful cryoablation in the noncoronary aortic cusp for a left anteroseptal accessory pathway. *J Interv Card Electrophysiol* 2008;**23**(3):205–11.

17 Daniels DV, Lu YY, Morton JB, *et al*. Idiopathic epicardial left ventricular tachycardia originating remote from the sinus of Valsalva: electrophysiological characteristics, catheter ablation, and identification from the 12-lead electrocardiogram. *Circulation* 2006;**113**(13):1659–66.

18 Asirvatham SJ. Correlative anatomy for the invasive electrophysiologist:outflow tract and supravalvar arrhythmia. *J Cardiovasc Electrophysiol* 2009;**20**(8):955–68.

19 Hasdemir CAN, Aktas S, Govsa F, *et al*. Demonstration of ventricular myocardial extensions into the pulmonary artery and aorta beyond the ventriculo-arterial junction. *Pacing Clin Electrophysiol* 2007;**30**(4):534–9.

20 Hai JJ, Chahal AA, Friedman PA, *et al*. Electrophysiologic characteristics of ventricular arrhythmias arising from the aortic mitral continuity – potential role of the conduction system. *J Cardiovasc Electrophysiol* 2015;**26**(2):158–63.

21 Suleiman M, Asirvatham SJ. Ablation above the semilunar valves: when, why, and how? *Part I. Heart Rhythm* 2008;**5**(10):1485–92.

22 Tabatabaei N, Asirvatham SJ. Supravalvular arrhythmia: identifying and ablating the substrate. *Circulation Arrhythmia Electrophysiol* 2009;**2**(3):316–26.

23 Gami AS, Venkatachalam KL, Friedman PA, *et al*. Successful ablation of atrial tachycardia in the right coronary cusp of the aortic valve in a patient with atrial fibrillation: what is the substrate? *J Cardiovasc Electrophysiol* 2008;**19**(9):982–6.

24 Liu XK, Barrett R, Packer DL, *et al*. Successful management of recurrent ventricular tachycardia by electrical isolation of anterolateral papillary muscle. *Heart Rhythm* 2008;**5**(3):479–82.

25 Crawford T, Mueller G, Good E, *et al*. Ventricular arrhythmias originating from papillary muscles in the right ventricle. *Heart Rhythm* 2010;**7**(6):725–30.

26 Hakim FA, Kendall CB, Alharthi M, *et al*. Parachute mitral valve in adults – a systematic overview. *Echocardiography* 2010;**27**(5):581–6.

27 Baxi AJ, Tavakoli S, Vargas D, *et al*. Bands, chords, tendons, and membranes in the heart: an imaging overview. *Curr Probl Diagn Radiol* 2016;**45**:380–91.

28 Rowin EJ, Maron BJ, Lesser JR, *et al*. Papillary muscle insertion directly into the anterior mitral leaflet in hypertrophic cardiomyopathy, its identification and cause of outflow obstruction by cardiac magnetic resonance imaging, and its surgical management. *Am J Cardiol* 2013;**111**(11):1677–9.

29 Syed FF, Hai JJ, Lachman N, *et al*. The infrahisian conduction system and endocavitary cardiac structures: relevance for the invasive electrophysiologist. *J Interv Card Electrophysiol* 2014;**39**(1):45–56.

30 Abdulla AK, Frustaci A, Martinez JE, *et al*. Echocardiography and pathology of left ventricular "false tendons". *Chest* 1990;**98**(1):129–32.

31 Kervancioglu M, Ozbag D, Kervancioglu P, *et al*. Echocardiographic and morphologic examination of left ventricular false tendons in human and animal hearts. *Clin Anat* 2003;**16**(5):389–95.

32 Joyner RW, Ramza BM, Tan RC. Effects of stimulation frequency on Purkinje–ventricular conduction. *Ann N Y Acad Sci* 1990;**591**:38–50.

33 Yamada T, Doppalapudi H, McElderry TH, *et al*. Electrocardiographic and electrophysiological characteristics in idiopathic ventricular arrhythmias originating from the papillary muscles in the left ventricle:relevance for catheter ablation. *Circulation Arrhythmia Electrophysiol* 2010;**3**(4):324–31.

34 Yamada T, McElderry TH, Okada T, *et al*. Idiopathic focal ventricular arrhythmias originating from the anterior papillary muscle in the left ventricle. *J Cardiovasc Electrophysiol* 2009;**20**(8):866–72.

35 Abouezzeddine O, Suleiman M, Buescher T, *et al*. Relevance of endocavitary structures in ablation procedures for ventricular tachycardia. *J Cardiovasc Electrophysiol* 2010;**21**(3):245–54.

36 Yokokawa M, Good E, Desjardins B, *et al*. Predictors of successful catheter ablation of ventricular arrhythmias arising from the papillary muscles. *Heart Rhythm* 2010;**7**(11):1654–9.

37 Del Carpio Munoz, F, Buescher TL, Asirvatham SJ. Teaching points with 3-dimensional mapping of cardiac arrhythmias: teaching point 3: when early is not early. *Circulation Arrhythmia Electrophysiol* 2011;**4**(2):e11–14.

38 Haïssaguerre M, Shah DC, Jais P, *et al*. Role of Purkinje conducting system in triggering of idiopathic ventricular fibrillation. *Lancet* 2002;**359**(9307):677–8.

39 Santoro F, Di Biase L, Hranitzky P, *et al*. Ventricular fibrillation triggered by PVCs from papillary muscles: clinical features and ablation. *J Cardiovasc Electrophysiol* 2014;**25**(11):1158–64.

40 Sriram CS, Syed FF, Ferguson EM, *et al*. Malignant bileaflet mitral valve prolapse syndrome in patients with otherwise idiopathic out-of-hospital cardiac arrest. *J Am Coll Cardiol* 2013;**62**(3):222–30.

41 Nogami A. Purkinje-related arrhythmias part I: monomorphic ventricular tachycardias. *Pacing Clin Electrophysiol* 2011;**34**(5):624–50.

42 Nakagawa H, Lazzara R, Khastgir T, *et al*. Role of the tricuspid annulus and the eustachian valve/ridge on atrial flutter. Relevance to catheter ablation of the septal isthmus and a new technique for rapid identification of ablation success. *Circulation* 1996;**94**(3):407–24.

43 Lachman N, Syed FF, Habib A, *et al*. Correlative anatomy for the electrophysiologist, Part I: the pericardial space, oblique sinus, transverse sinus. *J Cardiovasc Electrophysiol* 2010;**21**(12):1421–6.

44 Syed F, Lachman N, Christensen K, *et al*. The pericardial space: obtaining access and an approach to fluoroscopic anatomy. *Cardiac Electrophysiol Clin* 2010;**2**(1):9–23.

45 Cabrera JA, Ho SY, Climent V, *et al*. The architecture of the left lateral atrial wall: a particular anatomic region with implications for ablation of atrial fibrillation. *Eur Heart J* 2008;**29**(3):356–62.

46 D'Avila,A, Scanavacca M, Sosa E, *et al*. Pericardial Anatomy for the interventional electrophysiologist. *J Cardiovasc Electrophysiol* 2003;**14**(4):422–30.

47 Sánchez-Quintana D, Cabrera JA, Climent V, *et al*. How close are the phrenic nerves to cardiac structures? Implications for cardiac interventionalists. *J Cardiovasc Electrophysiol* 2005;**16**(3):309–13.

48 Di Biase L, Burkhardt JD, Pelargonio G, *et al*. Prevention of phrenic nerve injury during epicardial ablation: comparison of methods for separating the phrenic nerve from the epicardial surface. *Heart Rhythm* 2009;**6**(7):957–61.

6

Anatomy of the Outflow Tract Region: Relevance to Arrhythmias and Catheter Ablation

Andres Enriquez[1], Jason Bradfield[2], Kalyanam Shivkumar[2], and Fermin C. Garcia[3]

[1] *Division of Cardiology, Queen's University, Kingston, ON, Canada*
[2] *UCLA Cardiac Arrhythmia Center, UCLA Neurocardiology Research Center, Los Angeles, CA, USA*
[3] *Department of Medicine, Perelman School of Medicine, University of Pennsylvania, Philadelphia, PA, USA*

Introduction

The right and left ventricular outflow tracts (OTs) are the most common source of ventricular arrhythmias (VAs) in patients with structurally normal hearts [1–3] and are not an infrequent site of origin in structurally abnormal hearts, especially in the setting of non-ischemic cardiomyopathies (NICM). The clinical presentation of these arrhythmias includes isolated monomorphic frequent premature ventricular contractions (PVCs), repetitive non-sustained ventricular tachycardia (VT), sustained VT and, less commonly, triggers of ventricular fibrillation. Most of these arrhythmias can be effectively treated by catheter ablation, which has become a first-line therapy in symptomatic patients, in those with left ventricular (LV) dysfunction due to arrhythmia burden or in case of failure of antiarrhythmic therapy [4].

The OT is a relatively narrow anatomical region with complex relationships. When the heart is seen as *in situ* in the chest from an anterior view, the OT is dominated by the right ventricular outflow tract (RVOT) region between the tricuspid and pulmonic valves. The RVOT is anterior and leftward to the left ventricular outflow tract (LVOT), of which the only visible part in this view is the proximal ascending aorta crossing posterior and rightward to the RVOT and pulmonic artery. A posterior view of the heart allows a more panoramic view of the LVOT region, which consists of the LV ostium or opening of the LV and its components [5,6]. These include the ventricular muscle of the LV ostium, the aortic sinuses of Valsalva, the mitral annulus, the basal LV, and the LV summit (LVS) (Figure 6.1).

An organized approach to the mapping and ablation of OT arrhythmias starts with a detailed understanding of the anatomy and relationships of the OT structures followed by analysis of the 12-lead electrocardiogram (ECG) of the clinical arrhythmia [7]. This results in a hypothesis of where to direct the initial mapping efforts to guide the ablation stategy.

In this chapter, we review the gross anatomy of the OT region, the electrocardiographic correlations of the different structures, and the main anatomical relationships relevant for catheter ablation.

Right ventricular outflow tract

The right ventricle (RV) is the most anterior cardiac chamber, lying immediately behind the sternum, and wraps around the aorta, so its anterior aspect becomes the most leftward and highest OT structure. Beginning at the level of the tricuspid valve (TV), the RV is divided into two parts: an inflow tract or "sinus," higly trabeculated, particularly at the apex, and an outflow tract or "infundibulum (conus)," relatively glabrous (Figure 6.2). Both portions are separated by the crista supraventricularis, a prominent muscular ridge that extends from the interventricular septum to the RV free wall, becoming the moderator band [8]. Although the RV inflow and the TV lie to the right and anterior to the LV inflow and mitral valve (MV), the RVOT crosses the LVOT anteriorly and therefore the upper portion and the pulmonic valve (PV) lie to the left of the aortic valve [9]. The pulmonary trunk continues leftward and divides into a right and left pulmonary artery, the right of which will course below the aortic arch. The posterior wall of the infundibulum is in continuity with the LVOT and adjacent anterior interventricular septum, while its more distal portion is immediately adjacent to the left aortic cusps.

The anatomical relationship between the RVOT and LVOT can be better understood if one imagines that the RVOT wraps around the LVOT, so that the posteroseptal aspect starting in the septal leaflet of the TV continues wrapping around the right coronary cusp (RCC) and finishes in the septal pumonic valve (Figure 6.3).

Cardiac Mapping, Fifth Edition. Edited by Mohammad Shenasa, Gerhard Hindricks, David J. Callans, John M. Miller, and Mark E. Josephson.

Companion website: www.wiley.com/go/cardiacmapping5e

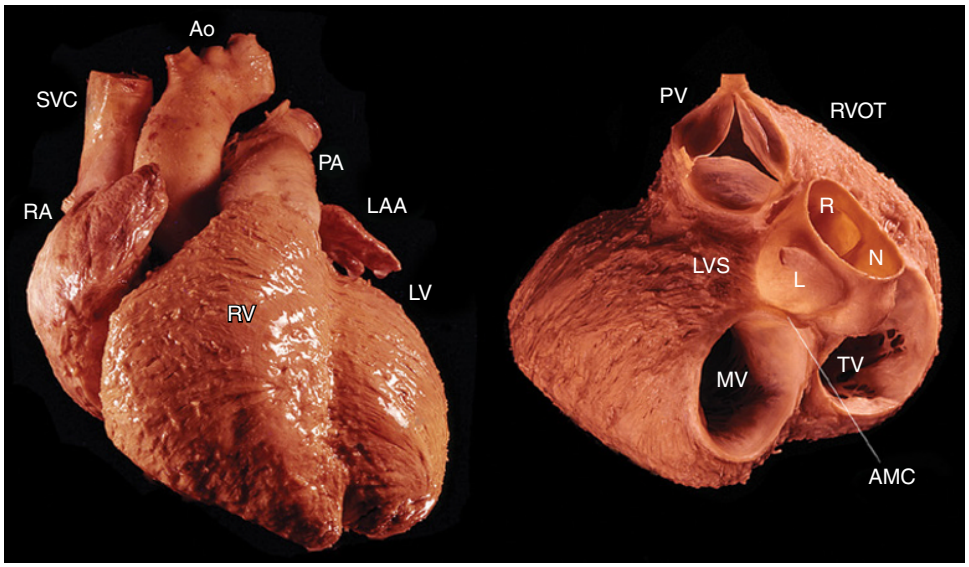

Figure 6.1 Anatomy of the outflow tract region. The anterior view is mostly dominanted by the RVOT wrapping around the aorta. In the posterior view the complex relationship of all the structures of the RVOT and LVOT becomes evident. AMC, aortomitral continuity; Ao, aorta; L, left coronary cusp; LAA, left atrial appendage; LV, left ventricle; LVS, left ventricular summit; MV, mitral valve; N, non-coronary cusp; PA, pulmonary artery; PV, pulmonic valve; R, right coronary cusp; RA, right atrium; RV, right ventricle; SVC, superior vena cava; TV, tricuspid valve. *Source:* Reproduced with permission from Dr K. Shivkumar. Copyright UCLA Cardiac Arrhythmia Center, Wallace A. McAlpine Collection.

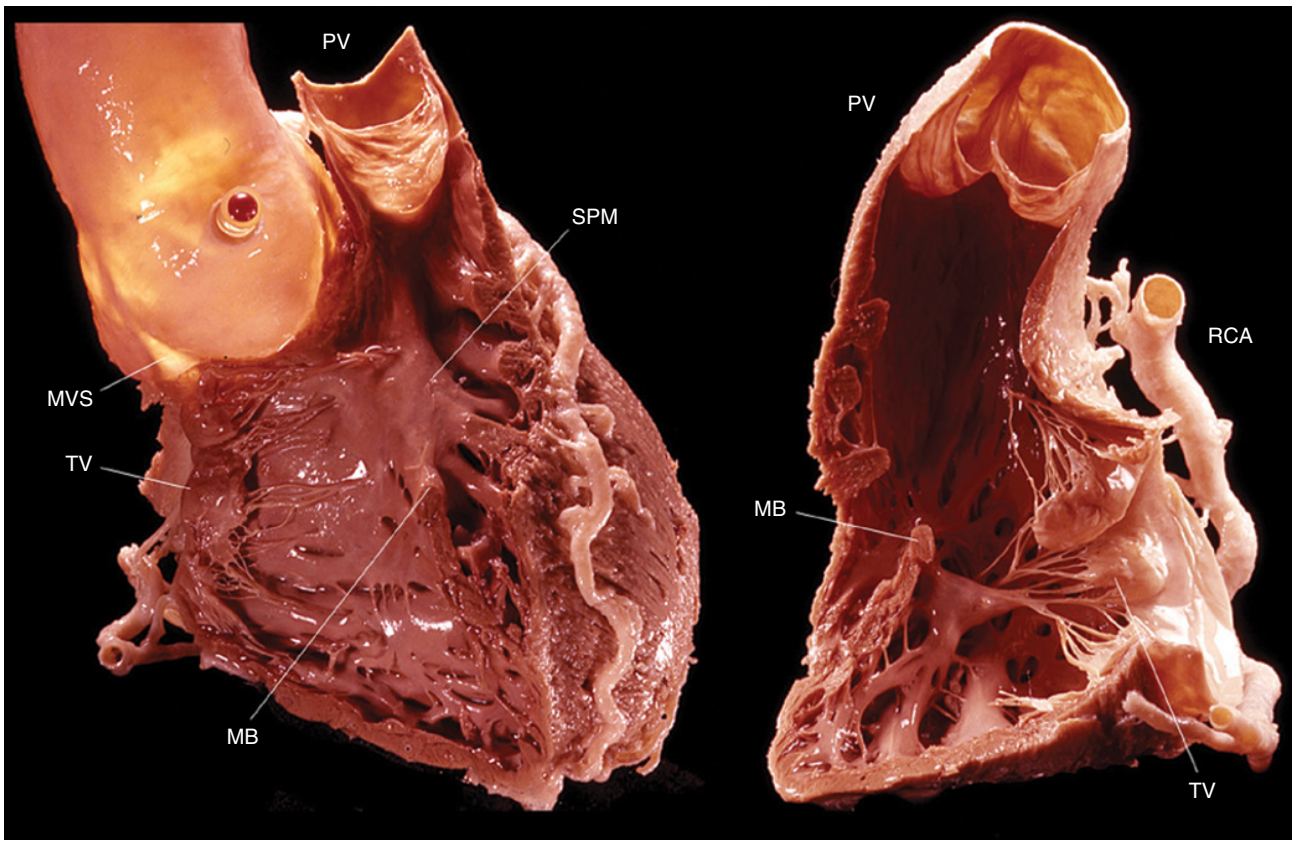

Figure 6.2 RV anatomy. The free wall was separated from the septal wall by creating incisions in the five points of attachment (anterior, pulmonic valve, posterior, tricuspid valve, and inferior). The RV is composed of an inflow portion (sinus) and an outflow portion (infundibulum or RVOT) demarcated by the infundibular muscles. The infundibulum wraps around the LVOT and has two opposing crescentic surfaces: anterior or "free wall" surface in contiguity with the sternum, and a posterior or "septal" surface, adjacent to the interventricular septum and more distally to the aortic cusps, in particular, the RCC and part of the LCC. MB, moderator band; MVS, membranous ventricular septum; PV, pulmonary valve; RCA, right coronary artery; SPM, septal papillary muscle; TV, tricuspid valve. *Source:* Reproduced with permission from Dr K. Shivkumar. Copyright UCLA Cardiac Arrhythmia Center, Wallace A. McAlpine Collection.

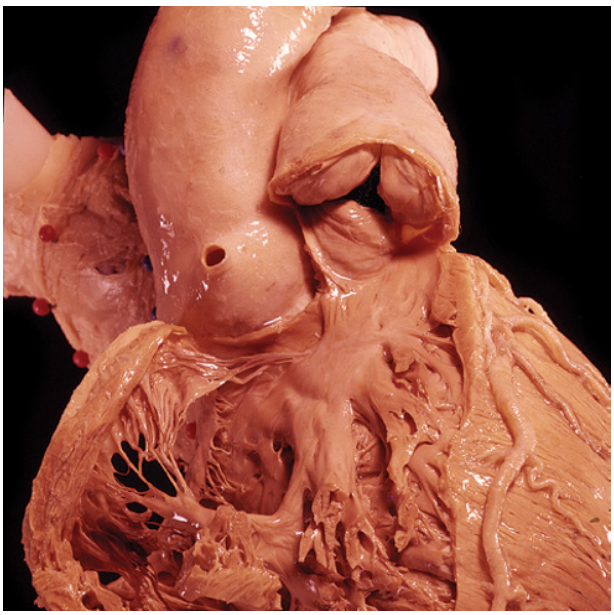

Figure 6.3 RVOT anatomy. In this image the RV free wall has been resected by an incision in the anterior attachment point, parallel to the LAD, the pulmonic valve, the posterior attachment, the TV, and the inferior attachment (not shown). This exposes the septal RV. The infundibulum wraps around the aorta, becoming the conus of the RVOT. The most anterior portion is below the pulmonic valve. *Source:* Reproduced with permission from Dr K. Shivkumar. Copyright UCLA Cardiac Arrhythmia Center, Wallace A. McAlpine Collection.

The anteroseptal aspect of the RVOT is adjacent to the left coronary cusp (LCC), in close proximity to the left anterior descending (LAD) and anterior interventricular vein (AIV).

The RVOT is the most common source of idiopathic VAs [3,10]. For the purpose of mapping, it can be divided into three zones, named 1 to 3 from posterior to anterior, each of which is subdivided into a septal and free wall site [11]. Most RVOT VAs originate from the anterosuperior aspect of septal aspect below the PV (septal sites 2 and 3). VAs originating from the RVOT typically have a left bundle branch block (LBBB) configuration with rare exceptions and an inferior axis. Free wall RVOT sites can be differentiated from septal sites by a smaller voltage in lead II and III, later precordial transition (V4–V5 versus V3–V4), a wider QRS duration (>140 ms) and the presence of characteristic notching in the inferior leads. In addition, the QRS morphology in lead I helps to distinguish posterior from anterior sites along the septum and free wall, with posterior locations (site 1) demonstrating a positive polarity in lead I (R wave) and more negative aVR than aVL, while anterior locations (site 3) exhibit a negative polarity in lead I (QS pattern) and more negative aVL than aVR [11]. Intermediate sites (site 2) demonstrate either a biphasic or multiphasic QRS pattern (rs, qrs) or an isoelectric segment preceding a small q or r wave.

Left ventricular outflow tract

The LVOT corresponds to the opening of the LV. McAlpine named the opening of the LV the LV ostium. This has an elliptical shape and is covered by the aortoventricular membrane, a fibrous structure that is perforated by the aorta anteriorly and the mitral valve posteriorly and laterally (Figure 6.4). In contrast to the RV infundibulum, which is composed entirely of muscle, the ventriculo-aortic junction is composed of a fibrous portion and a muscular portion [12,13]. The muscular portion, more extensive, corresponds to the interventricular muscular septum and is under the right coronary sinus and the anterior half of the left coronary sinus. The fibrous portion corresponds to the aortomitral continuity (AMC), a curtain of fibrous tissue that extends between the anterior leaflet of the MV and the noncoronary and left coronary leaflets of the aortic valve.

Ventricular arrhythmias may originate from the muscle of the LV ostium and they can be mapped and/or ablated directly from the subvalvular LV endocardium or indirectly from the coronary sinuses or the coronary venous circulation. If we start at the lateral top aspect of the LV ostium and move in a clockwise fashion (from the perspective of the PA view), the following structures can be used for mapping of LVOT arrhythmias (see Figure 6.4): the lateral and anterior aspect of the MV, the left fibrous trigone and AMC, the LCC, the right-left (R-L) cusp junction, and the RCC. VAs from the top of the MV can be mapped from below the valve or epicardially from the great cardiac vein. If we continue in a clockwise direction, VAs from the LV summit (see later) can be mapped from the LCC, below the valve in the LV or epicardially from the AIV. VAs from the more medial ventricular muscle can be mapped from the R-L junction or from below the valve. VAs from the anterior and septal portion of the LV ostium can be mapped from the RCC. Further clockwise rotation will take us to the membranous interventricular septum. This portion contains the penetrating portion of the His bundle and is devoid of muscle (and therefore cannot be a source of VAs). Even further clockwise rotation leads us to the posterior-superior process of the LV. This is the most inferior and posterior aspect of the LV and is adjacent to the inferior and medial aspect of the right atrium (RA) [14]. VAs from the posterior-superior process of the LV can be mapped from the LV endocardium below the NCC or from the adjacent RA.

Aortic root

The aortic valve occupies a central position within the heart and is composed of three cusps, each with relevant anatomical relationships. From an attitudinal perspective, the RCC is the most anterior and inferior cusp relative to

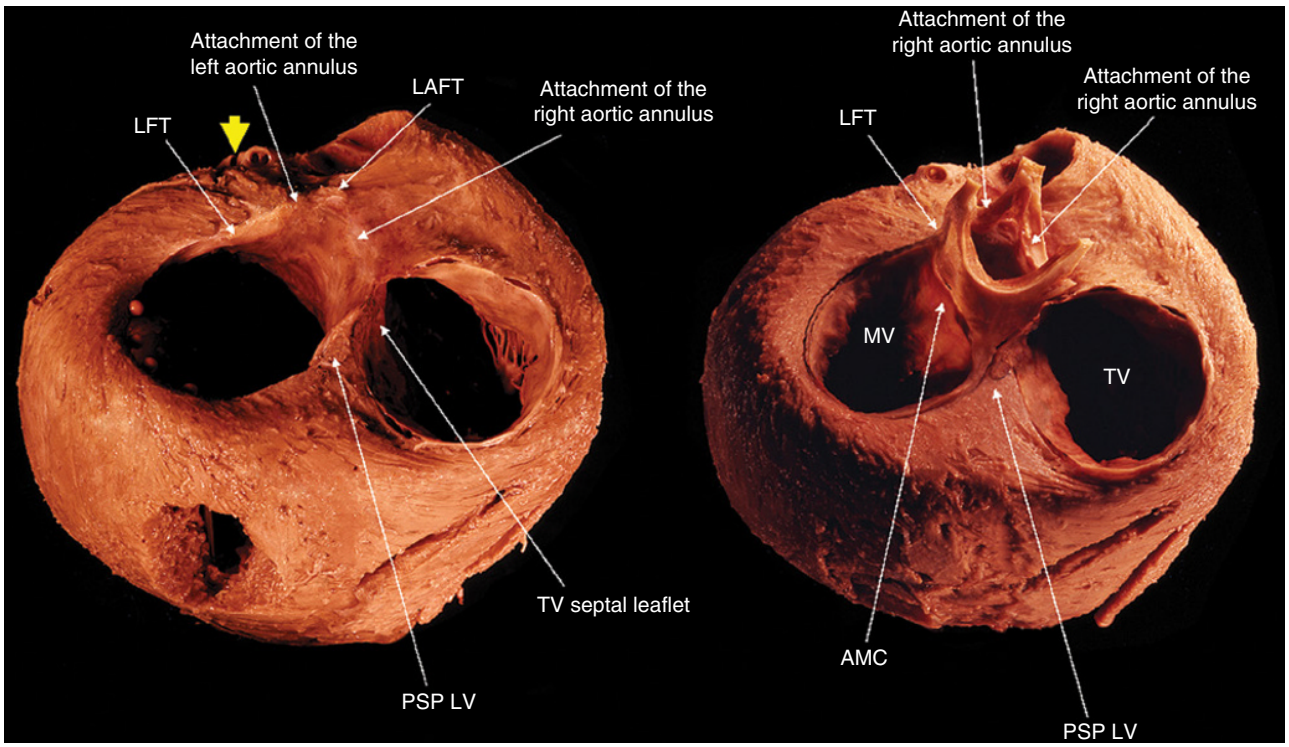

Figure 6.4 Anatomy of the LV ostium after removal of the atria and great vessels down to the annuli. AMC, aortomitral continuity; LFT, left fibrous trigone; LAFT, left anterior fibrous trigone; MV, mitral valve; PSP LV, posterior superior process of the LV; TV, tricuspid valve. Yellow arrow represents the LV summit. *Source:* Reproduced with permission from Dr K. Shivkumar. Copyright UCLA Cardiac Arrhythmia Center, Wallace A. McAlpine Collection.

the sternum, the NCC is posterior and rightward, and the LCC is posterior and leftward [9]. The RCC is in close proximity to the posteroseptal aspect of the RVOT, while the LCC is adjacent to the the anterior aspect of the LV ostium, in close proximity to the LAD and AIV/great cardiac vein (GCV) junction from the epicardial surface. On the other side, the NCC is in relationship to both the left and right atria separated by the interatrial septum. Below the commisure between the RCC and NCC lies the membranous ventricular septum, where the penetrating bundle of His is located.

According to a series, PVC/VTs ablated from the aortic root represent 71% of LVOT VAs and 17% of all idiopathic VAs [15]. Although sleeves of myocardial tissue may extend into the aortic sinuses and be a source of PVC/VT, most ventricular arrhythmias ablated from the aortic root are targeted at the R-L junction, where the ventricular myocardium of the LV ostium comes in direct contact with the aorta [16].

Ventricular arrhythmias from the RCC have a LBBB configuration with a QS pattern in V1 and precordial transition at V2 or V3, while those arising from the LCC have a predominant R wave in V1, often with a multiphasic pattern (M or W) [17]. VAs successfully ablated from the R-L junction typically demonstrate a QS complex with notching of the downstroke in lead V1, and precordial transition by lead V3 [16]. VAs originating from the NCC are extremely rare due to the absence of muscular fibers in this region.

Aortomitral continuity

As previously mentioned, the AMC is a curtain of fibrous tissue that extends between the anterior leaflet of the MV and the non-coronary and most posterior aspect of the left coronary cusp (Figure 6.5). Similar to what happens with the right/left cusp junction, the AMC does not contain muscle fibers, but ventricular arrhythmias may originate from the underlying ventricular myocardium of the LV ostium and thus can be ablated from this structure at its most anterior aspect.

Studies report that 11–16% of all idiopathic LVOT VTs are ablated from the AMC [3,6] and also reentrant VTs in patients with structural heart disease can be targeted from this structure [18]. The 12-lead ECG of VAs ablated from the AMC shows a right bundle branch block (RBBB) pattern in the majority of cases, with a positive vector in V1. Using pace mapping, Dixit et al. demonstrated that a qR pattern in lead V1 is relatively specific for pacing at the AMC [19], but the sensitivity of this finding is <50% [18,20].

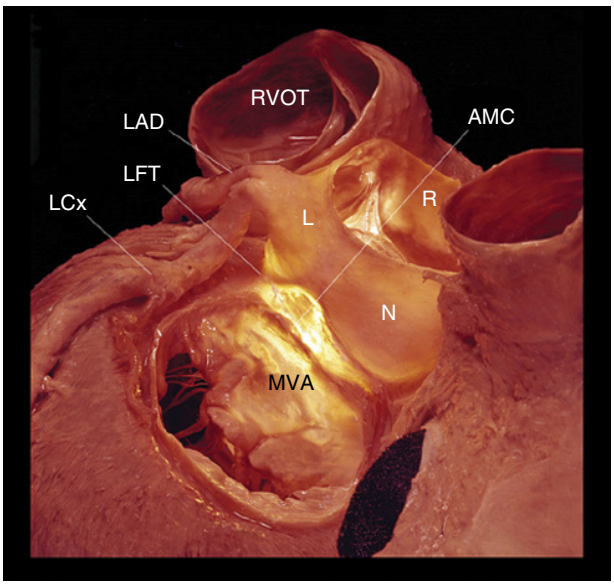

Figure 6.5 The LV ostium and its components after resection of the LA, showing the possible sources of LVOT ventricular arrhythmias and the structures from which ablation can be performed. The left anterior descending/left circumflex bifurcation covers the LV summit. AMC, aortomitral continuity; L, left coronary cusp; LAD, left anterior descending coronary artery; LCx, left circumflex coronary artery; LAD, left anterior descending; LFT, left fibrous trigone; LV, left ventricle; MVA, anterior mitral valve leaflet; N, non-coronary cusp; RVOT, right ventricular outflow tract. *Source:* Reproduced with permission from Dr K. Shivkumar. Copyright UCLA Cardiac Arrhythmia Center, Wallace A. McAlpine Collection.

Pulmonic valve

The pulmonic and aortic valves are not located at the same level. The pulmonic valve is cephalad to the aortic valve and faces to the left and slightly posteriorly. In relation to the heart, the pulmonary cusps are named anterior, left and right, but when viewed from an attitudinal perspective, the anterior cusp is actually anterior and leftward, the right cusp is anterior and rightward, and the left cusp is posterior.

Myocardial sleeves may extend above the pulmonary cusps and VAs originating within the pulmonary artery have been reported [21]. Electrocardiographic characteristics of these arrhythmias include a strong right inferior axis with tall R waves in II, III, and aVF, negative QRS in lead I and deeper S waves in aVL than aVR. These findings are explained by the fact that the site of origin within the PA is higher, more anterior and more leftward compared to most RVOT VAs. It is important to aknowledge that the LAD runs at the same level of the pulmonic valve in the interventricular sulcus and ablation above the PV could injure the proximal LAD with catastrophic consequences. Therefore, any attempt at ablation above the level of the PV should be preceded by careful definition of the coronary circulation.

Mitral valve annulus

The MV apparatus comprises the annulus, the two leaflets, the tendinous cords, and the papillary muscles (PMs) [22,23]. The mitral annulus has a D shape, with the straight border in fibrous continuity with the aortic valve, while the remaining two-thirds are mainly muscular.

Ventricular arrhythmias ablated from below the MV annulus represent a 5% of all idiopathic VTs/PVCs [3,24,25]. The most common location is anterolateral, followed by the posteroseptal and posterior regions.

The ECG typically shows a RBBB pattern and an S wave in lead V6. Precordial R wave transition usually occurs by V1 (positive concordance in precordial leads), but in some VTs mapped to the posteroseptal region, transition may occur between leads V1 and V2 [3,24,25]. Compared to septal sites, anterolateral and lateral sites exhibit a longer QRS duration along with predominantly negative forces in lead I. For mapping and ablation, access to the MV can be retrograde, via transeptal puncture or epicardial via the CS.

Left ventricular summit

The term *LV summit* describes the highest portion of the LV epicardium, above the upper end of the anterior interventricular sulcus [5] (Figure 6.6). It is a triangular region bounded by the bifurcation between the LAD and the left circumflex (LCx) coronary arteries [26]. It is bisected laterally by the GCV in two regions: a medial and more superior region, close to the apex of the triangle, that is inaccessible to catheter ablation due to close proximity to the major coronary vessels (the inaccessible area), and a more lateral and inferior region, toward the base of the triangle, that may be suitable for catheter ablation (the accessible area).

Left ventricular summit arrhythmias usually have a RBBB pattern with inferior axis and larger R waves in lead III than lead II, but VAs from the inaccessible area may also exhibit a LBBB with inferior axis and early transition (V2 or V3). An epicardial origin is suspected by prominent pseudo-delta waves [26–28].

Despite their epicardial origin, LV summit arrhythmias rarely can be ablated from the pericardial space due to close proximity to the major coronary vessels and the presence of a thick layer of epicardial fat. Instead, they are more often targeted from the coronary

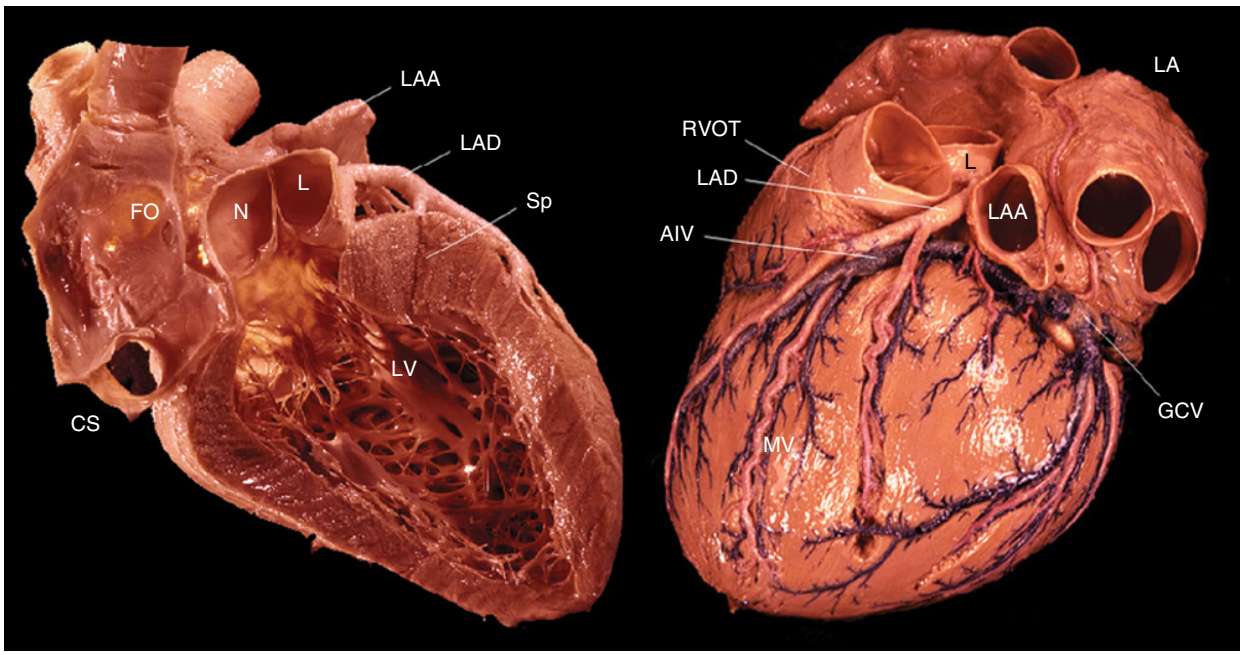

Figure 6.6 Left ventricular summit (LVS) with main anatomical relationships. The LVS is a triangular region bounded by the left anterior descending and left circumflex coronary artery, corresponding to the highest portion of the left ventricular epicardium. The great cardiac vein, which then becomes the anterior interventricular vein, bisects the LVS into an apical and medial portion (inaccessible area) and a basal and more lateral portion (accessible area). The venous circulation can be used to map the LVS but is in variable proximity to the LAD, which limits its utility. Also, epicardial access is limited by the presence of fat and the coronary arteries. AIV, anterior interventricular vein; CS, coronary sinus; FO, fossa ovale; L, left coronary cusp; LA, left atrium; LAA, left atrial appendage; LAD, left anterior descending; LV, left ventricle; N, non-coronary cusp; LV, left ventricle; RVOT, right ventricular outflow tract; Sp, septal perforator. *Source:* Reproduced with permission from Dr K. Shivkumar. Copyright UCLA Cardiac Arrhythmia Center, Wallace A. McAlpine Collection.

venous system (GCV-AIV) or adjacent endocardial structures such as the LCC, LVOT endocardium or anteroseptal RVOT [28].

General approach for ECG localization

A systematic approach to ECG analysis is helpful for predicting the likely site of arrhythmia origin, which is important for preprocedural planning and patient counseling regarding risks and success rates. All OT VAs share an inferiorly directed QRS axis, with positive forces in leads II, III, and aVF. Additional elements allow a more precise localization, including the bundle branch pattern, precordial transition, and frontal plane axis [7].

A first step is to discriminate between origin from the RVOT or LVOT regions. Typically, RVOT VAs exhibit a LBBB configuration with precordial R/S transition at or after lead V3. By contrast, LVOT VT usually manifests either a RBBB or a LBBB with precordial R/S transition at or before lead V3. This can be better understood if we imagine that the RVOT is anterior in the chest and the precordial leads register anterior to posterior (front to back) (Figure 6.7). Thus, as we move progressively more posterior from the RVOT free wall to the lateral mitral annulus, the precordial transition becomes progressively earlier (V4–V5 for RVOT free wall, V3–V4 for RVOT septum, V2–V3 for RCC) and finally transforms from an LBBB to a RBBB configuration at the top of the MV or LCC.

Differentiation between RVOT/LVOT may be challenging when the R/S transition is in V3, as this pattern can be seen in VAs from both the posteroseptal RVOT or the LVOT (especially RCC), and some ECG criteria have been proposed to predict the site of origin in these cases. One algorithm compares the precordial transition during VT/PVCs and sinus rhythm [29]. When VT/PVC transition occurs later than the sinus rhythm transition, the PVC origin is the RVOT (100% specificity). If the VT/PVC transition occurs at or earlier than the sinus rhythm transition, then the so-called V2 transition ratio is measured. This is calculated as the percentage R wave during VT/PVC divided by the percentage R wave during sinus rhyrhm. A ratio ≥0.6 predicts an LVOT origin with a sensitivity of 95% and a specificity of 100%. Another ECG criterion is the indexes of R wave duration

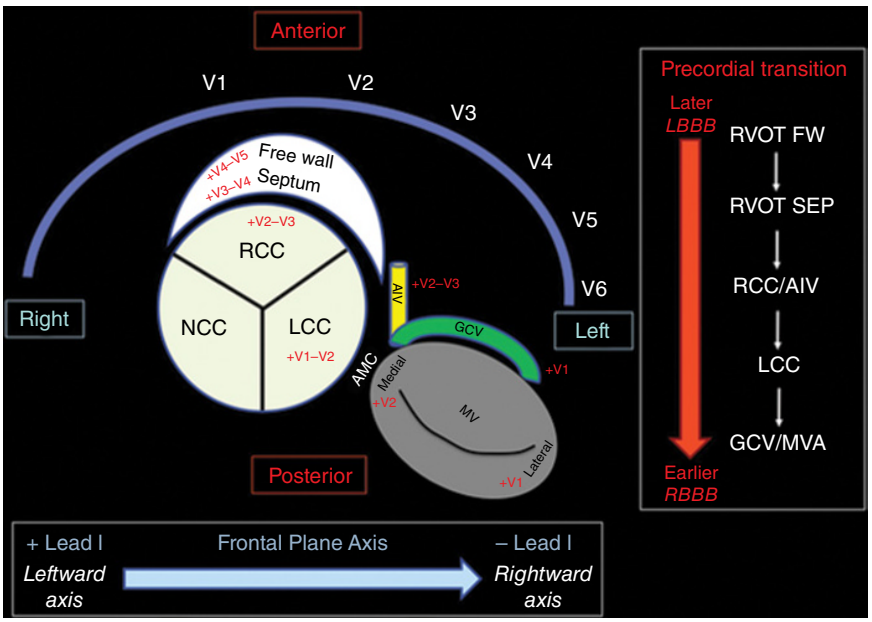

Figure 6.7 Attitudinally based schema to understand the ECG patterns of outflow tract ventricular arrhythmias. AIV, anterior interventricular vein; AMC, aortomitral continuity; FW, free wall; GCV, great cardiac vein; LBBB, left bundle branch block; LCC, left coronary cusp; MV, mitral valve; MVA, mitral valve annulus; NCC, non-coronary cusp; RBBB, right bundle branch block; RCC, right coronary cusp; RVOT, right ventricular outflow tract; SEP, septum. *Source:* Hutchinson and Garcia [7]. Reproduced with permission from John Wiley & Sons.

(QRS duration divided by the longer R wave duration in V1 or V2) and R/S wave amplitude (greater R/S wave amplitude ratio) in leads V1 and V2 [30]. A longer R wave duration index (>0.5) and higher R/S wave amplitude index (>0.3) suggest an LVOT origin.

Another important element to consider is the frontal plane QRS axis, reflected by the bipolar limb lead I and by the relative S wave amplitude in aVL compared to aVR (Figure 6.8). A positive QRS complex in lead I and a more negative aVR compared to aVL suggests an origin on the right side of midline. Such structures include the posterior RVOT, RCC, TV, the parahisian region, and the posterior LV. In contrast, a negative QRS complex in lead I and a more negative aVL than aVR suggests an origin on the left side of midline, including anterior RVOT, LCC, MV, and LV summit. The R–L junction can have characteristics of either the right or left side of the midline and its behavior in the frontal plane is less predictable, but a notch in the downstroke of V1 is suggestive of origin from this structure.

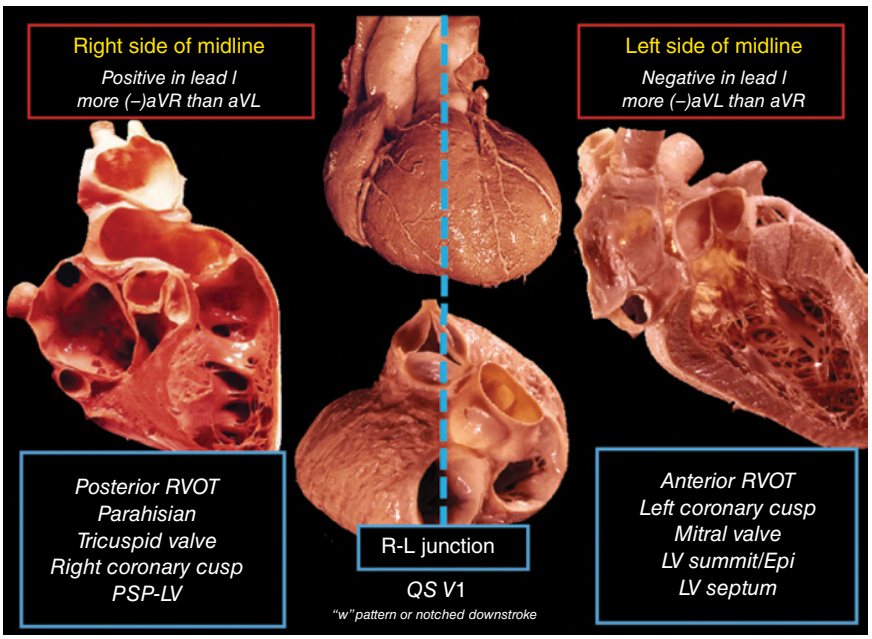

Figure 6.8 Determination of frontal plane axis to rapidly localize the site of origin of outflow tract ventricular arrhythmias. Ventricular arrhythmias are divided into those that are positive in lead I and those that are negative in lead I. The R–L junction could be in either group, but the signature "W" pattern in V1 helps guide mapping. Epi, epicardium; PSP-LV, posterior-superior process of the left ventricle; QS, RVOT, right ventricular outflow tract.

References

1 Buxton AE, Waxman HL, Marchlinski FE, Simson MB, Cassidy D, Josephson ME. Right ventricular tachycardia: clinical and electrophysiologic characteristics. *Circulation* 1983;**68**(5):917–27.

2 Kim RJ, Iwai S, Markowitz SM, Shah BK, Stein KM, Lerman BB. Clinical and electrophysiological spectrum of idiopathic ventricular outflow tract arrhythmias. *J Am Coll Cardiol* 2007;**49**(20):2035–43.

3 Tada H, Ito S, Naito S, *et al*. Idiopathic ventricular arrhythmia arising from the mitral annulus: a distinct subgroup of idiopathic ventricular arrhythmias. *J Am Coll Cardiol* 2005;**45**(6):877–86.

4 Priori SG, Blomström-Lundqvist C, Mazzanti A, *et al*. 2015 ESC Guidelines for the management of patients with ventricular arrhythmias and the prevention of sudden cardiac death: the Task Force for the Management of Patients with Ventricular Arrhythmias and the Prevention of Sudden Cardiac Death of the European Society of Cardiology (ESC). Endorsed by: Association for European Paediatric and Congenital Cardiology (AEPC). *Eur Heart J* 2015;**36**(41):2793–867.

5 McAlpine WA. *Heart and Coronary Arteries*. New York: Springer-Verlag, 1975.

6 Yamada T, Litovsky SH, Kay GN. The left ventricular ostium: an anatomic concept relevant to idiopathic ventricular arrhythmias. *Circ Arrhythm Electrophysiol* 2008;**1**(5):396–404.

7 Hutchinson MD, Garcia FC. An organized approach to the localization, mapping, and ablation of outflow tract ventricular arrhythmias. *J Cardiovasc Electrophysiol* 2013;**24**(10):1189–97.

8 James TN. Anatomy of the crista supraventricularis: its importance for understanding right ventricular function, right ventricular infarction and related conditions. *J Am Coll Cardiol* 1985;**6**(5):1083–95.

9 Asirvatham SJ. Correlative anatomy for the invasive electrophysiologist: outflow tract and supravalvar arrhythmia. *J Cardiovasc Electrophysiol* 2009;**20**(8):955–68.

10 Yamada T, McElderry HT, Doppalapudi H, Kay GN. Catheter ablation of ventricular arrhythmias originating in the vicinity of the His bundle: significance of mapping the aortic sinus cusp. *Heart Rhythm* 2008;**5**(1):37–42.

11 Dixit S, Gerstenfeld EP, Callans DJ, Marchlinski FE. Electrocardiographic patterns of superior right ventricular outflow tract tachycardias: distinguishing septal and free-wall sites of origin. *J Cardiovasc Electrophysiol* 2003;**14**(1):1–7.

12 Piazza N, de Jaegere P, Schultz C, Becker AE, Serruys PW, Anderson RH. Anatomy of the aortic valvar complex and its implications for transcatheter implantation of the aortic valve. *Circ Cardiovasc Interv* 2008;**1**(1):74–81.

13 De Kerchove L, El Khoury G. Anatomy and pathophysiology of the ventriculo-aortic junction: implication in aortic valve repair surgery. *Ann Cardiothorac Surg* 2013;**2**(1):57–64.

14 Santangeli P, Hutchinson MD, Supple GE, Callans DJ, Marchlinski FE, Garcia FC. Right atrial approach for ablation of ventricular arrhythmias arising from the left posterior-superior process of the left ventricle. *Circ Arrhythm Electrophysiol* 2016;**9**(7):ii.

15 Yamada T, McElderry HT, Doppalapudi H, *et al*. Idiopathic ventricular arrhythmias originating from the aortic root prevalence, electrocardiographic and electrophysiologic characteristics, and results of radiofrequency catheter ablation. *J Am Coll Cardiol* 2008;**52**(2):139–47.

16 Bala R, Garcia FC, Hutchinson MD, *et al*. Electrocardiographic and electrophysiologic features of ventricular arrhythmias originating from the right/left coronary cusp commissure. *Heart Rhythm* 2010;**7**(3):312–22.

17 Lin D, Ilkhanoff L, Gerstenfeld E, *et al*. Twelve-lead electrocardiographic characteristics of the aortic cusp region guided by intracardiac echocardiography and electroanatomic mapping. *Heart Rhythm* 2008;**5**(5):663–9.

18 Steven D, Roberts-Thomson KC, Seiler J, *et al*. Ventricular tachycardia arising from the aortomitral continuity in structural heart disease: characteristics and therapeutic considerations for an anatomically challenging area of origin. *Circ Arrhythm Electrophysiol* 2009;**2**(6):660–6.

19 Dixit S, Gerstenfeld EP, Lin D, *et al.* Identification of distinct electrocardiographic patterns from the basal left ventricle: distinguishing medial and lateral sites of origin in patients with idiopathic ventricular tachycardia. *Heart Rhythm* 2005;**2**(5):485–91.

20 Kumagai K, Fukuda K, Wakayama Y, *et al*. Electrocardiographic characteristics of the variants of idiopathic left ventricular outflow tract ventricular tachyarrhythmias. *J Cardiovasc Electrophysiol* 2008;**19**(5):495–501.

21 Sekiguchi Y, Aonuma K, Takahashi A, *et al*. Electrocardiographic and electrophysiologic characteristics of ventricular tachycardia originating within the pulmonary artery. *J Am Coll Cardiol* 2005;**45**(6):887–95.

22 McCarthy KP, Ring L, Rana BS. Anatomy of the mitral valve: understanding the mitral valve complex in mitral regurgitation. *Eur J Echocardiogr* 2010;**11**(10):i3–9.

23 Ho SY. Anatomy of the mitral valve. *Heart* 2002;**88**:iv5–iv10.

24 Wasmer K, Köbe J, Dechering DG, *et al*. Ventricular arrhythmias from the mitral annulus: patient characteristics, electrophysiological findings, ablation, and prognosis. *Heart Rhythm* 2013;**10**(6):783–8.

25 Kumagai K, Yamauchi Y, Takahashi A, *et al*. Idiopathic left ventricular tachycardia originating from the mitral annulus. *J Cardiovasc Electrophysiol* 2005;**16**(10):1029–36.

26 Yamada T, McElderry HT, Doppalapudi H, *et al*. Idiopathic ventricular arrhythmias originating from the left ventricular summit: anatomic concepts relevant to ablation. *Circ Arrhythm Electrophysiol* 2010;**3**(6):616–23.

27 Jauregui Abularach ME, Campos B, Park KM, *et al*. Ablation of ventricular arrhythmias arising near the anterior epicardial veins from the left sinus of Valsalva region: ECG features, anatomic distance, and outcome. *Heart Rhythm* 2012;**9**(6):865–73.

28 Enriquez A, Malavassi F, Saenz LC, *et al*. How to map and ablate left ventricular summit arrhythmias. *Heart Rhythm* 2017;**14**(1):141–8.

29 Betensky BP, Park RE, Marchlinski FE, *et al*. The V(2) transition ratio: a new electrocardiographic criterion for distinguishing left from right ventricular outflow tract tachycardia origin. *J Am Coll Cardiol* 2011;**57**(22):2255–62.

30 Ouyang F, Fotuhi P, Ho SY, *et al* Repetitive monomorphic ventricular tachycardia originating from the aortic sinus cusp: electrocardiographic characterization for guiding catheter ablation. *J Am Coll Cardiol* 2002;**39**(3):500–8.

7

Fundamentals of Cardiac Mapping

Fu Siong Ng[1,4], Caroline Roney[1,2,4], Chris D. Cantwell[3,4], and Nicholas S. Peters[1,4]

[1] *National Heart and Lung Institute, Imperial College London, UK*
[2] *King's College, London, UK*
[3] *Department of Aeronautics, Imperial College London, UK*
[4] *Imperial Centre for Cardiac Engineering, Imperial College London, UK*

Summary

A number of tools and techniques currently exist to map arrhythmias in the invasive cardiac electrophysiology laboratory to guide ablative treatments. The mapping technique chosen depends on the specifics and complexity of the arrhythmia, with each technique having its own advantages and disadvantages. Conventionally, mapping has been performed using a small number of recording catheters guided by fluoroscopy with activation mapping, pace mapping, and entrainment mapping used to identify the source or circuit of an arrhythmia. In recent years, numerous three-dimensional electroanatomical mapping systems have been developed to record electrophysiological data simultaneously with anatomical data. The latest challenge in cardiac mapping is to map complex arrhythmias with complex analysis methods such as phase mapping used to identify putative activation sources.

Introduction

Cardiac mapping refers to the recording of electrical signals from multiple sites across the heart to localize and characterize the substrate of an arrhythmia. This is performed in the invasive cardiac electrophysiology laboratory mainly to identify the mechanism underlying a particular arrhythmia and to guide appropriate ablative treatment. This chapter describes the different approaches to mapping arrhythmias in the electrophysiology laboratory, including conventional contact catheter mapping techniques and maneuvers, three-dimensional electroanatomical mapping using both contact and non-contact recordings, and also newer mapping approaches for myocardial fibrillation such as phase mapping and dominant frequency mapping.

Contact catheter mapping

Mapping in the electrophysiology laboratory is, on the whole, performed using catheters in direct contact with the myocardium. The conventional invasive electrophysiological study, used mainly for the diagnosis and treatment of supraventricular tachycardias, involves the introduction of four catheters through a large vein (femoral, subclavian or jugular), which are then positioned endocardially at the high right atrium, the right ventricular apex and close to the His bundle, and also in the coronary sinus. A further roving catheter, referred to as the mapping catheter, is also often introduced. These multipolar catheters are then used to record contact electrograms at different locations, and their relative timings of activation during pacing and during tachycardia can be used to discern the specific tachycardia mechanism. Figure 7.1 shows the conventional placement of recording catheters during a four-catheter electrophysiological study, and the electrograms recorded from those catheters.

Unipolar and bipolar recordings

Extracellular electrograms recorded by contact catheters are generated by the depolarization of cardiomyocytes that generate transmembrane currents between the intracellular and extracellular space, and are the fundamental raw data used in invasive cardiac electrophysiology [1]. These electrograms are recorded in either the unipolar or bipolar configuration. A unipolar electrogram is recorded between an electrode in contact with the myocardium and a fixed distant reference point, for example Wilson's central terminal [2]. As shown in Figure 7.2a, the unipolar electrogram morphology is useful in determining the direction of electrical propagation along a myocardial bundle. Electrograms recorded at sites where electrical propagation arises will have a negative ("QS") component only, whereas electrograms at the end of the bundle will have only a positive "R" component. Other sites will

Cardiac Mapping, Fifth Edition. Edited by Mohammad Shenasa, Gerhard Hindricks, David J. Callans, John M. Miller, and Mark E. Josephson.

Companion website: www.wiley.com/go/cardiacmapping5e

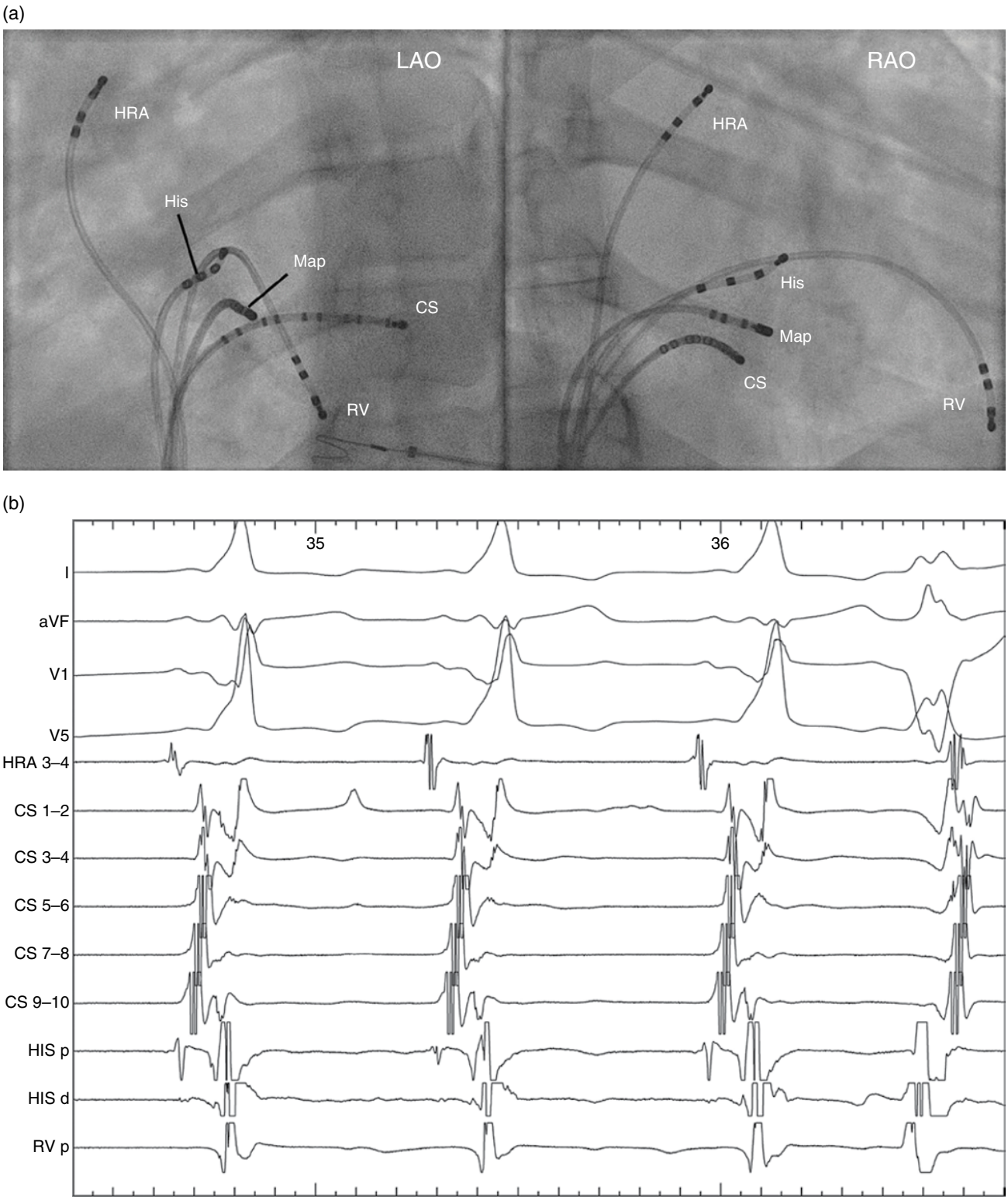

Figure 7.1 Conventional contact catheter mapping. (a) Fluoroscopic images in the left anterior oblique (LAO) and right anterior oblique (RAO) views demonstrating the locations for conventional catheter placement in an invasive electrophysiological study. A mapping catheter (Map) is also shown. CS, coronary sinus; His, His bundle; HRA, high right atrium; RV, right ventricular apex. (b) Selected surface ECG leads and bipolar electrograms are recorded from intracardiac catheters.

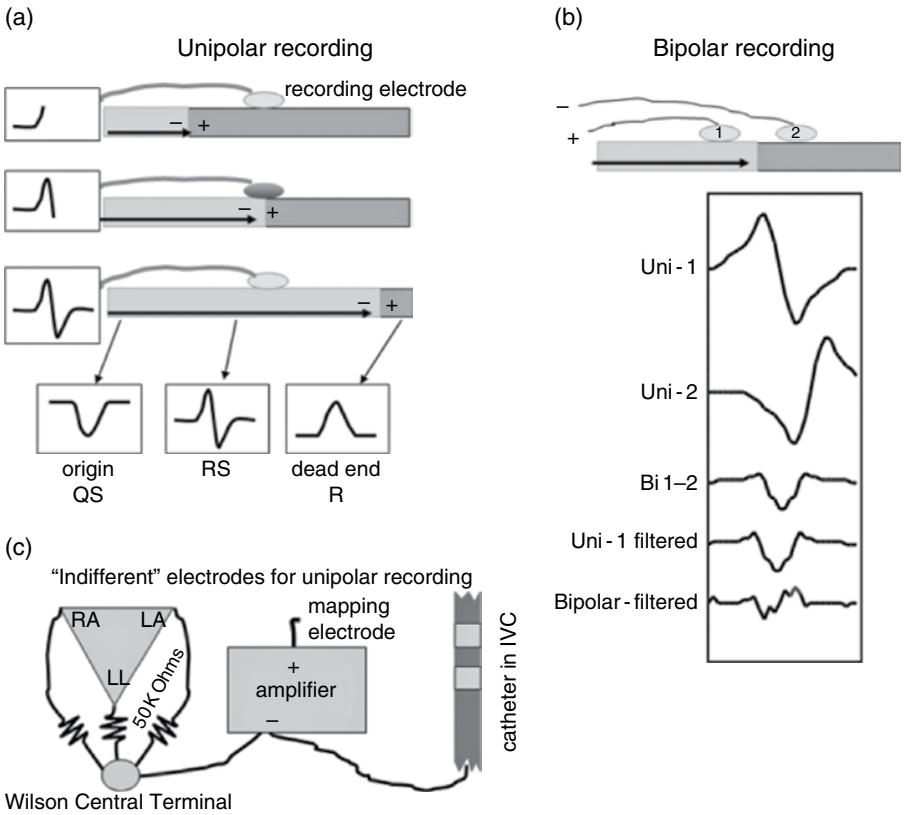

Figure 7.2 Unipolar and bipolar electrogram recordings. The bars in both (a) and (b) represent a sheet of myocardium, with propagation of the action potential wavefront from left to right. (a) A unipolar recording electrode at the middle of the sheet, as propagation approaches the electrode (*top*), a positive deflection (R wave) is inscribed. As it passes beneath the electrode, a negative S wave is inscribed, thus displaying the RS morphology (*middle*). Unipolar electrograms recorded from the origin will have QS morphologies, whereas unipolar electrograms recorded from the end of the sheet will have a monophasic R wave. (b) Bipolar electrograms are obtained by subtracting two closely spaced unipolar electrograms to remove far-field components and obtain more local information. (c) Indifferent electrode configurations for unipolar recordings. The indifferent electrode is commonly selected as the Wilson's central terminal, or a remote electrode such as one placed in the inferior vena cava (IVC). *Source:* Stevenson and Soejima [2]. Reproduced with permission of John Wiley & Sons.

exhibit biphasic "RS" unipolar electrograms, with an initial positive component (propagation towards that site) followed by a negative component (away from that site), with the point of maximum negative slope (dV/dt_{min}) representing the local activation time [3, 4]. The unipolar electrogram is useful for identification of foci of arrhythmia, which will have the "QS" unipolar electrogram morphology.

In contrast, a bipolar electrogram is recorded between two closely spaced electrodes on the recording catheter, and is derived as the difference between the unipolar electrograms recorded from the two electrodes (Figure 7.2b) [5]. The bipolar electrogram is more commonly used in the invasive electrophysiology laboratory as it contains more "local" information from the area of myocardium at the catheter tip between the two electrodes. Measuring the difference between two unipolar electrograms to obtain the bipolar electrogram results in significant attenuation of the far-field components of the electrogram, as the far-field components are common to both unipolar electrograms, thus accentuating the local components of the bipolar electrogram. However, the interpretation of the bipolar electrogram is more complicated, and the morphology of the bipolar electrogram is sensitive to the direction of wavefront propagation in relation of the orientation of the bipole [2]. A number of approaches are used to annotate activation time on a bipolar electrogram, with annotation of the first peak of the near-field, sharp, bipolar electrogram thought to be preferable to annotation of the earliest portion of the electrogram or the peak amplitude of the electrogram [2, 6].

Activation mapping

Several classic methods exist for mapping arrhythmia foci using contact catheters. A commonly used method is activation sequence mapping. This involves the recording of contact electrograms from multiple locations using a single roving mapping catheter, or a

combination of catheters, and determining the pattern and sequence of activation based on the activation times at each of the locations. For focal tachycardias, this allows the operator to pinpoint the location of the tachycardia focus by identifying the location of earliest activation with respect to a fixed reference, such as the surface P wave if mapping an atrial arrhythmia or the QRS if mapping a ventricular arrhythmia. This approach is commonly used to target ablation for ventricular outflow tract ectopy and focal atrial tachycardias. Activation mapping can also identify progression of activation along a macro-reentrant circuit, with activation times spanning the entire tachycardia cycle length recorded over a broad region.

Pace mapping

Pace mapping is used to approximate the location of a tachycardia focus or origin by comparing the P wave or QRS morphology during pacing from the roving mapping catheter with the P wave or QRS complex during tachycardia [7–9]. In practice, the P wave or QRS complex of the clinical tachycardia is first stored as a template and pacing is then performed at multiple locations using the mapping catheter. For the example of focal ventricular arrhythmias, at each location the degree of "pace match" between the paced QRS complex for all 12 surface ECG leads and the tachycardia QRS complex template is assessed. The closer the match between the paced QRS and the tachycardia QRS, the closer the mapping catheter is to the location of the tachycardia focus. Traditionally, the assessment of pace match is performed qualitatively, with a 12-out-of-12 qualitative pace match for all the surface ECG leads signifying that the mapping catheter is in close proximity to the tachycardia focus. Recently, automated template matching algorithms have been developed to quantitatively assess the degree of pace match by calculating the percentage of match across all ECG leads [10] (Figure 7.3). Pace mapping for focal tachycardias is often used in combination with activation mapping described above.

Entrainment mapping

For reentrant tachycardias, entrainment can be used to determine if the mapping catheter is within the reentrant circuit, and also to ascertain distance between the mapping catheter and the reentrant circuit [11, 12]. Entrainment can also help in distinguishing reentrant tachycardias from those resulting from automaticity or triggered activity.

Entrainment is a maneuver based on the principle that an excitable gap exists for any reentrant tachycardia, and that the excitation wavefront from a premature pacing stimulus can encounter the excitable gap and capture excitable myocardium within the circuit, propagating antidromically to collide with the previous wavefront, while also propagating in the orthodromic direction within the circuit, thus resetting the tachycardia. Entrainment is the continuous resetting of a reentrant circuit by a train of capturing pacing stimuli, delivered at a cycle length shorter than the tachycardia cycle length.

Several criteria exist to confirm entrainment of a tachycardia from within the tachycardia circuit, based on early work by Waldo and colleagues [13, 14]. Entrainment with concealed fusion refers to entrainment of the tachycardia with a P wave or QRS complex identical to that of the tachycardia, and with activation sequences from intracardiac recordings identical to those during tachycardia, and confirms that the pacing catheter is within the tachycardia circuit. A tachycardia can be entrained even if the pacing catheter is not within the tachycardia circuit, in which case the postpacing interval can give an indication of its proximity to the tachycardia circuit. The closer the pacing site is to the tachycardia circuit, the shorter the difference between the postpacing interval and the tachycardia cycle length, with the postpacing interval defined as the time from the final pacing stimulus to the next non-stimulated depolarization measured at the pacing site.

Electroanatomical mapping

The information obtained during conventional contact catheter electrophysiological studies using fluoroscopy is limited by the small number of catheters and electrodes, and the mapping of activation sequence using this approach is time-consuming and technically challenging. A further limitation of conventional electrophysiological mapping is the absence of anatomical information obtained during mapping.

In the past two decades, newer electroanatomical mapping techniques have been developed to overcome these limitations of conventional mapping [15, 16]. A number of different electroanatomical mapping systems currently exist that allow for the rapid collection of electrical data across multiple sites at high resolution, while simultaneously gathering anatomical data of the cardiac chamber. Although these electroanatomical mapping systems utilize different technologies, they have in common the advantages of increasing the efficacy of arrhythmia mapping and reducing fluoroscopic time and exposure. Electroanatomical mapping data are increasingly being combined with imaging data, obtained from cardiac magnetic resonance imaging (MRI) or computed tomography (CT), to further improve the

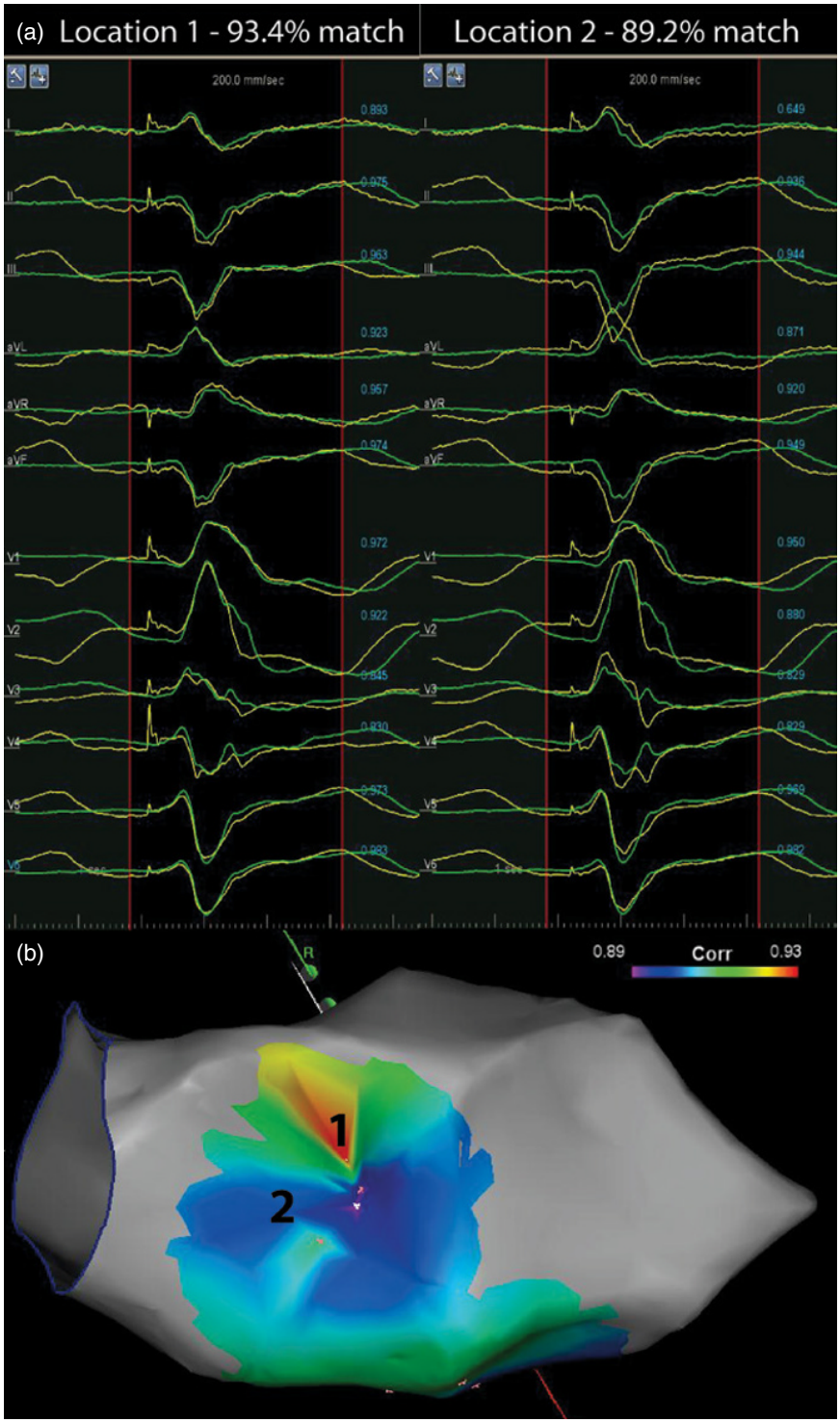

Figure 7.3 Pace mapping. Automated template-matching algorithm to quantify degree of pace match to localize ventricular ectopy (PaSo module of CARTO system shown). (a) Twelve-lead ECGs during clinical ventricular ectopy (*green*) and pacing from two locations at the inferior left ventricle (*yellow*) with superimposed QRS complexes are compared to quantify the degree of pace match. (b) The corresponding pace-match correlation map is shown, with areas in red exhibiting the best pace match correlations between clinical ectopy and pacing.

analysis and interpretation of the electrical recordings. Electroanatomical mapping is currently most commonly used in the setting of atrial fibrillation to facilitate pulmonary vein isolation and the creation of linear lesions, but is also often used for ablation of other arrhythmias including ventricular tachycardia, atrial tachycardia, atrial ectopy, and ventricular ectopy. Electroanatomical mapping systems can be divided into two groups, depending on whether the data are collected sequentially from across a cardiac chamber or collected simultaneously for the entire chamber.

Sequential mapping

A commonly used sequential electroanatomical mapping system is the CARTO mapping system (Biosense Webster Inc, Diamond Bar, CA, USA) (Figure 7.4a), which utilizes a low-level magnetic field delivered from three separate coils in a locator pad beneath the patient [15, 17]. The location and orientation of the catheter tip are calculated by triangulation, using the relative strength of the magnetic fields generated by the three coils that indicate the relative distance of the catheter tip to each coil. The location information obtained from the catheter allows the three-dimensional geometry of a cardiac chamber to be generated during mapping and for anatomical and electrophysiological information to be collected concurrently. The mapping catheter is moved systematically across a specific cardiac chamber and the anatomical and electrophysiological data are collected sequentially for different parts of the cardiac chamber.

Another commonly used mapping system is the EnSite NavX Precision system (Abbott, Chicago, IL, USA) (Figure 7.4b), which tracks the catheter location by sensing impedance changes between the catheter and specific reference points [18]. By applying a low-level current through orthogonally located skin patches, the distance from each skin patch can be calculated from the recorded voltage and impedance from this current and its location determined by triangulation [15].

In recent years, newer electroanatomical mapping systems have emerged, each with their specific advantages

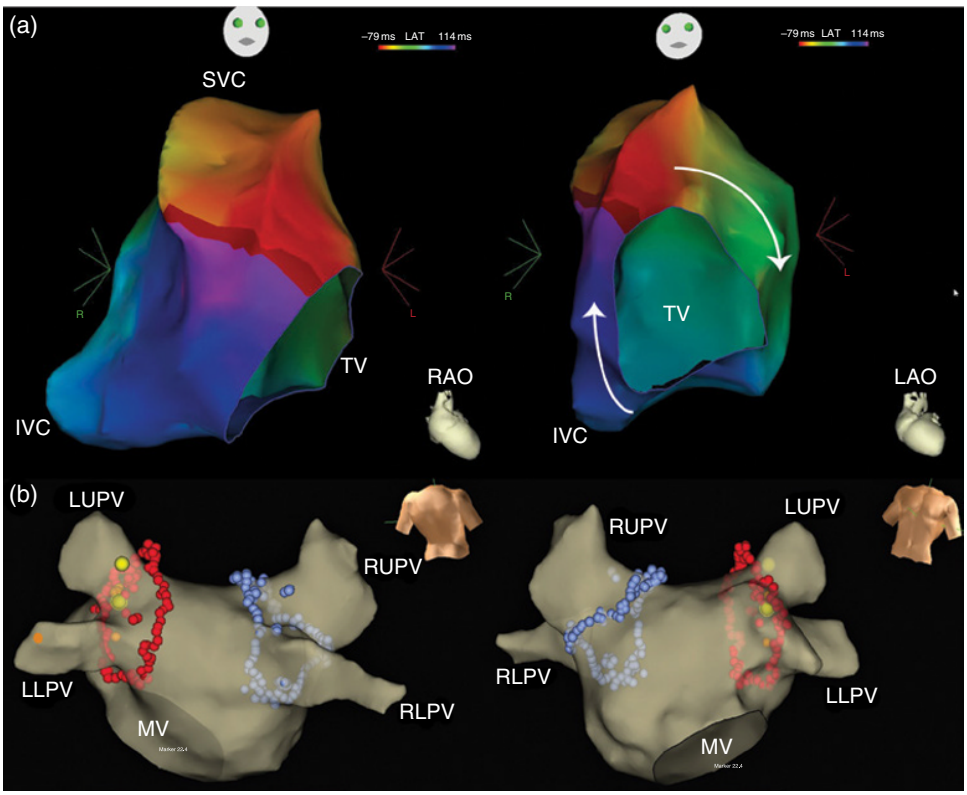

Figure 7.4 Commonly used electroanatomical mapping systems. (a) The CARTO electroanatomical mapping system. A common application of electroanatomical mapping is to map macro-reentrant tachycardias. A clockwise cavotricuspid isthmus-dependent atrial flutter is shown, with sequential atrial activation times through the entire tachycardia cycle around the tricuspid annulus. IVC, inferior vena cava; LAO, left anterior oblique; RAO, right anterior oblique; SVC, superior vena cava; TV, tricuspid valve annulus. (b) The NavX Velocity electroanatomical mapping system. Another common application of electroanatomical mapping is to guide atrial fibrillation ablation. Left atrial geometry is created and radiofrequency ablation is then performed to encircle the left-sided (*red*) and right-sided (*blue*) pulmonary veins to achieve pulmonary vein isolation. LLPV, left lower pulmonary vein; LUPV, left upper pulmonary vein; MV, mitral valve annulus; RLPV, right lower pulmonary vein; RUPV, right upper pulmonary vein.

and strengths. The Rhythmia mapping system (Boston Scientific Inc., Marlborough, MA, USA) is a new high-resolution electroanatomical mapping system, which utilizes a small basket array of 64 electrodes that can rapidly create high-density activation maps with little or no manual annotation of activation [19]. The ultra-high resolution of this system makes it eminently suitable for the mapping of localized microreentrant circuits and more complex tachycardia circuits (Figure 7.5).

Simultaneous global mapping

In contrast to sequential mapping systems, global mapping systems collect electroanatomical data from the entire cardiac chamber simultaneously, and data are analyzed for a single cycle of a tachycardia. For example, the Topera system (Abbott Electrophysiology, Palo Alto, CA, USA) uses basket catheters to provide extensive coverage of the atria to record electrophysiological information simultaneously from different parts of the atria, and has been used mainly to detect rotors in atrial fibrillation [20–22]. The global mapping approach has been argued to be superior in localizing fibrillatory drivers, compared with the sequential localized mapping approach, although it lacks the resolution of other sequential mapping systems.

Although the majority of electrophysiological data are obtained by direct electrode contact with the myocardium, several non-contact mapping systems exist for simultaneous global mapping. The Ensite multielectrode array catheter (St Jude Medical) is a 64-electrode balloon catheter that is deployed in a cardiac chamber, and the electrodes record far-field endocardial activity that is then transformed using inverse solution mathematics to computed equivalents of >3000 contact near-field electrograms, projected onto a virtual endocardial shell [23–25]. More recently, non-invasive mapping using body surface potentials has been introduced. The electrocardiographic imaging system (ECGI) uses body surface potentials recorded from a 252-electrode vest to reconstruct several thousand unipolar electrograms on an epicardial shell generated from a thoracic CT scan [26, 27] (Figure 7.6). This system has been used to aid location of focal ventricular arrhythmias [28], and to determine locations of fibrillatory drivers [29].

Mapping complex arrhythmias

With the advent of this wide range of new electroanatomical mapping technologies that can record a vast quantity of electroanatomical data, the key challenge is to analyze the spatiotemporal content of these signals in a way that maximizes diagnostically valuable information on the structural and functional properties of the underlying myocardium to guide ablation therapy,

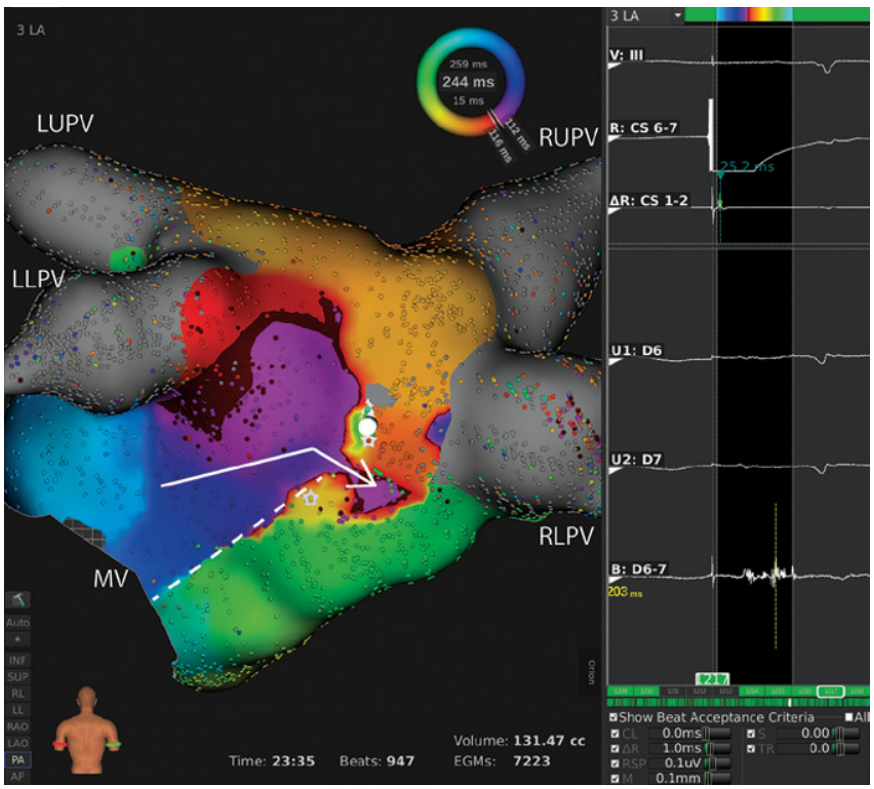

Figure 7.5 High-resolution electroanatomical mapping using the Rhythmia mapping system allows for the mapping of more complex tachycardia circuits. This example is of a patient who previously underwent a surgical maze procedure, and an atrial tachycardia was mapped. The activation map of the left atrium shows activation (*solid arrow*) across a gap in the previous inferior line (*dotted line*), and ablation at this gap terminated the atrial tachycardia. Electrograms recorded from the Orion basket catheter are shown on the right, with a fractionated signal (D6-7) at the gap in the inferior line. LLPV, left lower pulmonary vein; LUPV, left upper pulmonary vein; MV, mitral valve annulus; RLPV, right lower pulmonary vein; RUPV, right upper pulmonary vein.

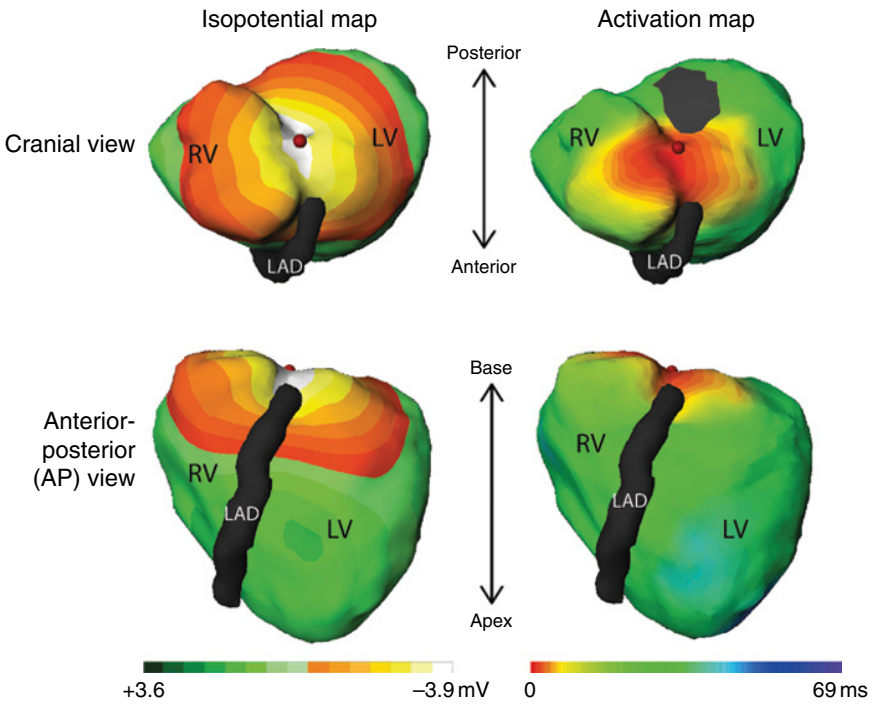

Figure 7.6 Non-invasive electrocardiographic imaging (ECGI) to localize ventricular ectopy. Electrocardiographic imaging uses body surface potentials recorded from a 252-electrode vest to calculate epicardial unipolar electrograms. Isopotential and activation maps are then generated during ventricular ectopic beats to localize the origin of the ectopy. In this case, the ectopy focus was located at the right ventricular outflow tract (*red dot*). LAD: left anterior descending artery.

especially in complex arrhythmias such as atrial fibrillation. For the remainder of this chapter, we discuss newer approaches to characterize and interpret mapping data, some of which are not yet directly available in current electroanatomical mapping systems.

Mapping putative activation sources

Dominant frequency mapping

During atrial fibrillation, the highest frequency of atrial activity is thought to indicate the frequency of electrical drivers maintaining the arrhythmia. Dominant frequency (DF) measures the fastest rate of activity and is defined for an individual electrogram as the frequency with the highest power in the frequency spectrum (Figure 7.7). Ablation strategies to target regions of atria with high DF, with the motivation of eliminating fibrillatory drivers, have been applied [30]. Prior to applying the Fourier transform, a sequence of preprocessing steps is applied in order to render the bipolar electrogram more sinusoidal and suitable for frequency analysis: first, bandpass filtering at 40 – 250 Hz, then signal rectification is performed, and subsequently low-pass filtering at 20 Hz [31]. The efficacy of the ablation strategy of targeting areas of high DF is dependent on the stability of such sites. However, there is conflicting evidence on the temporal stability of sites of high DF [32, 33], with some studies demonstrating that areas of high DF are not spatiotemporally stable, suggesting that they do not represent a fixed driver but perhaps wavefront collision [34]. More recent approaches to DF mapping include monitoring the movement of high DF sites over time, which require alternative methods for DF calculation, with improved temporal resolution [35]. Organizational index may help to distinguish drivers from other mechanisms causing high DF, such as wavefront collision, by determining the temporal organization of the spectrum as the mean ratio of the DF and its harmonics to the total power of the spectrum [36]. Targeting only high DF areas, which are spatiotemporally stable and with high organizational indices, may therefore be more effective.

Phase mapping

Phase mapping is a technique that has recently emerged to aid identification of fibrillatory drivers and guide ablation towards these regions [29]. Electrograms recorded during myocardial fibrillation are inherently complex and exhibit beat-to-beat variation in amplitude and duration and therefore wavefront propagation is complicated. Phase mapping, originally developed for optical mapping signals obtained during experimental electrophysiology, translates the periodicity in the fibrillatory signals into phase loops in a two-variable state space that represents the system [37]. The phase angle is then measured as the angle around these loops (Figure 7.8) and marks the location within the activation-recovery cycle. Phase maps calculated from a spatial arrangement of recordings can then be used to identify centers of rotational activity and wavebreak as these manifest as phase singularities, with stable phase singularities thought to represent rotors that drive fibrillation.

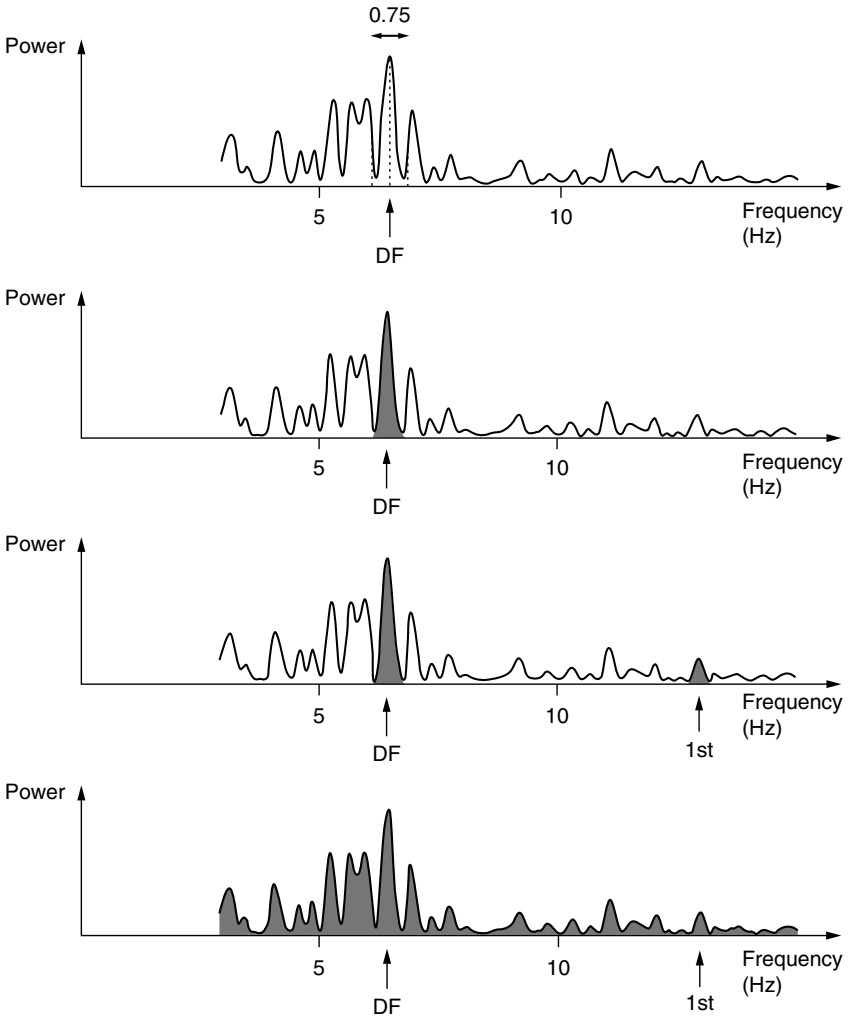

Figure 7.7 Calculation of dominant frequency and organisational index. The highest peak in the spectrum is marked as the dominant frequency (DF). To calculate the organizational index, the area within a band of 0.75 Hz on either side of the DF is calculated (shown in gray in the second panel). This area is added to the area under the first harmonic of the DF (*third panel*), and then divided by the total area under the entire frequency spectrum (*fourth panel*). *Source:* Jarman et al. [36]. Reproduced with permission of John Wiley & Sons.

Challenges in phase mapping include the correct choice of a second signal to generate a loop for each progression through an electrogram complex [38], as well as an appropriate origin from which to calculate the phase angle. The Hilbert transform may be used to create a suitable second signal, but it has the requirements that the signal must be sinusoidal and of zero mean [39]. As such, a variety of preprocessing techniques have been applied to electrograms to create a zero mean signal including empirical mode decomposition [38] and detrending algorithms [40]. Phase mapping has recently been applied to unipolar electrograms during ventricular fibrillation [40] and atrial fibrillation [41]. This is particularly challenging for atrial signals during atrial fibrillation due to the non-sinusoidal nature of the signals and the potentially long isoelectric segments. Recently, sinusoidal recomposition techniques for phase mapping of atrial unipolar electrograms have been developed to allow phase mapping to be better applied to atrial fibrillation unipolar electrograms [42].

Mapping of complex fractionated electrograms

A system of classifying unipolar electrograms into single, short-double, long-double, and fragmented electrograms was first introduced in 1997 by Konings et al., in which fragmented electrograms were hypothesized to represent either slow conduction or reentrant wavelet pivot points [43]. Nademanee et al. subsequently pioneered the approach of mapping and then ablating areas with fractionated electrograms in atrial fibrillation, termed complex fractionated atrial electrograms (CFAE) and thought to be fibrillatory drivers, with impressive success rates. Ablation of CFAEs terminated atrial fibrillation in 95% of the patients in their study [44], although other groups have failed to replicate this success [45]. One explanation for this discrepancy is that there are multiple definitions of CFAEs; the two most commonly used electroanatomical mapping systems, NavX and CARTO, use different algorithms and the resulting scores correlate poorly both with each other and with conduction velocity [46]. An alternative explanation is

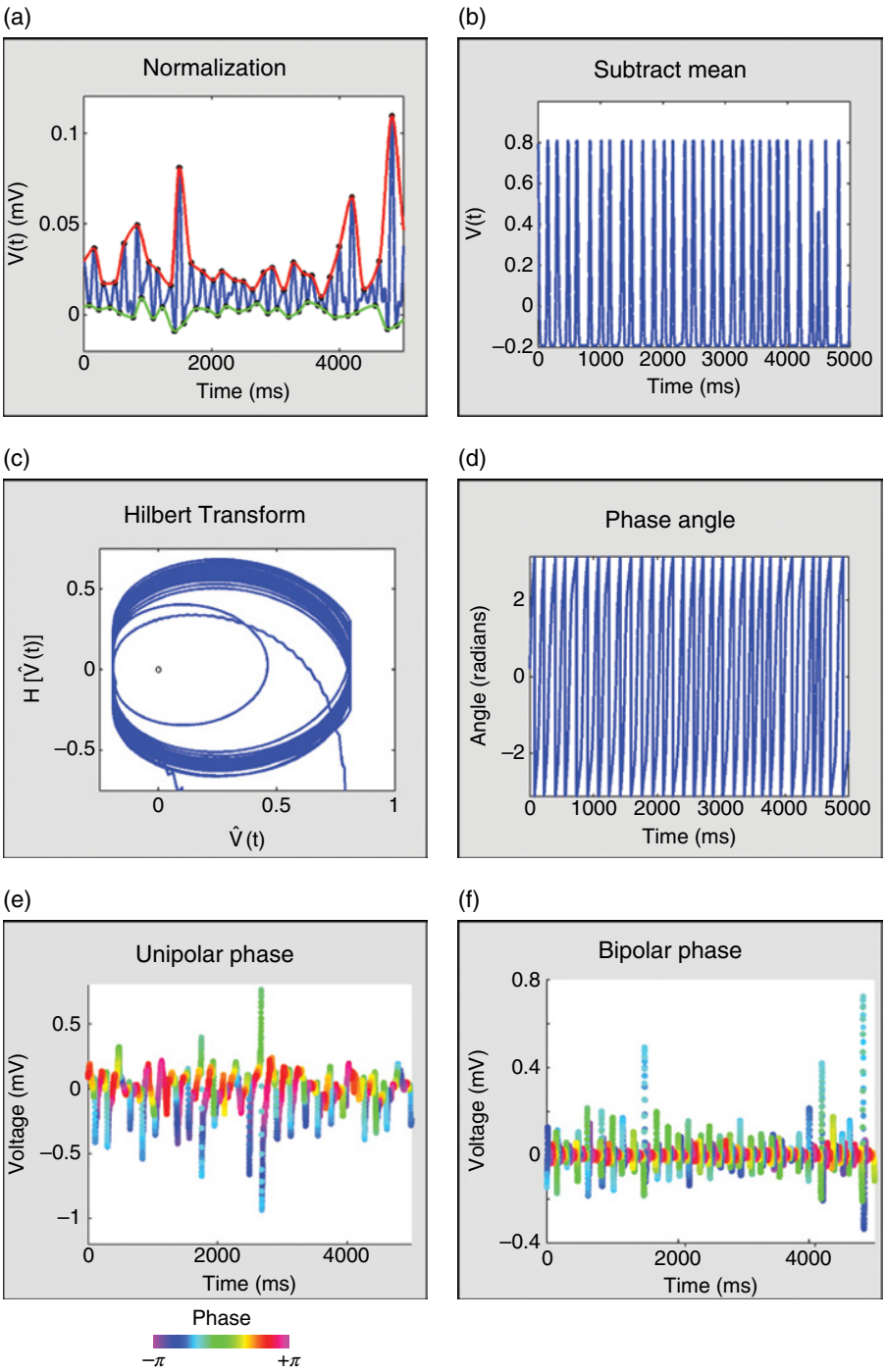

Figure 7.8 Phase mapping of electrogram signals. Filtered electrogram signals are processed as follows in order to calculate phase. (a) Maxima (*red*) and minima (*green*) of the signal are tagged and joined to create a moving maxima and minima. (b) These maxima and minima splines are used to normalize the signal, and a straight mean is removed to give a signal of zero mean. (c) The Hilbert transform of this zero mean signal is plotted against itself to give phase loops. (d) The angle around the trajectory is the phase angle. (e) Example of unipolar electrogram colored by phase angle. (f) Example of bipolar electrogram colored by phase angle.

that fractionation arises from multiple mechanisms, including focal or reentrant sources, as well as passive wave collision and slowing, which are difficult to distinguish. Classification of CFAEs by mapping local refractoriness of atrial tissue using monophasic action potential catheters demonstrated that far-field signals account for 67% of fractionation, while other CFAE types include rapid localized atrial fibrillation sites (8%), spatial disorganization (17%), and CFAE following atrial fibrillation acceleration (8%) [47].

Mapping and characterizing the arrhythmic substrate

Conduction velocity mapping

Local conduction velocity describes the propagation of the action potential wavefront through myocardial tissue and is defined empirically as the distance traveled by a propagating wavefront in a unit of time. Fibrosis and ion channel or gap junction remodeling leads to reduced macroscopic conduction velocity, and mapping regions of reduced local conduction velocity can identify regions of scar or adversely remodeled myocardium.

A number of approaches have been developed to determine localized myocardial conduction velocity, each with their strengths and weaknesses [48]. Triangulation provides planar conduction velocity estimation from triads of recording points through a trigonometric relation between interelectrode distances and activation times. With a sufficient number of electrograms, it can produce moderately high-density velocity maps and can allow for rapid velocity mapping (Figure 7.9) [49]. However, large distances between the vertices may lead to errors if the wavefront is not truly planar, while if the points are in very close proximity, the relative error in the estimation increases. Cosine-fit techniques extend triangulation to fit a planar or circular wavefront to a larger number of points [50], and are therefore more robust to noise, but are less localized in nature. A third approach is to use radial basis functions to interpolate local activation between electrode points. The gradient of the activation surface may then be computed to calculate conduction velocity [51].

There are a number of other approaches to conduction velocity estimation, including finite difference techniques [52], polynomial surface fitting [53], computing isopotential lines [54] or estimating propagation velocity based on time delays [55]. However, many of these have requirements which are not typically available in data acquired in the clinical electrophysiology laboratory and are limited to experimental cardiac electrophysiology.

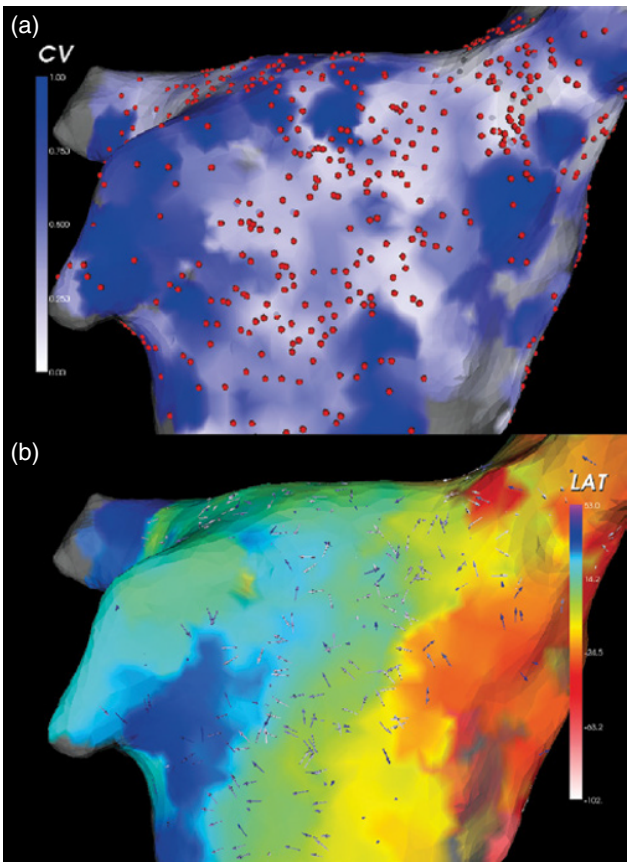

Figure 7.9 Conduction velocity mapping. Example of maps showing left atrial conduction velocity of electroanatomic mapping data, recorded during sinus rhythm. (a) Conduction speed calculated using the triangulation technique, applied to triads of electrodes. (b) Corresponding local activation time map with conduction velocity vectors. *Source:* Cantwell et al. [48]. Reproduced with permission of Elsevier.

Voltage mapping

Structural properties of tissue can also be estimated from the spatial distribution of electrogram amplitude, commonly known as voltage mapping. Low-amplitude bipolar electrograms are commonly associated with areas of fibrosis, which produce reduced electric fields and consequently lower potential differences between the measuring electrode and the reference point. Voltage maps are typically generated from summary statistics of amplitude of deflections within a signal over a fixed time window [56]. Frequently, the maximum deflection amplitude is chosen, although other statistical metrics and measures of variability may be used. Voltage mapping is used to guide substrate ablation in ventricular tachycardia by targeting ablation to low-voltage areas at the borders of infarct scars [57, 58], and more recently in atrial fibrillation, where areas of low-voltage are also targeted in a substrate modification approach [59, 60].

Conclusion

Multiple mapping approaches are currently available to guide the targeting of ablation therapy in the invasive cardiac electrophysiology laboratory. Conventional mapping approaches are most suited to simple arrhythmias such as focal arrhythmias. Electroanatomical mapping technologies record anatomical information in addition to electrophysiological data, and are commonly used in the ablation of atrial fibrillation, atrial tachycardia, and ventricular tachycardia. Electroanatomical mapping data is increasingly combined with imaging data from cardiac MRI or CT to improve analysis and interpretation of electrical recordings. For complex arrhythmias such as atrial fibrillation, newer mapping approaches such as phase mapping and dominant frequency mapping have been developed to identify locations of fibrillatory drivers.

References

1 De Bakker JMT, Wittkampf FHM. The pathophysiologic basis of fractionated and complex electrograms and the impact of recording techniques on their detection and interpretation. *Circ Arrhythm Electrophysiol* 2010;**3**(2):204–13.

2 Stevenson W, Soejima K. Recording techniques for clinical electrophysiology. *J Cardiovasc Electrophysiol* 2005;**16**(9):1017–22.

3 Spach MS, Miller WT, Miller-Jones E, Warren RB, Barr RC. Extracellular potentials related to intracellular action potentials during impulse conduction in anisotropic canine cardiac muscle. *Circ Res* 1979;**45**(2):188–204.

4 Steinhaus BM. Estimating cardiac transmembrane activation and recovery times from unipolar and bipolar extracellular electrograms: a simulation study. *Circ Res* 1989;**64**(3):449–62.

5 Gallagher JJ, Kasell JH, Cox JL, Ideker RE, Smith WM. Techniques of intraoperative electrophysiologic mapping. *Am J Cardiol* 1982;**49**(1):221–40.

6 Del Carpio Munoz F, Buescher T, Asirvatham SJ. Teaching points with 3-dimensional mapping of cardiac arrhythmias: taking points: activation mapping. *Circ Arrhythm Electrophysiol* 2011;**4**(3):e22–5.

7 Waxman HL, Josephson ME. Ventricular activation during ventricular endocardial pacing: I. Electrocardiographic patterns related to the site of pacing. *Am J Cardiol* 1982;**50**(1):1–10.

8 Josephson ME, Waxman HL, Cain ME, Gardner MJ, Buxton AE. Ventricular activation during ventricular endocardial pacing. II. Role of pace-mapping to localize origin of ventricular tachycardia. *Am J Cardiol* 1982;**50**(1):11–22.

9 Moreno M, Pérez-Castellano N, Villacastin J. Pacemapping. *Indian Pacing Electrophysiol J* 2005;**5**(1):35–42.

10 Casella M, Carbucicchio C, Russo Dello A, *et al*. Radiofrequency catheter ablation of life-threatening ventricular arrhythmias caused by left ventricular metastatic infiltration. *Circ Arrhythm Electrophysiol* 2011;**4**(2):e7–10.

11 Stevenson WG, Sager PT, Friedman PL. Entrainment techniques for mapping atrial and ventricular tachycardias. *J Cardiovasc Electrophysiol* 1995;**6**(3):201–16.

12 Deo R, Berger R. The clinical utility of entrainment pacing. *J Cardiovasc Electrophysiol* 2009;**20**(4):466–70.

13 Okumura K, Henthorn RW, Epstein AE, Plumb VJ, Waldo AL. Further observations on transient entrainment: importance of pacing site and properties of the components of the reentry circuit. *Circulation* 1985;**72**(6):1293–307.

14 Henthorn RW, Okumura K, Olshansky B, Plumb VJ, Hess PG, Waldo AL. A fourth criterion for transient entrainment: the electrogram equivalent of progressive fusion. *Circulation* 1988;**77**(5):1003–12.

15 Bhakta D, Miller JM. Principles of electroanatomic mapping. *Indian Pacing Electrophysiol J* 2008;**8**(1):32–50.

16 Koutalas E, Rolf S, Dinov B, *et al*. Contemporary mapping techniques of complex cardiac arrhythmias - identifying and modifying the arrhythmogenic substrate. *Arrhythmia Electrophysiol Rev* 2015;**4**(1):19–27.

17 Gepstein L, Hayam G, Ben-Haim SA. A novel method for nonfluoroscopic catheter-based electroanatomical mapping of the heart. In vitro and in vivo accuracy results. *Circulation* 1997;**95**(6):1611–22.

18 Estner HL, Deisenhofer I, Luik A, *et al*. Electrical isolation of pulmonary veins in patients with atrial fibrillation: reduction of fluoroscopy exposure and procedure duration by the use of a non-fluoroscopic navigation system (NavX). *Europace* 2006;**8**(8):583–7.

19 Nakagawa H, Ikeda A, Sharma T, Lazzara R, Jackman WM. Rapid high resolution electroanatomical mapping: evaluation of a new system in a canine atrial linear lesion model. *Circ Arrhythm Electrophysiol* 2012;**5**(2):417–24.

20 Narayan SM, Krummen DE, Shivkumar K, Clopton P, Rappel W-J, Miller JM. Treatment of atrial fibrillation by the ablation of localized sources: CONFIRM (Conventional Ablation for Atrial Fibrillation With or Without Focal Impulse and Rotor Modulation) trial. *J Am Coll Cardiol* 2012;**60**(7):628–36.

21 Buch E, Share M, Tung R, *et al*. Long-term clinical outcomes of focal impulse and rotor modulation for

treatment of atrial fibrillation: a multicenter experience. *Heart Rhythm* 2016;**13**(3):636–41.

22 Benharash P, Buch E, Frank P, *et al*. Quantitative analysis of localized sources identified by focal impulse and rotor modulation mapping in atrial fibrillation. *Circ Arrhythm Electrophysiol* 2015;**8**(3):554–61.

23 Gornick CC, Adler SW, Pederson B, Hauck J, Budd J, Schweitzer J. Validation of a new noncontact catheter system for electroanatomic mapping of left ventricular endocardium. *Circulation* 1999;**99**(6):829–35.

24 Schilling RJ, Peters NS, Davies DW. Feasibility of a noncontact catheter for endocardial mapping of human ventricular tachycardia. *Circulation* 1999;**99**(19):2543–52.

25 Schilling RJ, Peters NS, Davies DW. Simultaneous endocardial mapping in the human left ventricle using a noncontact catheter: comparison of contact and reconstructed electrograms during sinus rhythm. *Circulation* 1998;**98**(9):887–98.

26 Ramanathan C, Ghanem RN, Jia P, Ryu K, Rudy Y. Noninvasive electrocardiographic imaging for cardiac electrophysiology and arrhythmia. *Nat Med* 2004;**10**(4):422–8.

27 Burnes JE, Taccardi B, Rudy Y. A noninvasive imaging modality for cardiac arrhythmias. *Circulation* 2000;**102**(17):2152–8.

28 Jamil-Copley S, Bokan R, Kojodjojo P, *et al*. Noninvasive electrocardiographic mapping to guide ablation of outflow tract ventricular arrhythmias. *Heart Rhythm* 2014;**11**(4):587–94.

29 Haissaguerre M, Hocini M, Denis A, *et al*. Driver domains in persistent atrial fibrillation. *Circulation* 2014;**130**(7):530–8.

30 Mansour M, Mandapati R, Berenfeld O, Chen J, Samie FH, Jalife J. Left-to-right gradient of atrial frequencies during acute atrial fibrillation in the isolated sheep heart. *Circulation* 2001;**103**(21):2631–6.

31 Ng J, Kadish AH, Goldberger JJ. Effect of electrogram characteristics on the relationship of dominant frequency to atrial activation rate in atrial fibrillation. *Heart Rhythm* 2006;**3**(11):1295–305.

32 Sanders P, Berenfeld O, Hocini M, *et al*. Spectral analysis identifies sites of high-frequency activity maintaining atrial fibrillation in humans. *Circulation* 2005;**112**(6):789–97.

33 Salinet JL, Tuan JH, Sandilands AJ, Stafford PJ, Schlindwein FS, Ng GA. Distinctive patterns of dominant frequency trajectory behavior in drug-refractory persistent atrial fibrillation: preliminary characterization of spatiotemporal instability. *J Cardiovasc Electrophysiol* 2014;**25**(4):371–9.

34 Jarman JWE, Wong T, Kojodjojo P, *et al*. Spatiotemporal behavior of high dominant frequency during paroxysmal and persistent atrial fibrillation in the human left atrium. *Circ Arrhythm Electrophysiol* 2012;**5**(4):650–8.

35 Salinet JL, Masca N, Stafford PJ, Ng GA, Schlindwein FS. Three-dimensional dominant frequency mapping using autoregressive spectral analysis of atrial electrograms of patients in persistent atrial fibrillation. *Biomed Eng Online* 2016;**15**(1):28.

36 Jarman JWE, Wong T, Kojodjojo P, *et al*. Organizational index mapping to identify focal sources during persistent atrial fibrillation. *J Cardiovasc Electrophysiol* 2014;**25**(4):355–63.

37 Gray RA, Pertsov AM, Jalife J. Spatial and temporal organization during cardiac fibrillation. *Nature* 1998;**392**(6671):75–8.

38 Bray M-A, Wikswo J. Considerations in phase plane analysis for nonstationary reentrant cardiac behavior. *Phys Rev E* 2002;**65**(5):051902.

39 Umapathy K, Nair K, Masse S, *et al*. Phase mapping of cardiac fibrillation. *Circ Arrhythm Electrophysiol* 2010;**3**(1):105–14.

40 Nash MP, Mourad A, Clayton RH, *et al*. Evidence for multiple mechanisms in human ventricular fibrillation. *Circulation* 2006;**114**(6):536–42.

41 Haissaguerre M, Hocini M, Shah AJ, *et al*. Noninvasive panoramic mapping of human atrial fibrillation mechanisms: a feasibility report. *J Cardiovasc Electrophysiol* 2013;**24**(6):711–17.

42 Kuklik P, Zeemering S, Maesen B, *et al.* Reconstruction of instantaneous phase of unipolar atrial contact electrogram using a concept of sinusoidal recomposition and Hilbert transform. *IEEE Trans Biomed Eng* 2015;**62**(1):296–302.

43 Konings KT, Smeets JL, Penn OC, Wellens HJ, Allessie MA. Configuration of unipolar atrial electrograms during electrically induced atrial fibrillation in humans. *Circulation* 1997;**95**(5):1231–41.

44 Nademanee K, McKenzie J, Kosar E, *et al*. A new approach for catheter ablation of atrial fibrillation: mapping of the electrophysiologic substrate. *J Am Coll Cardiol* 2004;**43**(11):2044–53.

45 Estner HL, Hessling G, Ndrepepa G, *et al*. Acute effects and long-term outcome of pulmonary vein isolation in combination with electrogram-guided substrate ablation for persistent atrial fibrillation. *Am J Cardiol* 2008;**101**(3):332–7.

46 Lau DH, Maesen B, Zeemering S, *et al*. Indices of bipolar complex fractionated atrial electrograms correlate poorly with each other and atrial fibrillation substrate complexity. *Heart Rhythm* 2015;**12**(7):1415–23.

47 Narayan SM, Wright M, Derval N, *et al.* Classifying fractionated electrograms in human atrial fibrillation using monophasic action potentials and activation mapping: evidence for localized drivers, rate acceleration, and nonlocal signal etiologies. *Heart Rhythm* 2011;**8**(2):244–53.

48 Cantwell CD, Roney CH, Ng FS, Siggers JH, Sherwin SJ, Peters NS. Techniques for automated local activation time annotation and conduction velocity estimation in cardiac mapping. *Comput Biol Med* 2015;**65**:229–42.

49 Kojodjojo P, Kanagaratnam P, Markides V, Davies DW, Peters N. Age-related changes in human left and right atrial conduction. *J Cardiovasc Electrophysiol* 2006;**17**(2):120–7.

50 Roney CH, Cantwell CD, Qureshi NA, *et al*. An automated algorithm for determining conduction velocity, wavefront direction and origin of focal cardiac arrhythmias using a multipolar catheter. Conference Proceedings of the IEEE Engineering in Medicine and Biology Society. *IEEE Trans Biomed Eng* 2014;**2014**:1583–6.

51 Mase M, Greco MD, Marini M, Ravelli F. Velocity field analysis of activation maps in atrial fibrillation: a simulation study. World Congress on Medical Physics and Biomedical Engineering, Munich, Germany, 2009, pp. 1014–17.

52 Salama G, Kanai A, Efimov IR. Subthreshold stimulation of Purkinje fibers interrupts ventricular tachycardia in intact hearts. Experimental study with voltage-sensitive dyes and imaging techniques. *Circ Res* 1994;**74**(4):604–19.

53 Bayly PV, KenKnight BH, Rogers JM, Hillsley RE, Ideker RE, Smith WM. Estimation of conduction velocity vector fields from epicardial mapping data. *IEEE Trans Biomed Eng* 1998;**45**(5):563–71.

54 Kay MW, Gray RA. Measuring curvature and velocity vector fields for waves of cardiac excitation in 2-D media. *IEEE Trans Biomed Eng* 2005;**52**(1):50–63.

55 Dubois R, Labarthe S, Coudiere Y, Hocini M, Haissaguerre M. Global and directional activation maps for cardiac mapping in electrophysiology. *Comput Cardiol* 2012;**39**:349–52.

56 Miyamoto K, Tsuchiya T, Narita S, *et al*. Bipolar electrogram amplitudes in the left atrium are related to local conduction velocity in patients with atrial fibrillation. *Europace* 2009;**11**(12):1597–605.

57 Marchlinski FE, Callans DJ, Gottlieb CD, Zado E. Linear ablation lesions for control of unmappable ventricular tachycardia in patients with ischemic and nonischemic cardiomyopathy. *Circulation* 2000;**101**(11):1288–96.

58 Soejima K, Stevenson WG, Maisel WH, Sapp JL, Epstein LM. Electrically unexcitable scar mapping based on pacing threshold for identification of the reentry circuit isthmus: feasibility for guiding ventricular tachycardia ablation. *Circulation* 2002;**106**(13):1678–83.

59 Jadidi AS, Lehrmann H, Keyl C, et al. Ablation of persistent atrial fibrillation targeting low-voltage areas with selective activation characteristics. *Circ Arrhythm Electrophysiol* 2016;**9**(3):e002962.

60 Rolf S, Kircher S, Arya A, *et al*. Tailored atrial substrate modification based on low-voltage areas in catheter ablation of atrial fibrillation. *Circ Arrhythm Electrophysiol* 2014;**7**(5):825–33.

8

Troubleshooting to Avoid Failed Ablation

Krishna Kancharla[1], Suraj Kapa[2], and Samuel J. Asirvatham[2,3]

[1] *Heart and Vascular Institute, University of Pittsburgh Medical Center, Pittsburgh, PA, USA*
[2] *Department of Cardiovascular Diseases, Mayo Clinic, Rochester, MN, USA*
[3] *Department of Pediatrics and Adolescent Medicine, Mayo Clinic, Rochester, MN, USA*

Summary

Successful therapy for arrhythmias after ablation starts with proper case selection, preprocedural planning, selection of case-specific tools, and an arrhythmia-specific strategy. Understanding arrhythmia mechanism and key components for maintenance of arrhythmia is paramount in planning ablation strategy. Furthermore, identifying hurdles intraoperatively (e.g., arrhythmias caused by an endocavitary structure) and methods to overcome such hurdles (e.g., use of ICE) need to be considered. Finally, effective energy delivery to the target tissue with an objective assessment of outcomes is necessary to avoid failed ablation.

Introduction

The goal of therapy in patients with arrhythmia depends on the type of arrhythmia, symptoms associated with it, and morbidity or mortality attributable to the arrhythmia. In current practice, patients and care providers, after assessment of risks and benefits of therapy, may elect to proceed with either conservative methods or intervention with medical therapy or ablation and sometimes a combination. While ablation is performed most often with catheter-based techniques, surgical therapy may rarely be considered in selected cases. In this chapter, we will discuss a general approach to optimizing ablation success followed by specific arrhythmia scenarios.

Goals of invasive therapy

When making clinical decisions to proceed with cardiac ablation, it is critical to define the goals of the procedure. For example, for a patient with frequent monomorphic premature ventricular complexes (PVCs) with significant symptomatic palpitations and otherwise normal cardiac function, the goal of ablation is symptom relief. On the other hand, for a patient with equally frequent PVCs that are asymptomatic but induce rare events of ventricular fibrillation, the goal may be life-saving. In general, ablation can be considered successful when prespecified goals are met without the occurrence of new arrhythmias or complications resulting in long-term morbidity or mortality. While the abolition of clinical arrhythmia with ablation is universally accepted as a success, it may be equally qualified to define success when the prespecified goals are met despite the continued occurrence of clinical arrhythmia at a lower burden.

Assessment of outcomes of ablation

Both objective and subjective assessments should be considered before and after ablation to measure the outcomes of the ablation. A subjective assessment, while providing a powerful understanding of the patient's perspective and often meeting the prespecification of symptom relief as the ablation goal, often can be nonspecific in its association with arrhythmia. As a result, an objective assessment is often needed in addition to the subjective assessment. In the electrophysiology (EP) lab acutely, this assessment is typically achieved with attempts to induce tachycardia via various techniques (e.g. pacing maneuvers) or medications after the ablation. However, assessment based on inducibility is not without its limitations [1]. After the procedure, monitoring in the immediate postoperative period and ambulatory monitoring after hospital discharge can be a helpful addition in objective assessment of the results. The extent and duration of monitoring and follow-up should be tailored to the patient, arrhythmia characteristics, and immediate results of the ablation.

Cardiac Mapping, Fifth Edition. Edited by Mohammad Shenasa, Gerhard Hindricks, David J. Callans, John M. Miller, and Mark E. Josephson.

Companion website: www.wiley.com/go/cardiacmapping5e

Preprocedural planning (table 8.1)

Understanding the arrhythmia being targeted

A successful ablation starts with a clear definition of the clinical arrhythmia. Effort should be made to document the arrhythmia episodes, precipitating factors, frequency and duration of arrhythmia, and details of its termination. A multilead surface electrocardiogram of certain arrhythmias obtained before the procedure can be extremely helpful in procedural planning, patient counseling, and confirming the target arrhythmia during the procedure. In patients with infrequent episodes who are considered for therapy, prolonged ambulatory monitoring or implantable recorders can be very helpful in documenting the clinical arrhythmia. A full list of potential diagnoses and exclusions should be created before the procedure for adequate procedural planning.

Understanding pathophysiology/substrate being targeted

An assessment of cardiac structure and function is also essential in all patients for decision making and procedural preparation. Imaging often sheds light on the primary pathology resulting in the arrhythmia. While transthoracic echocardiogram gives significant and sufficient information in most cases, cardiac computed tomography angiogram (CTA) and/or cardiac magnetic resonance imaging (CMR) can be very valuable in some scenarios. For example, in patients undergoing ablation for atrial tachycardia or atrial fibrillation, an understanding of the atrial size, pulmonary venous anatomy, venous anomalies, and relation to surrounding structures like the esophagus or phrenic nerve can be extremely helpful in recognizing potential complications or nuances in the procedural approach. Assessment of atrial or ventricular fibrosis by CMR can also be helpful in understanding substrate and thus planning a strategy for ablation. Use of intraprocedural imaging, for example intracardiac echo (ICE), can further facilitate the understanding of arrhythmia and relation to the substrate.

Table 8.1 Preprocedural and procedural preparation checklist.

Preprocedural planning	Procedural planning
Documentation of clinical arrhythmia characteristics	Anesthesia considerations to avoid suppression of arrhythmia
Clear definition of goals of the invasive therapy	Hemodynamic support
Understanding the arrhythmia being targeted – differential diagnosis	Planning access – venous, arterial, and pericardial
Understanding the substrate being targeted	Choosing procedural tools specific to arrhythmia and patient
Maximizing the chance of occurrence of arrhythmia during procedure	Image integration
Consideration for preprocedural imaging	Consideration of energy sources

Maximizing the chance of occurrence of clinical arrhythmia

Even with extensive preprocedural planning, most arrhythmias cannot be fully anticipated until the patient presents to the EP lab. In patients with arrhythmias that are hemodynamically well tolerated (e.g. atrial flutter), it may be best to take the patient to the lab while the arrhythmia is active in order to ensure the arrhythmia being mapped is also the one targeted. In many cases, however, this is not feasible as the arrhythmias are either intermittent (e.g. paroxysmal supraventricular tachycardia (SVT)) or not hemodynamically tolerable. Drug therapy should be stopped at a minimum of five half-lives before the procedure day to optimize the likelihood of inducing the arrhythmia in the lab. For patients who have hemodynamically intolerable arrhythmias off medical therapy, hospital admission should be considered as the drug therapy is weaned so short-acting medications can be considered during this period until the day of the procedure (e.g. in patients with ventricular tachycardia (VT) storm). In patients with implantable devices, arrhythmia inducibility can be tested with a non-invasive study using the implantable device before intravenous lines or catheters are introduced.

Procedural preparation

Anesthesia and ventilation planning

Care should be taken to avoid drugs that decrease the potential for inducibility of arrhythmias. There are insufficient data to guide the choice of anesthetics/analgesia in the EP lab based on the arrhythmia being targeted. Most inhaled or intravenous (IV) anesthetics and analgesics alter autonomic tone or cardiac conduction/repolarization. Propofol [2] and isoflurane [3,4] have not demonstrated significant effects on atrioventricular (AV) nodal properties. In general, local anesthetic at vascular access sites and short-acting IV agents (e.g. propofol) with quick reversal are the most commonly used analgesics and anesthetics during EP procedures. During induction of arrhythmia, particularly if non-inducible in the anesthetized state, anesthetics and analgesics should be stopped to wake up the patient for adequate assessment.

When ablating an arrhythmia that may arise close to structures whose function may be affected by the use of specific anesthetics (e.g. the phrenic nerve during atrial fibrillation ablation), drugs such as neuromuscular blocking agents should be avoided to allow for assessment of diaphragm contraction.

Another factor to consider during anesthesia is the importance of position stability, which is often critical to properly represent data on the cardiac map and thus guide arrhythmia therapy. In the case of most mapping systems, anatomy is registered against a static reference other than the patient (in the case of currently approved magnetic-based mapping systems) or the patches themselves (in the case of impedance-based mapping systems). Jet ventilation is another anesthetic support tool in ventilated patients that can be considered to reduce the respiratory variation of the heart during mapping and ablation and also to improve catheter stability [5].

Hemodynamic support

Most tachyarrhythmias cause some hemodynamic alteration, especially under sedation, and may need transient vasopressor support during the procedure. If the clinical arrhythmia being ablated is known to be hemodynamically unstable or ischemia provoking due to untreatable coronary disease, a mechanical assist device may be considered, especially if it is felt that mapping needs to be done during the arrhythmia. In cases where the primary method of ablation may involve targeting substrate (e.g. regions of scar), mapping during the arrhythmia may not be as critical as in other cases where the substrate is not as certain (e.g. midmyocardial scar where bipolar endocardial and epicardial maps may appear otherwise preserved).

Vascular access

Based on the differentials considered for the arrhythmia, vascular access should be planned and thoroughly discussed with the patient before the procedure. In addition to standard multiple venous accesses, arterial access, transseptal access, and epicardial access should be considered on a case-by-case basis for mapping and ablation. In rare cases, venous access via non-traditional sites may be considered, for example, internal jugular or subclavian access in case of inferior vena cava (IVC) obstruction and sometimes for improved catheter orientation and contact (e.g. right free wall accessory pathway or superior tricuspid annular mapping and ablation). In patients with an atrial baffle, a thorough understanding of the anatomy and cardiac hemodynamics is important as some patients may require evaluation in otherwise non-accessible areas with a transbaffle access.

Procedural tools

The diagnostic and interventional tools used should be tailored to the case. In general, having multiple diagnostic catheters with closely spaced bipoles spanning the areas of interest for the evaluation of tachycardia can provide valuable information early in the case. With the ultimate goal of stable contact in the chamber of interest, specific mapping catheters and sheaths should be selected. Based on chamber size, a catheter with an adequate distal curve should be selected to facilitate contact. Steerable sheaths provide an additional dimension of maneuverability and may be considered as needed, especially in patients with significant chamber enlargement. When difficulty with contact is anticipated, contact force sensing can be considered.

A thorough appreciation of the mechanism of tachycardia in relation to the anatomy is critical to success and avoiding complications. Electroanatomical mapping should be considered as useful for a three-dimensional appreciation of the structure being mapped. CT or MR image integration and correlation with the electroanatomical map can be valuable in appreciation of how the location of potential areas of interest based on the electrical mapping correlates with presumptive substrate on the basis of preprocedural imaging. For example, fibrosis in the ventricle during ventricular tachycardia mapping may be integrated with the map to determine whether assessment of scar is consistent between the two modalities. Direct visualization of the tissue being mapped with ICE can also be valuable in assessing contact, especially on intracardiac structures like papillary muscles and thick trabeculated tissue in the ventricles. ICE image integration with the electroanatomical map can also be considered for a better three-dimensional appreciation of the structures being mapped.

Equipment that may be needed for ablation should also be made available well in advance. While radiofrequency ablation (RFA) is commonly utilized for most arrhythmias, cryoablation may be considered when the source of the arrhythmia lies close to critical structures such as the AV node/His bundle or phrenic nerve. When advanced ablation therapies like bipolar ablation, alcohol ablation, or needle ablation are considered in specific circumstances, additional personnel or supplies may also be needed and may require special consideration for consent well in advance.

Reasons for failed ablation

Common reasons for failed ablation for arrhythmia can be categorized as follows.

Inability to identify the mechanism of arrhythmia and critical target sites

- Inability to induce tachycardia.
- Misdiagnosis as another tachycardia, for example, mistaking the arrhythmia mechanism during SVT in a patient with AV node reentry tachycardia (AVNRT) and a bystander anterograde conducting pathway as pathway-mediated tachycardia (antidromic tachycardia).
- More than one clinical tachycardia. For example, in some patients both AVNRT and accessory pathway-mediated tachycardias may exist, and symptoms may not be clearly distinguishable (Figure 8.1).
- Inability to identify a change of tachycardia during mapping and ablation. For example, one can have a change from one atrial flutter to another during mapping that is not predictable, making consistent activation or entrainment mapping difficult or impossible.
- Inability to identify the critical tissue needed for the tachycardia, for example, typical AVNRT involving a left inferior extension and the fast pathway. Ablation of the right inferior extension of the AV node may not cause the elimination of tachycardia and unless left-sided mapping is considered, the critical tissue might not be identified.
- Presumed inability to access the arrhythmogenic tissue due to lack of reach with tools being used or incomplete mapping. For example, tissue between the endocardial surface and the papillary muscle head in the left or right ventricle may be thought to have been adequately mapped due to presence of a "complete shell" but these deep interspaces with potentially large regions of tissue that can be arrhythmogenic may not have been adequately mapped.
- Inability to access the arrhythmogenic tissue due to true anatomical constraints, for example, if a region of tissue has been anatomically separated from a prior surgical procedure like reduction atrioplasty with part of the atrium folded and sutured closed or in the case of midmyocardial scar.
- Misrepresentation/interpretation of the electroanatomical map performed.

Failure to cause irreversible tissue death at the target site

- Inadequate contact/stability resulting in poor energy delivery.
- Contact-induced loss of conduction leading to inability to assess arrhythmia and results of ablation.
- Inability to deliver energy due to poor flow and temperature rise leading to low power.
- Cooling of the tissue being ablated. For example, ablation of the mitral isthmus area endocardially with ongoing cooling from the coronary sinus and circumflex artery epicardially may limit ability to reach adequate tissue temperatures to achieve transmural lesion formation.
- Shunting of energy due to contact with adjacent structures, for example ablation close to a mechanical valve.
- Arrhythmogenic tissue distant from the endocardial/epicardial site of catheter contact for ablation, for example midmyocardial substrate for ventricular tachycardia in a patient with non-ischemic cardiomyopathy.

Figure 8.1 Conversion of orthodromic reentry tachycardia into AVNRT after a His refractory PVC.

Close proximity to another critical structure, ablation of which can result in major morbidity or mortality

- Proximity to critical conduction tissue, for example, a midseptal pathway with proximity to the AV node and His bundle.
- Concern for collateral damage, for example, proximity to a coronary artery (often seen with outflow tract epicardial PVC ablation which may arise close to the left anterior descending artery), esophagus, or phrenic nerve.

Recurrence of arrhythmia due to the development of a new substrate

- Atrial fibrillation recurrence due to a new trigger after previous successful pulmonary vein isolation.
- Reengagement of reentry circuit due to the availability of another slow conducting zone that may not have been apparent during the first ablation.

The occurrence of new arrhythmia as a result of ablation

- Creation of new substrate from prior ablation, for example, the occurrence of cavotricuspid isthmus flutter after ablation for typical AVNRT on the septum or an atypical atrial flutter after pulmonary vein isolation.

Troubleshooting to avoid failed ablation (Box 8.1)

Evaluation of arrhythmia mechanism and critical components

Identification of the arrhythmia mechanism and vital tissue is the number one priority when trying to achieve successful ablation. First, distinguishing between reentry versus automatic or triggered for atrial and ventricular arrhythmias is important because while focal tachycardias typically need ablation of only a small region of tissue, macro-reentrant arrhythmias often involve ablation of a critical isthmus and anchoring of that site to electrically inert structures on either side to be successful. Furthermore, interpretation of activation information may be affected by whether the arrhythmia is focal or not.

In the case of reentrant arrhythmias, differentiating areas within regions of scar with no conduction (with no signal and no capture despite contact or area of double potentials) versus slow conduction (e.g. low voltage but capture or areas of fractionated signals) may help define the circuit. Entrainment maneuvers/subthreshold pacing maneuvers should also be considered to identify critical circuit components [6]. Areas of slow conduction that serve as the isthmus may be excellent targets for ablation. While termination of tachycardia may occur with ablation at this site, further ablation should still be performed in other areas of slow conduction to eliminate alternative potential circuits for arrhythmia. Sometimes the change of tachycardia rate or activation can happen when a change of reentrant circuit occurs and can be a clue for the existence of alternative circuits.

Box 8.1 Checklist to avoid failed ablation.

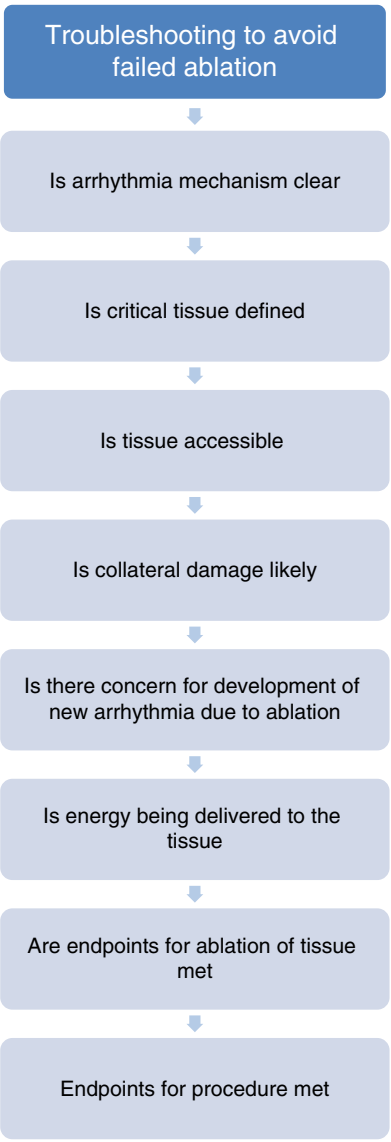

Specific clinical cases

Supraventricular arrhythmias

The most common reason for failure in SVT ablation is misdiagnosis. Common scenarios include:

- AVNRT or atrial tachycardia with bystander accessory pathway, which can be confused with a pathway-mediated tachycardia

- junctional tachycardia with AVNRT due to near-simultaneous activation of atrium and ventricles
- an atriofascicular pathway-mediated antidromic reciprocating tachycardia (ART) with bundle branch ventricular tachycardia or moderator band-related ventricular tachycardia.

A high index of suspicion should be maintained in these scenarios with a thorough evaluation performed during mapping to delineate the mechanism of tachycardia and confirm/exclude the participation of different structures in the tachycardia.

The presence of more than one SVT can be another reason for failure. A careful observation of tachycardia with an interpretation of maneuvers can often make this clear. However, sometimes it is difficult to interpret and will only be clear after therapy for one of the two potential tachycardias.

While most patients with AVNRT are amenable to successful ablation with ablation of the right inferior extension of the AV node, a small proportion of patients need further delineation of the components of the AVNRT circuit. Once AVNRT is considered, an evaluation for both the anterograde and retrograde limb of the tachycardia can help provide additional understanding of the circuit. In cases of typical AVNRT (retrograde conduction over fast pathway), entrainment at different locations in the atrium and coronary sinus (CS) can be considered to identify the anterograde limb of the tachycardia (in particular, the triangle of Koch and the distal and proximary coronary sinus). In cases where atrial activation in AVNRT is not early at the fast pathway location, atrial activation may be mapped to identify the retrograde limb of the tachycardia. This evaluation can be followed by a strategic ablation at the earliest site to improve success in AVNRT.

Yet another scenario when AVNRT ablation may fail is where the arrhythmia is either confused with atrial tachycardia (AT) due to more atrial activation (As) than ventricular activation (Vs) or with VT due to the presence of more Vs than As. In these cases, it is important to recognize that upper or lower common pathway block above and below the level of the critical circuit components comprising AVNRT may result in A-V dissociation in either direction, with AVNRT primarily driving either the A *or* the V. Additional testing should be considered to delineate mechanism clearly before planning therapy in these scenarios.

Fascicular tachycardia

The mechanism in fascicle/Purkinje-mediated tachycardia is most often reentrant, but a triggered mechanism may also be seen [7]. When feasible, the mechanism should be evaluated with pacing and entrainment techniques which can guide the mapping and ablation strategy. Please refer to mapping considerations below for further discussion.

Atrial fibrillation (AF)

Understanding the pathophysiology of AF specific to an individual patient is important before making a therapeutic plan. An attempt to understand the triggers and substrate for maintenance of AF may help in formulating a treatment plan which may include trigger isolation/elimination or substrate modification in the form of focal or linear ablation. For example, a pulmonary vein isolation procedure may not be sufficient in a patient with an AF trigger in the superior vena cava (Figure 8.2). In some patients, a pathway-mediated tachycardia, AVNRT, or atrial flutter could also be a major trigger, and elimination may prevent paroxysms of AF.

Mapping considerations

Common pitfalls in utilization of a three-dimensional electroanatomical mapping system and troubleshooting to avoid these pitfalls include the following.

Choice of an unstable reference

During electroanatomical mapping of a tachycardia in comparison to a chosen reference, care should be taken to ensure that the reference location is stable. For example, in the case of ventricular arrhythmias, the peak of the QRS in a specific lead may be chosen. However, in certain arrhythmia cases (e.g. fascicular tachycardia), the QRS morphology may vary. Similarly, using an intracardiac reference that is unstable in position may lead to mischaracterization of activation time. In such cases, a screw-in lead to maintain a stable reference can be of value.

Change in body position

Change in patient position in relation to the mapping system references can affect the map. Most systems will indicate that the patient has moved relative to the mapping reference and that the map may need to be recreated. However, each system has different thresholds based on relative motion of the patches to a reference (in most cases, a magnetic reference), and thus minor motion that can cause subtle shifts of relative point positioning may not be readily appreciated.

Comprehensive mapping

The number of points needed to make a comprehensive map should be tailored to the tachycardia and mechanism in consideration (Video 8.1). In general, the areas of possible involvement should be densely mapped while keeping local anatomy in mind to prevent missing data from critical locations, while the remaining areas may be sparsely mapped to exclude the participation

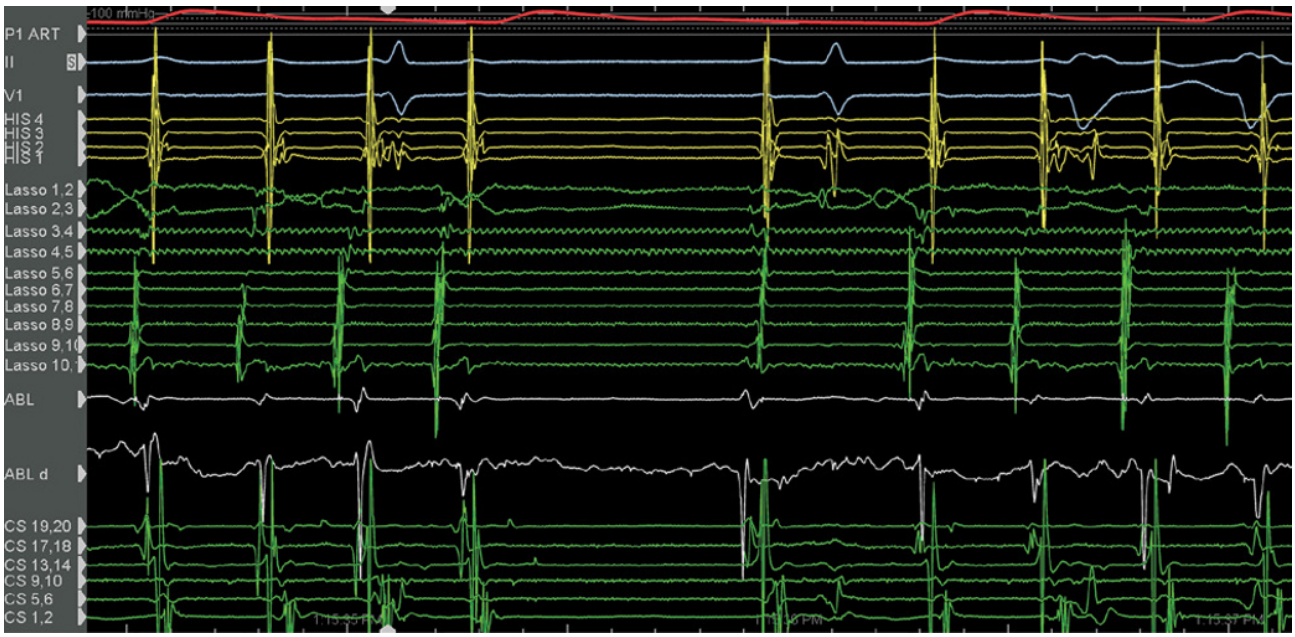

Figure 8.2 Patient on isoproterenol testing. Lasso catheter in SVC, ablation catheter in right atrium and CS catheter in coronary sinus. Atrial tachycardia and AF were noted repeatedly to start from SVC in this patient. SVC isolation was performed for therapy.

of those tissues. One example is PVCs from the outflow tract where dense mapping of both outflow tracts and nearby surrounding structures (e.g. the coronary sinus) may be needed, but dense mapping of the rest of the ventricles may not prove useful. In comparison, in the case of substrate mapping in a patient with structural ventricular disease and multiple VT morphologies, more extensive mapping of one or both ventricles may be needed.

Annotation of points

A uniform standard should be adopted throughout the mapping process for annotation of points for electrical activation. Stable tissue contact with the catheter should be assured when the point is annotated. Use of both bipolar and unipolar electrograms may facilitate proper annotation [8]. The rapid downstroke on unipolar electrogram and the first peak of the bipolar electrogram may be considered for local activation timing. However, when dealing with complex fractionated electrograms, this paradigm becomes less clear. When in doubt, anatomical tagging for fractionation should be considered instead of timing annotation. Furthermore, care should be taken to ignore annotation of possible mechanical signals from cardiac or valve motion.

Anatomical considerations

One critical factor involved in mapping is to understand the real anatomy of the structure of interest. While electroanatomical maps create often smooth, continuous surfaces, this reflects a limitation of spatial interpolation. All cardiac chambers are characterized by the presence of ridges, trabeculations, and potential arrhythmogenically active endocavitary structures. One common but underappreciated difficulty in complete mapping is in areas of trabeculated cardiac tissue. While a CTA/MRI provides an understanding of the anatomy, ICE can provide real-time guidance in mapping. This should be considered especially when there is missing information in the tachycardia after a presumed complete map. A separate notation of an intracavitary structure often provides a better three-dimensional appreciation of the structure and characterization of electrical activation during arrhythmia.

Reentry versus point source tachycardia

An assessment of whether an arrhythmia is focal versus reentrant based on the electroanatomical map alone has limitations. A focal tachycardia, for example, may appear to take the entire P-P interval once both atria are mapped due to presence of slow intra- or interatrial conduction. Similarly, reentrant tachycardias in one chamber may be misinterpreted as arising from another chamber if solely relying on the appearance of activation when performing electroanatomical mapping. For example, a left atrial flutter in a patient with prior cavotricuspid isthmus ablation can appear like counterclockwise reentry around the cavotricuspid isthmus (CTI) if the conduction time is coincidentally similar to the tachycardia cycle length (Video 8.2).

Further considerations in the interpretation of a reentrant arrhythmia based on electroanatomical mapping

In general, either electroanatomical or entrainment mapping may be used for evaluation of a reentrant atrial or ventricular arrhythmia before ablation. When an electroanatomical map is created, it is good practice to assess for proper annotation of points and for relevant but unmapped areas. This should especially be considered when a portion of the tachycardia circuit is unidentified. After mapping, an evaluation for potential circuits should be considered. Based on potential circuits identified, entrainment should be considered for confirmation of participation of presumed critical sites. The addition of entrainment data to electroanatomical mapping can aid in an improved understanding of the tachycardia circuit.

Consideration in the interpretation of a focal tachycardia

If a focal source of tachycardia is suspected and electromagnetic mapping is used, it is critical to have a clear, stable reference. While the presence of early activation significantly earlier than the surface ECG morphology (P wave in AT or QRS in PVCs) is likely the source of tachycardia, an origin away from this site is also possible. For example, a right ventricular outflow map in a patient with PVC from the left sinus of Valsalva may appear relatively focal, particularly if the annotated electrogram was the far-field component. In addition, if there is a diffuse area of early activation, this generally suggests a site of early activation from a different chamber.

Consideration in the mapping of a fascicular or Purkinje-mediated tachycardia

Mapping a fascicular or Purkinje-mediated tachycardia can pose additional nuances that should be considered.

- *Mapping the earliest ventricular activation.* In fascicular tachycardia there may often be more than one exit site and ablation of such sites only modifies the activation. This is characterized by variable surface QRS morphology during tachycardia, which may also be seen in other types of tachycardia (e.g. papillary muscle VT). For this reason, mapping for fascicular and Purkinje activation should be considered over mapping earliest ventricular activation.
- *Mapping earliest Purkinje site.* While mapping the earliest Purkinje site is of advantage in focal arrhythmias, it is not sufficient in reentrant arrhythmias where there is no start or end for activation in an arrhythmia occurring in a circuitous manner. Use of high- and low-output pacing to capture Purkinje tissue may sometimes help identify potential sites of participation. However, comparative mapping techniques may similarly afford further data, wherein timing of fascicular and Purkinje relative to ventricular signals may be done during both sinus rhythm and tachycardia at each site, as exemplified in Figure 8.3.

Consideration in mapping of an accessory pathway

Common pitfalls in mapping of an accessory pathway are as follows.

- *Mapping sites of shortest AV interval.* Due to the presence of slant in some accessory pathways, atrial and ventricular activation may overlap along the annulus away from the site of the accessory pathway. Thus, attempts to identify the pathway potential and the earliest site of ventricular activation when anterograde mapping or the earliest site of atrial activation in retrograde mapping may help to better differentiate the site of optimal ablation.
- *Mapping earliest activation.* It is common practice to map the earliest activation to identify the pathway insertion. A common pitfall here is failure to recognize

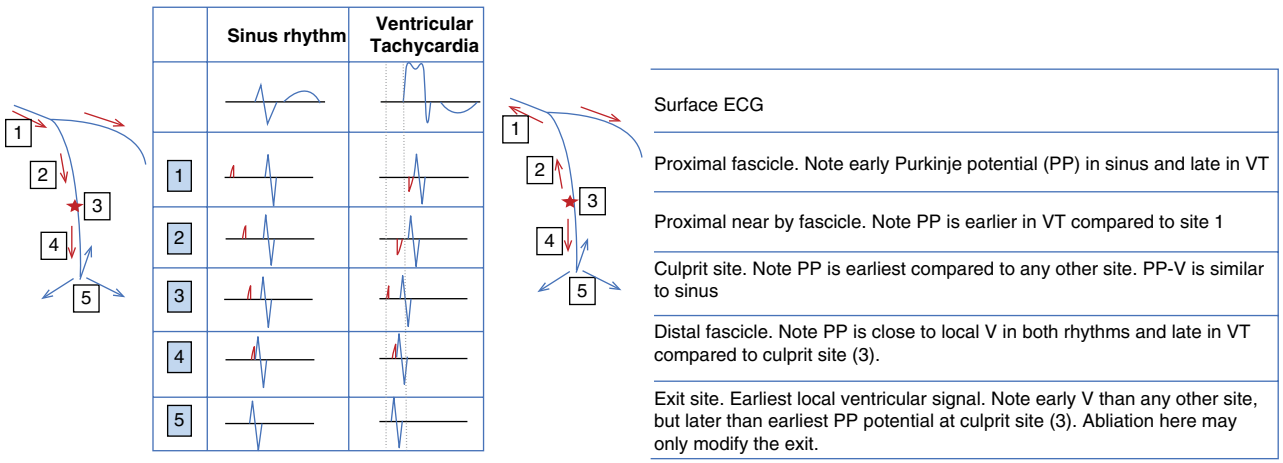

Figure 8.3 Comparative mapping between sinus rhythm and ventricular tachycardia to evaluate fascicular arrhythmia. ECG, electrocardiogram; VT, ventricular tachycardia.